INVESTIGATING THE MOLECULAR BASIS OF RESISTANCE AND PYRETHROID SELECTIVITY AT ACARINE SODIUM CHANNELS

Alix Dawn Blockley

MBiol (Hons)

Thesis submitted to Birkbeck, University of London

for the degree of

Doctor of Philosophy

September 2016

Declaration

I declare that the work in this thesis is the candidates own.

Signed:

Alix Dawn Blockley

Acknowledgements

Firstly, this work would not have been possible without the guidance of my wonderful supervisory team: Andreas Turberg, Bonnie Wallace, Emyr Davies, and in particular Lin Field and Martin Williamson. I thank you all for your advice and encouragement when it just would not work. Again. You have taught me how to supervise a student well. Thank you for always having an open door when I needed it.

I particularly thank my "adoptive" supervisor, Ian Mellor at the University of Nottingham. Your advice, practical encouragement and supportive words, particularly when I was low on time and high on leak currents, made this work possible.

I would also like to thank all those I have worked with at Rothamsted Research in the Insect Molecular Biology group and beyond. Thank you for making each day in the lab a good day. In particular, I thank Joel González-Cabrera, for his guidance at the start of my PhD, for providing the native *Varroa destructor* VGSC, and critically for sharing the frustrations of cloning arthropod VGSCs. I also thank Andrew Mead for his help with analysis of bioassay data and Rob King for bioinformatics support.

To my lab group at Nottingham University: Rohit Patel, Neville Ngum, Abu Izuddin, Mahmoud Sherif, Maria Kor and David Richards. Thank you so much for the shared commiserations and congratulations, and for making me part of the team. In particular, I thank John Grzeskowiak for his friendship and for teaching me the basics of electrophysiology. I hope we can co-supervise a student or twenty!

Lastly, I thank my husband James for his love and support, for keeping his phone on, washing my bike, and for not going to the Peaks without me. Your face.

I dedicate this work to Sarah Bough, without whom I would never have started this PhD, wish you were here; and to my dad, who would have been a brilliant biologist.

Contents

List of Tables:

List of Figures:

1 Abbreviations Used

AMP = Ampicillin

ATP = Adenosine triphosphate

AUC = Area under the curve

BLAST = Basic local alignment search tool

°C = Degrees Celsius

Ca2+ = Calcium ions

CI = Confidence Interval

cDNA = Complementary deoxyribonucleic acid

cRNA = Complementary ribonucleic acid

CTP = Cytidine triphosphate

DDT = Dichloro-diphenyl-tricloroethane

DMSO = Dimethyl-sulphoxide

DNA = Deoxyribonucleic acid

dATP = Deoxyadenosine triphosphate

dCTP = Deoxycytidine triphosphate

dGTP= Deoxyguanosine triphosphate

dNTP = Deoxynucleotide triphosphate: N indicating that this may refer to any deoxyribonucleotide: dATP, dCTP, dGTP or dTTP

dTTP = Deoxythymidine triphosphate

dsRNA = Double stranded ribonucleic acid

DTT = Dithiothreitol

EC_{50} = Effective concentration causing 50% of the maximum response

EDTA = Ethylenediaminetetraacetic acid

exp = Exponential

G = Conductance

g = Local gravitational acceleration

G_{max} = Maximum conductance

GTP = Guanosine triphosphate

HEPES = (4-(2-hydroxyethyl)-1-piperazineethanesulfonic acid)

Hz = Hertz

I = Current

IC_{50} = Concentration causing 50% response inhibition

ID = Internal diameter

I_{peak} = Peak current

I_{tail} = Tail current

IPTG = Isopropyl β-D-1-thiogalactopyranoside

k = Slope factor

K+ = Potassium ion

Kdr = Knockdown resistance

kHz = Kilohertz

L = Litre

LB = Lysogeny broth

Log 10 = Log to the based 10 of a value

M = Molar

M7G = 7-Methyl guanosine

MΩ = Megaohm

mg = Milligram

M_i = Integral modification

ml = Millilitre

mM = Millimolar

mRNA = Messenger ribonucleic acid

ms = Millisecond

mV = Millivolt

µg = Microgram

µl = Microliter

µM = Micromolar

n = Number of cells/individuals in a test group

Na+ = Sodium ion

ng = Nanogram

nl = Nanolitre

nm = Nanometre

NTP = Nucleotide triphosphate: N indicating that this may refer to any ribonucleotide: ATP, CTP, GTP or UTP

OD = Optical Density

OIE = World organisation for animal health

p = Phosphate

PCR = Polymerase chain reaction

RCF = Relative centrifugal force

RNA = Ribonucleic acid

rpm = Revolutions per minute

S.E. = Standard error

SEM = Standard error of the mean

Skdr = Super knockdown resistance

SNP = Single nucleotide polymorphism

SOC= Super optimal broth with catabolite repression

ssDNA = Single stranded deoxyribonucleic acid

TAE = Trisacetate ethylene diamine tetra acetic acid

TEVC = Two electrode voltage clamp

Tris = Tris(hydroxymethyl)aminomethane

UTP = Uridine triphosphate

UV = Ultraviolet radiation

V = Voltage

$V_{50.act}$ = Half-activation voltage (voltage causing 50% of the maximum response)

$V_{50.inact}$ = Half-inactivation voltage(voltage causing 50% of maximum inactivation)

VGSC = Voltage-gated sodium channel

V_{rev} = Reversal potential

V_T = Test potential

$V_{T.inact}$ = Inactivating pre-pule potential

WHO = World health organisation

X-gal = 5-bromo-4-chloro-3-indolyl-β-D-galactoside

2 Abstract

Many acarine (tick and mite) species are ectoparasites of humans, livestock and domestic pets, where they spread disease and impact adversely on health. They are normally controlled through the application of acaricides; however, the prolonged use of individual compounds has resulted in many species developing resistance to specific pesticides. This thesis describes investigations into the molecular properties that determine the resistance to and selectivity of pyrethroids, an important class of pesticides that act on the voltage-gated sodium channels (VGSCs) of arthropod neurons. Comparison of insect and acarine VGSC sequences, coupled with molecular modelling studies, have identified a residue at amino-acid position 933 (*M. domestica* numbering) found within a putative pyrethroid binding pocket that may contribute to a greater selectivity of pyrethroids with comparatively larger halogenated groups for acarine VGSCs compared to those of insects. This is due to the presence of a smaller glycine residue at position 933 in acarine channels, compared to a cysteine residue in insect channels, which may enhance the binding of such pyrethroids (O'Reilly et al., 2014). This model is supported by the findings of Jonsson et al 2010, that *R. microplus* cattle ticks carrying the amino acid substitution G933V, are resistant to the pyrethroid flumethrin, which has a comparatively larger halogenated group, but not the pyrethroid cypermethrin, which has a comparatively smaller halogenated group. Work in this thesis describes progress made in the investigation of such specificity; involving sequencing studies, two-electrode voltage clamp electrophysiology in *Xenopus laevis* oocytes involving insect and acarine VGSCs, and whole arthropod bioassays. While this work cannot conclusively disprove the model proposed by O'Reilly *et al* 2014, it suggests that the mechanisms of selectivity for pyrethroids in arthropods may involve the interplay of several factors, rather than being solely based upon structural variations in their VGSCs.

Abstract Word Count: 295

3 General Introduction

3.1 Acari

Acari are members of the subphylum chelicerata, one of the three major lineages that diverged early on in the evolution of the phylum arthropoda. The chelicerata are named after their claw-like feeding appendages called chelicerae that they use as fangs or pincers. Most extant chelicerates are arachnids, a group comprised of spiders, scorpions, ticks and mites - and it is the ticks and mites that make up the subgroup acari (Campbell et al., 2015). At the time of writing over 55,000 acarine species have been described, making it the most diverse group of the Arachnida, totalling nearly half of all known Arachnida species and 3.5 % of all Animalia species discovered so far (Zhang et al., 2011). However, this is likely to be a conservative estimate, with some entomologists estimating that the total number of mite and tick species is between 500,000 and 1,000,000 (Zhang et al., 2011). Acari range in size, from the smallest mites, at around 0.1 mm in length, to the largest ticks, at a little over 30 mm in length; they also range in shape from round to elongated forms and can be hard or soft bodied. The larvae of acari have three pairs of legs, but during development into nymphs and adults, they develop an additional pair, marking them as distinct from insects (Online: Online: Encyclopædia Britannica 2016).

Acari are distributed globally in a wide range of habitats, they have been recorded at 5,000 m above sea level on the slopes of Mount Everest and at 5,200 m below sea level in the Northern Pacific Ocean, they are found in hot springs, deserts, tundra and even the Antarctic (Online: Encyclopædia Britannica 2016). Their habitats also intersect with areas inhabited by humans; unfortunately, this is not always beneficial from a human standpoint, since many acari are vectors of diseases transmissible to humans, other animals (including domestic livestock and companion animals), and crop plants (Online: Encyclopædia Britannica 2016). The need to prevent the transmission of these diseases means that there is an associated need to control vectorial acarine species, and some of the challenges involved in meeting this need are addressed in this Thesis.

3.2 Mites

3.2.1 Mite Anatomy and Lifestyle

Mites, like all acari, have eight legs. They can be distinguished from ticks as they have hairs or bristles called setae on their legs and bodies and they do not have teeth on the hypostome of the mouthparts (Service, 2012). The term “mite” comes from old English and means “a very small creature” and in fact most are less than 1 mm in length and none are longer than a few millimeters (Walter and Proctor, 1999). Mites live in a wide range of habitats, such as fresh and brackish water, hot springs, soil, and as parasites on plants, mammals, birds and insects; as a consequence of this habitat diversity mites exhibit a wide range of body forms, mating strategies, and lifecycles (Service, 2012; Walter and Proctor, 1999).

Mites can reproduce sexually or asexually (both as haploid arrhenotoky and as thelytoky) and different species exhibit a variety of lifecycles that often involve a combination of stages. The sarcoptiform mites and many trombidiformans begin their lives as, usually spherical, eggs that hatch into either prelarvae and then go on through development to become larvae, protonymphs, deutonymphs, tritonymphs and finally adult mites. The prostigmatans skip the tritonymph stage and in most heterostigmatans, the adult stage is only separated from the egg by a single larval stage. However, in some heterostigmatan species females are physogastric, meaning that the abdomen is able to swell to accommodate growing young, and in these mites all development, and mating, occurs within the body of the mother and she gives birth to fully formed and already mated adult offspring (Walter and Proctor, 1999).

3.2.2 Mite Damage and Mite-Borne Disease

Mites can be benign or even, on balance, beneficial from a human standpoint, being critical players in the formation of soil and acting as important agents of biological pest control (Walter, 1999; Online: Encyclopædia Britannica 2016). However; they can be threatening to humans, with crop-feeding mites causing damage to our food supply by

feeding on plant tissue and/or by transmitting plant viruses (Van Leeuwen et al., 2015), and some animal-feeding mites acting as vectors for disease or causing skin irritation or allergies (Deplazes et al., 2016; Service, 2012).

For human health issues the species of most importance are *Sarcoptes scabiei* (the scabies mite), trombiculid mites (including the scrub typhus mites), house dust mites and follicle mites (Service, 2012). *S. scabiei* causes scabies, a skin condition resulting from the direct burrowing action of the mite, which is particularly prevalent in areas where people live in close contact with one another. Scabies starts by a female mite being transmitted onto a person's skin, where it will dig out a small pocket in which to wait until it encounters a male mite and can mate. Once fertilized the female mite begins to burrow down through the outer layers of the skin, feeding on the liquids produced from broken dermal cells. Mites usually choose to burrow in places where the skin is thin and creased, commonly the hands, wrists and elbows; this burrowing occurs at a rate of around 0.5-5mm per day and burrows can be seen on the skin as thin lines. Each fertilized female will then lay 1-3 eggs per burrow, which hatch into larvae after 3-4 days (Service, 2012). *S. scabei* is not a disease vector, but rather affects the host by causing an allergic reaction; giving rise to an itchy rash and the scratching reaction that this rash induces in the host frequently gives rise to secondary bacterial infections. As the rash is caused by an allergic response it can persist even after all the mites are destroyed (Service, 2012).

In Northern Europe and the USA *Neotrombicula autumnalis* (the harvest mite) and *Eutrombicula alfreddugesi* (the red bug) are trombiculid mites responsible for bites and irritation to humans walking through long grass or scrub in the summer or autumn (Service, 2012). However; in South East Asia, in an area known as the "tsutsugamushi triangle", some species of trombiculid mites are responsible for the spread of a serious disease, scrub typhus (Online: World Health Organisation 2016). Scrub typhus, also known as Tsutsugamushi disease, is caused by the bacterium *Orientia* (formerly *Rickettsia*) *tsutsugamushiwas* and was first described in 1899 in Japan. The symptoms are often non-specific, making misdiagnosis common. Disease presentation begins with flu-like symptoms including chills, shaking, a fever, intense headache, infection of

the mucous membrane surrounding the eyes and swelling of the lymph nodes. A rash may also be present on the infected person's trunk, as may a dry, dark scab known as an eschar at the bite site. Mortality rates in untreated patients can be as high as 30% (Online: World Health Organisation 2016).

Also in humans house dust mites (a collection composed of around twenty mite species) can aggravate conditions such as asthma and follicle mites (*Demodex* species) can cause skin complaints such as acne, rosacea, impetigo contagiosa or blepharitis (Service, 2012). Whilst not seemingly serious; the aggravation of asthma and other conditions and the allergic complaints caused by these mites can certainly be life-altering and even life-threatening in extreme cases (Service, 2012).

In livestock mites can also cause numerous skin problems and systemic allergies. The mite species responsible include *Psoroptes, Chorioptes, Demodex, Cheyletiella, Notoedres, Trombicula,* and *Otodectes*, along with *S. scabei* (Taylor, 2001), but McNair (2015) has noted *Psoroptes ovis* (the sheep scab mite) and *Dermanyssus gallinae* (poultry mites) are of particular veterinary importance in livestock.

P. ovis represents a major economic burden in the UK, and is found in sheep-producing countries worldwide, except for New Zealand and Australia, where it has been successfully eradicated (Sargison et al., 2007). *P. ovis* are small (0.75mm) and live below the fleece on the skin surface, where they feed on tissue fluid, in a similar way to *S. scabei* (van den Broek et al., 2000). The disease is not usually fatal but the severe itching in infected animals frequently leads to secondary bacterial infections and also distracts the animal from eating, causing weight loss (Kirkwood, 1986). Coupled with damage to the fleece, this weight loss reduces the value of the animal to the farmer and since mites can survive for up to 16 days off the animal, the condition can spread quickly through a flock (McNair, 2015; O' Brien et al., 1994).

D. gallinae is very common in in hen houses worldwide, especially in Europe, where it is estimated that up to 90% of hen houses in Italy and up to 60% of hen houses in the UK are infested (Fiddes et al., 2005; Marangi et al., 2012). *D. gallinae* is

haematophagous, feeding on the blood of the chickens and causing anaemia, which decreases egg production and can sometimes be fatal (Kirkwood, 1967). Furthermore, it is thought that these mites can act as vectors for bacterial and viral infections (Valiente Moro et al., 2005). *D. gallinae* mites are very small, around 1mm long, and as such are difficult to treat with acaricides, as they can easily hide in small inaccessible nooks during the day, with feeding activity taking place at night. (Kirkwood, 1967). Furthermore, *D. gallinae* can also infest other animals, including the humans who work in the hen houses and so can be transported between populations (Rosen et al., 2002).

Companion animals can be infested by many diverse species of mites and given the close contact between these animals and humans, mites which infest companion species are of particular concern as the transmissive agent of zoonotic diseases (Deplazes et al., 2016), defined as "diseases and infections that are transmitted naturally between vertebrate animals and man" (Online: World Health Organisation 1959).

In the order Prostigmata the genera *Demodex*, *Cheyletiella* and *Trombicula* are important ectoparasites of dogs and cats, but will also attack other companion animals and humans (Deplazes et al., 2016). *Demodex* species are small-legged, cigar-shaped mites that are extremely host-specific; *Demodex canis* is a particularly important ectoparasite of dogs, causing fur loss as mites multiply to excess in hair-follicles, often leading to secondary bacterial infections in the skin which can be extremely severe. This condition, called demodicosis, can also present in cats, goats, cattle, pigs and horses (Deplazes et al., 2016). *Cheyletiella* (fur mites) are common on dogs, cats and rabbits; though they can colonise humans. In dogs, cats, and humans the mites (termed "walking dandruff") can cause dandruff, itching and eczema, but the condition may also be asymptomatic (Deplazes et al., 2016). *Trombicula* mites, as discussed above, are important carries of disease in humans (Service, 2012; Online: World Health Organisation 2016) but also infest animals, providing a zoonotic transmission route for both the mites and, in South East Asia, for scrub typhus (Tsutsugamushi disease) (Deplazes, 2016; Online: World Health Organisation 2016). These mites are not host-specific, and the larvae will attack any mammal or bird, typically *en masse*, meaning

that one individual may be attacked by thousands of mites. This causes extreme itching and occasionally convulsions or seizures, with symptoms lasting for several days after the larvae have left the host (Deplazes et al., 2016).

Outside of the order Prostigmata, other important mites of companion animals include *Ornithonyssus bacoti* (the tropical rat mite), a haematophagous mite (family Macronyssidae) which causes itching, rough fur and restlessness in rodent pets including hamsters, gerbils, rats and mice. These mites may also use humans as hosts, with children who are in close contact with their pets often being affected by itchy, erythematous papules. Also in the family Macronyssidae, *Ophionyssus natricis* (the common snake mite) is the most pathogenic ectoparasite of domestic snakes and can also affect lizards and again can move to humans, causing itchy skin lesions and vesicular exanthema along with secondary effects from scratching (Deplazes et al., 2016). Mange is another mite-caused condition that can occur in companion animals and is caused by a variety of species such as *Otodectes cynotis* (ear mange in cats and dogs), *S. scabiei* variants (Sarcoptes manage in horses, canids and mustelids), *Notodres* species (Notoedrosis in cats and rabbits) and *Trixacarus caviae* (Trixacarosis in Guinea pigs). All of these can temporarily infest humans causing pseudoscabies or temporary dermatitis (Deplazes et al., 2016).

There are many phytophagous mites that infect crop plants, posing critical threats to the production of many human and animal-feed plant species including fruits, vegetables, corn, soybean and cotton (Jeppson et al., 1975; Van Leeuwen et al., 2015). Mite species belonging to the family *Tetranychidae* (spider mites), the *Tenuipalpidae* (false spider mites), the *Tarsonemidae* (tarsonemid mites) and the *Eriophyidae* (gall and rustmites) pose a particularly serious economic threat by both direct feeding effects and by the spread of numerous plant pathogens (Van Leeuwen et al., 2010a; Van Leeuwen et al., 2010b). The spider mites *Tetranychus urticae*, *Panonychus citri* and *Panonychus ulmi* are considered to be the most devastating pests, with *P. citri* and *P. ulmi* mainly infesting citrus and apples respectively and *T. urticae* infecting over 1000 reported host species belonging to more than 250 plant families (Online: Alain Migeon And Franck Dorkeld Spider Mites Web: a comprehensive database for the

Tetranychidae 2006-2015). A comprehensive review of the impact of agricultural mites estimates that worldwide the control of these pests is worth over €900 million, with the majority of this being spent to control the three spider mite species (Van Leeuwen et al., 2015).

Alongside their direct effects on crop plants, mites may also have a deleterious effect on food production via the infestation of insects required for crop pollination, most notably *Varroa destructor* and *Acarapis woodi* mites and their deleterious effects on the honeybee, *Apis mellifera*. *A. mellifera* plays a critical role in human health and the global economy, both as honey producer and as the main pollinator of food crops (Decourtye et al., 2010).

V. destructor causes varroosis of the European honey bee, now the most common bee disease in Europe, and this disease is now also present in North and South America, Russia and Africa; spreading from hive to hive and country to country via the long range transportation of bees, with the mites spreading between bees through drones, workers, robber bees and swarming behaviour (Deplazes et al., 2016). Female mites lay eggs in the brood cells of hives before the brood cells are capped, and these develop into adults over approximately 8 days on the bee larvae; adult females mites leave the brood, already fertilised, together with the bee once it hatches, whilst male mites die within the brood cell once fertilisation has occurred (Deplazes et al., 2016). It is the female mites that feed on the bee's haemolymph, depleting energy resources so that when infected individuals hatch they are significantly smaller and have considerably shorter life-spans than uninfected bees; in heavy infestations young bees may not be viable at all (Deplazes et al., 2016). In addition damage by direct feeding, *V. destructor* is known to play a role in the transmission and virulence of the globally-distributed deformed wing virus, which causes shrivelled wings in infected bees, rendering them unable to fly and therefore feed. Furthermore, *V. destructor* infestation also causes immunosuppression in developing bees, making them more vulnerable to the virus (de Miranda and Genersch, 2010; Genersch and Aubert, 2010; Yang and Cox-Foster, 2005). Without *V. destructor* mite control a honeybee colony will collapse in the third or fourth year after primary infestation, and varroosis is so serious

as to be a World Organisation for Animal Health (OIE) listed notifiable disease (Online: World Organisation for Animal Health 2016). Effective elimination of *V. destructor* is currently not possible, due to transmission of mites from other hives, so bee keepers aim to reduce the number of mites to below a damage threshold (Deplazes et al., 2016).

Tracheal mite disease (Acarapiosis) caused by *A. woodi* infestations is also on the OIE notifiable list (Online: World Organisation for Animal Health 2016). These mites develop within the trachea of honey bees (so are an internal mite) and puncture the tracheal wall to ingest haemolymph. This obstructs air circulation, causing general weakness and can render the bees unable to fly and can cause death, particularly in spring. Acarapiosis is found worldwide, except in Australia and New Zealand, and is spread only by direct bee to bee contact; however, affected colonies tend to swam, facilitating the spread of the mites. Bees are only susceptible until the age of four days, after which the spiracles are protected by strongly chitinised bristles, and the mites can no longer penetrate into the trachea (Deplazes et al., 2016; Sammataro et al., 2000).

3.3 Ticks

3.3.1 Tick Anatomy and Lifestyle

The term tick (suborder *Ixodida*) refers to any of approximately 867 species of invertebrates in the order Parasitiformes (subclass acari) (Jongejan and Uilenberg, 2004). Most ticks are 15 mm or less, however some can grow up to 30 mm. Ticks are closely related to mites, from whom they differ by the presence of a “Haller’s organ”, a sensory disk found on the tip segment of the first of four pairs of legs (Haller 1881 - As cited in (Foelix and Axtell, 1972)) they also lack setae on their bodies and have a toothed hypostome (Service, 2012). All tick species belong to one of three families: The Nuttalliellidae or the Ixodidae, which together comprise the hard ticks, or the Argasidae, the soft ticks (Jongejan and Uilenberg, 2004; Service, 2012). There are some obvious physical differences, allowing easy differentiation between hard and soft ticks,

with hard ticks having a hard cuticle and a scutum (protective shield) either completely or partially covering the dorsal region, and soft ticks having more leathery bodies and no scutum (Mehlhorn, 2001). Hard and soft ticks also differ in their life cycles. Soft ticks live on their host animal and feed intermittently, before detaching and retreating to a hiding place, off the host. Adult soft ticks mate off the host, and females generally lay eggs after each blood meal. There are then several nymphal stages, which are always parasitic (Jongejan and Uilenberg, 2004) and like the adults nymphs attach to the host for a relatively short time. Soft ticks tend to feed on many different individual hosts, often from different species, during their lifetime and are referred to as "many-host" ticks (Service, 2012). Hard ticks feed continuously on host blood for several days during each life stage (larvae, nymph, adult) and have one, two or three hosts, and usually mate on a host animal. When an adult female has obtained a blood meal, she drops from the host, lays a single large mass of eggs, and dies. The male may remain on the host for several months (Jongejan and Uilenberg, 2004). Many species of hard tick are host specific, for example, some feed almost exclusively on birds, others on reptiles and others on certain groups of mammals, such as canids. However, others will feed on any available host, including humans (Service, 2012).

3.3.2 Tick Damage and Tick-Borne Disease

Ticks were the first arthropods to be recognised as vectors of disease and, along with mosquitoes, are the major arthropod vectors of diseases in livestock, companion animals and humans (Colwell et al., 2011; Jongejan and Uilenberg, 2004). They transmit more pathogens, including protozoans, rickettsiae, spirochetes and viruses, than any other arthropod species (Ghosh et al., 2007). A tick is considered a vector for a pathogen if it will feed on an infected host, acquire the pathogen during the blood meal, maintain the pathogen through one or more life stages, and then pass the pathogen on to other hosts (Jongejan and Uilenberg, 2004; Kahl et al., 2002). Ticks are responsible for the spread of a large number of potentially life-threatening diseases of humans, such as tick-borne encephalitis (caused by viruses of the family Flaviviridae), babeosis (a febrile, malaria-like parasitic disease caused by protozoa of the *Babesia* genus), ehrlichiosis (febrile illnesses caused by bacterial infection of white blood cells

by bacteria of the genus *Ehrlichia*) and Lyme borreliosis (Dantas-Torres et al., 2012; Jongejan and Uilenberg, 2004; Telford and Goethert, 2004).

Worryingly, there is evidence that the incidence of tick-borne diseases is increasing (Dantas-Torres et al., 2012; Nicholson et al., 2010; Piesman and Eisen, 2008), and it is thought that changes in human and tick behaviour will increasingly lead to the conditions required for tick-borne disease to spread (Randolph, 2010; Sutherst, 2004). A good example of this is Lyme borreliosis, or Lyme disease, in the United Kingdom (UK). This human disease is caused by bacteria of the *Borrelia* genus vectored predominantly by *Ixodes ricinus* in the UK (Alao and Decker, 2012) and was first described in the late 1970's in Lyme, Connecticut (Steere et al., 1977). Early symptoms include a bull's-eye rash and flu-like symptoms that are treatable with antibiotics (Online: Centers for Disease control and Prevention 2015). However, if not treated, complications involving the nervous, cardiovascular and musculoskeletal systems can occur (Alao and Decker, 2012; Uzzell et al., 2012). From 2001 to 2011, the number of confirmed cases of Lyme disease in England and Wales rose from 268 to 959 (Online: Health Protection Agency 2013) suggesting that the disease is on the increase here, although this seeming increase may result from improved disease detection methods (Uzzell et al., 2012),

A further example of a tick-borne disease increasing in humans is Spotted Fever Rickettsiosis (SFR) in the USA. SFR is actually a group of diseases caused by bacteria of the *Rickettsia* genus, which are spread to humans by various hard tick species, via a range of domestic and wild animal hosts. It includes the well-documented Rocky Mountain spotted fever. Symptoms of an SFR include fever, headache, fatigue, muscle aches, a maculopapular or petechial rash and often blackened or crusted skin at the site of the tick bite (Online: Centers for Disease control and Prevention 2016). The severity depends on the species of *Rickettsia* involved and varies from self-resolving to potentially fatal (Online: Centers for Disease control and Prevention 2016). Reported cases in the United States increased from 1.7 cases per million person-years in 2000 to 14.3 cases per million person-years in 2012, suggesting that favourable ecological

changes influencing vector tick populations and disease transmission may be occurring (Drexler et al., 2016).

Ticks may also cause direct health problems in in humans and other animal hosts by substances in tick salvia, which cause “tick paralysis” and “non-paralytic tick toxicosis”. Tick paralysis typically causes a progressive paralysis starting in the lower limbs that slowly reaches the upper body, possibly with other symptoms including vomiting and a typhus-like rash depending on the host and tick species involved. Non-paralytic tick toxicosis gives a multitude of symptoms ranging from fever, sweating, breathing difficulties, to nervous incoordination and death (Estrada-Pena and Mans, 2014). Tick paralysis occurs globally, involving more than 70 tick species and including both Ixodid and Agrasid ticks, with the most important species being *Dermacentor andersoni* and *Dermacentor variabilis* in the United States and Canada, and *Ixodes holocyclus* in Australia (Estrada-Pena and Mans, 2014; Mans et al., 2004).

For non-humans the host range of ticks is wide and includes mammals, birds, reptiles and amphibians, and both hard and soft tick species can be found as parasites associated with livestock and companion animals (Deplazes et al., 2016; Guzman-Cornejo et al., 2011; Jongejan and Uilenberg, 2004; Service, 2012). As for mites, animal tick infestation links animal and human health via zoonoses; for example, in the United Kingdom, *Ixodes ricinus*, the main vector of Lyme disease (Uzzell et al., 2012), has been reported on both domestic dogs and cats (Jameson and Medlock, 2011) and provides a potential route for disease transmission from companion animals to humans. In fact, most tick-borne diseases infecting to animals are caused by pathogens that can also infect humans, so livestock and companion animals can be reservoirs for human tick-borne disease (Deplazes et al., 2016).

In livestock tick-borne diseases occur in domestic poultry, cattle, sheep, goats and camels (Jongejan and Uilenberg, 2004). In cattle alone, tick-borne diseases affect over 80% of the population, posing a considerable constraint to livestock production and hence the health of many humans living in rural areas (Marcelino et al., 2012). Ticks can cause severe damage to the health of livestock animals simply through their role

as haematophagous feeders, which damages the skin and coat of infected animals, and causes anaemia through blood-loss, leading to lower milk/meat production. Furthermore, ticks also transmit a large variety of disease pathogens to livestock animals, for example anaplasmosis and babesiosis (Deplazes et al., 2016). Anaplasmosis is caused by intracellular parasites of the genus *Anaplasma* (Alessandra and Santo, 2012). In sheep and goats, the condition tick fever is predominantly caused by *Anaplasma ovis* and less commonly by *Anaplasma phagocytophilum* (Alessandra and Santo, 2012). *A. ovis* is spread by the ticks *Rhipicephalus bursa*, *Rhipicephalus bursa turanicus*, *Dermacentor silvarum*, *Dermacentor marginatus*, *D. andersoni* and *Haemaphysalis sulcate* (Alessandra and Santo, 2012); while *A. phagocytophilum* is spread by *I. ricinus* in Europe and *Ixodes scapularis* and *Ixodes pacificus* in the US (Richter et al., 1996). In cattle the causative agent of anaplasmosis is usually *Anaplasma marginale,* spread mainly by *Rhipicephalus microplus*, along with other members of the *Rhipicephalus* and *Dermacentor* species. *Amblyomma variegatum* and *Hyalomma* species can also spread anaplasmosis, in the form of *Anaplasma bovis* (Deplazes et al., 2016; Marcelino et al., 2012). Babeosis in small ruminants and cattle is caused by protozoa of the genus *Babesia*, which infect erythrocytes causing, among other symptoms, severe anaemia (Perez de Leon et al., 2014), for example *Babesia ovis* in sheep with a mortality rate of 30-50% (Alessandra and Santo, 2012). *Babesiidae* are transmitted by many different ticks including *Amblyomma*, *Dermacentor*, *Ixodes*, *Haemaphysalis*, *Hyalomma*, and *Rhipicephalus* species (Deplazes et al., 2016).

Common companion animals such as cats, dogs and horses all suffer from ticks and tick-borne disease (Jongejan and Uilenberg, 2004; Reichard et al., 2010; Service, 2012) and issues for animal welfare and disease transmission can be very significant (Kiss et al., 2012). Dogs are particularly affected, for example in tropical, sub-tropical and some temperate zones dogs may contract babesiosis that can be highly pathogenic. *Babesia* causing canine babesiosis are spread by *D. reticulatus* in Europe and Asia, by *Rhipicephalus sanguineus* in America, and by *Haemaphysalis bispinosa* and *Haemaphysalis leachi* in Australia and Africa (Deplazes et al., 2016). Ehrlichiosis in dogs also occurs in several global regions, the vectors being *R. sanguineus* and *D. variabilis*, and can be fatal (Jongejan and Uilenberg, 2004). Cats can also be affected by tick-

borne disease, for example feline cytauxzoonosis, vectored by *Amblyomma americanum* and caused by the protozoan *Cytauxzoon felis*, is fatal in almost all cases (Meinkoth and Kocan, 2005; Reichard et al., 2010).

3.4 Acarine Control

The widespread threats from mites and ticks to both human and animal health and to crop production means that there is a pressing need for good, sustainable, control strategies. As a species, human beings are existing in a time of immense and rapid changes in the global environment, such as an increased level of atmospheric carbon dioxide and global temperature rise (Solomon et al., 2007), which could have an impact on acarine-borne disease, causing human (and therefore animal) movement into acarine infested areas (Colwell et al., 2011; Randolph, 2010) and triggering changes to both acarine longevity and their habitat range (Sutherst, 2004).

One line of defence against human and animal acarine-borne disease is avoidance of areas inhabited by acari during their peak periods of activity, and various agencies such as the Centers for Disease Control and Prevention in the USA, the European Centre for Disease Control, and the Health Protection Agency in the UK have produced detailed and easily accessible web-based information to help to educate the public in acarine, and thus acarine-borne disease, avoidance and bite prevention (Online: Centers for Disease control and Prevention 2015b; Online: European Centre for Disease Prevention and Control 2016; Online: Health Protection Agency 2012; Online: World Health Organisation Regional Office for South East Asia, 2016). For example, it is possible to reduce the risk of human exposure to Lyme borreliosis in far western North America, simply by encouraging people to avoid dense woodland, with ground cover dominated by fir needles or leaf litter, between mid-April and mid-June, because this is the peak activity time for nymphs of the tick *Ixodes pacificus* (Clover and Lane, 1995; Eisen et al., 2003; Eisen et al., 2004; Talleklint-Eisen and Lane, 2000). If entry into tick or mite infested areas is unavoidable, an alternative is simple personal avoidance behaviours, for example, sticking close to the centre of trail paths and not wandering into areas covered by tall grass or leaf litter (Online: Centers for Disease control and Prevention

2015b) or the wearing of suitable protective clothing (Piesman & Eisen, 2008; Online: World Health Organisation Regional Office for South East Asia, 2016). However, there is currently little information into how effective such strategies are in reducing the incidence of acarine-borne disease (Mowbray et al., 2012). Furthermore, trying to mitigate the effects of acarine-borne diseases in animals by behavioural changes is not very effective and is not applicable to control of mites affecting crop production. It is therefore important that novel and more effective methods for acarine control are in constant development, including biological control, novel vaccines, RNAi technologies, plant-derived (or natural) chemical acaricides and repellents, and synthetic chemical acaricides and repellents (Dietemann et al., 2012; Kiss et al., 2012; McNair, 2015; Van Leeuwen et al., 2015).

3.4.1 Biological Acarine Control

Biological control has been defined as "the use of an organism to reduce the population density of another organism" (van Lenteren, 2012). For pest mite species in a crop setting, this primarily involves augmenting biocontrol using natural enemies, reared on mass and released into an agricultural/horticultural setting. Such mass production and sale of natural enemies has been in operation for around 120 years and has been successful in fruit orchards, vineyards, cotton fields, maize crops and greenhouses; proving to be an environmentally sound and economically valid method of pest control. This includes biological control of mite pest species (van Lenteren, 2012), which has been used since around 1968 (van Lenteren, 2012). In 2010 it was estimated that 170 species of invertebrate natural enemies were sold worldwide for controlled release to allow the biological control of over 100 crop pest species (Cock et al., 2010). However, despite the availability and successes of this technology, augmented biological control was used on only approximately 0.4% of land under cultivation in 2010 (Cock et al., 2010). This could be due to serval factors, including target specificity of the natural predators; which may seem to be a positive trait, but actually limits return on investment in terms of sales (Barzman et al., 2015; van Lenteren, 2012). Furthermore, most farmers are accustomed to the use of pesticides and may be reluctant to change to an unproven method, with regulations on the

application and collection of biological control agents that can delay or even prevent them from being used (Cock et al., 2010; van Lenteren, 2012).

Biological control can also be achieved using fungal-based acaricides, known as mycoacaricides, which have been in use for many years in crop-pest situations. For example, Mycar, a mycoacaricide based on *Hirsutella thompsonii*, was granted registration for the control of the citrus rust mite, *Phyllocoptruta oleivora*, in the United States in 1981 (de Faria and Wraight, 2007) and entomopathogenic fungi have been used to successfully control many pest-mite species on crops both in the laboratory and in the field (Bugeme et al., 2015; Marcic, 2012; Naik and Shekharappa., 2009; Shi and Feng, 2006; Shi et al., 2008; Ullah and Lim, 2015). Entomopathic fungi have also been used in animal pest-mite control, for example in beehives to control *V. destructor* mites (Kanga et al., 2003; Meikle et al., 2007). However, in this case the beneficial effects of the fungus may be outweighed by negative effects on the bees themselves, namely increased mortality and reduced adult body mass (Hamiduzzaman et al., 2012). Furthermore, two large field trials involving the fungal pathogen *Metarhizium anisopliae* showed no significant *V. destructor* control (James et al., 2006). Recently, conidia of *M. anisopliae* were shown to be effective against eggs of the tick *R. sanguineus* under laboratory conditions (Luz et al., 2016). However, this study used egg clutches of only 25, rather than the thousands seen in a wild clutch, and since efficacy was affected by both concentration and formulation, further investigation would be needed to see if this fungus could be used in the field. *M. anisopliae* and *Beauveria bassiana* have been shown to give 100% mortality against adult *P. ovis* sheep scab mites *in vitro* at temperatures and humidity simulating that of sheep skin (Lekimme et al., 2008) and initial *in vivo* tests showed that both can infect *P. ovis* on a host sheep, with *B. bassiana* giving the highest infection levels. However, in the latter trials, the sheep were housed indoors, so further investigations are required to establish efficacy under outdoor conditions (with their varying levels of UV radiation, rainfall, and humidity) (Abolins et al., 2007). Combining conidia from *B. bassiana* with a desiccant dust was effective against the poultry red mite *D. gallinae* in laboratory testing arenas, although again tests would be needed to show efficacy in both chicken house and free-range situations (Steenberg and Kilpinen, 2014).

There have been several mycoacaricidal products that began registration for use against ticks and mites (de Faria and Wraight, 2007), but at present, although there are mycoacaricidal products marketed as suitable for use against agricultural pest mite species, none are detailed as being suitable for use against mites on animals. Only one that was original marketed as suitable for use in outdoor tick control, Met52®EC, is available to buy from Monsanto BioAg™, although this is no longer stated in the online literature as being suitable for use against ticks and no mention is made of animal mites (Online: Monsanto 2014).

Bacterial toxins have also been investigated for mite control, for example toxins from strains of the bacterium *Bacillus thuringiensis* have been found to be effective as a control agent against *V. destructor* mites in *A. mellifera* hives. With some of the toxins having only a limited toxic effect on the bees at doses 14 times higher than the LD 50 for the mites. However, field trials would be needed to confirm efficacy of this toxin, refining the delivery method and monitoring the wellbeing of any hive undergoing treatment (Alquisira-Ramirez et al., 2014). Proteins from *B. thuringiensis* strain GP532 have also shown an *in vitro* acaricidal effect on the scabies mite *Psoroptes cuniculi*, isolated from New Zealand rabbits, but again field trials of the protein would be needed before it could be seen as a viable treatment option for this form of mange (Dunstand-Guzman et al., 2015).

3.4.2 Vaccination

The use of vaccination in animals against ectoparasite mite species has been trialled (McNair, 2015) and recently a recombinant vaccine, based on a cocktail of seven antigens, has proven effective against *P. ovis* in lambs, giving a reduction in both mite numbers (56%) and lesion size (57%). This may be seen as progress towards a commercial vaccine, which could be developed following the necessary field trials and optimisation of vaccine production (Burgess et al., 2016).

For ticks vaccination against the pathogenic agent causing a tick-borne disease is an alternative option to tick-avoidance, and this has shown some successes. However in

humans, the only tick-borne disease currently controlled by a proven efficacious vaccine, is Tick-borne encephalitis (TBE) (Piesman and Eisen, 2008). There are currently four licenced vaccines available for TBE, FSME-Immun® and Encepur®, used mainly in Europe, and TBE-Moscow® and EnceVir®, used mainly in Russia [Online: World Health Organisation 2011]. Immunization campaigns in Australia between 1991 and 2000 were estimated to have saved the equivalent of 80 million US dollars by reducing costs associated with caring for patients, loss of productivity and premature retirement due to post-infection neurological complications (Online: World Health Organisation 2011). A more recent study showed that the current adult vaccination programme in Slovenia is also cost-effective (Smit, 2012). However, caution should be observed when considering vaccination programmes. The World Health Organisation (WHO) states that cost-effectiveness will be "strongly influenced by the price of the vaccine and by how well the target populations are defined", recommending large scale vaccination only in areas where the disease is highly endemic and that any vaccination should be targeted to at-risk groups in areas where the disease incidence is moderate or low (Online: World Health Organisation 2011).

In stark contrast to the success of TBE vaccines, LYMErix™, the Lyme borreliosis vaccine designed for use in humans, was withdrawn in 2002, after just four years on the market, despite being relatively safe and efficacious (Steere et al., 1998) (Piesman and Eisen, 2008). This was due to several factors including the need for frequent boosters, high cost, exclusion of children from vaccination, fear of vaccine induced Lyme disease like symptoms and litigation related to the vaccine, which compounded to give low sales (Hanson and Edelman, 2003).

In companion animals and livestock, vaccines are available against anaplasmosis, heartwater (ehrlichiosis), babeosis, tropical theileriosis and Lyme borreliosis (Dantas-Torres et al., 2012; Hebert and Eschner, 2010; Marcelino et al., 2012; Schetters, 2005; Suarez and Noh, 2011). As with their human counterparts, these animal vaccinations against the pathogenic agents vectored by ticks have also shown mixed results. For example, in companion animals, vaccinations against Lyme borreliosis and canine babeosis are currently available for dogs. However, these require boosters after one

year and six months, respectively, and in the case of babesiosis, there is little efficacy data available. Therefore, the costs involved in annual or bi-annual vaccination make it more cost effective to use other control measures, such as the application of tick repellents, and overall the current position is that it would be unadvisable to rely on vaccination alone as a means of protecting companion animals against ticks (Day, 2011). Furthermore, although livestock vaccinations against heartwater, tropical theileriosis, anaplasmosis and babesiosis can be successful, most of those currently available vaccines are live, blood-derived, attenuated forms of the pathogen itself (Marcelino et al., 2012) or forms of the pathogen with naturally low pathogenicity (Shkap et al., 2007). This may pose many problems such as the spread of silent pathogens from the blood of culture donors (for example bovine leukaemia virus), the risk of reversion to virulence of the pathogen, uncertainties in standardising the dose, quality control of the vaccine, the maintenance of donor animals which may themselves become reservoirs for ticks, and difficulties in transportation and storage at the end user (Shkap et al., 2007). All of these factors can reduce the efficacy of vaccination programmes against tick-borne diseases in livestock (Marcelino et al., 2012).

There is also the possibility of vaccination against the ticks themselves, to reduce of the vector and hence disease transmission. This is currently done on large scale in cattle against the tick *R. microplus*, using two commercially available vaccines, Gavac™ and TickGARD™, both based on the *R. microplus* gut antigen Bm86 (Kiss et al., 2012). Vaccination with Bm86 triggers antibody production in the host animal, and ingestion of these antibodies damages the feeding ticks (Willadsen, 2001), reducing the number, weight and reproductive capacity of engorged females (Kiss et al., 2012). However, as with vaccination against a tick-vectored pathogen, such vaccination against the ticks themselves shows variable efficacy. For example *R. microplus* Bm86-based vaccines, that elicit protective immune responses against *R. microplus* feeding, vary considerably in their efficacy depending on the genetic variability of the tick and bovine populations. Furthermore, although there is some evidence of cross-protective immunity, an antigen against one type of tick may not provide resistance against another species (Parizi et al., 2012). To serve as a true preventer of tick-borne disease,

anti-tick vaccines must disrupting tick feeding before any pathogen has chance to pass into the host animal. This may require anti-tick vaccines that disrupt tick attachment rather than tick feeding (Piesman and Eisen, 2008).

3.4.3 RNAi Gene Silencing

RNAi gene silencing is an interesting novel method that has been proposed for control of some acari. The technique has been shown to be effective in the crop pest *T. urticae* by using double-stranded (ds) RNA injection to silence the Distal-less gene (Khila and Grbic, 2007). For *V. destructor*, dsRNA has been delivered by injection and immersion of the mites into a dsRNA solution (Campbell et al., 2010) and also by feeding mites on bees which have, in turn, been fed dsRNA (Garbian et al., 2012). The latter trial involved injecting a mixture of dsRNA designed to silence 14 genes in *V. destructor* that are thought to be responsible for fundamental housekeeping functions as well as apoptosis inhibition in mite cells, and gave a 60% reduction in the mite population on the bees, without a significant reduction in bee numbers compared to an uninjected control. Further studies are now needed in the field, to test the effects of dsRNA-treatment in *V. destructor*-infected honeybee colonies. The first step is to find target-genes that have the greatest effect on mite survival with the least amount of dsRNA needing to be fed to the bees (Garbian et al., 2012).

In 2002 RNAi methods proved successful in the tick *A. americanum*, where injection of histamine binding protein (HBP) dsRNA into females gave a reduction in the HBP transcripts (Aljamali et al., 2002). Following this, RNAi was used to silence the subolesin gene in *D. variabilis* (de la Fuente et al., 2006). Subolesin is a highly-conserved protein in tick species that is involved in feeding and reproduction, and its knockdown resulted in a decrease in tick survival and the production of sterile ticks. This has led to the suggestion that the release of subolesin-silenced ticks could be a method for the control of tick populations, as the release of *R. microplus* subolesin-silenced ticks achieved tick-control in cattle populations when used in combination with a cattle-based recombinant subolesin vaccination (Merino et al., 2011).

However, while the release of sterile acari represents a potential approach to tick and mite control, some concerns have been expressed about releasing genetically modified vectors into the environment, and this may prevent further use of the technology (Sparagano and De Luna, 2008).

3.4.4 Plant-Derived Chemical Acaricides

Plants are one of the greatest sources of organic compounds, and many show pesticidal properties; furthermore, they are generally more biodegradable and have reduced environmental effects when compared to synthetics pesticides, and so the anti-parasite (including anti-acari) activity of plant extracts is being increasingly investigated (Flamini, 2006). In fact a large number of products are already in commercial use, for example neem oil (from the neem tree) is reported to have biocidal effects against over 200 species of arthropod pests (Isman, 2006).

Contact acaricidal activity of plant extracts has been shown against a variety of crop plant-infesting mite species including *Tetranychus cinnabarinus* and *T. urticae* (Isman, 2000; Lee et al., 1997; Tunc and Sahinkaya, 1998). Interestingly in the case of *T. urticae*, EcoTrol, a Rosemary oil-based pesticide, not only gave complete pest mortality at concentrations not phytotoxic to the host plant, but also proved not toxic to the predatory mite *Phytoseiulus persimilis* at these concentrations in both laboratory and greenhouse experiments. Offering potential integrated pest management options against this species (Miresmailli and Isman, 2006). Essential oils generally show great promise for use in crop species, as most are volatile and rapidly evaporate from the foliage or degrade due to UV and temperature exposure, minimising residues on food crops (Miresmailli and Isman, 2006). Furthermore, in contrast to certain synthetic insecticides, neither bioaccumulation nor bio-magnification has been reported for any plant-derived pesticides to date and for many mammalian toxicity is low and environmental persistence is short (Regnault-Roger et al., 2012). Many plant-based compounds have toxic, repellent, anti-feedant or growth regulatory effects when used in the laboratory against both tick and mite ectoparasites. However, their efficacy is variable and dependent upon many factors including the target species, species life-

stage, the pest feeding mechanism, the method of extraction of the plant active, the type of solvent used, the time of harvest, and the working concentration (George et al., 2008; Kiss et al., 2012; McNair, 2015).

Although plant-derived products are thought to be less environmentally damaging than their synthetic alternatives, there are worrying opinions that people may falsely believe that naturally-derived products are inherently safe, when in actuality very few of these products have undergone toxicological testing against mammals and non-target organisms (Attia et al., 2013; Shaalan et al., 2005). Furthermore, as field studies have a large cost implication, not least because of the high cost of extraction for plant-derived compounds, a successful active needs to show great promise to progress to reach this stage of testing (Attia et al., 2013; George et al., 2008; Kiss et al., 2012). In particular, great care must be taken when using plant-derived pesticidal products in beehives, as they tend to have broad-spectrum toxicity against arthropods (George et al., 2008).

3.4.5 Synthetic Chemical Acaricides

Synthetic chemical repellents and acaricides are currently the most widely used and effective method of controlling ticks and mites and hence the diseases they vector (Kiss et al., 2012; McNair, 2015; Van Leeuwen et al., 2015).

The following effects can be achieved when using acaricides:

i. Repellency: When the compound causes the tick/mite to move away from an area, plant or animal.
ii. Disruption of attachment to the host: When feeding is prevented by the compound.
iii. Direct kill: A true acaricidal effect.

(Adapted from (Halos et al., 2012)).

Repellents and acaricides can be applied directly to the fur or skin of an animal or human, or applied indirectly by addition to collars, clothing or bedding (Beugnet and

Franc, 2012; Jongejan and Uilenberg, 2004; Katz et al., 2008; Piesman and Eisen, 2008). They can also be sprayed directly onto crop plants (Van Leeuwen et al., 2015). Other methods treat areas off the host, for example, acaricides sprayed onto vegetation in an area-wide attempt to reduce tick-borne diseases (Piesman and Eisen, 2008).

In humans, repellents such as N,N-diethyl-meta-toluamide (DEET) and permethrin-based products, have proven reasonably safe to use and effectively reduce the risk of bites from a variety of species when applied directly to the skin or onto clothing (Carroll et al., 2005; Kumar et al., 1992; Lane, 1989; Pretorius et al., 2003; Schreck et al., 1986; Service, 2012; Solberg et al., 1995). On companion and livestock animals, a wide variety of repellents and acaricides are used including organophosphates, pyrethroids, carbaryl, fipronil, macrocyclic lactones and amitraz, all of which have been shown to be effective against ectoparasites (Beugnet and Franc, 2012; Deplazes et al., 2016; Guerrero et al., 2012; McNair, 2015; Stanneck et al., 2012) and a similarly wide-range of products are licensed for use in crop plant protection (Van Leeuwen et al., 2015).

The widespread use of acaricides has led to the development of resistance in many acari worldwide, leading to a real concern that the armoury of effective compounds will be exhausted unless concerted action is taken to develop new products and reduce the spread of resistance (McNair, 2015; Rinkevich et al., 2013; Van Leeuwen et al., 2015; Van Leeuwen et al., 2010a). Acaricide resistance to multiple compounds is seen in several agriculturally and economically important acari, including the two-spotted spider mite *T. urticae* (a costly pest of a wide range of outdoor and protected crops), *S. scabei* (the causative agent of scabies in animals), the Southern cattle tick *R. microplus*, the red poultry mite *D. gallinae*, and *V. destructor* (a major threat to food security due to its parasitism of honey bees) (Reviewed in (McNair, 2015; Van Leeuwen et al., 2015; Van Leeuwen et al., 2010a)). The development of new resistance-management strategies, to prolong the use of existing synthetic acaricidal compounds, and the design of novel synthetic acaricides has therefore become a critical area of study in recent years (Davies et al., 2007; O'Reilly et al., 2014; Van Leeuwen et al., 2015).

3.5 Pyrethroid Pesticides and the Arthropod VGSC

3.5.1 Pyrethroid Discovery and Development

A major component in acarine control is the use of the pyrethroid pesticides (Deplazes et al., 2016; McNair, 2015; Rinkevich et al., 2013; Van Leeuwen et al., 2015; Van Leeuwen et al., 2010b). Synthetic pyrethroids were first introduced in the 1970's and represented a new class of environmentally friendly, highly effective and selective insecticides. At the time it was introduced, the pyrethroid deltamethrin was the most effective insecticide on the market, being 100 times more active than DDT without the same bioaccumulation problems (Khambay and Jewess, 2005).

Pyrethroids are the synthetic analogues of naturally occurring compounds found in the flowers of plants of the *Chrysanthemum* genus. The dry flowers were probably used as insecticides in ancient China as early as the 1st Century AD, and by the middle Ages they were being used for pest control in Persia. They arrived in Europe around 200 years ago, where they were traded as "Persian dust" (Davies et al., 2007). The insecticidal compounds within the *Chrysanthemum* flowers are esters of chrysanthemic acid (pyrethrins I) and pyrethric acid (pyrethrins II) and the alcohol moiety of the pyrethrins exists as three natural varieties, so that the complete pyrethrin series is pyrethrin I and II, jasmolin I and II and cinerin I and II (Casida, 1980). Pyrethroid insecticides were commercially produced from *Chrysanthemum* flowers in the mid-19th Century, with the main active ingredients being pyrethrins I and II (Figure 1). However, these compounds show low photostability and were costly to produce. There followed a period of structural modification of the pyrethrin series to produce the first synthetic pyrethroids, and between 1967 and the late 1980's many highly insecticidal, photostable, compounds with low mammalian toxicity were synthesised; including permethrin, cypermethrin and deltamethrin (synthesised by Elliot and co-workers at Rothamsted Research, England) and fenvalerate (synthesised by the Sumitomo Chemical Company, Japan) (Casida, 1980; Khambay and Jewess, 2005).

Pyrethroids are divided into two groups based on both their biological action and their chemical structures. Type I pyrethroids are generally good 'knockdown' agents (they incapacitate rapidly, but relatively high concentrations are needed to kill an arthropod) and Type II pyrethroids are generally good killing agents (being slower acting than Type I pyrethroids, but killing arthropods at lower concentrations) (Elliott, 1989; Soderlund, 2012). The differing symptoms seen with Type I and Type II pyrethroids have been associated with an α-cyano group at the α-benzylic position in Type II; however, the presence of this group does not always lead to increased kill at a lower concentration, so it is likely that Type I and Type II represent extremes of a spectrum of activity, from knockdown to kill, rather than discrete groups (Khambay and Jewess, 2005) (Figure 3.1).

Figure 3.1: Pyrethrins I and II and Exemplar Type I and II Pyrethroids

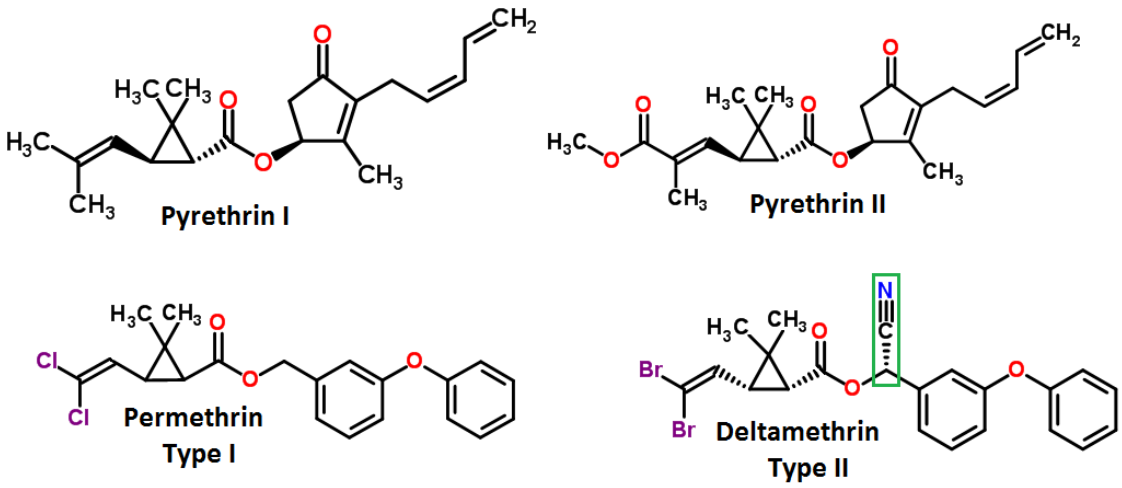

Pyrethrins I and II are shown to illustrate their structural similarity to the modern synthetic pyrethroids, Permethrin and Deltamethrin. Permethrin is an example of a Type I pyrethroid and Deltamethrin an example of a Type II pyrethroid. The α-cyano group found in Type II pyrethroids is highlighted on Deltamethrin by a green box. All structures are adapted from ChemSpider 2016.

3.5.2 Expression of VGSCs

The target-site for pyrethroid action is the voltage-gated sodium channel (VGSC) of the arthropod nervous system (Vais et al., 1997; Williamson et al., 1993a; Williamson et al., 1993b). Like all ion channels, VGSCs are macromolecular proteins that form pores in cell membranes, and form one of the excitable elements in nerve cells allowing for the

propagation of nerve impulses (Hille, 2001). The first arthropod VGSC gene was cloned from *Drosophila melanogaster*, and was named *para* based on temperature-sensitive paralytic mutations (Loughney et al., 1989). Since then *para*-orthologous VGSC genes have been found in a wide-range of arthropod species (Rinkevich et al., 2013).

In mammals, nine genes are thought to be responsible for the coding of distinct VGSC α-subunits with different gating properties, this allows differential expression of VGSCs to fulfil unique physiological roles in different cell types, tissues, and developmental stages; however, in those arthropods sequenced to date only one functional VGSC is encoded from one gene (Catterall, 2012; Dong et al., 2014; Goldin, 2001). Thus in arthropods extensive RNA splicing and RNA editing are employed on VGSC transcripts to give a variety of channels with distinct gating properties (Du et al., 2009b; Lin et al., 2009; Liu et al., 2004; Olson et al., 2008; Song et al., 2004; Tan et al., 2002). RNA splicing in arthropod VGSC genes was first shown in the *para* (or $DmNa_V$) gene in D. melanogaster (Loughney et al., 1989; Thackeray and Ganetzky, 1994, 1995). It has since been shown that splicing sites are conserved in the VGSC genes of several other arthropods including: *Blattella germanica* (German cockroach), *Bombyx mori* (Silkworm), *Heliothis virescens* (Tobacco Budworm), *Musca domestica* (House Fly), and *Plutella xylostella* (Diamondback moth) (Lee et al., 2002; Park et al., 1999; Shao et al., 2009; Sonoda et al., 2006; Tan et al., 2002). Further VGSC transcript modification, in the form of RNA editing, has so far been found in VGSC transcripts from *D. melanogaster* (Hanrahan et al., 2000; Olson et al., 2008) and *B. germanica* (Liu et al., 2004; Song et al., 2004).

3.5.3 VGSC Structure and Function

The VGSCs of arthropods are highly homologous to mammalian VGSC α-subunits; being comprised of 4 internally homologous domains (DI-DIV), each comprising 6 membrane-spanning segments (S1-S6) connected by intracellular linkers (Noda et al., 1984). To make the functional channel, the S5 and S6 segments of each of the four domains come together to form a central ion-conducting pore, whilst the S1-S4 segments form the voltage-sensing part of the channel (Figure 3.2).

Figure 3.2: A Representative VGSC

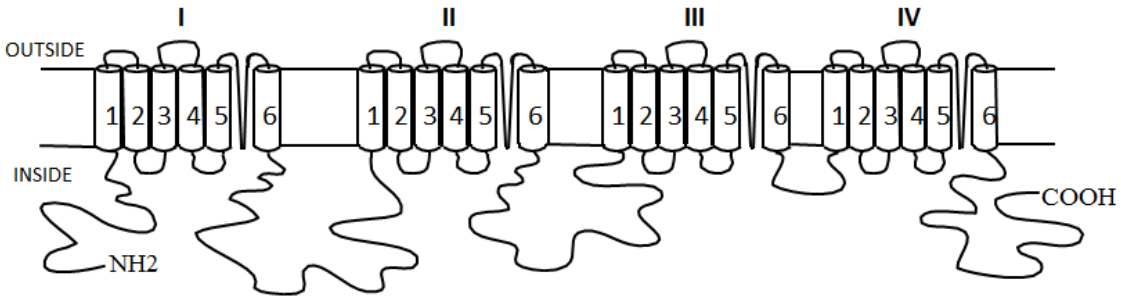

An exemplar VGSC showing domains I-IV and their six membrane-spanning domains (1-6).

The voltage sensor for the channel is comprised of repeating motifs of a positively charged amino acid residue, followed by two hydrophobic residues that are found in each S4 segment. Hairpin loops between the S5 and S6 segments form a narrow ion-selective filter at the extracellular end of the pore, within these loops sodium ion selectivity is determined by the amino-acids D, E, K and A in analogous positions in domains I, II, III, and IV respectively (a sequence known as the “DEKA” motif). The intracellular loop between DIII S6 and DIV S1 contains the amino-acid motif “IFM” in mammalian cells or “MFM” in arthropods, and this creates an inactivation gate, critical for fast inactivation of the channel and facilitating the refractory period required between action potentials. (Dong et al., 2014; Hille, 2001; McCusker et al., 2012; O'Reilly et al., 2006; Payandeh et al., 2011). The availability of crystal structures from bacterial homologues of VGSCs, in both open and closed conformations, suggest that the mechanism for channel gating primarily involves the C-terminal end of the S6 helices. Here a rotation around the backbone angle of one amino-acid residue in the middle of S6 helices swings those subunits away from the central pore, thus opening up the bottom of the VGSC allowing fully-hydrated sodium ions to traverse (McCusker et al., 2012) (Figure 3.3).

Figure 3.3 VGSC Structure

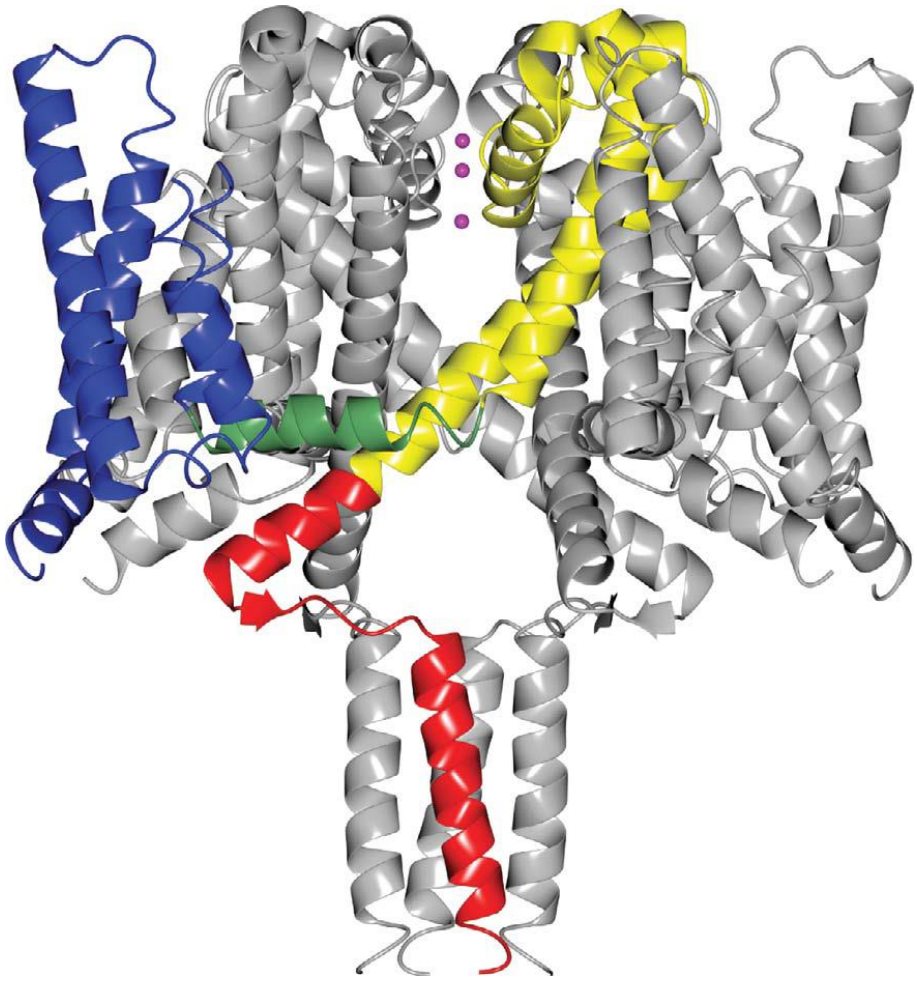

Ribbon "cartoon" representation of the open crystal structure of the heterotetrameric *Magnetococcus marinus* NavMs VGSC as viewed from the membrane. This channel is structurally homologous to arthropod VGSCs. One monomer is coloured to show: The voltage sensor (blue), the S4–S5 linker (green), the pore helices (yellow), the C-terminal domain (red), and sodium ions entering the channel (purple). The other three monomers are depicted in grey, for ease of viewing. Kindly provided for this work by Professor Bonnie Wallace.

Alongside the pore-forming VGSC α-subunit, mammalian sodium channels have one or more auxiliary subunits, known as β-subunits. These small transmembrane proteins are known to modulate activity of the mammalian VGSC (Brackenbury and Isom, 2011; Catterall, 2012). Similarly, insect VGSCs are also known also have both pore-forming and auxiliary subunits, the TipE and TEH protein in *D. melanogaster* and their orthologues in other insects, which are functionally homologous to the β-subunits in mammals (Dong et al., 2014). However, interestingly in acari any such auxiliary proteins have yet to be discovered (Li et al., 2011).

Vertebrate NaV_1 VGSCs show selectivity for sodium over potassium with permeability ratios ranging from 12-21, while potassium channels select potassium over sodium by a ratio of 100-1000 (Hille, 2001; Lim and Dudev, 2016). Thus, these channels allow the selective, directional, movement of these two ions across the cell-membrane of axon, making them critical in maintaining the normal functioning of an animal's nervous system by allowing the propagation of action potentials (Campbell et al., 2015) (Figure 3.4).

Figure 3.4: Representation of an Action Potential in a Nerve Cell Axon

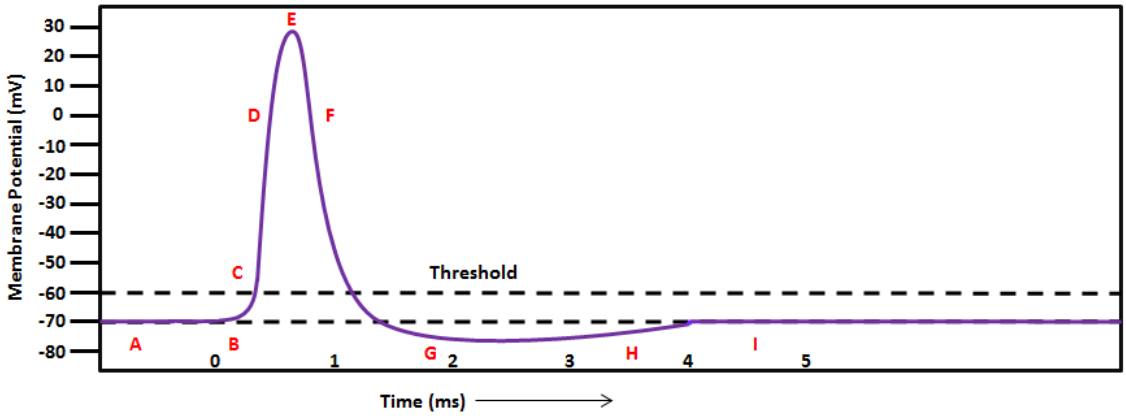

A: Membrane is at resting potential of -70mV. Voltage gated sodium channels are in a closed resting state.

B: A depolarising stimulus arrives.

C: Depolarising stimulus causes the membrane to depolarise to the threshold. Voltage gated sodium channels open to give their active state and Na^+ ions enter the cell. Voltage gated potassium channels slowly open.

D: The rapid entry of Na^+ ions depolarises the cell. Giving the rising phase of the action potential.

E: Voltage gated sodium channels close and inactivate. Potassium channels continue to open.

F: K^+ ions move out of the cell into the extracellular fluid.

G: K^+ ions continue to leave the cell hyperpolarising it.

H: Voltage-gated potassium channels close and some K^+ ions return into the cell through leak channels.

I: Resting membrane potential is restored. Voltage-gated sodium channels return to closed resting state (via their deactivated state).

A representation of changes in neuronal axon membrane potential elicited by a stimulatory nervous impulse (action potential).

VGSCs are thought to exist in four states mediated by two defined "gates", the activation gate and the inactivation gate. At the resting membrane potential, the VGSC is in a closed resting state; the activation gate (the channel pore) is closed, but the inactivation gate (the linker region between Domains III and IV at the intracellular base of the channel pore) is open and not blocking the pore. In response to a graded depolarisation in a dendrite or cell body, the channel undergoes a structural change to

give an open, or activated, state allowing a selective influx of sodium ions through the pore (McCusker et al., 2012). After a short delay the inactivation gate occludes the pore mouth and the channel forms the inactivated state, which is followed by a fourth state, the deactivated state, when the pore is closed at both the activation and inactivation gates. Once the membrane has returned to resting potential the inactivation gate moves away from the intracellular pore mouth and the channel is returned to the closed resting state, ready for another action potential (Figure 3.5) (Wakeling et al., 2012).

Figure 3.5: The Four States of the VGSC

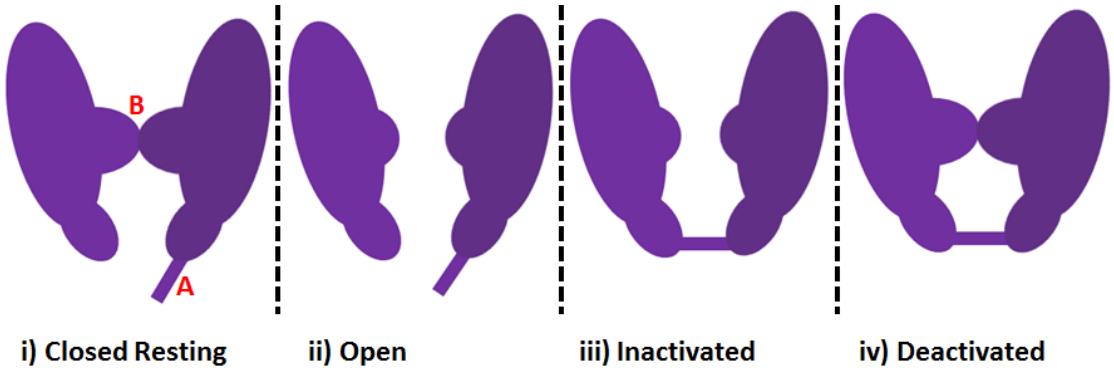

A diagrammatic representation of the four states of the VGSC: i) Closed resting, ii) Open, iii) Inactivated, iv) Deactivated. Where A) indicates the inactivation gate and B) indicates the activation gate.

3.5.4 Pyrethroid Action at the Arthropod VGSC

To allow normal propagation of an action potential, VGSCs must transit between the four transition states: i) “closed resting”, ii) “open” iii) “inactivated” and iv) “deactivated” and toxins may act by altering the equilibrium between the transition states and thus disrupt normal nerve signalling (Catterall, 1980). It is proposed that pyrethroids bind to arthropod VGSCs at a specific site; speculated to be a long, narrow, hydrophobic cavity bounded by the DIIS4-S5 linker and the DIIS5 and DIII S6 helices (Davies et al., 2008; O'Reilly et al., 2006). Upon binding, pyrethroids lock arthropod VGSCs in the open conformation causing prolonged current flow through the channel, resulting in repetitive firing of nerve impulses, hyper-excitability and/or death (Wakeling et al., 2012; Zlotkin, 1999) (Figure 3.6).

Figure 3.6: Exemplar Effect of Pyrethroids Generating Persistent Current in Arthropod VGSCs

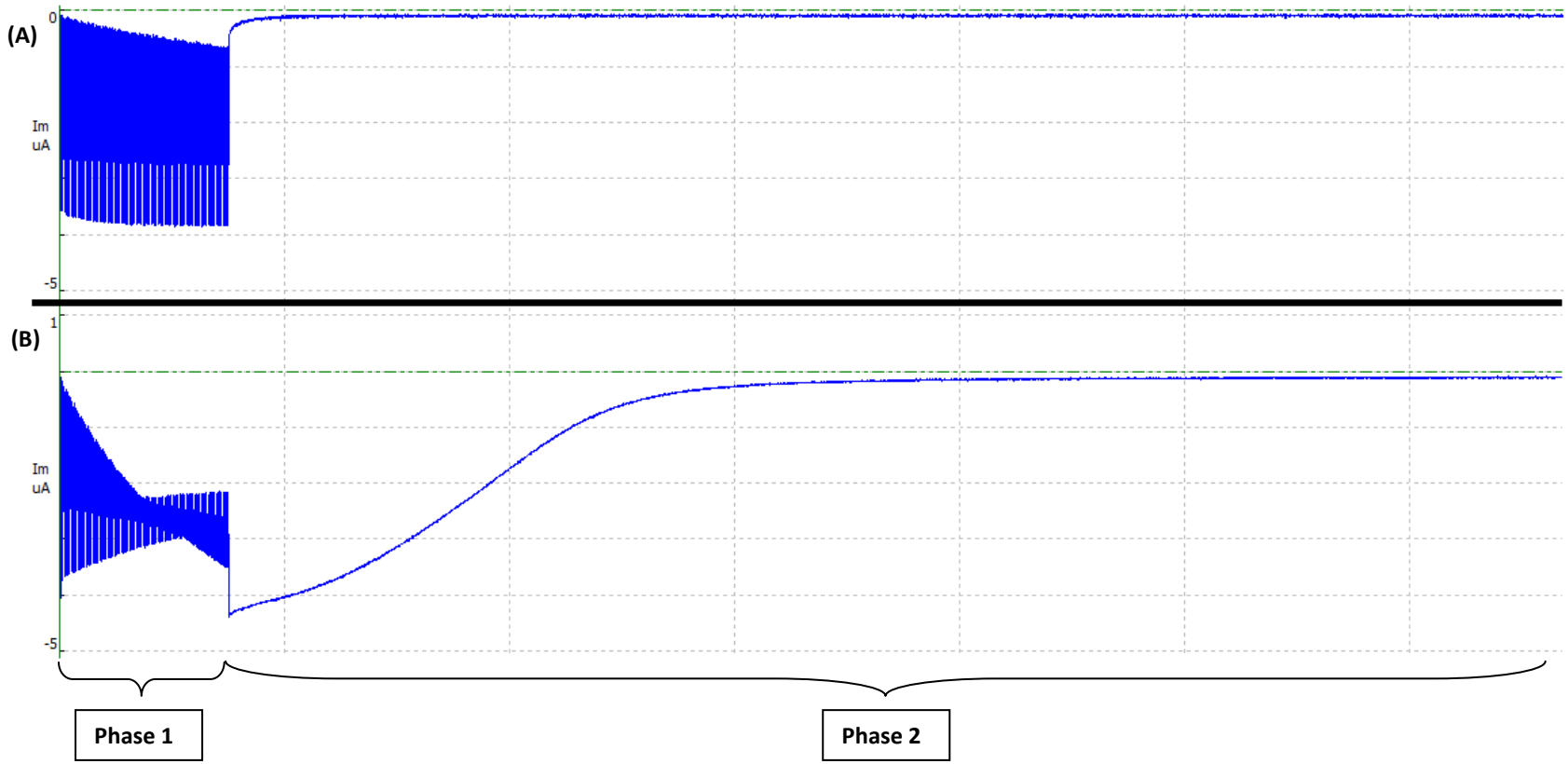

The effect of pyrethroid pesticides on arthropod VGSCs as exemplified by Deltamethrin. The persistent current recorded from the *V. destructor* VGSC using Two-Electrode Voltage Electrophysiology in a *Xenopus laevis* oocyte. Voltage across the oocyte membrane has been manipulated such that: (Phase 1) Expressed VGSCs would undergo a period of rapid opening and closing events, allowing pyrethroid binding while VGSCs are in their open conformation. (Phase 2) All VGSCs should be closed and current flow should be zero. Any persistent current in this second phase is due to VGSCs within the oocyte membrane being held open. Persistent current flow through the VGSC population in the oocyte is shown in the presence of (A) No pyrethroid and (B) 1 µM Deltamethrin.

The success of pyrethroids as insecticides results mainly from the relative insensitivity of the mammalian VGSC to these compounds (Khambay and Jewess, 2005), which can be explained, at least in part, by differences in channel structure. Mammalian VGSCs differ from those found in arthropods by the presence of an isoleucine, rather than a methionine, in the DIIS4-S5. The absence of this methionine in mammalian channels would prevent the formation of a key sulphur-aromatic interaction with pyrethroids, rendering them relatively insensitive to the compounds (Davies et al., 2008; O'Reilly et al., 2006). This effect is enhanced as pyrethroids preferentially target the open state of arthropod VGSCs, accessing their binding site through fenestrations in the VGSC that are much larger when the channel is activated (Bloomquist, 1996; McCusker et al., 2012) (Figure 3.7).

Figure 3.7: VGSC Structure and Pyrethroid Binding

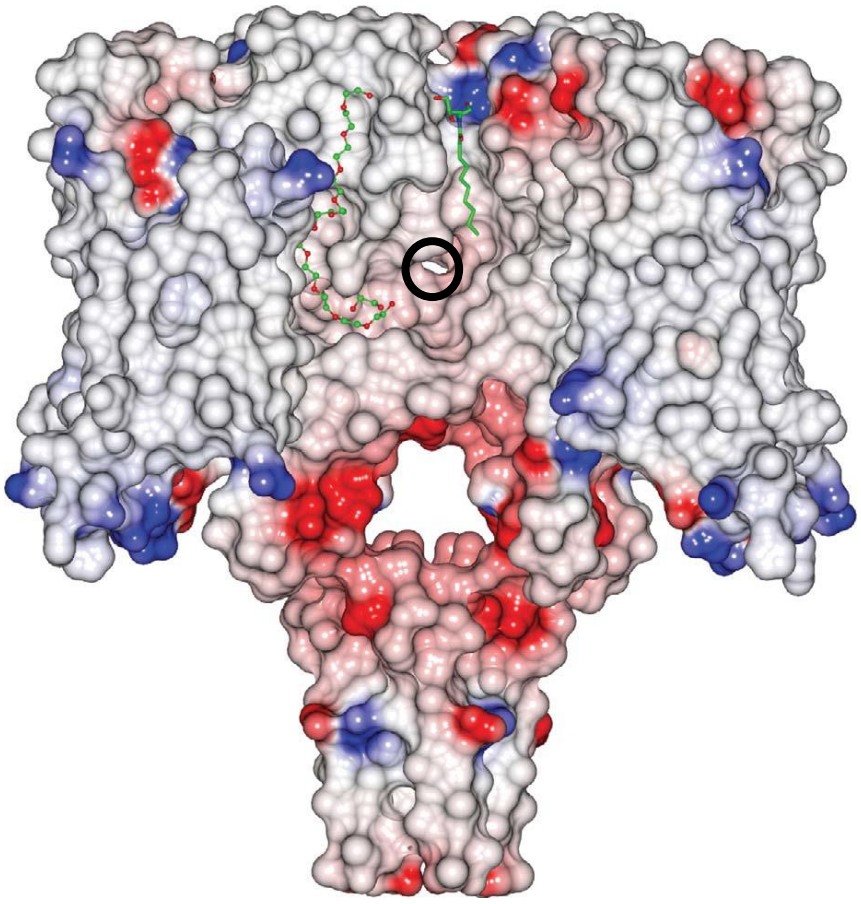

Space filling model (coloured according to electrostatics) of the open crystal structure of the *M. marinus* NavMs tetrameric channel as viewed from the membrane. This channel is structurally homologous to arthropod VGSCs. The locations of detergent and polyethylene glycol molecules are shown on the surface in green and red stick format. The location of the fenestration leading to the hydrophobic cavity, which pyrethroid insecticides could enter for binding in homologous arthropod VGSCs, is circled in black. Kindly provided for this work by Professor Bonnie Wallace.

3.5.5 The VGSC and Pyrethroid Resistance in Arthropods

Extensive use of pyrethroids around the globe has led to widespread resistance to these compounds amongst target species, including ticks/mites. Such resistance arises through modifications to the target site protein, increased metabolism or sequestration of the acaricide, or a reduction in the ability of the acaricide to penetrate the tick exoskeleton (Guerrero et al., 2012). Pyrethroid insensitivity based on target site resistance (mediated by mutations in the gene encoding the VGSC) is of particular importance to both acarine and insect control (Williamson et al., 1996). A comprehensive review of the many VGSC target-site mutations thought to be associated with pyrethroid resistance in insects and acari can be found in (Rinkevich et al., 2013).

Pyrethroid target-site resistance, termed *knockdown resistance (kdr)* (Busvine, 1951), has several forms including the more potent *super-kdr* variants, which confer up to 500-fold resistance to Type II pyrethroids (Sawicki, 1978). Modelling of the VGSC with pyrethroids has suggested that several of the mutations conferring *super-kdr* are located within a putative binding pocket, whilst further *kdr*-associated mutations, found away from the proposed binding site, are in positions which may contribute to changes affecting channel kinetics and therefore pyrethroid binding (Davies et al., 2007; Davies et al., 2008; O'Reilly et al., 2006).

For ticks, three point mutations conferring amino acid substitutions have been associated with target-site pyrethroid resistance *R. microplus*; the first in Mexico (He et al., 1999) and the others in Australia (Jonsson et al., 2010; Morgan et al., 2009) (Table 3.1). Pyrethroid resistance has also been reported in *Rhipicephalus sanguineous*, although this has not been associated with target site changes (Eiden et al., 2015; Miller et al., 2001).

Table 3.1: VGSC Substitutions in *R. microplus*

Domain	Segment	Amino Acid Substitution	Reference Code
III	S6	Phe-Ile	F1538I
II	S4-5 LINKER	Leu-Ile	L925I
II	S4-5 LINKER	Gly-Val	G933V

Summary of amino acid substitutions detected in the VGSC channel and associated with pyrethroid resistance in *R. microplus*. Reference code numbering comes from alignment with *M. domestica*.

In mites pyrethroid resistance is relatively common, with many important species reported to have target site substitutions (Table 3.2) (Gonzalez-Cabrera et al., 2013; Van Leeuwen et al., 2010a).

Table 3.2: VGSC Substitutions in Important Mite Species

Affected Organism	Domain	Segment	Amino Acid Substitution	Reference Code
V. destructor	II	S5	Leu-Val	L925V
T. urticae	II	S6	Leu-Val	L1024V
T. urticae	II-III	S6-S1 LINKER	Ala-Asp	A1215D
V. destructor	III	S6	Phe-Leu	F1528L
S. scabiei	III	S6	Gly-Ala	G1535A
T. urticae	III	S6	Phe-Ile	F1538I
V. destructor	III-IV	S6-S1 LINKER	Leu-Pro	L1595P
V. destructor	IV	S5	Ile-Val	I1752V
V. destructor	IV	S6	Met-Ile	M1823I

Summary of amino acid substitutions detected in the VGSC channel and associated with pyrethroid resistance in some economically important mite species. Reference code numbering comes from alignment with *M. domestica*.

3.5.6 Pyrethroids as Acaricides

Although the pyrethroids were developed first as insecticides, some are reported to be more effective at killing acari than they are at killing insects. This offers the possibility of selective control of acari without damaging beneficial insects (species of environmental and/or human importance). For example, the pyrethroid Tau-

Fluvalinate is used against *V. destructor* mites in *A. mellifera* (honey bee) colonies, as it can kill the mites without affecting the bees (Gonzalez-Cabrera et al., 2013).

Investigations into why some pyrethroids show specificity for acari over insects have suggested that it is due to differences between their VGSCs. Modelling studies by O'Reilly *et al* in 2014 suggested that the interaction between pyrethroids and the VGSC involves the amino acid at position 933 (*M. domestica* numbering is used throughout). Pyrethroids with selective acaricidal activity differ from other pyrethroids by having large halogenated substituents in their acidic moiety, which it is proposed, could be accommodated by acarine channels with the smaller glycine/alanine at position 933 but not by insect channels with the larger cysteine residue (O'Reilly et al., 2014).

This view is supported by the finding of a mutation in the VGSC of Australian cattle ticks, which leads to a replacement of the normal glycine at residue 933 with a valine; ticks with the valine are sensitive to cypermethrin, which has a comparatively small acidic moiety, but resistant to flumethrin, which has a comparatively large acidic moiety (Jonsson et al., 2010). The O'Reilly *et al* 2014 model suggests that the slightly larger valine residue would preclude binding of the acarine-specific flumethrin, but allow the binding of cypermethrin, with the smaller acidic moiety (O'Reilly et al., 2014) (Figure 3.8).

Figure 3.8: Example Pyrethroids with Large and Small Acidic Moieties

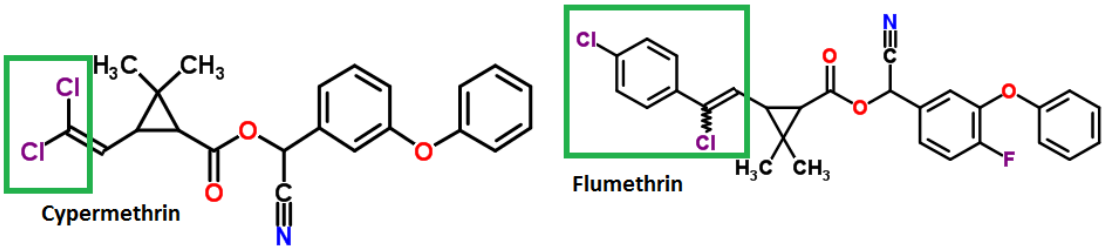

Cypermethrin and flumethrin shown as examples of pyrethroids with relatively small and large acidic moieties. Areas of interest within the acidic portion are highlighted by green boxes. Both pyrethroid structures are from ChemSpider 2016.

3.6 Electrophysiological Methods to Study VGSC Activity

In 1881 Sidney Ringer showed that a solution containing sodium, potassium, and calcium ions was required to keep a frog's heart beating, thus creating "Ringer's Solution". Since then, it has been understood that ions play a role in the functioning of the nervous system (Hille, 2001). However, it was in the period from 1935-1952 when classical biophysics established the ionic theory of membrane excitation, showing that ion permeability changes were responsible for the electrical signals seen in the nervous systems of animals (Hille, 2001). Today we can use techniques developed during this period to study how ion channels function.

3.6.1 Two Electrode Volt Clamp (TEVC) Electrophysiology

In 1982 Ricardo Miledi and co-workers successfully expressed nicotinic acetylcholine receptors (nACHRs) in oocytes from *Xenopus laevis* (the African clawed frog) by injecting nACHR mRNA isolated from cat muscle, allowing study of the changing currents that arose across the oocyte membrane due to expression of the protein (Miledi et al., 1982). The same group then went on to study more than a dozen different ion channels and receptors, injecting mRNA isolated from various tissues. When cloning of receptors and channels became possible, the *X. laevis* oocyte system allowed single cDNAs encoding specific channels to be expressed and compounds with selectivity for specific receptor subtypes or channels to be identified (Papke and Smith-Maxwell, 2009). The relatively large size of the *X. laevis* oocyte (1mm diameter on average) makes them easy to handle, and their very low levels of endogenous channels and receptors makes it possible to study currents arising from expressed exogenous channels (Goldin, 2006). This is particularly pertinent for tests involving pyrethroid pesticides, which are known to be able to bind to other channels besides VGSCs (Casida et al., 1983; Khambay and Jewess, 2005). The basic method of TEVC electrophysiology can be used to study VGSCs, which are exogenously expressed in oocytes following micro-injection of cloned RNA (Section 7.2.7). In this system, the oocyte is placed in the middle of a recording chamber filled with a conductive solution known as Xenopus Ringer, based on the original solution made by Sidney Ringer in

1881 (Hille, 2001). The chamber is connected via a conductive bridge to an input on an amplifier, also connected to the amplifier are two microelectrodes and these are carefully inserted into the oocyte. One is used to measure the membrane-potential of the oocyte membrane by recording the internal voltage of the oocyte relative to the experimental chamber, and the other is configured to inject a current into the oocyte (Dascal, 2001; Goldin, 2006; Papke and Smith-Maxwell, 2009). If the experimental chamber is considered "zero" in terms of electrical potential, it is possible to set the voltage across the oocyte membrane by adjusting the amount of current injected, thus "clamping" the oocyte at a desired membrane potential. For example, the typical resting membrane potential of a *X. laevis* oocyte is between -10 and -40 mV, the typical resting potential of a nerve axon is around -70mV. Therefore, clamping an oocyte injected with a VGSC at -70mV will mimic the conditions found in the axon of a nerve cell at rest. Any alterations of the set voltage will trigger responses in the exogenous VGSCs in line with those seen in their native cell (Hille, 2001).

3.6.2 Studying Pyrethroids and VGSCs Using TEVC Electrophysiology

Since the *D. melanogaster para* VGSC was first functionally expressed in *X. laevis* oocytes (Feng et al., 1995) it has been possible to use this channel as a model to study the effects of target-site mutations suspected of conferring pyrethroid resistance. As described, pyrethroids act by stabilising the VGSC in the open "activated" conformation and causing repetitive firing of action potentials via a continuous flow of sodium ions into the intracellular matrix (Catterall, 2000; Vais et al., 1997; Zlotkin, 1999). This can be observed using TEVC electrophysiology whereby the application of a pyrethroid results in wild-type *D. melanogaster para* channels showing a delay in returning from an open "activated" to a closed "inactivated" state. This is seen as an increase in the amount of current needed to restore the membrane potential from one in which the channels would be mostly open, to a more-negative potential at which the channels would be mostly closed, and the period over which this channel inactivation occurs. In channels containing an amino acid substitution that confers pyrethroid resistance, this delayed closure is no longer observed, and channels return more rapidly to a closed state (Vais et al., 2000b; Warmke et al., 1997).

3.7 Aims and Objectives

From the background described in the introduction to this work there is a clear need for good control of acari, and to date the pyrethroids have played an important role in this. However, there are now concerns over resistance developing to these compounds presenting a need to understand more about their mode of action and any potential acarine selectivity.

The study reported here set out to understand the interactions of acaricides with the VGSCs of arthropods to elucidate efficacy levels and any acarine specificity.

The specific objectives of this work were:

- To identify known or novel mutations in the VGSC sequences of different acarine species that confer resistance to pyrethroids, to inform effective pest management strategies (Chapter 5).

- To attempt to fully sequence and clone a tick VGSC for expression in X. laevis oocytes (Chapter 6).

- To examine the molecular interactions of pyrethroids at amino acid position 933 of arthropod VGSCs, postulated by O'Reilly *et al* 2014 to contribute to the increased activity and selectivity of certain pyrethroids at acarine VGSCs compared to closely related insect VGSCs (Chapter 7).

- To look at the *in vitro* toxicity of acaricides on live arthropods to examine the accuracy of reported pyrethroid selectivity in insects and acari (Chapter 8).

4 General Experimental Methods

Unless otherwise stated all protocols were performed at room temperature (20-25°C). All methods in this chapter are adapted from standard protocols as found in "Molecular Cloning: A Laboratory Handbook" by Sambrook and Green, 2012.

4.1 Source Organisms

Tick species were obtained via Andreas Turberg and Melania Akkoese at Bayer Animal Health, Monheim, Germany. Bayer Animal Health sources tick species as follows: *Amblyomma americanum* (lone star tick) from Oklahoma State University, Stillwater, Oklahoma, USA; *Amblyomma hebraeum* (bont tick) from the Bayer Animal Health Breeding Lab, Monheim, Germany (Origin: Understepoort Isolate, South Africa), *Ixodes ricinus* (castor bean tick) and *Dermacentor reticulatus* (ornate cow tick) from Insect Services, Berlin, *Rhipicephalus microplus* (cattle tick) Parkhurst strain from the Bayer Animal Health Breeding Lab, Monheim, Germany (Origin: Parkhurst Isolate, State of Queensland Department of Primary Industries and Fisheries, Queensland, Australia), *Rhipicephalus sanguineous* (brown dog tick) and *Dermacentor variabilis* (American dog tick) from EL LABS, Soquel, California, USA.

Mite species were obtained from a variety of sources. *Dermanyssus gallinae* (red poultry mite) was obtained from Melania Akkoese Bayer Animal Health, Monheim, Germany. *Psoroptes ovis* (sheep scab mite) RNA was a gift from Dr Stuart Burgess at the Moredun Research Institute, Scotland, UK. For bioassays *Varroa destructor* (honey-bee mites) were taken from bees at The Honey Farm, Imkerei Ullmann, Erlensee, Germany. The RNA source for *V. destructor* VGSC cloning was from mites collected by Pete Kennedy from the DL colony at the Rothamsted Research farm, Harpenden, England.

The insect species *Musca domestica*, strain WHO(N), was bred at Bayer Animal Health, Monheim, Germany.

All species were known to be pyrethroid susceptible, with the exception of *R. microplus* (Parkhurst) ticks, which had previously been described as pyrethroid resistant (Morgan et al., 2009; Nolan et al., 1989); and *V. destructor* mites, which were untested for their susceptibility to pyrethroids.

4.2 Agarose Gel Electrophoresis

Agarose gels were used to check the size and quality of nucleic acid samples. Gels were made by dissolving molecular biology grade agarose (ThermoFisher Scientific) in 1 x TAE (Tris-acetate-EDTA) buffer (pH8.3) at an appropriate percentage of agarose for the size of the nucleic acids being visualized (See (Sambrook and Green, 2012)) before the addition of Ethidium Bromide to a final concentration of 0.4 µg/ml. The mixture was then poured into a gel mould and combs added to create wells into which nucleic acid samples could be loaded. Once set gels were placed into electrophoresis tanks and submerged in 1 x TAE buffer (pH8.3). Nucleic acid samples were mixed with an appropriate loading dye and added into the wells alongside a DNA size ladder (ThermoFisher Scientific), to allow size estimation of nucleic acid strands (bands). RNA samples were first denatured by heating to 65°C for five minutes in RNA loading dye. Samples were run through the gel by the application of an electrical current until sufficient separation of bands had occurred as would allow size differention. Bands were visulaised, such that quality and size could be estimated, using the Gene Genius Bio-imaging System (Syngene).

4.3 Extraction of Total RNA from Ticks and Mites

Total RNA was extracted from whole ticks/mites using the Bioline Isolate RNA Mini Kit, using half the manufacturers recommended volumes of reagents. When RNA was extracted for the purpose of whole species VGSC sequencing several individuals were used per reaction to increase RNA yield; however, RNA was isolated from a single arthropod when it was required for assertaining the pyrethroid resistance status of an individual. Filter tip pipettes were used throughout the extraction process to reduce the likelihood of RNase contamination and sample degradation and to prevent cross-

contamination. Acari were placed into 1.5 ml microcentrifuge tubes and snap frozen in liquid nitrogen at the point of collection, then immediately stored at -80°C to limit RNA degradation. When removed form storage each sample was transferred to a 1.5 ml microcentrifuge tube and the tubes floated in liquid nitrogen for 1 minute; the samples were then ground to a powder until complete breakage of the exoskeleton was achieved, using sterile plastic pestles that had been pre-chilled by dipping in liquid nitrogen. The tubes were then placed at room temeperature and 225 µl of lysis buffer R was added, they were then further homogenised with the pestle to ensure adequate cell lysis. Samples were then cetnrifuged for 1 minute with a relative centrifugal force (RCF) of 16168 x g and the resulting supernatant carefully pipetted onto R1 spin columns that had been placed over sterile 1.5 ml microcentrifuge tubes. Samples were then were centrifuged at room temperature for 2 minutes at 10037 x g, R1 spin columns were discarded, and 1 volume (~200 µl) of sterile (microfiltered) 70% ethanol was added to the resulting filtrates. Mixtures were vortexed briefly, before being carefully pipetted to labelled R2 spin columns placed over fresh sterile 1.5 ml microcentrifuge tubes and then centrifuged for 2 minutes at 10037 x g. Microcentrifuge tubes were discarded and R2 spin columns were placed over fresh 1.5 ml microcentrifuge tubes and 500 µl wash buffer AR was added to the R2 columns. Samples were centrifuged for 2 minutes at 10037 x g, the filtrate discarded, and 700 µl wash buffer BR added to the R2 columns. Samples were centrifuged again for 2 minutes at 10037 x g and again the filtrate was discarded. This centrifugation step was repeated to ensure that all wash buffer was removed from the R2 columns. R2 columns were then placed over fresh sterile 1.5ml microcentrifuge tubes and 30 µl of nuclease-free sterile distilled water was added to the centre of each R2 column to elute acarine RNA. Columns were incubated at room temperature for 1 minute then centrifuged for 2 minutes at 10037 x g. The RNA concentration of each sample was determined using a Nanodrop spectrophotometer (ThermoScientific) and a small amount (apporximately 500 ng each smaple) was run on a 1.5% agarose electrophoresis gel to check the quality of the extracted RNA (See Chpater 4.2). All RNA samples were stored at -80°C.

4.4 Reverse Transcription of RNA

Reverse transcription of RNA into cDNA was done using the RevertAid Premium First Strand complementary DNA (cDNA) Synthesis Kit (ThermoFisher Scientific). All centrifugation steps were at 4°C in a table top centrifuge. Specific primers were diluted to 100 ng/µl immediately prior to use. To begin cDNA synthesis 0.5 µl oligo dT primer, 0.5 µl 10 mM dNTP mix and 0.1 µl of each gene specific primer were mixed on ice in 0.25 ml thin-walled microcentrifuge tubes. The gene specific primers used in each case were 1147R (a degenerate primer designed bind in Domain II of the acarine VGSC) and 2187R (a degenerate primer designed to bind downstream of Domain IV of the acarine VGSC); except in one instance with *R. microplus*, where only the 1147R gene specific primer was used, in an attempt to enhance cDNA synthesis from the 5' end of the tick VGSC RNA (Table 4.1).

Table 4.1: Degenerate Primers for cDNA synthesis of Acarine VGSCs

Name	Target Domain (D)	Sequence 5'-3'	Base Pairs
1147_R	DII	TCDAWNGCYTCYTGHAGYTTYTTNGT	26
2187_R	DIV	CCADATYTCRTARTACATRTC	21

Following this 0.5 µl (~1 µg) RNA was added to each reaction mix, along with nuclease-free sterile distilled water if required to give a final volume of 7.25 µl. Samples were heated at 65°C for 3 minutes, chilled on ice, pulse centrifuged to collect the contents in the base of the tube, then placed back on ice. Next 2 µl of 5xRT buffer, 0.25 µl Ribolock and 0.5 µl RevertAid premium was added to each sample, reactions were mixed gently then incubated at 50°C for 1 hour (double the time suggested in the suggested protocol to allow time for synthesis of the long (~6500bp) VGSC sequences. Resulting cDNA samples were stored at -80°C.

4.5 Polymerase Chain Reaction (PCR) Protocols

Reactions were optimised on a reaction-by-reaction basis; based on the melting temperature of the primers, the type of polymerase used, the length of the desired amplicon, the GC-content (or suspected GC content) of the target amplicon, and the volume of PCR product required. Further details are given where appropriate in the methods section of results chapters. PCR products were stored at -20°C.
For each PCR a negative control was prepared containing no template cDNA to ensure observed bands were not the result of spurious-template contamination.

4.6 Primers

Degenerate primers were designed by the author with the help of Joel Gonzales, all other primers were designed solely by the author unless otherwise stated. All primers were synthesised by Sigma-Aldrich. Specific sequence and melting temperature (Tm) details are given in the methods section of the results chapters.

4.7 Media and Antibiotics

Liquid Lysogeny Broth (LB) media (Bertani, 1951) was prepared by adding 10 g bacto-tryptone, 5 g bacto-yeast extract and 10 g NaCl to 950 ml of deionized water and the mixture stirred until all solutes had dissolved. The pH was adjusted to 7.0 with 5M NaOH and the volume made to 1 L with deionized water and the resulting solution sterilized by autoclaving. If agar-plates were required, 15 g of bacto-agar was added to the mixture. Any antibiotics required for bacterial selection were added just prior to use of the media. Super Optimal Broth with Catabolite Repression (SOC) media was prepared by adding 20 g bacto-tryptone, 5 g bacto-yeast extract and 0.5 g NaCl to 950 ml of deionized water and the mixture stirred until all solutes had dissolved. 10 ml of a 250 mM KCl solution was added and the pH adjusted to pH7.0 with 5M NaOH. The volume of the solution was adjusted to 1 L with deionized water and the resulting solution sterilized by autoclaving. Just before use, 5 ml of a sterile solution of 2 M $MgCl_2$ and 20 ml of filter-sterilised 1 M glucose solution were added along with any

desired antibiotics. The antibiotics Ampicillin (Amp) and Carbenicillin were made as 50 mg/ml stocks and used at a working concentration in media of 50 µg/ml.

4.8 Gel Purification of PCR Products

DNA was purified from agarose-gel slices using a QIAquick Gel Extraction Kit (Qiagen). This allows purification of up to 10 µg of DNA of lengths between 70 bp and 10 Kb. All centrifugations were at room temperature at 16168 x g in a bench-top microcentrifuge. Gel slices containing the DNA fragments were excised using a clean, sharp scalpel and placed in 1.5 ml microcentrifuge tubes. Samples were weighed and 3 volumes of Buffer QG was added for every 1 volume of gel slice (100 mg gel being taken as ~ 100 µl). Samples were then incubated at 50°C for 10 min (or until the gel slice had completely dissolved), with vortexing every 2-3 minutes to help dissolve the gel. Mixtures were confirmed to be still yellow, indicating a pH of ≤7.5 as needed for adsorption of the DNA onto QIAquick column membranes, before the addition of 1 gel volume of isopropanol to each sample and samples were mixed by inversion. To bind the DNA samples were added to QIAquick spin columns, placed over 2 ml collection tubes, and centrifuged at 16168 x g for 1 minute. Flow through was discarded and the columns placed back into the same tubes, sample volumes of >800 µl were applied to the columns in multiple steps. To ensure maximum DNA purity an extra 500 µl Buffer QG was applied to the columns, samples were re-centrifuged at 16168 x g for 1 minute, the flow-through discarded, and the columns placed back into the same collection tube. Columns were washed with 750 µl Buffer PE (with ethanol added as per manufacturer's instructions), which was left on the columns for approximately 5 minutes prior to centrifugation for 1 minute. The flow-through was discarded and the columns placed back in the collecting tubes, samples were re-centrifuged at 16168 x g for a further 1 minute to completely remove the wash buffer (as residual ethanol from the buffer can inhibit subsequent enzymatic reactions). The columns were then transferred to clean 1.5 ml microcentrifuge tubes and the DNA eluted by the addition of 50 µl nuclease-free water, followed by incubation for four minutes, and to centrifugation for 1 minute. Purified DNA was then analysed by agarose gel electrophoresis (Section 4.2) and stored at -20°C.

4.9 Cloning of DNA for Sequence Analysis

PCR products were purified by gel extraction then cloned into the vector pJET1.2/blunt using the CloneJET™ PCR Cloning Kit (ThermoFisher Scientific). This vector was chosen because:

i) Recircularised pJET1.2/blunt vector expresses a lethal restriction enzyme after transformation, so only recombinant clones containing a plasmid with the desired insert survive.

ii) The 5'-ends of the pJET1.2/blunt cloning site have phosphoryl groups so phosphorylation of the PCR primers is not required.

iii) The direction of the insert in the vector was not important, and blunt-end cloning raises the chances of correct ligations (compared to a TA cloning vector).

iv) All common laboratory *Escherichia coli* strains may be directly transformed with pJET1.2/blunt ligation products.

v) pJET1.2/blunt contains the β-lactamase gene, conferring resistance to ampicillin, which can be used for the selection and maintenance of recombinant *E. coli*.

Plasmids with inserts were transformed into *E. coli* Stratagene's Xl10 Gold ultracompetent cells following manufacturers' instructions, except that SOC media, rather than NZY^+ broth, was used as the growth medium (Section 4.7 and 4.10). Following transformation, cultures were plated onto LB plates containing 50 μg/ml ampicillin to allow the selection of transformants. Plates were incubated at 37°C overnight and then stored at 4°C.

4.10 Transformation of Plasmids into *E. coli*

The following E. coli strains were used for DNA transformations in this work:

- Stratagene's XL10 Gold cells: These have the genotype Tet^{r}Δ(*mcrA*)*183 Δ*(*mcrCB-hsdSMR-mrr*)*173 endA1 supE44 thi-1 recA1 gyrA96 relA1 lac* Hte [F´ *proAB lacI*^{q}Z*ΔM15* Tn*10* (Tet^r) Amy Cam^r]. XL10 Gold cells were chosen for the cloning of VGSC fragments that would not produce functional channels. These cells possess the Hte phenotype, which increases the transformation efficiency of ligated DNA molecules. Also they are not ampicillin resistant, allowing selection of correctly ligated pJET1.2/blunt-DIV plasmids.

- Stratagene's XL1 Blue ultracompetent cells: These have the genotype *recA1 endA1 gyrA96 thi-1 hsdR17 supE44 relA1 lac* [F´ *proAB lacI*q*ZΔM15* Tn*10* (Tetr)]. This cell line was chosen for the transformation of full-length VGSC constructs, as XL1 blue cells had maintained arthropod VGSCs in that past that had proven fatally toxic to other *E. coli* strains (Martin Williamson personal communication).

- Invitrogen's MAX Efficiency® Stbl2™ competent cells: These have the genotype F- *mcr*A Δ(*mcr*BC-hsdRMS-*mrr*) *rec*A1 *end*A1*lon gyr*A96 *thi sup*E44 *rel*A1 λ- Δ(*lac-pro*AB). These are recommended for use with unstable inserts and proved successful for the mutant *V. destructor* G933V VGSC construct (Chapter 7).

For all transformations *E. coli* cells were thawed on ice and 50 µl aliquots were added to pre-chilled 14 ml BD Falcon polypropylene round-bottom tubes. β-Mercaptoethanol provided by the manufacturer was then added to cells as per manufacturer's instructions. For XL1 Blue and Xl10 gold cells, tubes were mixed gently then incubated on ice for 10 minutes, with gentle mixing every 2 minutes (Stbl2 cells did not require this step). Following incubation with β-Mercaptoethanol, 2 µl of a ligation mix, or 0.5µl of a plasmid control, was added to individual cell aliquots. Cells were then incubated on ice for 30 minutes, then heat-shocked according to manufacturer's instructions. Following heat-shock 450 µl of preheated (42°C) SOC broth was added to

each sample and the tubes were incubated at 30°C for 1.5 to 2 hours with shaking at 225–250 rpm. After this recovery period 250 µl of each ligation reaction (or between2.5 and 25 µl of each control) was plated onto LB-Ampicillin, LB-Carbenicillin or LB-Ampicillin[X-gal/IPTG] plates, depending on blue/white selection or growth control needs (Section 4.7). The latter plates were prepared by pipetting a 100 µl pool of SOC medium onto LB agar surface, then 30 µl of 10 mM Isopropyl β-D-1-thiogalactopyranosid (IPTG) and 30 µl of 2% 5-Bromo-4-Chloro-3-Indolyl β-D-galactopyranoside (X-gal) were added and the mixture spread over the plate at least 30 minutes prior to plating the transformations. Plates were incubated at temperatures between 21 and 30°C for at least 24 hours to allow bacterial growth.

4.11 Colony PCR

Single colonies of *E. coli* containing recombinant plasmids were picked from agar plates using 10 µl filter pipette tips. These cells were streaked onto a fresh LB/Amp plates (colony plates), which were incubated for ~8hrs at 37°C then stored at 4°C. The cells remaining on the tips were then washed into nuclease-free water in the wells of a sterile 96 well plate and left to incubate at room temperature. These cells were then used in PCR reactions designed to amplify the insert contained within their recombinant plasmids. PCR protocols varied according to the length of the inserts and primer used (Section 4.5).

For colonies containing the vector pJET1.2 carrying inserts (of less than 1 Kb) composed of sections of tick VGSCs the PCR reactions contained:

0.5 µl pJET1.2 Forward Sequencing Primer ~10 µM*
0.5 µl pJET1.2 Reverse Sequencing Primer ~10 µM*
2 µl cells
9.5 µl Water, nuclease-free
12.5 µl ThermoFisher Scientific's DreamTaq PCR Master Mix (2X)
Total volume 25 µl

***Primers supplied with the CloneJET™ PCR Cloning Kit (ThermoFisher Scientific).**

Tubes were flicked to mix the contents, pulse centrifuged to collect the contents in the base of the tube, then placed into a thermocycler where the protocol in Table 4.2 was applied.

Table 4.2:

Step	Temperature	Time
Initial Denaturation	95°C	3 minutes
25 Cycles	94°C	30 seconds
	60°C	30 seconds
	72°C	I minute per Kb of amplicon
Final Extension	72°C	5 minutes
Hold	10°C	∞

For colonies containing the vector pGH19 (Section 6.2.1) carrying full-length VGSC inserts (of over 5 Kb) PCR reactions were carried out using New England Biolabs's Q5® High-Fidelity DNA Polymerase (Q5). The reagents, pGH19-specific primers, and PCR conditions listed in Tables 4.3 and 4.4 were used.

Table 4.3: Reaction Setup

Component	Negative control	Reactions	[Final]
5X Q5 Reaction Buffer	10 µl	10 µl	1X
10 mM dNTPs	2 µl	1 µl	400 µM
10 µM 5'_UTR_3_F* GGGATGTGCTGCAAGGCGATTAAG	2.5 µl	2.5 µl	0.5 µM
10 µM 3'_UTR_3_R* GTATAGATACTCAAGCTAGCCTCG	2.5 µl	2.5 µl	0.5 µM
Template	2 µl dH_2O	2 µl Cells	
Nuclease-Free Water	32 µl	3 µl	
Q5 High-Fidelity DNA Polymerase	0.5 µl	0.5 µl	0.02 U/µl

***Primers designed by Joel Gonzales**

Table 4.4: Thermocycling Conditions

Step	Temperature	Time
Initial Denaturation	98°C	30 seconds
35 Cycles	98°C	10 seconds
	68°C	20 seconds
	72°C	7 minutes
Final Extension	72°C	5 minutes
Hold	10°C	∞

The DNA fragments produced by the colony PCR reactions were analysed by electrophoresis on a 1.5% agarose gel (Section 4.2).

4.12 Nucleic Acid Precipitation

Nucleic acids were precipitated by the addition of an equal volume of sodium acetate (4 M, pH 5.2) and 5 x the sample volume (calculated before addition of sodium acetate) of filter sterilized 100% ethanol. Samples were incubated at room temperature for at least 5 minutes prior to centrifugation at 16168 x g for 30 minutes at 4°C. Following centrifugation supernatants were carefully discarded and nucleic acid pellets rinsed with 500µl 75% sterile filtered ethanol. Samples were then centrifuged at 16168 x g for 15 minutes at 4°C and the supernatants discarded. Nucleic acid pellet s were air-dried and re-suspended in 10-50 µl of nuclease-free water, depending on the desired final concentration. Nucleic acid concentrations were checked using a Nanodrop spectrophotometer (ThermoFischer Scientific) and gel electrophoresis was used to confirm the quality of samples (Section 4.2).

4.13 Extraction of Plasmid DNA from *E. coli*

Extractions of plasmid DNA from *E. coli* used the QIAprep Spin Miniprep Kit from Qiagen, designed to purify up to 20 µg of high-copy plasmid DNA from up to 5 ml cultures of *E. coli* grown in LB medium. Firstly, bacterial cultures were pelleted by centrifugation then resuspended to give a homogenous solution in 250 µl Buffer P1 (with RNase added as per manufacturer's instructions). Samples were transferred to 1.5 ml microcentrifuge tubes and 250 µl Buffer P2 was added to each reaction,

solutions were then mixed thoroughly by inversion. This lysis step was allow to proceed for no more than five minutes before the addition of 350 µl Buffer N3 to each sample. The solutions were mixed immediately and thoroughly by inversion to give a cloudy solution then centrifuged for 10 minutes at 16168 x g in a table-top microcentrifuge. Resulting supernatants were carefully applied to QIAprep 2.0 spin columns (in collecting tubes) and centrifuged at 16168 x g for 30-60 seconds. Spin columns were then washed with 0.75 ml Buffer PE (with ethanol added as per the manufacturer's instructions) and centrifuged at 16168 x g for 1 minute; the flow-through was discarded and samples were re-centrifuged at 16168 x g for an additional 1 min to remove all residual wash buffer (residual ethanol from the buffer could have resulted in inhibition of subsequent enzymatic reactions). To elute plasmid DNA from the columns, columns were placed into clean 1.5 ml microcentrifuge tubes and 50 µl nuclease-free water was added to each sample, these were left to incubate for 1 minute prior to centrifugation at 16168 x g for 1 minute. Columns were then discarded and the concentration of plasmid DNA determined using a Nanodrop spectrophotometer (ThermoFischer Scientific) and gel electrophoresis (Section 4.2).

4.14 Sequencing and Sequence Analysis

All sequencing was done by Eurofins MWG Operon. Sequence analysis used Geneious software created by Biomatters and available from http://www.geneious.com/

4.15 Site-Directed Mutagenesis of Cloned VGSC Sequences

Mutagenesis of the *D. melanogaster para* VGSC construct *(para* 13-5) and of pgh19 vectors containing the *V. destructor* VGSC construct (*Varroa* 13-5) (Sections 6 and 7) used the QuikChange II XL Site-Directed Mutagenesis Kit (Agilent Technologies). In each experiment the pWhitescript 4.5-Kb control plasmid was used to demonstrate the efficiency of mutagenesis; this plasmid contains a stop codon (TAA) at a position which is normally a glutamine codon (CAA) in the ß-galactosidase gene, so that that *E. coli* cells transformed with this plasmid appear white on LB-Ampicillin[x-gal/IPTG] plates. The control primers create a point mutation in pWhitescript that changes the stop

codon (TAA) in the ß-galactosidase gene back to a glutamine codon (CAA), so that following transformation colonies that have undergone successful mutagenesis appear blue on LB-Ampicillin[x-gal/IPTG] plates.

Mutagenesis control reactions contained:

5 µl of 10× reaction buffer

2 µl (10 ng) of pWhitescript 4.5 Kb control plasmid (5 ng/ µl)

1.25 µl (125 ng) of oligonucleotide control primer #1 [34-mer (100 ng/ µl]

1.25 µl (125 ng) of oligonucleotide control primer #2 [34-mer (100 ng/ µl]

1 µl of dNTP mix

3 µl of QuikSolution reagent

36.5 µl of double-distilled water (ddH2O) to a final volume of 50 µl

After samples were mixed and pulse centrifuged to collect the contents in the base of the tube, 1 µl of *PfuUltra* HF DNA polymerase (2.5 U/µl) was added and samples were cycled using conditions outlined in Table 4.5.

Table 4.5:

Segment	Cycles	Temperature	Time
1	1	95°C	1 minute
2	18	95°C	50 seconds
		60°C	50 seconds
		68°C	1 minute per Kb of plasmid
3	1	68°C	7 minutes

Sample mutagenesis reactions contained:

5 µl of 10× reaction buffer

X µl (Around 50 ng) of Template DNA

1.25 µl (125 ng) of each forward oligonucleotide primer

1.25 µl (125 ng) of each reverse oligonucleotide primer

1 µl of dNTP mix

3 µl of QuikSolution

X µl ddH2O to a final volume of 50 µl

After samples were mixed and pulse centrifuged to collect the contents in the base of the tube, 1 µl of *PfuUltra* HF DNA polymerase (2.5 U/µl) was added and samples were cycled using specific cycling parameters depending on the construct (Sections 6 and 7).

Following the temperature cycling, reaction tubes were placed on ice for 2 minutes to cool the reactions to ≤37°C, then 1 µl of the *Dpn*I restriction enzyme (10 U/ µl) was added and samples were mixed by pipetting. Sample tubes were briefly spun in a microcentrifuge, then incubated at 37°C for 1 hour to digest the parental (non-mutated) supercoiled dsDNA. Following the *DpnI* digestion samples were transformed into *E. coli* (Section 4.10) and mutagenesis reaction samples were plated onto LB-Ampicillin plates, mutagenesis control reaction were plated on LB-Ampicillin[x-gal/IPTG] plates to allow for blue/white selection (Section 4.10).

4.16 Data Analysis

Details pertaining to the data analysis of experimental work can be found in the methodological sections of Chapters 6-8.

5 Amplification and Sequencing of Acarine VGSCs

5.1 Chapter Introduction and Aims

Since the introduction of pyrethroid insecticides their extensive use has led to the development of widespread resistance to these compounds in many arthropod species, including mites and ticks of agricultural, animal health, and medical importance (Rinkevich et al., 2013). This resistance reduces the effectiveness of pyrethroids, thus it is critical to be able to determine which species are resistant, and their geographical location, in order to limit the spread of resistance and create effective acarine control measures where needed. Target-site resistance to pyrethroids results from mutations in the gene encoding the VGSC, and these mutations cluster around a proposed pyrethroid-binding site (O'Reilly et al., 2006). Therefore, the use of PCR amplification and sequencing in the region of the proposed binding site can give a good indication of any potential resistance mutations present in an acarine species, and can allow the development of high throughput diagnostics to monitor the presence and spread of target-site pyrethroid resistance. Furthermore; the suggested specificity of pyrethroids with larger halogenated groups for acarine species over insects has led to speculation that this could be due to variation in their VGSCs, especially at amino acid residue 933, where most acarine species have a glycine and insect species sequenced to date have a cysteine (O'Reilly et al., 2014). The hypothesis is that the presence of the glycine will allow the binding of pyrethroids with larger halogenated groups, compounds whose binding would be precluded by the presence of a cysteine. This model is supported by the finding that a glycine to valine substitution at position 933 (G933V) in the VGSC of Australian cattle ticks, results in cypermethrin remaining effective but flumethrin becoming ineffective (Jonsson et al., 2010; O'Reilly et al., 2014).

This chapter reports the sequencing of cDNA from individuals belonging to several acarine species, to identify any potential target-site pyrethroid resistance mutations and to elucidate the amino-acid present at position 933 in the VGSCs of these acari. Sequencing was done using PCR to amplify and sequence the region of the VGSC gene around this residue. Initially using degenerate primers, to look at a wide-range of

acarine species rapidly, and then with species-specific primers as needed. Following initial acarine VGSC sequencing the *R. microplus* VGSC was chosen for further study, because of its relevance to animal health and because it was the only tick species in which target-site mediated resistance to pyrethroids had been detected (Rinkevich et al., 2013; Van Leeuwen et al., 2010a). Rapid Amplification of cDNA Ends (RACE) and the construction of an Illumina transcriptome were done with the aim of obtain a full-length tick VGSC construct for study in *X. laevis* oocytes. The aim of all investigations being to garner a greater knowledge of the potential efficacy of these compounds at acarine VGSCs and thus inform the judicious use of these compounds against acari.

Throughout this study the numbering of the amino acid residues in the VGSC is according to the published numbering for the *M. domestica* channel (Williamson et al., 1993a).

5.2 Chapter Specific Methods

5.2.1 Primers for VGSC Amplification and Sequencing

For initial sequencing degenerate primers were designed for the targeted amplification of membrane-spanning domains of previously un-sequenced acarine VGSCs. These primers were based on published partial or putative mRNA channel sequences from ten acarine species: *I. scapularis* (accession number XM_002407075), *Metaseiulus occidentalis* (accession number XM_003741689), *R. microplus* (accession number AF134216), *S. scabiei type hominis* (accession number DQ077148), *S. scabiei type canis* (accession number EF041516), *S. scabiei type suis* (accession number DQ145115), *T. cinnabarinus* (accession number JX290514), *Tetranychus evansi* (accession number HM117902), *T. urticae* (accession number JN881331) and *V. destructor* (accession number AY259834). The sequences of the primers and the domains they were designed to amplify (target domains) are shown in Table 5.1. Primers in Table 5.1 were designed by the author with the help of Joel González-Cabrera.

Table 5.1: Degenerate Primers Targeting Acarine VGSC Sequences

Primer Name	Target Domain (D)	Primer Sequence 5'-3'	Primer Length (Base Pairs)
484_F	DI	AARRGMAARGAYATMTTYCG	20
490_F	DI	AARGAYATMTTYCGBTTYAG	20
898_R	DI	TCCWGGWACDAYAGCDACBG	20
903_R	DI	TTBARTCCWGGWACDAYAGC	20
819_F	DII	GAYGTNATGGTNCTRAAYGA	20
924_F	DII	ATGGCNATGGAYCAYCAYGAYATG	24
1146_R	DII	TCYTGHAGYTTYTTNGTRTC	20
1147_R	DII	TCDAWNGCYTCYTGHAGYTTYTTNGT	26
1710_F	DIII	ATHTTYTGGCTVATHTTYTC	20
1712_F	DIII	TGGCTVATHTTYTCNATHATG	21
1814_F	DIV	TAYTTYGTNTTYTTYATHAT	20
1816_F	DIV	GTNTTYTTYATHATHTTYGG	20
1850_R	DIII	TCYTCNGTCATRAACATYTC	20
1853_R	DIII	TTYTGRTCYTCNGTCAT	17
2185_R	DIV	TCRTARTACATRTCRTARTC	20
2187_R	DIV	CCADATYTCRTARTACATRTC	21

Further degenerate primers were designed for the amplification of Domain IV (DIV) of acarine channels (Table 5.2), using mRNA sequences from one tick and four mite species with available Domain IV sequences: *I. scapularis* (accession number XM_002407075), *M. occidentalis* (accession number XM_003741689), *T. cinnabarinus* (accession number JX290514), and *V. destructor* (accession number AY259834) for both forward and reverse primers and *T. urticae* (accession number JN881331) for the forward primers only. These primers were used to amplify and sequence DIV from *D. gallinae*, *P. ovis*, *A. hebraeum*, D. *variabilis*, and *R. sanguineus*.

Table 5.2: Degenerate Primers Targeting Acarine VGSC Domain IV

Primer Name	Target Domain (D)	Primer Sequence 5'-3'	Primer Length (Base Pairs)
DIVFA	DIV	GAARAARATGGGMTCWAARAARCC	24
DIVRA	DIV	GRUCGAAMYGCUGCCARAUC	20
DIVFB	DIV	CCAMGRTTYAAACTTCARGC	20
DIVRB	DIV	GCUGCCARAUCUCRUAGUAC	20

Degenerate primers were designed to amplify the region just before DI (Pre-DI) and just after DIV (Post-DIV) of the acarine VGSC, using mRNA VGSC sequences from *M. occidentalis* (accession number XM_003741689), *T. cinnabarinus* (accession number JX290514), *T. urticae* (accession number JN881331) and *V. destructor* (accession number AY259834). These were used to amplify the *R. microplus* (Parkhurst) VGSC sequence past the domain-spanning region to aid RACE primer design (Table 5.3).

Table 5.3: Primers Used to Amplify and Sequence the *R. microplus* VGSC

Primer Name	Target Domain (D)	Primer Sequence 5'-3'	Primer Length (Base Pairs)
Pre-DIFA	Pre-DI	TDTTYMGRCCKTTYACSAGRG	21
Pre-DIRA	Pre-DI	CATGAGGACGCAGTTGACGA	20
Pre-DIFB	Pre-DI	GRCCKTTYACSAGRGARWSYYTSGC	25
Pre-DIRB	Pre-DI	CAGTTGACGAGAATGGTTAC	20

Primers to amplify the full domain-spanning region of the *R. microplus* VGSC and the 3' end including the 3' untranslated region (UTR) are shown in Tables 5.4 and 5.5. Primers in Table 5.4 were designed to sequence a full-length *R. microplus* domain-spanning VGSC PCR product that included the 3' UTR region. This PCR product was created using the primers shown in Table 5.5, designed from sequence information obtained using Pre-DI primers in Table 10 at the 5' end and using raw reads from a *R. microplus* Illumina transcriptome at the 3' end.

Table 5.4: Primers Used to Sequence the *R. microplus* VGSC

Primer Name	Primer Sequence 5'-3'	Primer Length (Base Pairs)
RM DIS1 R	GGTGCACTAGGATGCAGATG	20
RM DIS1 F	CATCTGCATCCTAGTGCACC	20
RM DIS3 F	GGATTTTGTTGTTATATCTCTAGCG	25
RMSeqCheck5'	CGCTAGAGATATAACAACAAAATCC	25
DI-II FCP F	CCTGGGCTCCTTCTATCTAGT	21
DI-II FCP R	AGCAATTGGCCATGCACTTG	20
DII FCP F	CGCTATTCATGGCCATGGAC	20
RM DIIS2 R	CATAAGCTTCATTCCAGC	18
RM DIIS2 F	GCTGGAATGAAGCTTATG	18
RM DII-III R	GTCGGGATTCGCTTGGGACAG	21
RM DII-III F	CTGTCCCAAGCGAATCCCGAC	21
RM DII-III RB	GTGTCCACATCTTCCGTGTC	20
RM DII-III FB	GACACGGAAGATGTGGACAC	20
D II-III FCP R	ATCGCGTGTAACACCAGTCG	20
RM DIIIS5 R	CTTTCCCGCAAGCATCTGGA	20
RM DIIIS5 F	TCCAGATGCTTGCGGGAAAG	20
RM DIVS3 R	AGGTCCTTTAGCACCGTACC	20
RM DIVS3 F	GTGCTAAAGGACCTGATCGC	20
RMSeqCheck3'	CTTGTGATGTTCATCTACGC	20
ParaRMCheckF	ACCTCATCATCAGCTTCCTCG	21
RM PostDIV R	TTGGTCAGGTTGGAGTAGGC	20
RM PostDIV F	GCCTACTCCAACCTGACCAA	20

Table 5.5: Primers Used to Amplify the Functional Region of the *R. microplus* VGSC and the 3' UTR

Primer Name	Primer Sequence 5'-3'	Primer Length (Base Pairs)
RMFL0115 FPA	CCTTTCACGCGAGAGTCCCTAGCC	24
RMFL0115 RPA	CGCGAGAGTCCCTAGCCGCCCAAG	24
RMFL0115 FPB	GGTGCTTCTGCGTCGAGGGTACG	23
RMFL0115 RPB	CTTCTGCGTCGAGGGTACGTAGC	23

5.2.2 PCR Protocols

For each amplification of regions of the VGSC, two rounds of PCR were carried out, the first (PCR 1) with a set of outer primers and the second (PCR 2) with at least one inner (nested) primer. This enabled the synthesis of enough PCR product for sequencing reactions.

Standard PCR reactions used the ThermoFisher Scientific's DreamTaq PCR Master Mix (2X), containing DreamTaq DNA Polymerase and proprietary PCR buffer containing KCl and (NH4)2SO4 at a ratio optimized for best performance of the DreamTaq DNA Polymerase, dNTPs, and 4mM $MgCl_2$. The buffer also includes a density reagent, allowing direct loading onto agarose gels and two tracking dyes for monitoring electrophoresis. The master mixes also contained 1 µl of each primer (forward and reverse) from a stock made to 100ng/µl. PCR 1 reactions contained 2 µl cDNA as a template, cDNA concentration is unknown, due to RNA and nucleotide contamination of the mix; however, 2 µl insect cDNA prepared in the manner outlined in Section 4.4 had previously been shown to be effective in PCR experiments (Joel González-Cabrera and Martin Williamson personal communication). Nested PCR 2 reactions contained 1 µl of PCR 1. Control reactions contained nuclease-free water in place of the template DNA. Unless otherwise stated, PCR reactions started with an initial denaturation step at 95°C for 3-5 minutes followed by 25 to 45 PCR cycles, each with denaturation steps of 95°C for 45 seconds and extension steps of 72°C that allowed approximately 1 min of extension time per Kb of sequence to be amplified. Primer annealing steps were 45 seconds and Tm's were primer specific.

Amplification reactions with degenerate primers from Table 5.1 were done on all acarine species tested in this study using ThermoFisher Scientific's DreamTaq PCR Master Mix (2X), with Tm's and primer combinations as shown in Table 5.6.

Table 5.6: Effective Primer Combinations and Tm's Used for Primers in Table 5.1

Primer Name	Target Domain (D)	PCR	Tm (°C)
484_F	DI	1	45
898_R	DI	1	45
490_F	DI	2	44
903_R	DI	2	44
819_F	DII	1	45
1146_R	DII	1	45
924_F	DII	2	53
1147_R	DII	2	53
1710_F	DIII	1	54
1850_R	DIII	1	54
1712_F	DIII	2	50
1853_R	DIII	2	50
1814_F	DIV	1	45
2185_R	DIV	1	45
1816_F	DIV	2	45
2187_R	DIV	2	45

Reactions with primers from Table 5.2 were used in protocols designed to amplify DIV from *D. gallinae*, *P. ovis*, *A. hebraeum*, D. *variabilis*, and *R. sanguineus*, using ThermoFisher Scientific's DreamTaq PCR Master Mix (2X) and Tm's and primer combinations as shown in Table 5.7.

Table 5.7: Effective Primer Combinations and Tm's Used for Primers in Table 5.2

Primer Name	Target Domain (D)	PCR	Tm (°C)
DIVFA	DIV	1	54
DIVFB	DIV	1	54
DIVRA	DIV	2	51
DIVRB	DIV	2	51

Degenerate Pre-DI primers shown in Table 5.3 were used to amplify a region of the *R. microplus* (Parkhurst) VGSC past the domain-spanning region. These reactions used ThermoFisher Scientific's DreamTaq PCR Master Mix (2X) with Tm's and primer combinations as shown in Table 5.8.

Table 5.8: Effective Primer Combinations and Tm's Used for Primers in Table 5.3

Primer Name	Target Domain (D)	PCR	Tm (°C)
Pre-DIFA	Pre-DI	1	48
Pre-DIRA	Pre-DI	1	48
Pre-DIFB	Pre-DI	2	54
Pre-DIRB	Pre-DI	2	54

Primers shown in Table 5.5 were used designed to try to obtain the full membrane-spanning domain region of the *R. microplus* VGSC, using PCR reactions with New England Biolabs's Q5® High-Fidelity DNA Polymerase (Q5) All reaction mixes contained 1X Q5 Reaction Buffer (New England Biolabs), 0.5 µM of each primer (forward and reverse), 400 µM dNTPs (from an equal mix of dATP, dCTP, dGTP, and dTTP nucleoside triphosphates) and 0.04 U/µl High-Fidelity DNA Polymerase (Q5). PCR 1 reactions contained 1 µl cDNA as a template and nested PCR 2 reactions contained 1 µl of the PCR 1 reaction as a template. Control reactions contained nuclease-free water in place of the template DNA. Following an initial denaturation step of 98°C for 30 seconds, PCR amplification occurred over 25 cycles, each with denaturation steps of 98°C for 10 seconds and extension steps of 72°C for 6 minutes. Primer annealing steps were 20 seconds in duration and Tm's and primer combinations are shown in Table 5.9.

Table 5.9: Effective Primer Combinations and Tm's Used for Primers in Table 5.5

Primer Name	Target Domain (D)	PCR	Tm (°C)
RMFL0115 FPA	Full Channel	1	72
RMFL0115 RPA	Full Channel	1	72
RMFL0115 FPB	Full Channel	2	72
RMFL0115 RPB	Full Channel	2	72

Following PCR amplification, samples were either sequenced directly following DNA precipitation or after cloning (see Chapter 4).

5.2.3 Rapid Amplification of cDNA Ends (RACE)

5’ and 3’ RACE reactions for VGSCs were done using the FirstChoice® RLM-RACE Kit (Ambion) on RNA from *I. ricinus*, *R. microplus* and *R. sanguineus* and the SMARTer™ RACE cDNA Amplification Kit (Clontech) and the GeneRacer™ Kit (Invitrogen) for *R. microplus* RNA only (the latter kit being used in amplification of only the 5’ end). All reactions were according to manufacturer’s instructions; however, with the FirstChoice® RLM-RACE Kit the “small scale” reaction protocol was followed and with the SMARTer™ RACE cDNA Amplification Kit, half volumes of reactants were used. All gene-specific RACE amplification primers were designed according to manufacturer’s directions and are shown in Tables 5.10, 5.11 and 5.12.

The PCR mix for amplification using the FirstChoice® RLM-RACE Kit (Ambion) was adapted to accommodate the use of a range of primers and DNA polymerases, specifically ThermoFisher Scientific’s DreamTaq PCR Master Mix (2X), New England Biolabs’s Q5® High-Fidelity DNA Polymerase (Q5) and the KAPA2G Robust DNA Polymerase from KAPA Biosystems. The PCR mix for amplification using the SMARTer™ RACE cDNA Amplification Kit was adapted to accommodate the use of a range of primers and DNA polymerases, specifically ThermoFisher Scientific’s DreamTaq PCR Master Mix (2X), New England Biolabs’s Q5® High-Fidelity DNA Polymerase (Q5), ThermoFisher Scientific’s Long PCR Enzyme Mix and the KAPA2G Robust DNA Polymerase from KAPA Biosystems.

In all PCRs the extension time was set to allow for the size of the product expected plus extra time to take account of untranslated regions at the 5’ and 3’ ends of the VGSC.

Table 5.10: Primers Used with the FirstChoice® RLM-RACE Kit (Ambion)

Primer Name	Target Species	Primer Sequence 5'-3'	Primer Length (Base Pairs)
Tick 5' Outer Primer A	*I. ricinus; R. microplus*; *R. sanguineus*	GAGGACRCAGTTGACGAGAATGG	23
Tick 5' Outer Primer B	*I. ricinus; R. microplus*; *R. sanguineus*	GATTCRAACGTGTAGATTGTGGT	23
Tick 5' Outer Primer C	*I. ricinus; R. microplus*; *R. sanguineus*	GCTARAGATATAACAACAAAATC	23
Tick 5' Inner Primer A	*I. ricinus; R. microplus*; *R. sanguineus*	GACRCAGTTGACGAGAATGGTTAC	24
Tick 5' Inner Primer B	*I. ricinus; R. microplus*; *R. sanguineus*	AACGTGTAGATTGTGGTGAATAT	23
Tick 5' Inner Primer C	*I. ricinus; R. microplus*; *R. sanguineus*	AGATATAACAACAAAATCCAACC	23
Tick 3' Outer Primer A	*I. ricinus; R. microplus*; *R. sanguineus*	CGTCTCSTACCTCATCATCAG	21
Tick 3' Outer Primer B	*I. ricinus; R. microplus*; *R. sanguineus*	GAYTGCAACCGSCCCACCGAC	21
Tick 3' Outer Primer C	*I. ricinus; R. microplus*; *R. sanguineus*	CTACGGCGTCGACGAGAACT	20
Tick 3' Inner Primer A	*I. ricinus; R. microplus*; *R. sanguineus*	CTCSTACCTCATCATCAGCTTCC	23
Tick 3' Inner Primer B	*I. ricinus; R. microplus*; *R. sanguineus*	TGCAACCGSCCCACCGACGA	20
Tick 3' Inner Primer C	*I. ricinus; R. microplus*; *R. sanguineus*	GCGTCGACGAGAACTTCAAC	20
5' Outer Primer A	*R. microplus*	AGAAGCTGAAAAGTGGGTGCA	21
5' Outer Primer B	*R. microplus*	ATGGTCATGAGGACGCAGTT	20
5' Inner Primer	*R. microplus*	TGCAGATGGCCAGTCTCCTGA	21
3' Outer Primer	*R. microplus*	CCCTTCGGGACTGCCTACCA	20
3' Inner Primer	*R. microplus*	TTGGACCTTACGCGCACGCT	20
5' RACE Chance Outer Primer	*R. microplus*	AGCTGACAAAGCAGTCTCGG	20
5' RACE Chance Inner Primer	*R. microplus*	GACAAAGCAGTCTCGGCGGG	20

Table 5.11: Primers Used with the SMARTer™ RACE cDNA Amplification Kit (Clontech)

Primer Name	Target Species	Primer Sequence 5'-3'	Primer Length (Base Pairs)
Tick 5' Outer Primer C Extended	*R. microplus*	CGCAAGGCGCTCAGGTTYCCCAAATTAA	28
Tick 5' Inner Primer C Extended	*R. microplus*	CAAAATCCAACCARTTCCAYGGATCTCGAAG	31
Tick 3' Outer Primer C Extended	*R. microplus*	GGCATGTCYTTCTTYATGCACGTSAAGC	28
Tick 3' Inner Primer C Extended	*R. microplus*	CGCTAYGGCGTCGACGAGAACTTYAACTTYG	31
RmSpec3'A	*R. microplus*	GCGGCCTACTTCGTGTCGCCCAC	23
RmSpec3'B	*R. microplus*	CCCTGGCCATGTCATTGCCGGCAC	24
RmSpec5'A	*R. microplus*	CGATGGGCGTGGCGATGAGCTCG	23
RmSpec5'B	*R. microplus*	GATCGGCGTCCTTGTGGTCTCGCGAG	26

Table 5.12: Primers Used with the GeneRacer™ Kit (Invitrogen)

Primer Name	Target Species	Primer Sequence 5'-3'	Primer Length (Base Pairs)
RACE12.2015GSP1	*R. microplus*	GTAGTCGTCGCCTGCCGGGATGCCC	25
RACE12.2015GSP2	*R. microplus*	TCGATGGGCGTGGCGATGAGCTCGG	25

5.2.4 Transcriptomics

Alongside RACE the *R. microplus* transcriptome was sequenced using the Illumina HiSeq2000 method in order to try to obtain the full-length *R. microplus* VGSC sequence. *R. microplus* total RNA (from larvae + adults) was sent to Eurofins/MWG/Operon (Ebersberg, Germany) for cDNA library preparation and normalisation. The cDNA was processed and sequenced using 2 full lanes of HiSeq2000 with 1 x 100bp paired end reads protocol. Each lane generated just over 100 million reads, giving a combined total of 208 million reads. Initial read data were analysed for quality using FastQC (Online: Babraham Bioinformatics 2016), digitally normalised to further reduce the abundance of the more common transcripts and then assembled using the programme Trinity (Grabherr et al., 2011). This resulted in 250,000 contigs of average length 950bp, which were put into the DeCypher server at Rothamsted allowing sequence-specific searching using a Basic Local Alignment Search Tool (BLAST). Raw reads were also put into a Geneious (Section 4.14) server for BLAST searching.

5.3 Results

5.3.1 Comparing the Pyrethroid Binding Site of Insect and Acarine VGSCs

PCR primers targeting Domains DI, DII and DIII of the VGSC (Table 5.1) were used successfully on all nine acarine species to amplify and sequence regions of the VGSC; with the exception of DI from *P. ovis*, which failed to amplify (Figure 5.1).

Figure 5.1: Acarine VGSC Sequencing Coverage

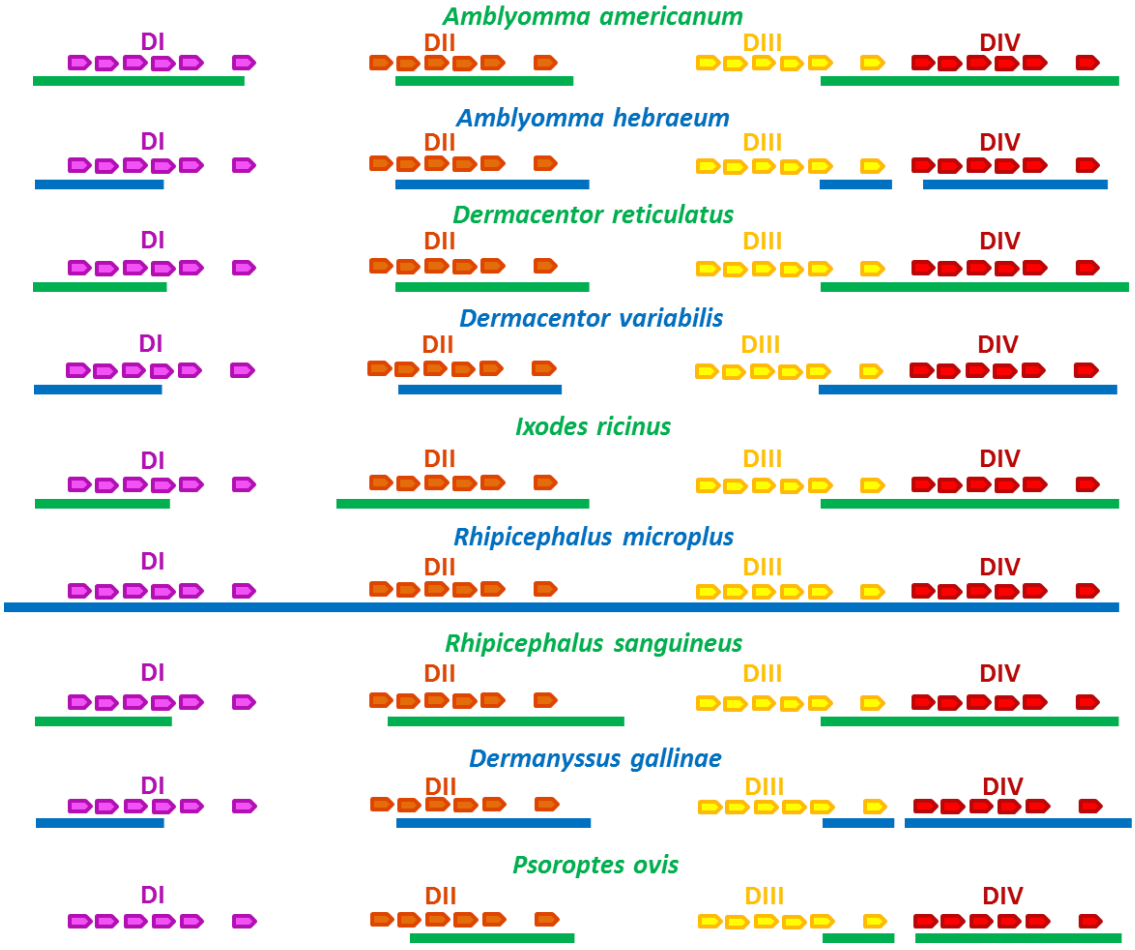

Summary of VGSC areas in different acarine species covered by sequencing in this study to date. VGSC Domains I-IV are shown split into their S1-6 segments. Blue and green lines represent sequence coverage for each organism.

Further amplification of the *P. ovis* VGSC DI was attempted with alternative primers; but despite several PCR protocol iterations all attempts to gain this portion of the channel failed. Primers targeting Domain DIV (Table 5.1) were successful for *A. americanum*, *D. reticulatus*, *I. ricinus* and *R. microplus* only and molecular cloning and colony PCR prior was needed to get enough material for sequencing (Chapter 4). Sequence details for the acarine VGSCs sequenced in this study can be found in Appendices 1 and 2.

For *R. microplus*, the entire domain-spanning sequence of the VGSC has been elucidated, along with the 3' UTR, using both PCR and bioinformatics-based methods. Initially degenerate primers (Table 5.1) were used to amplify domain spanning segments of the channel, then Pre-DI primers (Table 5.3) were used to extend the sequence at the 5' end for later RACE protocols, Post-DIV primers were also synthesised to try to extend the sequence at the 3' end prior to RACE, but amplification with these was unsuccessful. Several RACE protocols using three different RACE methods and various PCR amplification steps using a range of primers, cycling protocols, DNA polymerases and Tm's were tested. However, all proved unsuccessful in gaining either the 5' or 3' ends of the channel. As an alternative, a *R. microplus* transcriptome from mixed larvae and adults was sequenced using the Illumina HiSeq2000 method and this did generate reads corresponding to the 3' end of the gene, including the stop codon and the 3' UTR. The transcriptome was assembled using Trinity (Grabherr et al., 2011), but resulting assemblies discarded contigs corresponding to the 3' end, so direct sequence mapping to the *I. scapularis* (accession number XM_002407075) VGSC sequence using the raw Illumina reads in Geneious (Section 4.14) was used to obtain the sequence of the 3' UTR.

Primers which enabled the full amplification and sequencing of the *R. microplus* domain-spanning region (Table 5.5) were RMFLNMFA ("*R. microplus* full-length non-mutant forward A"), RMFLNMRA ("*R. microplus* full-length non-mutant reverse A"), RMFLFA ("*R. microplus* full-length forward A"), RMFLRA ("*R. microplus* full-length reverse A"). Note that the latter two primers change the channel by adding AflII and

AbsI restriction sites to the 5’ and 3’ ends, this was to allow the subsequent cloning of the products (Chapter 6).

The sequencing reported here gave some interesting results regarding the similarity of acarine VGSCs around the pyrethroid binding site and subtle differences between acarine and insect channels. Overall, the acarine channels sequenced to date are very conserved and are very similar to the *M. domestica* insect channel across the putative pyrethroid binding site (O'Reilly et al., 2006) at the protein level (Figure 5.2). The mites used in this study, *D. gallinae* and *P. ovis*, show the greatest level of variation when compared to each other and to the tick and *M. domestica* channels.

Within Domain II at residue 933 (Figure 5.2 “Domain II S5”), there is a clear difference between the acari sequenced in this study and the insect VGSCs sequenced to date. This residue is a glycine in most acari, including those sequenced here, and a cysteine in insects, so sequencing in the current study supports the theory proposed in O’Reilly *et al* 2014, that the specificity of certain pyrethroids for acarine toxicity may be due to differences between acarine and insect VGSCs at position 933. With the smaller glycine in acarine channels being able to support pyrethroids with larger halogenated groups that would be excluded by the larger cysteine found in insect VGSCs (O'Reilly et al., 2014).

Figure 5.2: Acarine VGSCs over the Proposed Pyrethroid Binding Site

The Domain II S4-S5 Linker:

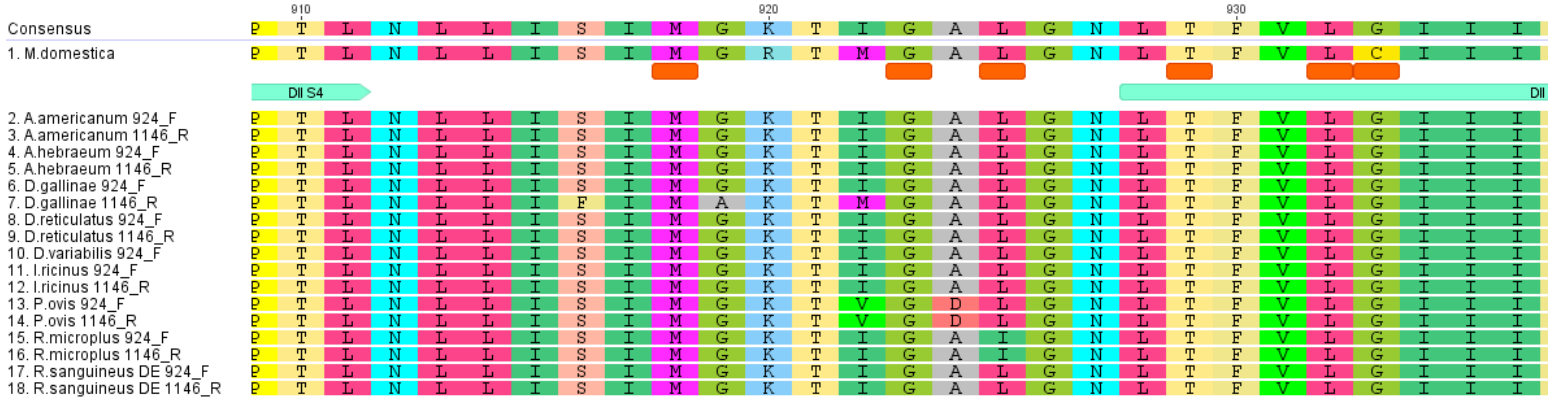

Domain II S5:

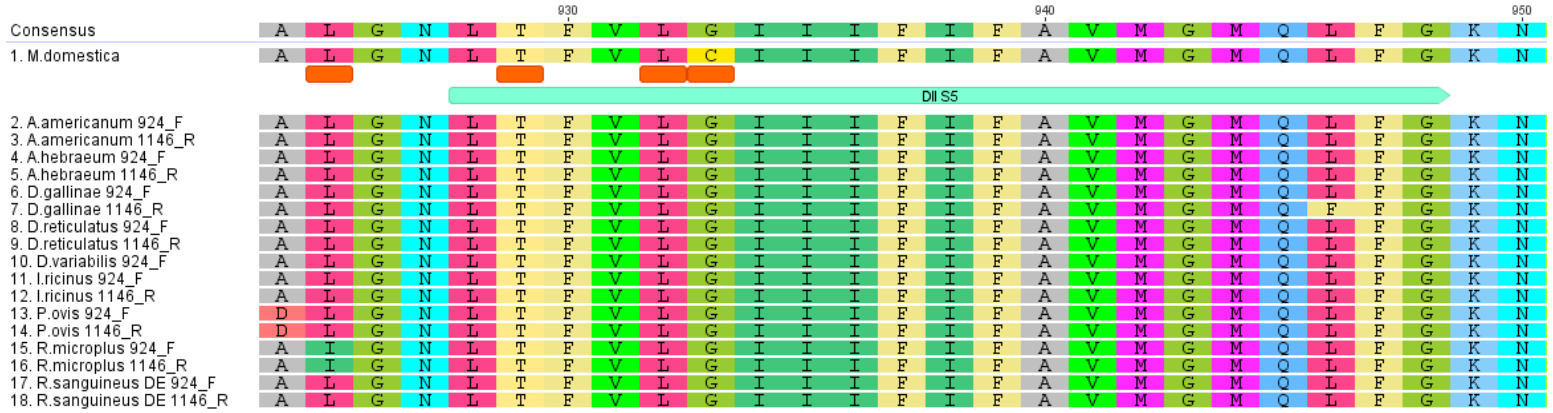

Domain III S6:

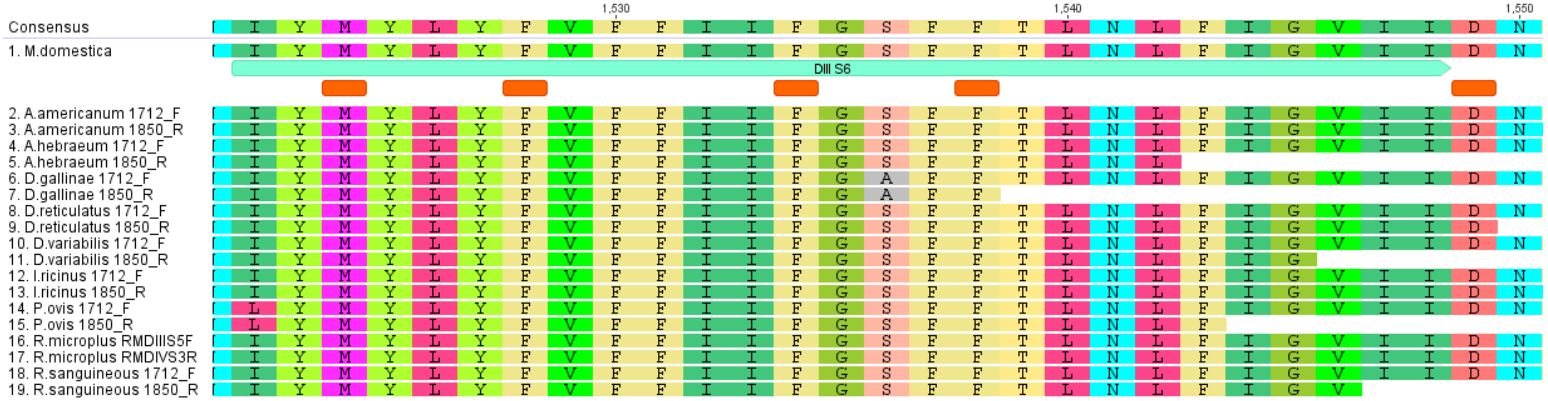

Comparisons of acarine protein sequences as sequenced in this study at the putative pyrethroid binding site (O'Reilly et al., 2006) using *M. domestica* (accession number AF461154) as an insect reference. Species names and the primers used for sequencing the domain segments shown are on the left hand side of the sequence diagrams (Tables 5.1-5.5). Orange boxes represent the sites of VGSC target-site mutations associated with pyrethroid resistance as reported in arthropod species to date (Rinkevich et al., 2013). Note that at these sites all acarine species sequenced carry the same amino acid as the pyrethroid susceptible *M. domestica* comparison.

5.3.2 Pyrethroid Resistance in *R. microplus* and *R. sanguineus*

During the course of the acarine sequence analysis reported in this study amino acid substitutions linked with target-site pyrethroid resistance were located in two tick species; *R. microplus* (Parkhurst strain) and *R. sanguineus* (Field individuals).

The *R. microplus* strain used in this study is a lab strain, known to be pyrethroid resistant, reared by Bayer Animal Health in Monheim, but originally isolated from the field in Australia (Nolan et al., 1989). This strain has previously been characterised as carrying target-site resistance for pyrethroids in the form of a leucine to isoleucine amino-acid substitution at position 925 (L925I) and this amino acid substitution was confirmed in the present study (Morgan et al., 2009; Nolan et al., 1989).

During sequence analysis a novel amino acid substitution, located in DII S6 (Figure 5.3), was identified in *R. microplus* (Parkhurst). The mutation causing this was shown to be homozygous by molecular cloning and sequence analysis (Chapter 4) and results in a valine at position 1010 being swapped for a phenylalanine (V1010F). The substitution is close to other sites where substitutions have been reported to be associated with resistance, i.e. I1011M/V, L1014F/H/S and V1016G/I (Figure 5.1) (Rinkevich et al., 2013).

Figure 5.3: The V1010F Aino Acid Substitution in R. microplus (Parkhurst Strain)

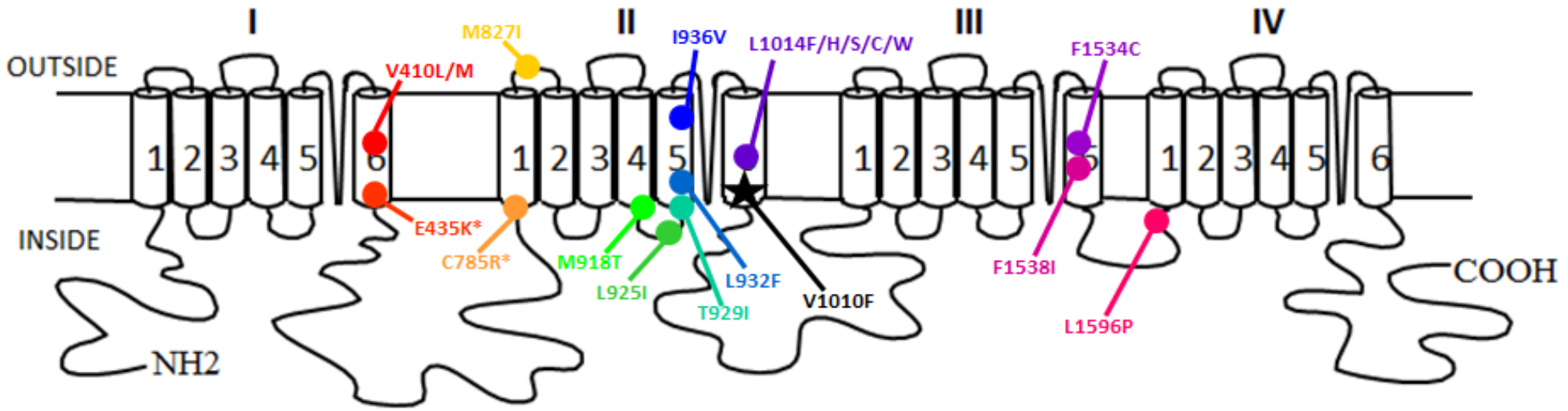

i) A representative insect/acarine VGSC showing domains I-IV and their six membrane-spanning domains illustrating the relative position of V1010F in *R. microplus* (Parkhurst) (black star) compared to previously identified VGSC mutations (coloured circles) that have been confirmed to confer resistance to pyrethroids in *X. laevis* oocyte TEVC experiments (Reported in Dong *et al* 2014). Mutations with a * do not confer pyrethroid resistance alone but enhance resistance conferred by L1014F or V410M.

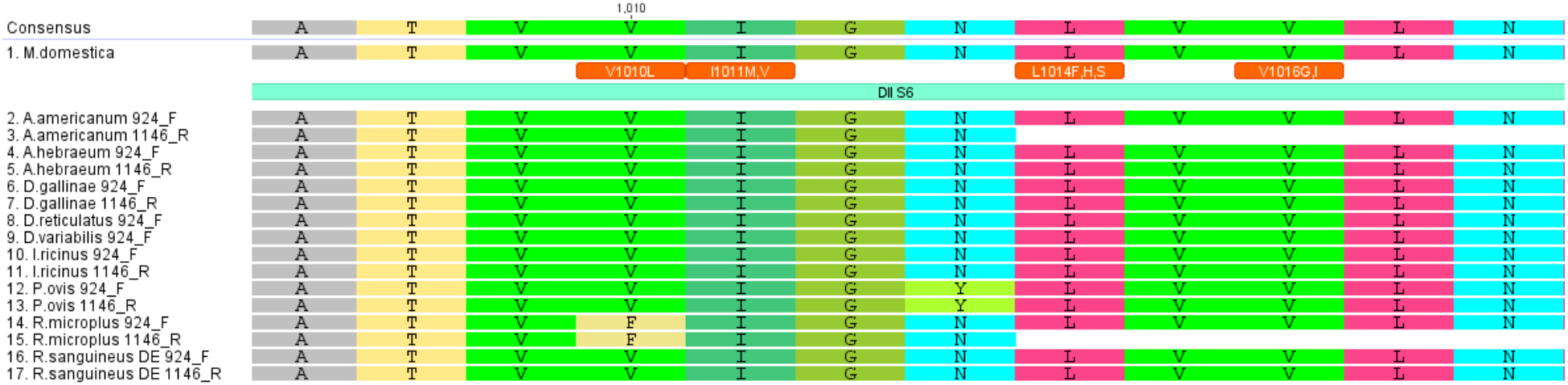

ii) Comparisons of acarine protein sequences as sequenced in this study around V1010F using *M. domestica* (accession number AF461154) as an insect reference. Species names and the primers used for sequencing the domain segments shown are on the left hand side of the sequence diagrams (Table 5.1). Orange boxes represent the sites of VGSC target-site mutations associated with pyrethroid resistance reported in arthropod species to date (Rinkevich et al., 2013).

For *R. sanguineus* field samples, collected by Bayer Animal Health (Monheim, Germany) were tested for resistance to pyrethroids by exposing individuals to permethrin dissolved in acetone. Sample collection, including the location of collection sites, bioassay protocols, and further sequence details are the confidential property of Bayer Animal Health. Following bioassays, individuals were frozen at -80°C and then sent to Rothamsted Research for PCR amplification and sequencing using primers shown in Tables 5.1 and 5.2 (Section 5.2.1) and PCR protocols detailed in Section 5.2.2. Where mutations were found, PCR products were cloned to establish if the mutations were homozygous (on just one allele) or heterozygous (on both alleles). Mutations resulting in amino acid substitutions in the VGSC found in *R. sanguineus* individuals during this study are shown in Table 5.13 and Figure 5.4.

Table 5.13: Resistance Profiles of *R. sanguineus*

Name of Individual	Description	Mutations Present		
		L925I	G933V	F1538L
RST1	Control (Acetone treated only)	WT[#] L/L	Homozygous V/V	WT F/F
RST2	Survivor 180 ppm* permethrin	Heterozygous L/I	Heterozygous G/V	Heterozygous F/L
RST3	Survivor 180 ppm permethrin	WT L/L	Heterozygous G/V	Heterozygous F/L
RSA4	USA[⌂] Presumed WT.	WT L/L	WT G/G	WT F/F

[#]Wild Type
[*]parts per million
[⌂]EL LABS, Soquel, California, USA

Figure 5.4: Mutations Found in Permethrin Resistant *R. sanguineus* Individuals

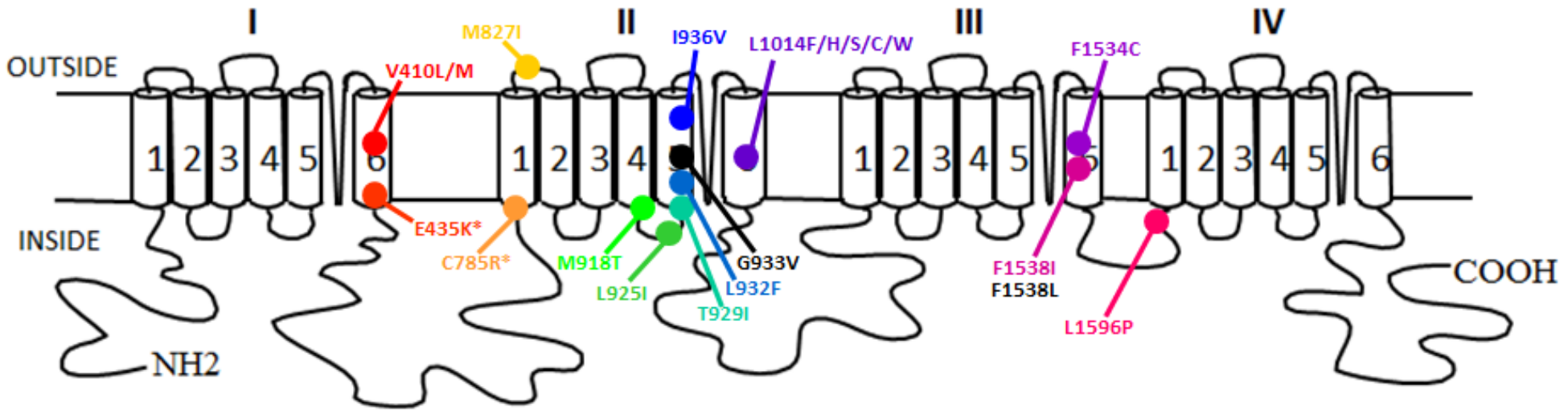

A representative insect/acarine VGSC showing domains I-IV and their six membrane-spanning domains illustrating the relative position of L925I, G933V and F1538L mutations found in *R. sanguineus* individuals in the present study. These are compared to previously identified VGSC mutations (coloured circles) that have been confirmed to confer resistance to pyrethroids in *X. laevis* oocyte TEVC experiments (Reported in Dong *et al* 2014). Mutations with a * do not confer pyrethroid resistance alone but enhance resistance conferred by L1014F or V410M. Note that L925I is shown only once as a coloured circle, as it has already been confirmed to confer pyrethroid resistance in *X. laevis* oocyte TEVC experiments (Usherwood et al., 2007).

R. sanguineus individual RST1, used in the acetone control bioassay, was homozygous for G933V, found in the putative pyrethroid binding site (O'Reilly et al., 2006) of the VGSC. Individual RST2 had three heterozygous amino-acid substitutions; L925I and G933V, located within the pyrethroid binding site in the Domain II S4-S5 linker of the VGSC, and F1538L in Domain III S6 (Figure 5.4). Cloning experiments showed that L925I and G933V are on the same allele for this individual, whilst F1538L is on the opposite allele. Individual RST3 also had G933V and F1538L, present heterozygously on opposite alleles.

5.4 Discussion

Work described in this Chapter describes the sequencing of acarine VGSCs from a variety of species and the detection of amino acid substitutions associated with resistance to pyrethroids.

Significant progress was made in obtaining new sequence information for the membrane-spanning domains of the VGSCs from nine acarine species, *A. americanum*, *A. hebraeum*, *D. gallinae*, *D. reticulatus*, D. *variabilis*, *I. ricinus*, *P. ovis, R. microplus (Parkhurst)* and *R. sanguineus*. In the case of *R. microplus* the sequencing covers almost the entire length of the channel, with just the 5' start sequence being missing (Figure 5.1). The results highlight the striking similarity of amino acid sequences between arthropod VGSCs over their functional membrane spanning domains, in particular around the putative pyrethroid binding site (O'Reilly et al., 2006). This has supported the view that amino acid 933 could play a role in pyrethroid selectivity. As more acarine samples become available, future work should focus on further examining the similarities and differences between the channels of a wider variety of acari and insects, leading to stronger clarification on the mechanisms of pyrethroid binding and selectivity.

The novel amino acid substitution, V1010F, identified in the *R. microplus* (Parkhurst) VGSC could be playing a role in pyrethroid resistance in this strain, especially since it is located in close proximity to other mutations already reported to be associated with

target-site resistance to pyrethroids in other organisms (Rinkevich et al., 2013) (Figure 5.3). A similar leucine to valine, V1010L has been found in *Anopheles culicifacies* (malaria mosquitoes) in India by Singh *et al* in 2010 and in this case V1010L was always found in conjunction with L1014S heterozygous on the same allele (Singh et al., 2010). L1014S is commonly associated with resistance to pyrethroids in insects, but this mutation was not found in the acari in the present study. It is worth noting that V1010L has had no associations to pyrethroid resistance as no *A. culicifacies* mosquitoes in the Singh *et al* 2010 study were screened for their pyrethroid susceptibility (Singh et al., 2010). At present it is also not possible to link V1010F with resistance to pyrethroids in *R. microplus* due to the interfering effects of L925I, which has been shown to be associated strongly with pyrethroid resistance in arthropods and has been confirmed as conferring pyrethroid resistance in electrophysiological studies with the *D. melanogaster para* VGSC (Morgan et al., 2009; Morin et al., 2002; Usherwood et al., 2007). However, both the proximity of V1010F to other substitutions in the VGSC that have been confirmed to confer pyrethroid resistance (Rinkevich et al., 2013) and its presence as a homozygous mutation marks it as a potential subject for further electrophysiological study.

The study has also led to the characterisation of resistance in *R. sanguineus* individuals, the first time that pyrethroid resistance in this species has been linked to target site mutations. The substitution L925I, found in *R. sanguineus* individual RST2 has been linked previously with pyrethroid resistance in several other species (Morin et al., 2002; Rinkevich et al., 2013) and has been confirmed to reduce VGSC sensitivity to pyrethroids by expression in in *X. laevis* oocytes (Usherwood et al., 2007); therefore it is likely that this mutation contributes to conferring the resistance to permethrin shown by RST2. L925I in RST2 is found heterozygously with G933V and with another substitution, F1538L, found in Domain III S6 (Figure 5.2). F1538L has been reported as potentially linked to pyrethroid resistance in the VGSC of the pollen beetle *Meligethes aeneus* (Wrzesinska et al., 2014); and a substitution at the same position, F1538I (He et al., 1999) has been found in several species to date (Rinkevich et al., 2013) and has been confirmed to reduce VGSC sensitivity to pyrethroids by expression in *X. laevis* oocytes (Du et al., 2011). Cloning experiments show that for *R. sanguineus* RST2, L925I

and G933V are found on the same allele, whilst F1538L is found on the opposite allele; therefore, it is possible that in this case the substitutions work in concert to give the observed phenotypic levels of permethrin resistance.

Individual RST1 was homozygous for the substitution G933V, found in the putative pyrethroid binding site (O'Reilly et al., 2006) of Domain II S5 of the VGSC (Figure 8). This was also present in *R. microplus* ticks from Australia, where, the homozygous form remained sensitive to the pyrethroid cypermethrin, which has a comparatively small acidic moiety, but gave resistance to the pyrethroid flumethrin, which has a comparatively large acidic moiety (Jonsson et al., 2010). This specific sensitivity supports the pyrethroid-selectivity model suggested by O'Reilly *et al*, in that the slightly larger valine residue found in resistant ticks would preclude binding of flumethrin but allow the binding of cypermethrin (O'Reilly et al., 2014). It is a shame, therefore, that the resistance phenotype of RST1 is unknown, as this would have given a valuable insight not only into its pyrethroid resistance profile, but into the relationship between residue 933 and pyrethroid selectivity. Like cypermethrin, permethrin has a comparatively small acidic-moiety (Figure 5.5); therefore, the O'Reilly model implies that it is unlikely that the G933V mutation alone would give permethrin resistance; permethrin being small enough to fit into the VGSC without hindrance from the comparatively larger valine residue.

Figure 5.5: The Pyrethroids Cypermethrin and Permethrin

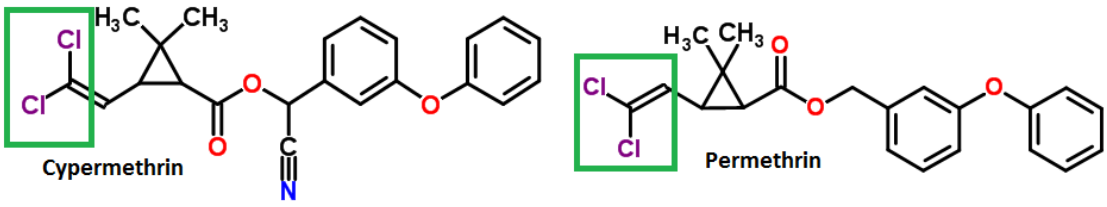

Cypermethrin and permethrin are shown as examples of pyrethroids with small acidic moieties. Areas of interest within the acidic portion are highlighted by green boxes. Both pyrethroid structures are from ChemSpider 2016.

In flumethrin-resistant Australian *R. microplus* ticks, G933V and L925I were found heterozygously on opposite alleles (Jonsson et al., 2010), suggesting that they may act in combination to confer resistance. Interestingly, the resistance profile of these individuals showed them to be resistant to flumethrin but not to cypermethrin (Jonsson et al., 2010); supporting the model proposed by O'Reilly *et al* 2014. In the *R. sanguineus* individual RST3 in the present study, G933V and F1538L are also found heterozygously on opposite alleles, suggesting that they too could act in combination in a similar manner to confer resistance. However, if the model proposed by O'Reilly *et al* 2014 is correct, then the combination of G933V and F1538L in RST3 would not confer resistance to permethrin; its comparatively small acidic moiety would allow it to bind to channels containing a valine at position 933 (Figure 5.5). It could be that F1538L alone gives target site resistance, as suggested case for heterozygous F1538L pollen beetles (Wrzesinska et al., 2014). Alternatively, in both RST3 and pollen beetles metabolic resistance could be involved, and such resistance has been characterised previously in both species (Miller et al., 2001; Philippou et al., 2011).

It would be useful to do further studies of the *R. sanguineus* ticks from this geographical area to get a better understanding of their resistance to permethrin and how this might inform the pyrethroid binding model, proposed by O'Reilly *et al* in 2014, and which is under investigation in the present study. It would be relevant to test the susceptibility of such ticks to a range of pyrethroids, to see whether their resistance profiles differ for pyrethroids with large acidic moieties such as flumethrin. Further examination of sequence data from both survivors and susceptible individuals could then identify any target site mutations involved. If ticks which survive a flumethrin treatment, but not a permethrin treatment, are homozygous for G933V (like RST1), this would support the model.

6 Progress in Obtaining a Chimeric Arthropod VGSC

6.1 Chapter Introduction and Aims

Study of a tick VGSC by expression in *X. laevis* oocytes has been frustrated by the lack of a complete sequence encoding such a channel. Attempts to use of Rapid Amplification of cDNA Ends (RACE) and a *R. microplus* Illumina transcriptome to provide the sequence of a 5' end of a tick VGSC were also unsuccessful in the current study (Chapter 5). Therefore, the aim of the present chapter was to produce a chimeric channel with the domain-spanning sequence and functionality (voltage sensing and pore forming domains) of a *R. microplus* channel but with the N and C termini of an insect, *D. melanogaster*, VGSC. The resulting construct would be expected to function as a *R. microplus* channel when expressed in *X. laevis* oocytes and could thus be used to investigate pyrethroid activity at an acarine VGSC; allowing comparison of pyrethroid selectivity between acarine and insect VGSCs to inform targeted pesticide application.

R. microplus was chosen because of the economic burden of treatment against this parasite, and because it was the only tick species that had been shown to have target-site mediated pyrethroid resistance (Rinkevich et al., 2013).

6.2 Chapter Specific Methods

6.2.1 *para* 13-5 Mutagenesis and Primer Design

A construct containing a functional *D. melanogaster para* VGSC was supplied by Martin Williamson (Rothamsted Research, Hertfordshire, UK). This construct, *para* 13-5 (Warmke et al., 1997), is the plasmid vector pGH19 containing the *D. melanogaster para* VGSC flanked by the 5' and 3' untranslated *X. laevis* beta-globin sequences, to stabilize heterologous cRNAs expressed in *X. laevis* oocytes (Liu et al., 1996).

To create a *R. microplus/D. melanogaster* chimeric VGSC construct, it was first necessary to find sites that would allow the creation of unique restriction sites in *para* 13-5 by site-directed mutagenesis to enable the insertion of the domain-spanning (or functional) region of the *R. microplus* VGSC into the *D. melanogaster para* channel. The *D. melanogaster para* VGSC gene and the *R. microplus* domain regions were aligned in Geneious (Section 4.14) and two suitable restriction enzymes were identified; AflII (New England Biolabs® Incorporated) at the 5' end and AbsI (SibEnzyme®) at the 3' (Figure 6.1). The primers used to create AbsI and AflII sites in the *D. melanogaster para* VGSC are listed in Table 6.1.

Figure 6.1: The *para* 13-5 Construct Showing the Modifications Needed to Generate the *R. microplus/D. melanogaster para* chimeric VGSC Construct

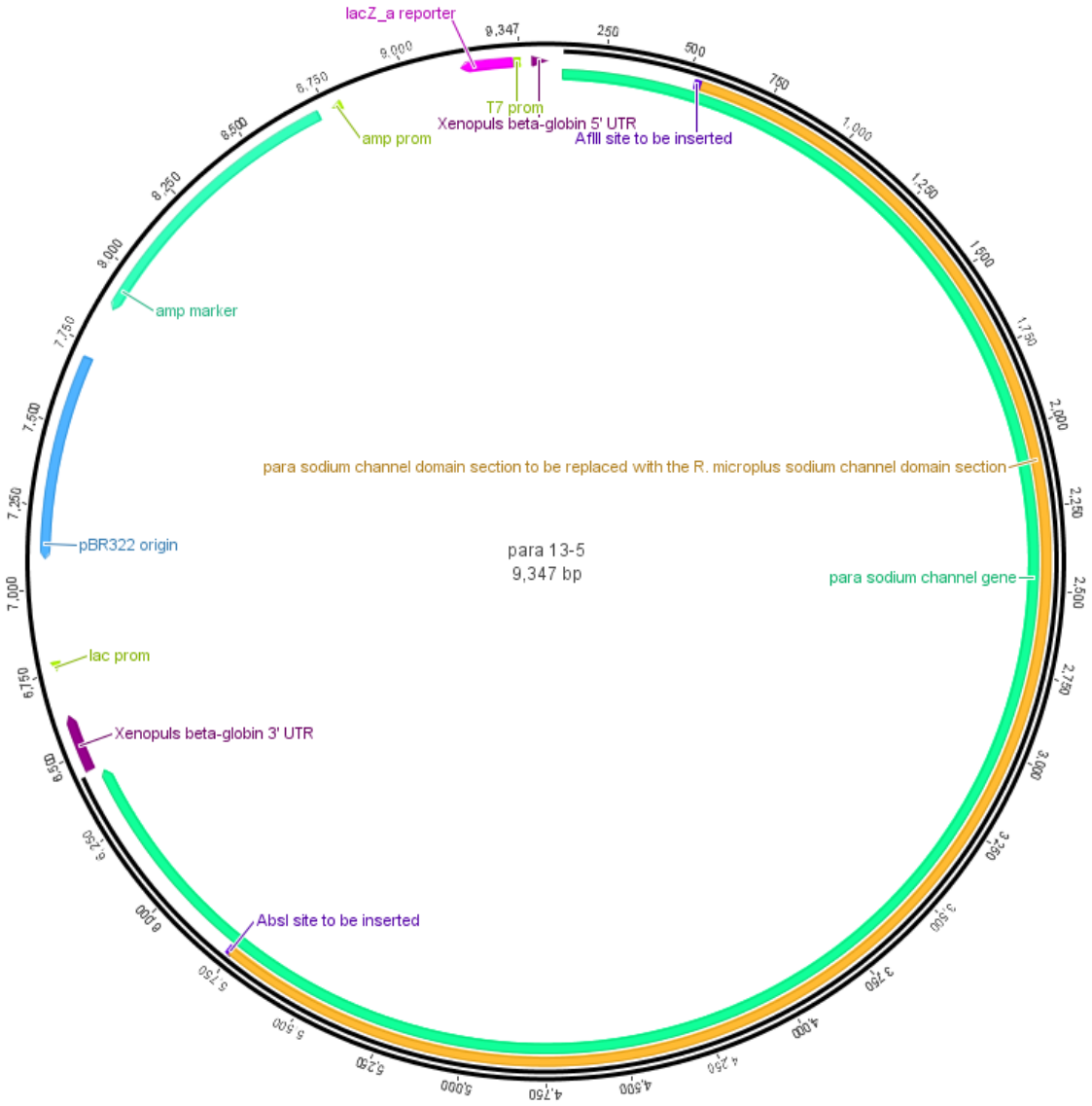

The *para* 13-5 construct used in the creation of a *D. melanogaster para*/R. *microplus* chimeric VGSC. To create the channel construct, mutagenesis of the existing *para* 13-5 construct was performed to insert cut sites for the restriction enzymes AflII and AbsI. At the same time, PCR was used to generate complimentary sites at the end of the domain-spanning regions of the *R. microplus* VGSC. Restriction digestion and subsequent ligation would give a chimeric *D. melanogaster para/R. microplus* VGSC channel construct.

Table 6.1: Primers Used to Create AbsI and AflII Sites in the *D. melanogaster para* gene in *para* 13-5

Name	Restriction Site Progress	Sequence 5'-3'	Base Pairs
ParaMut5'F3M	First 3 mutations towards AflII site	GCAATGTGGCTCTTCGATCCATTCAATCCGATACGTCGTGTGGCC	45
ParaMut5'R3M	First 3 mutations towards AflII site	GGATTGAATGGATCGAAGAGCCACATTGCTTTTGATGCAGAAAAGCG	47
ParaMut5'F	AflII site complete	GCAATGTGGCTCTTAAGTCCATTCAATCCGATACGTCGTG	40
ParaMut5'R	AflII site complete	GGATTGAATGGACTTAAGAGCCACATTGCTTTTGATGCAG	40
ParaMut3'F3M	First 3 mutations towards AbsI site	TTCCTGGACGCCCTCGAGCCCCCGCTGCAGATCC	34
ParaMut3'R3M	First 3 mutations towards AbsI site	TCTGCAGCGGGGGCTCGAGGGCGTCCAGGAATTCG	35
ParaMut3'F	AbsI site complete	TTCCTGGACGCCCTCGAGGAGCCGCTGCAGATCC	34
ParaMut3'R	AbsI site complete	TCTGCAGCGGCTCCTCGAGGGCGTCCAGGAATTCG	35

Mutagenesis of *para* 13-5 to create the AflII and AbsI sites used the QuikChange II XL Site-Directed Mutagenesis Kit (Agilent Technologies) and the primers shown in Table 6.1. Two rounds of mutagenesis were required; in the first reaction, primers were designed to generate the first three mutations needed to create each restriction site, and in the second reaction the primers were designed to give complete restriction sites. Each mutagenesis reaction the cycling parameters shown in Table 6.2.

Table 6.2: PCR Conditions for the Creation of AbsI and AflII Sites in *para* 13-5.

Segment	Cycles	Temperature	Time
1	1	95°C	1 minute
2	18	95°C	50 seconds
		60°C	50 seconds
		68°C	1 minute per Kb of plasmid
3	1	68°C	10 minutes

After the mutagenesis of *para* 13-5 the sequence was checked by sequencing a second AbsI site, previously unknown in the plasmid due to a prior sequencing discrepancy, was located. This was removed by a further round of site-directed mutagenesis using the same protocol as shown in Table 6.2 and the primers shown in Table 6.3.

Table 6.3: Primers Used to Remove Second AbsI Sites from *para* 13-5

Name	Sequence 5'-3'	Base Pairs
AbsI2MutF	CGGCCGCCTCCAGGCTAGCTTGAGTATC	45
AbsI2MutR	AAGCTAGCCTGGAGGCGGCCGCCTGCAGG	47

6.2.2 Amplification of the Domain-Spanning Region of the *R. microplus* VGSC

The full-length domain (FLD) spanning region of the *R. microplus* VGSC was amplified using the nested PCR protocols detailed in Tables 6.4-6.7. Primers RMFLFA and RMFLRA were designed to create AflII and AbsI sites at the 5’ and 3’ ends respectively of the *R. microplus* VGSC such that the amplicon could be inserted, in frame, into the sites created in *para* 13-5 as detailed in Section 6.2.1. All primer Tm’s were calculated using New England Biolabs’s Q5 Tm Calculator.

Table 6.4: PCR1 Reaction Setup

Component	Negative Control	Reactions	[Final]
5X Q5 Reaction Buffer	10 µl	10 µl	1X
10 mM dNTPs	1 µl	1 µl	200 µM
10 µM RMFLNMFA GACTACGTCCACCACTCGC	2.5 µl	2.5 µl	0.5 µM
10 µM RMFLNMRA TTGCGGGCGAAGAAGTCC	2.5 µl	2.5 µl	0.5 µM
Template	2 µl dH_2O	2 µl cDNA	
Nuclease-Free Water	31.5 µl	31.5 µl	
Q5 High-Fidelity DNA Polymerase	0.5 µl	0.5 µl	0.02 U/µl

Table 6.5: Thermocycling Conditions

Step	Temperature	Time
Initial Denaturation	98°C	1 minute
35 Cycles	98°C	30 seconds
	69°C	30 seconds
	72°C	5 minutes
Final Extension	72°C	5 minutes
Hold	10°C	∞

Table 6.6: PCR2 Reaction Setup

Component	Negative control	Reactions	[Final]
5X Q5 Reaction Buffer	10 µl	10 µl	1X
10 mM dNTPs	1 µl	1 µl	200 µM
10 µM RMFLFA GCGCTGTTTCTCTTAAGCCCCTTCAACC	2.5 µl	2.5 µl	0.5 µM
10 µM RMFLRA GGATCTGCAGAGGCTCCTCGAGGGCGTTCACG	2.5 µl	2.5 µl	0.5 µM
Template	2 µl dH_2O	2 µl PCR1	
Nuclease-Free Water	31.5 µl	31.5 µl	
Q5 High-Fidelity DNA Polymerase	0.5 µl	0.5 µl	0.02 U/µl

CTTAAG = AflII restriction endonuclease site

CCTCGAGG = AbsI restriction endonuclease site

Table 6.7: Thermocycling Conditions

Step	Temperature	Time
Initial Denaturation	98°C	1 minute
35 Cycles	98°C	30 seconds
	72°C	30 seconds
	72°C	5 minutes
Final Extension	72°C	5 minutes
Hold	10°C	∞

The resulting PCR product was fully sequenced using primers shown in Table 5.4.

6.2.3 Ligation Reactions to Create a Chimeric Arthropod VGSC Construct

Firstly a total of 3 µg each of the doubly mutated *para* 13-5 plasmid (the vector) (Section 6.2.1) and the *R. microplus* VGSC PCR product (the insert) (Section 6.2.1) were cut with AflII in 1X CutSmart® Buffer (50 mM Potassium Acetate, 20 mM Tris-acetate, 10 mM Magnesium Acetate, 100 µg/ml BSA) (New England Biolabs® Incorporated) in a total reaction volume of 50µl at 37°C for one hour. Samples were then heated to 65°C for 20 minutes to denature the AflII enzyme. In the same manner 500 ng of un-mutated *para* 13-5 was treated with AflII as a negative control for AflII digestion (Control A). This was frozen along with another control (Control B) of 5 µl cut vector DNA, to act as both a positive vector digestion and a ligation control.

AflII cut Control B (4 µl), insert, and the remaining vector DNA was ethanol precipitated as (Section 4.12) and the pellet resuspended in 49µl AbsI 1X Reaction Buffer (10 mM Tris-HCl (pH 9.0 at 25°C), 10 mM MgCl2, 50 mM KCl, 1mM DTT) (SibEnzyme®). After 1 µl of vector and insert DNA was removed (to act as a control for the efficiency of ethanol precipitation) 2µl of AbsI was added to the AflII-cut vector and insert tubes and both were incubated at 37°C for one hour. Concurrently the following control digestions (controls C-F) were performed in 1X AbsI or 1X Fast Digest reaction buffer at 37°C, in a total volume of 25 µl (Table 6.8).

Table 6.8: Control Reactions

Control	Contents
C	500ng *para* 13-5 cut with Fast Digest NotI (ThermoFisher Scientific).
D	500ng *para* 13-5 with AbsI only.
E	500ng vector with NotI (ThermoFisher Scientific).
F	500ng vector with AbsI only.

All resulting controls and double-digested vector and insert DNA were run overnight on a 1% agarose gel, along with uncut parental *para* 13-5 and uncut vector and insert DNA. The next day the gel was stained with ethidium bromide (0.75 µg/ml) for 30 minutes, then de-stained in 300 ml distilled water before visualisation (Figure 6.2).

Figure 6.2: Gel of DNA Fragments used in the Creation of a Chimeric *D. melanogaster para* and *R. microplus* VGSC Construct.

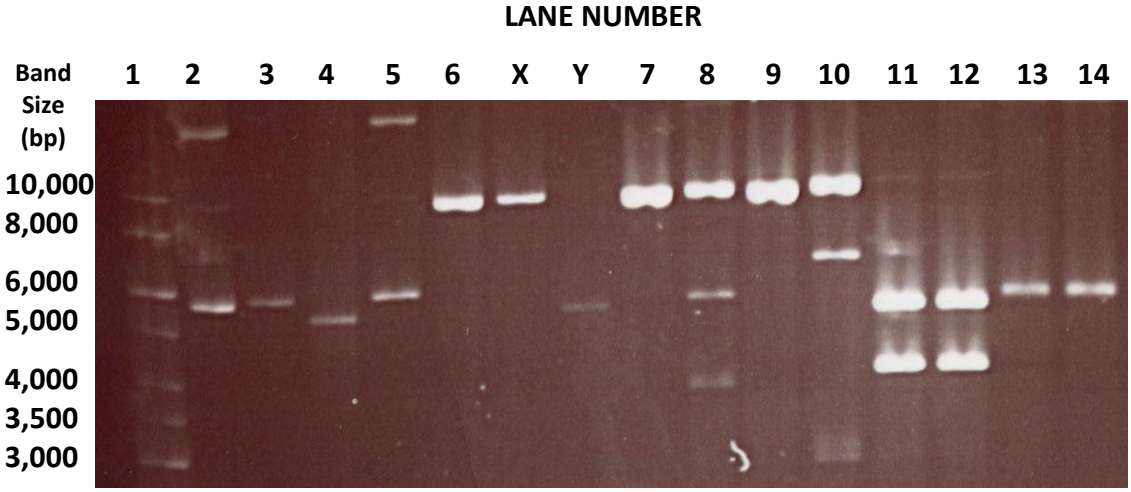

Lane 1 is a 1Kb DNA Ladder (GeneRuler™, Fermentas) with the size, in base pairs, of each band on the left-hand side of the gel image. Lane 2 is uncut *para* 13-5 plasmid, Lane 3 uncut vector and Lane 4 uncut insert. Lane 5 is Control A and Lane 6 Control B (see 6.2.3). Lanes X and Y have 1 µl each of ethanol purified AflII cut vector and insert respectively. Lanes 7-10 are Controls C-F. Double AflII/AbsI digested vector was split between Lanes 11 and 12 and insert between Lanes 13 and 14.

The gel (Figure 6.2) showed that the control A DNA (Lane 5) was uncut, indicating that *para* 13-5 does not have any additional AflII sites. In contrast, Control B (Lane 6) showed that the mutated *para* 13-5 had been cut successfully with AflII to give a linear band. Control X and Y, composed of 1 µl of ethanol purified AflII cut vector and insert DNA, show that DNA was not being lost during the ethanol precipitation process. Controls C and D (Lanes 7 and 8 respectively), showed that *para* 13-5 was cut

successfully with NotI and with AbsI as expected. Controls E and F (Lanes 9 and 10 respectively) showed that the vector was cut successfully with NotI and also with AbsI, although the AbsI digestion was less efficient and possibly showed star activity. The double digested vector DNA (in both Lanes 11 and 12) showed a fragment at approximately 5,200bp, representing the *D. melanogaster para* VGSC domains being removed and a fragment of approximately 4,100 bp, representing the pGH19 vector with *D. melanogaster para* 5' and 3' VGSC tails, as needed to make the chimeric construct. The double digested insert is shown in Lanes 13 and 14. After visualisation bands representing all vector and insert fragments (including the removed *D. melanogaster para* VGSC fragment) and control bands B-F were cut from the gel and the DNA extracted (Section 4.8). Note that the upper vector gel fragments from lanes 11 and 12 were combined, the lower vector gel fragments from lanes 11 and 12 were combined and insert fragments from lanes 13 and 14 were combined to increase the amount of DNA. Samples were eluted into 50 µl nuclease-free water and 1 µl of each was run on a 1% agarose gel to check DNA recovery.

The ligation of the DNA fragments used New England Biolabs's® High-concentration T4 DNA ligase and the ligation mix contained 1000 cohesive end units in a total reaction volume of 10 µl in 1X DNA ligase buffer (50 mM Tris-HCl, 10 mM MgCl2, 1 mM ATP, 10 mM DTT). The construct was made from 2.5µl of prepared vector (pGH19 with 5' and 3' D. melanogaster para channel tails) and 5µl of prepared insert DNA with a DNA quality and ligation control comprising 2.5 µl of prepared vector (pGH19 with 5' and 3' *D. melanogaster para* channel tails) and 5µl of the *D. melanogaster para* VGSC domains removed by double-digest. As a ligation efficacy control 5µl of Controls B-F were added to further separate ligation mixes. The ligations were incubated at 16°C overnight and then 2µl of each was removed and used to transform XL1 Blue *E. coli* (Section 4.10). The remainder of each ligation mix was then incubated for a further 48 hours at 4°C and then 2µl of each was removed and used to transform XL1 Blue *E. coli* (Section 4.10). Plates were incubated for 24 hours at 32°C, resulting colonies were picked and overnight cultures were prepared in 2 ml LB broth containing 50 µg/ml ampicillin (Section 4.7). DNA was prepared from the cultures using a Qiagen mini-prep kit to remove plasmid DNA (Section 4.13). Extracted DNA was sent for sequencing

(Section 4.1) to check the presence and reading frame of the *R. microplus* full-length domain-spanning insert using primers shown in Table 6.9.

Table 6.9: Primers Used to Sequence Chimeric VGSC Constructs

Primer Name	Primer Sequence 5'-3'	Primer Length (Base Pairs)
T7*	TAATACGACTCACTATAGGG	20
RM DIS1 R	GGTGCACTAGGATGCAGATG	20
RM DIS1 F	CATCTGCATCCTAGTGCACC	20
RM DIS3 F	GGATTTTGTTGTTATATCTCTAGCG	25
RMSeqCheck5'	CGCTAGAGATATAACAACAAAATCC	25
DI-II FCP F	CCTGGGCTCCTTCTATCTAGT	21
DI-II FCP R	AGCAATTGGCCATGCACTTG	20
DII FCP F	CGCTATTCATGGCCATGGAC	20
RM DIIS2 R	CATAAGCTTCATTCCAGC	18
RM DIIS2 F	GCTGGAATGAAGCTTATG	18
RM DII-III R	GTCGGGATTCGCTTGGGACAG	21
RM DII-III F	CTGTCCCAAGCGAATCCCGAC	21
RM DII-III RB	GTGTCCACATCTTCCGTGTC	20
RM DII-III FB	GACACGGAAGATGTGGACAC	20
D II-III FCP R	ATCGCGTGTAACACCAGTCG	20
RM DIIIS5 R	CTTTCCCGCAAGCATCTGGA	20
RM DIIIS5 F	TCCAGATGCTTGCGGGAAAG	20
RM DIVS3 R	AGGTCCTTTAGCACCGTACC	20
RM DIVS3 F	GTGCTAAAGGACCTGATCGC	20
RMSeqCheck3'	CTTGTGATGTTCATCTACGC	20
ParaRMCheckF	ACCTCATCATCAGCTTCCTCG	21
RM PostDIV R	TTGGTCAGGTTGGAGTAGGC	20
RM PostDIV F	GCCTACTCCAACCTGACCAA	20

***T7 Universal Primer designed to anneal to the T7 promoter sequence found in pGH19 (Sambrook and Green, 2012).**

6.2.4 Removal of a NotI Site from the *R. microplus* Sequence

As the native *R. microplus* channel (Section 10.1 Appendix 1) contains a NotI restriction site and this enzyme was used to linearize plasmid vector pGH19 prior to cRNA transcript preparation (Chapter 7) the chimeric constructs underwent site-directed mutagenesis to remove this site following the protocol shown in Table 6.2 and the primers shown in Table 6.10. The constructs were fully sequenced after this process (using primers shown in Table 6.9) to check for additional any mutations that might have been introduced.

Table 6.10: Primers Used to Remove Second NotI Sites from Chimeric Constructs

Name	Sequence 5'-3'	Base Pairs
NotI Removal F	CCGGAGTCGCGCCCGCGCTCCGCCGCC	27
NotI Removal R	GCGGAGCGCGGGCGCGACTCCGGGTAG	27

6.3 Results

6.3.1 Creation of R. microplus/D. melanogaster para Chimeric VGSCs

Three chimeras were successfully created, constructs C*himera L2*, *Chimera L4* and *Chimera LC* (Figure 6.3). All three resulted in slow growth when they transformed *E. coli* a characteristic noted previously in *E. coli* containing functional arthropod VGSCs (Martin Williamson and Joel González-Cabrera personal communication). However, whilst all constructs contained the *R. microplus* functional domains successfully ligated into the *D. melanogaster para* channel, subsequent sequencing revealed that all sequences contained premature stop codons. Note that these were present in *Chimera LC* and *Chimera L4* both before and after removal of the NotI site. *Chimera L2* and *Chimera L4* were found to be identical, and both contained a frame-shift mutation between Domains I and II, caused by the deletion of amino acids and resulting in the creation of many stop codons before the start of Domain II in both clones (Figure 6.3). A further deletion also occurred in these clones, in an area homologous to optional exon b, a removal variation first described in the D*. melanogaster para* VGSC and since documented several arthropod species (Dong et al., 2014; Loughney et al., 1989). This deletion alone would not cause a frame shift in the channel (Figure 6.3). Finally, a probable alternative exon is was present in *Chimera L2/L4*, in a homologous position to that of variations seen in other arthropods. This variable region was first described as the mutually exclusive exons k and l in the *M. domestica Vssc1* and D*. melanogaster para* VGSCs, and was subsequently documented in two other arthropod species, *B. germanica* and *V. destructor* (Dong et al., 2014; Lee et al., 2002). *Chimera* LC was found to contain a point-mutation encoding a stop codon between Domains I and II, in place of a tryptophan in the native *R. microplus* channel (Figure 6.3). The full sequences of *Chimera LC* and *Chimera L2/L4* can be found in Section 10.3 Appendix 3.

Figure 6.3: Comparison of the *R. microplus*, *Chimera L2*, *Chimera L4*, and *Chimera LC* VGSCs over Variable Regions of Interest.

Chimera constructs *Chimera LC*, *Chimera L2* and *Chimera L4* compared over variable regions to each other and the *R. microplus* full-length domain PCR product shown in Section 10.1 Appendix 1 and detailed in Chapter 5.

(A)

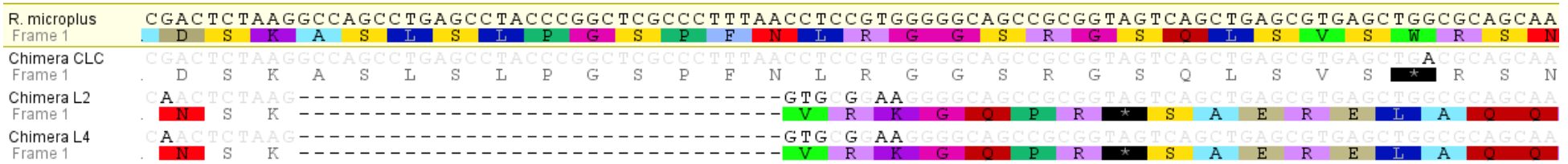

The first deletion region in *Chimera L2* and *Chimera L4*, giving a frame shift in these clones and causing subsequent stop codon creation. Also the guanine to adenine mutation resulting in the creation of a tryptophan to stop substitution in *Chimera LC*. The *R. microplus* PCR product (Chapter 5) (Section 10.1 Appendix 1) is set as the reference sequence and colour highlighting indicates variations from this sequence.

(B)

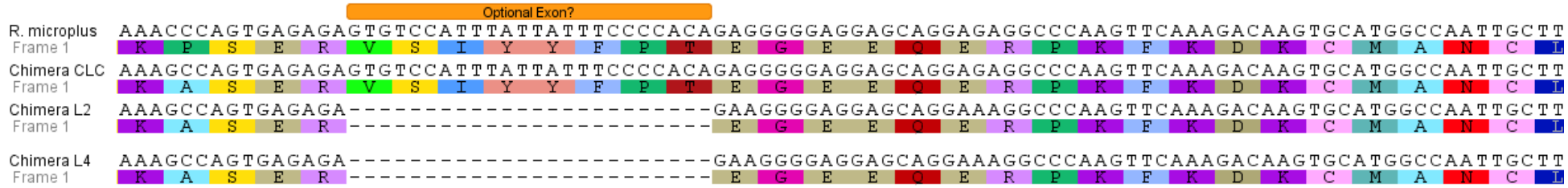

The second deletion region in *Chimera L2* and *Chimera L4* around a region corresponding to optional exon b in other arthropods (Dong et al., 2014). This is shown removing the frame shift created by the first deletion for clarity.

(C)

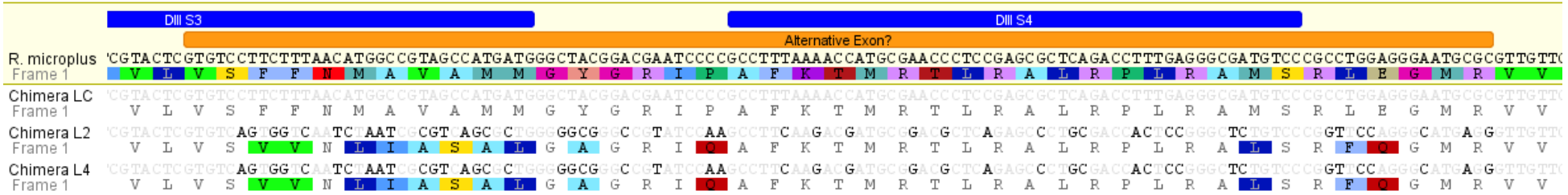

The variable region found in *R. microplus* constructs corresponding to the mutually exclusive exons k and l in *D. melanogaster* and *M. domestica*, exon 3 in *V. destructor* (Wang et al., 2003), and exons G1, G2 and G3 in *B. germanica* (Tan et al., 2002). The *R. microplus* PCR product (Chapter 5) (Section 10.1 Appendix 1) is set as the reference sequence and colour highlighting indicates variations from this sequence.

Given the importance of obtaining a functioning *R. microplus*/*D. melanogaster* VGSC, attempts were made using site-directed mutagenesis to change the stop codon in *Chimera LC* back to a tryptophan, and to remove a guanine nucleotide from around the Exon b removal site in *Chimera L4* and *Chimera L2* to correct the frame shift. Although the mutagenesis reactions were successful, all resulting constructs were further mutated, presumably by the *E. coli*, and would not be expected to express functional VGSCs. As found when *X. laevis* oocytes were injected with cRNA from a similarly truncated channel from *B. germanica* (Tan et al., 2002). Further attempts to obtain a functional VGSC used Chimera *LC* as a start point. These attempts included:

- Changing the *E. coli* cell type used for growth following mutagenesis (XL1 Blue, XL10 Gold and Stbl2 cells were all used),
- Lowering the growth temperature to room temperature,
- Using carbenicillin in place of ampicillin in LB growth media,
- Mutagenesis then removal of the T7 promoter from the construct,
- Colony PCR of transformed *E. coli* prior to liquid culture growth using primers designed to amplify the full-length chimeric channel,
- A "ZIP-PCR" as an alternative to site-directed mutagenesis; this involves two rounds of PCR, with the first designed to amplify the two halves of the construct and in the process remove the stop codon, and the second to "zip" these two halves together and give a full-length channel.

6.4 Discussion

In summary none of the attempts to create *R. microplus*/*D. melanogaster* chimeric VGSC constructs for functional studies were successful, which was very disappointing. However, future work on the constructs might produce a functional channel. Moving the chimeric VGSC and *X. laevis* Beta-globin sequences to different bacterial expression vectors, to see if this stabilises the construct in *E. coli*, is a potential solution. As is moving these regions to an insect expression vector, then attempting maintenance, and even chimeric channel expression, in insect cells. Any VGSC expression could then be monitored using patch-clamp techniques.

In addition, there are some interesting wider inferences to be made from the data obtained in this study. Despite their frame-shift deletion, *Chimera L2* and *Chimera L4* showed possible alternative exon usage within the *R. microplus* VGSC, which is comparable to that seen in other arthropods (Dong et al., 2014). Firstly around an area homologous to optional exon b, a variation first described in the D*. melanogaster para* channel and since documented in several arthropod species (Dong et al., 2014; Loughney et al., 1989). This exon is suspected to be involved in the modulation of current flow, as removal of this region has been shown to increase current expression of *B. germanica* and *V. destructor* channels (Du et al., 2009a; Song et al., 2004). Furthermore, *Chimeras L2/L4* showed alternative exon usage in a homologous position to that of mutually exclusive exons k/l, a variation first described in the *M. domestica Vssc1* and D*. melanogaster para* VGSCs (Dong et al., 2014; Lee et al., 2002) (Figure 15). This region is also homologous to sites of variation documented in two other arthropod species, *B. germanica and V. destructor*. In *B. germanica* the same region contains one of three mutually exclusive exons G1, G2 or G3, with G3 encoding a stop codon and thus a truncated channel protein that is not functional in *X. laevis* oocytes (Tan et al., 2002). In *V. destructor* the same region contains exon 3, which interestingly is either present or absent, and thus would also encode a truncated channel protein (Wang et al., 2003). The arrangement of this region is homologous to, and conserved in, the vertebrate VGSC $Na_v1.6$. As found in mice, humans and fish (Plummer et al., 1997). This level of conservation suggests that alternative splicing in this region is likely

of ancient evolutionary origin and that it may play a role in the control of VGSC expression and/or function (Dong et al., 2014). Indeed it has been shown that the amino acid sequence within this exon region modulates the generation of a persistent current in the *D. melanogaster para* channel, with channels containing exon l showing greater persistent currents (so maintaining the open state for longer) than those containing exon k (Lin et al., 2009). This is supported by findings that alternative splicing that includes exon l over exon k is associated with increased neuronal activity (Lin et al., 2012). All chimeric constructs created in the present study show a slightly greater level of similarity to exon l in *D. melanogaster para* (Figure 6.4). However, *Chimera LC* and the *R. microplus* PCR product (Chapter 5) (Section 10.1 Appendix 1) show less similarity to this exon than do *Chimeras L2*/*Chimera L4*, and interestingly these sequences also show less similarity to the published sequence for *I. scapularis* and *V. destructor*. It could be therefore that *Chimera LC* and the *R. microplus* PCR product represent an “exon k” or “G2” type variant in *R. microplus*.

Figure 6.4: A Comparison of the Conserved Variable Region in Domain III Segments 3 and 4 of Arthropod VGSCs

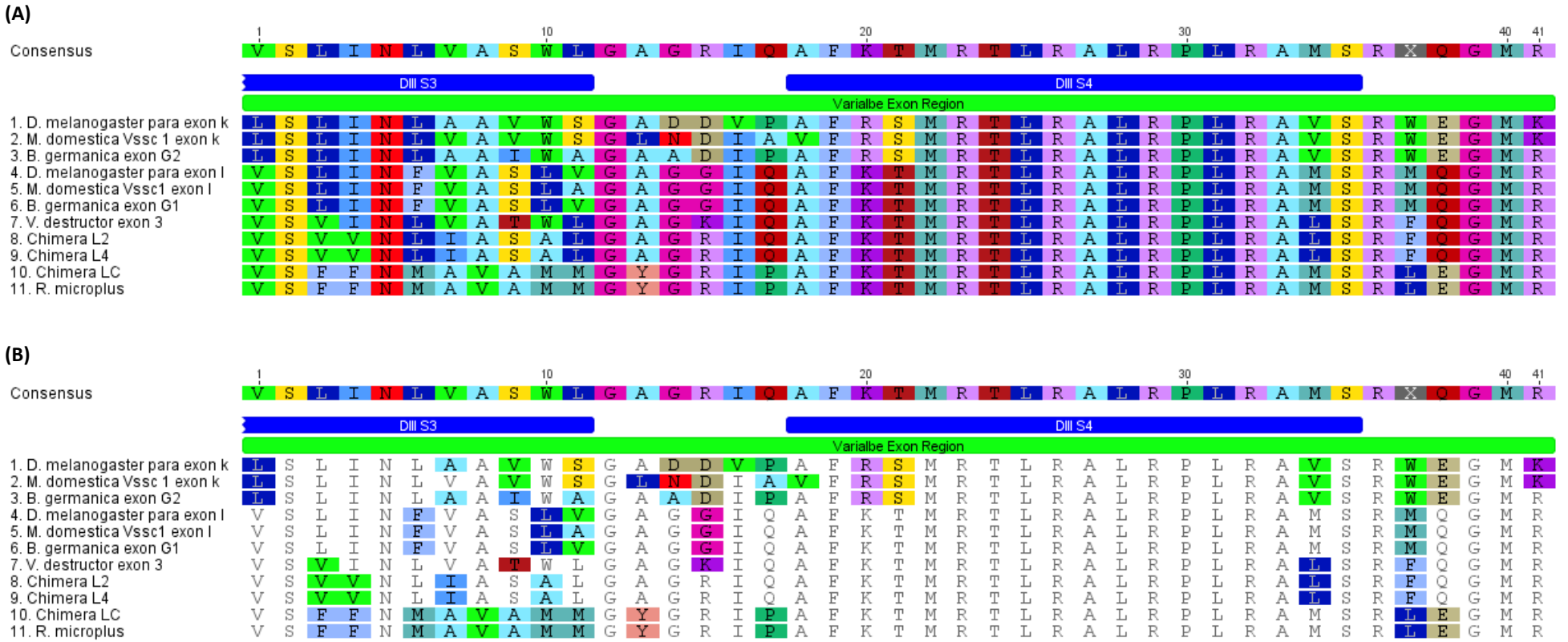

Comparison of the variable region found in Domain II Segments 3 and 4 of selected arthropod VGSCs. (A) The region with no highlighting. (B) The region highlighting differences to the sequence consensus. The sequence for *D. melanogaster* and *M. domestica* was taken from Lee *et al* 2002, *B. germanica* from Tan *et al* 2002, and *V. destructor* from Wang *et al* 2003. Sequences for *R. microplus* and chimeric constructs are from the current study.

It would be interesting to investigate the use of alternative exons found in this study in *R. microplus*, including in different developmental stages and tissue types, as this could help target pyrethroid control strategies to a particular tick life-stage. Variation in expression is already seen in exon G1/G2/G3 in different life stages of *B. germanica* (Tan et al., 2002). This could be informative from an acarine control perspective, as such variation in channel structure could affect pyrethroid action at the *R. microplus* VGSC, given that pyrethroids act by increasing current persistence (Davies et al., 2008) and considering the link between exon k/l variation and current persistence reported (Lin et al., 2009). Furthermore, *D. melanogaster para* VGSCs expressing the k exon variation have been reported to be 24 times less sensitive to the pyrethroid deltamethrin than those expressing the l exon variation (Burton, 2012), Further work could therefor also involve inserting the suspected *R. microplus* exon "l" and "k" sequences separately in place of the same region in the *D. melanogaster para* or *V. destructor* VGSC. By employing the same investigative methods as in Chapter 7, it would then be possible to investigate the effects of *R. microplus* "exon k/l" usage on pyrethroid sensitivity using electrophysiological methods.

7 Electrophysiological Studies of Acarine and Insect VGSCs

7.1 Chapter Introduction and Aims

The aim of this chapter was to compare insect and acarine VGSC function and test the idea, proposed by O'Reilly *et al* 2014, that residue 933 is involved in pyrethroid selectivity; to this end both native and mutated versions of the arthropod VGSCs were expressed in *X. laevis* oocytes. Differences in VGSC responses to pyrethroid insecticides with large and small halogenated-groups could then be recorded using TEVC techniques (Section 3.6). Disappointingly, a *R. microplus*/*D. melanogaster* chimeric channel could not be successfully maintained in *E. coli* (Chapter 6) so the studies were done using native and mutant VGSCs from *D. melanogaster* and the honeybee mite *V. destructor*. The native VGSC constructs used were *D. melanogaster para* 13-5 (as cloned by Feng *et al* 1995) (Section 6.2.1) and *V. destructor* 13-5 (the plasmid vector pGH19 containing the *V. destructor* VGSC flanked by the 5' and 3' untranslated *X. laevis* beta-globin sequences, as cloned by Joel González-Cabrera at Rothamsted Research).

7.2 Chapter Specific Methods

7.2.1 Mutagenesis of *D. melanogaster para* VGSC at Residue 933

Mutagenesis of the *D. melanogaster para* VGSC construct *D. melanogaster para* 13-5 was carried out using the QuikChange II XL Site-Directed Mutagenesis Kit (Agilent Technologies) (Section 4.15). Primers (Table 7.1) were designed to change the residue from a cysteine in most native insect VGSCs, including the *D. melanogaster para* VGSC, to either:

- An alanine: As found in some mite species at position 933.
- A glycine: As found at position 933 in all tick and most mite species sequenced to date.
- A valine: As found at position 933 in *R. microplus* ticks which are sensitive to cypermethrin (which has a relatively small acidic moiety), but resistant to flumethrin (with a relatively large acidic moiety) (Jonsson et al., 2010).

Table 7.1: Primers Used to Change Residue 933 of the *D. melanogaster para* VGSC

Name	Sequence 5'-3'	Base Pairs
ParaMutC933AF	GTAATCTGACATTTGTACTTGCCATT ATCATCTTCATCTTTGCGGTGATG	50
ParaMutC933AR	CGCAAAGATGAAGATGATAATGGCA AGTACAAATGTCAGATTACCCAAAG	50
ParaMutC933GF	GTAATCTGACATTTGTACTTGGCATT ATCATCTTCATCTTTGCGGTGATG	50
ParaMutC933GR	CGCAAAGATGAAGATGATAATGCCA AGTACAAATGTCAGATTACCCAAAG	50
ParaMutC933VF	GTAATCTGACATTTGTACTTGTCATT ATCATCTTCATCTTTGCGGTGATG	50
ParaMutC933VR	CGCAAAGATGAAGATGATAATGACA AGTACAAATGTCAGATTACCCAAAG	50

All mutagenesis reactions were cycled using the cycling parameters shown in Table 7.2

Table 7.2: PCR Conditions Used for Mutagenesis of Residue 933 of the *D. melanogaster para* VGSC

Segment	Cycles	Temperature	Time
1	1	95°C	1 minute
2	18	95°C	50 seconds
		60°C	50 seconds
		68°C	10 minutes
3	1	68°C	10 minutes

Following mutagenesis, 2µl of each sample was transformed into Stratagene's XL1 Blue ultracompetent cells and with non-mutated *D. melanogaster para* 13-5 was used as a growth control (Section 4.10). Following growth at 30°C, small colonies that grew in the same way as the control colonies containing the native *D. melanogaster para 13-5,* were picked, along with a control colony, and grown in LB liquid media containing 50 µg/ml Amp. After 24-48 hours, plasmid DNA from colonies that grew at the same rate as the native *D. melanogaster para* 13-5 control were purified using a mini-prep (Qiagen), plasmid DNA was also purified form a colony of the native *D. melanogaster para* 13-5 control (Section 4.13). Extracted plasmids were then used as templates in PCR reactions that amplified the *D. melanogaster para* VGSC gene region of the constructs, along with the 5' and 3' untranslated *X. laevis* beta-globin sequences. This allowed an increase in the amount of VGSC gene DNA available for sequencing. PCR

reactions were carried out using New England Biolabs's Q5® High-Fidelity DNA Polymerase (Q5) the reagents, pGH19-specific primers, and cycling conditions are shown in Tables 7.3 and 7.4.

Table 7.3: PCR Reagents Used in the Amplification of VGSCs in *D. melanogaster para* 13-5

Component	Negative Control	Reactions	[Final]
5X Q5 Reaction Buffer	10 µl	10 µl	1X
10 mM dNTPs	2 µl	1 µl	400 µM
10 µM 5'_UTR_3_F Primer GGGATGTGCTGCAAGGCGATTAAG	2.5 µl	2.5 µl	0.5 µM
10 µM 3'_UTR_3_R Primer GTATAGATACTCAAGCTAGCCTCG	2.5 µl	2.5 µl	0.5 µM
Template	0.5 µl dH_2O	0.5 µl *para* 13-5 Template	
Nuclease-Free Water	32 µl	32 µl	
Q5 High-Fidelity DNA Polymerase	0.5 µl	0.5 µl	0.02 U/µl

Table 7.4: PCR Reaction Conditions Used in the Amplification of VGSCs in *D. melanogaster para* 13-5

Step	Temperature	Time
Initial Denaturation	98°C	30 seconds
35 Cycles	98°C	10 seconds
	68°C	20 seconds
	72°C	7 minutes
Final Extension	72°C	5 minutes
Hold	10°C	∞

The products of the PCR reactions were analysed for the presence of the required PCR product using gel electrophoresis on a 1% agarose gel in 1xTAE. The DNA was then precipitated (Section 4.2) and sent for sequencing (Section 4.14) using the primers shown in Table 7.5, to check the success of the mutagenesis reaction and confirm that no additional mutations had occurred during the transformation into *E. coli*.

Table 7.5: Primers Used to Sequence VGSCs in *D. melanogaster para* 13-5

Name	Sequence 5'-3'	Base Pairs
598_F_Dm	TGCCCGTTTACGTATCTTAGAG	22
705_R_Dm	TCGCAGGGCTGCTAGATTAC	20
1251_F_Dm	TTTGATTTTGGCCATTGTTG	20
1353_R_Dm	AGCTTCTTCCGCTTCACGTA	20
1909_F_Dm	TATACCTCGCATCAGTCCCG	20
2001_R_Dm	CTCCTTGGTCATTGTGCTGA	20
2548_F_Dm	TATTTCTTCACCGCCACCTT	20
2640_R_Dm	GAAGATGTTCCAGCCCTCCT	20
3203_F_Dm	GGGTTAAGCGTAATATTGCTGA	22
3854_F_Dm	TGAGTAGCTTAGCTTTGGCA	20
3953_R_Dm	AATATAACCGTAAATATTCTGTCCA	25
4497_F_Dm	ACCAATTCGTGAAACGAACA	20
4594_R_Dm	TGATAACACCAATGAACAGATTGA	24
5158_F_Dm	CTGTTCAACATCTGCCTGCT	20
5800_F_Dm	GAGATTGGTGAGATAGCGGC	20
5898_R_Dm	GATTAGCCGGGCGCAGTA	18

7.2.2 Mutagenesis of the *V. destructor* VGSC at Residue 933

Mutagenesis of the *V. destructor* VGSC was done as described in 7.2.1 using the QuikChange II XL Site-Directed Mutagenesis Kit (Agilent Technologies) (Section 4.15). Primers were designed (Table 7.6) to change the residue at position 933 in the *V. destructor* VGSC to either:

- A cysteine: As found at position 933 in most insect species including *D. melanogaster*.
- A valine: As found at position 933 in *R. microplus* ticks which are sensitive to cypermethrin (which has a relatively small acidic moiety), but resistant to flumethrin (with a relatively large acidic moiety) (Jonsson et al., 2010).

Table 7.6: Primers Used to Change Residue 933 of the *Varroa* 13-5 at Residue 933

Name	Sequence 5'-3'	Base Pairs
VarroaMutG933CF	GCTCTGGGTAACCTGACCTTT GTGTTGTGCATTATCATCTTC	42
VarroaMutG933CR	GATGATAATGCACAACACAAA GGTCAGGTTACCCAGAGCTCC	42
VarroaMutG933VF	GCTCTGGGTAACCTGACCTTT GTGTTGGTAATTATCATCTTC	42
VarroaMutG933VR	GATGATAATTACCAACACAAA GGTCAGGTTACCCAGAGCTCC	42

All mutagenesis reactions were cycled using the cycling parameters shown in Table 7.7.

Table 7.7: PCR Conditions Used for Mutagenesis of Residue 933 of the *V. destructor* VGSC

Segment	Cycles	Temperature	Time
1	1	95°C	1 minute
2	18	95°C	50 seconds
		60°C	50 seconds
		68°C	10 minutes
3	1	68°C	10 minutes

Following mutagenesis samples were cloned into Stratagene's XL1 Blue and XL10 Gold ultracompetent cells and Invitrogen's MAX Efficiency® Stbl2™ competent cells a non-mutated *D. melanogaster para 13-5* was used as a growth control (Section 4.10).

Following growth at 30°C, small colonies that grew in the same way as the control colonies were picked, along with a control colony and grown in LB liquid media containing 50 µg/ml Amp. The same colonies were used in colony PCR reactions (Section 4.11) to obtain the full-length *V. destructor* VGSC gene region of the *V. destructor 13-5* constructs, along with the 5' and 3' untranslated *X. laevis* beta-globin sequences needed to stabilize the heterologous cRNAs when expressed in *X. laevis* oocytes (Liu et al., 1996). Following colony PCR, the wild-type *V. destructor 13-5* construct and each amplicon was used as a template in a nested PCR reaction to amplify the gene region of the *V. destructor 13-5*, along with the 5' and 3' untranslated *X. laevis* beta-globin sequences. This allowed an increase in the amount of DNA available for sequencing and provided linear products for reverse transcription. PCR

reactions were carried out using New England Biolabs's Q5® High-Fidelity DNA Polymerase (Q5). The reagents, pGH19-specific primers and cycling conditions in Tables 7.8 and 7.9.

Table 7.8: Reagents Used Nested PCR to Amplify *V. destructor* 13-5 Products Following Colony PCR

Component	Negative Control	Reactions	[Final]
5X Q5 Reaction Buffer	10 µl	10 µl	1X
10 mM dNTPs	2 µl	1 µl	400 µM
10 µM Nested 5'_UTR_3_F GGCGATTAAGTTGGGTAACG	2.5 µl	2.5 µl	0.5 µM
10 µM Nested 3'_UTR_3_R TACTCAAGCTAGCCTCGAGG	2.5 µl	2.5 µl	0.5 µM
Template	0.5 µl dH_2O	0.5 µl *Varroa 13-5* Template	
Nuclease-Free Water	32 µl	32 µl	
Q5 High-Fidelity DNA Polymerase	0.5 µl	0.5 µl	0.02 U/µl

Table 7.9: Nested PCR Conditions Used in the Amplification of *Varroa* 13-5 Products Following Colony PCR

Step	Temperature	Time
Initial Denaturation	98°C	30 seconds
35 Cycles	98°C	10 seconds
	64°C	20 seconds
	72°C	7 minutes
Final Extension	72°C	5 minutes
Hold	10°C	∞

The products of the PCR reactions were analysed for the presence of the required PCR product using gel electrophoresis on a 1% agarose gel in 1xTAE (Section 4.2). The DNA was then precipitated (Section 4.12) and sent for sequencing (Section 4.14) using the primers shown in Table 7.10, to check the success of the mutagenesis reaction and confirm that no additional mutations had occurred during the transformation into *E. coli*.

Table 7.10: Primers Used to Sequence *V. destructor* VGSC Products from Colony PCR and Nested PCR Amplification of *Varroa* 13-5 Constructs

Name	Sequence 5'-3'	Base Pairs
T7*	TAATACGACTCACTATAGGG	20
Vd_420_R	CTCTACAGGTGTGGCGATCA	20
Vd_653_F	CCGAAACAATATTCACGACG	20
Vd_1356_F	CAATCTGATTCTCGCCATTG	20
Vd_2043_F	CGTAGACGCTCAGGAACACC	20
Vd_2751_F	TTTCTTCACCGCTACCTTCG	20
Vd_3448_F	GGTAAACAGCGCAACCAGAT	20
Vd_4146_F	CGCAGAAGGAAAAGAAAACG	20
Vd_4846_F	GGCAGATTCTACCACTGCGT	20
Vd_5560_F	CTTTCGATCCTTGGCACAGT	20
Vd_6251_F	AGTACAAGCTGATCGCGCTG	20

***T7 Universal Primer designed to anneal to the T7 promoter sequence found in pGH19 (Sambrook and Green, 2012).**

7.2.3 Preparation of DNA for in vitro Transcription

Prior to *in vitro* transcription of VGSCs contained in pGH19, the plasmids were linearized using the NotI as shown in Table 7.11.

Table 7.11: Components of Plasmid Linearization Reactions Using Not1

Component	Amount
para 13-5 DNA	~3 µg
Buffer FastDigest 10X*	3 µL
Fast-Digest NotI*	3.5 µL
Nuclease-Free H_2O	To 30 µL

*** ThermoFisher Scientific**

Samples were incubated at 37 °C for 2 hours before the addition of 20 µL of distilled nuclease-free H_2O; giving a final volume of 50 µL. To this, 2 µL of proteinase K (5 mg/mL) was added to a final concentration of 200 µg/mL, along with 2.5 µL of 10% SDS to a final concentration of 0.5 %. Samples were incubated at 50 °C for 30 minutes prior to the addition of 2.5 µL of 0.5 M EDTA to a final concentration of 25 mM. Following incubation, samples were purified by the addition of a ½ volume of saturated phenol (28.5 µL) and a ½ volume of chloroform (28.5 µL). Samples were mixed by vortexing, then centrifuged at 16168 x g at 4°C for 5 minutes. The aqueous phase (upper) layer was pipetted into a new tube and 57 µL of chloroform added, before vortexing and

then centrifugation at 16168 x g at 4°C for 1 minute. Another phenol:chloroform purification was done and the final aqueous phase (upper) was pipetted into a new tube and the DNA precipitated using 1 volume of 4 M Ammonium Acetate and 5 volumes of ice cold 100% ethanol (500 µL) incubated overnight at -20 °C. The samples were then centrifuged at 16168 x g for 20 minutes at 4 °C and the supernatant carefully removed. The remaining pellet was washed with 500 µL of ice cold 70% ethanol, centrifuged at 16168 x g for 5 minutes at 4 °C, the supernatant was carefully removed, and samples vacuum dried until no liquid was present. The pellets were re-suspended in 10 µL nuclease-free water and 0.5 µL was run on a 1 % agarose gel to check the purity of the product (Section 4.2).

In addition to VGSC constructs, another pGH19 construct containing cDNA needed to transcribe the *D. melanogaster* TipE protein, was also prepared for *in vitro* transcription. TipE is a VGSC accessory protein shown to greatly enhance activity of *D. melanogaster para* VGSCs in *X. laevis* oocytes (Feng et al., 1995). The TipE construct used in this study was made by Vais *et al* in 2000.

7.2.4 Preparation of cRNA Transcripts for Expression in *X. laevis* Oocytes

Linearized VGSC or TipE pGH19 plasmids, or already linear *V. destructor* VGSC PCR products, were used as DNA templates for *in vitro* transcription to created capped cRNA for use in *X. laevis* microinjection. This protocol was carried out using ThermoFisher Scientific's T7 mMESSAGE mMACHINE® kit. The starting mix was as shown in Table 7.12.

Table 7.12: Reverse Transcription Mix

Template	DNA	2 X NTP/CAP*	10 X Buffer	GTP	Enzyme	Water
PCR Product or linearized plasmid	1 µg	5 µL	1 µL	0.5 µL	1 µL	To 10 µL

*** 2X NTP/CAP is a neutralized buffered solution containing ATP (15 mM), CTP (15 mM), UTP (15 mM), GTP (3 mM), 5' RNA cap analog $m^7G(5')ppp(5')G$ (12 mM).**

Samples were incubated for 2 hours at 37 °C. For each 10 µL reaction, 0.5 µL Turbo DNAse was added and samples were mixed then incubated for 15 minutes at 37 °C. 57 µL distilled Nuclease free H_2O and 7.5 µL ammonium acetate stop solution were added to a final volume of 75 µL. Samples were then purified by phenol:chloroform precipitation as described in 7.2.3. The final pellets were re-suspend in 10 µL nuclease-free water and the concentration of the RNA was checked using a nanodrop spectrophotometer (ThermoScientific). Samples (~500ng of RNA) were run on a 1 % agarose gel (Section 4.2) to check the products. All cRNA transcripts were stored at -80°C.

7.2.5 Preparation of *X. laevis* Oocytes

X. laevis ovaries were obtained from The European *Xenopus* Resource Centre (EXRC) at Portsmouth University, details of housing and production conditions can be found at:http://www.port.ac.uk/research/exrc/holdingandproducingconditions. At least ten separate batches of oocytes were used to collect the data found in this work. The ovaries were delivered on wet ice in EXRC Modified Barth's Solution (MBS) containing NaCl (88 mM), KCl (1 mM), $NaHCO_3$ (2.4 mM), $MgCl_2 \cdot 6H_2O$ (0.82 mM), $Ca(NO_3)_2 \times 2H_2O$ (0.33mM), $CaCl_2 \times 6H_2O$ (0.41mM) and HEPES (10mM) pH 7.5 - pH 7.6, with a final concentration of 5 U/ml penicillin and 5 µg/ml streptomycin. Once received, the *X. laevis* ovaries were torn into approximately $1cm^3$ pieces and placed into Ca^{2+}-free MBS, containing NaCl (88 mM), KCl (1 mM), Tris pH 7.6 (15 mM), $NaHCO_3$ (2.4 mM) and $MgCl_2 \cdot 6H_2O$ (0.82 mM), this was adjusted to pH 7.5 using hydrochloric acid before filtering using a 2 µm Nalgene vacuum filtration system. To this solution 1-2 mg/ml Type 1A Collagenase enzyme (Sigma-Aldrich) was added and oocytes were treated for 30-45 minutes at room temperature with gentle shaking to remove connective tissue. The oocytes were then washed in fresh Ca^{2+}-free MBS a minimum of five times to remove excess collagenase and to prevent total loss of the follicular tissue which surrounds each egg. The healthiest oocytes of the correct development stage (stage IV or V) were then selected according to the guidelines for shape, size, and colour developed at Nottingham University (Eldursi et al., 1997). Follicular tissue was then removed from the oocytes using forceps.

7.2.6 Microinjection of cRNA Transcripts

Microinjection of cRNA transcripts was done with an auto-nanolitre-injector, Nanoject II (Drummond Scientific) at a volume of 50.6 nl of cRNA per oocyte. Injecting tips were pulled from 3.5 nanolitre glass capillaries (World Precision Instruments) using a horizontal pipette puller. Prior to injection, the ends of the tips were opened by carefully breaking under the microscope to give a slanted tip of approximately 10 µM diameter. Injection tips were filled with mineral oil and secured onto the Nanoject II needle to create an injection pipette. cRNA transcripts for native or mutant D*. melanogaster para* 13-5 and for Tip E were diluted with sterile nuclease-free water to a final concentration of 0.5 ng/nl and mixed at a ratio of 1 part Tip E transcript, 1 part VGSC transcript and 3 parts nuclease-free water, giving a final concentration for each cRNA of 0.1 ng/nl. Native or mutant *V. destructor 13-5* transcripts were diluted with nuclease-free water to a final concentration of 1 ng/nl but these were not mixed with Tip E, as this has been shown to hinder expression of the *V. destructor* VGSC (Du et al., 2009a). Transcript cRNA was gently drawn into the injection pipette, taking care to avoid any air bubbles. Defolliculated oocytes were then placed in a bath of Ca^{2+}-free MBS (Section 7.2.5) where they were each injected with 50.6 nl of transcript solution. Following injection, the oocytes were incubated for either 2-4 days for *D. melanogaster para* 13-5/TIP E transcripts or 4-5 days for *V. destructor* 13-5 transcripts at 18°C in 24 well VWR® multi-well plates (VWR) with no more than 3 oocytes per well. Each well contained Ca^{2+}-containing MBS, which was Ca^{2+}-free MBS (Section 7.2.5) with the addition of $CaCl_2 \cdot 2H_2O$ (0.77 mM), penicillin (100U/ml), streptomycin (100µg/ml), kanamycin (4 µg/ml), and tetracycline (50 µg/ml), antibiotics were added as advised by Alin Mirel Puinean and as used in (Puinean et al., 2013). Once TEVC recordings had begun on a batch of VGSC-expressing oocytes any remaining cells from that batch were stored at 4°C.

7.2.7 Recording VGSC Signals Using TEVC Electrophysiology

TEVC, as introduced in Section 3.6, was used to measure current flow at fixed voltages across an oocyte membrane. Oocytes were placed in sterile disposable 35 mm petri dishes containing 2ml of Xenopus Ringer: NaCl (96 mM), KCl (2 mM), CaCl2 (1.8 mM), MgCl2 (1 mM), and HEPES (5 mM), adjusted to pH 7.5 with NaOH. Electrodes inserted into the oocyte for recording (E1) and injecting (Ei) current were prepared from Borosilicate thin walled Clark capillary glass (with filament, OD 1.5 mm, ID 1.17 mm, Length 100mm) (Harvard Apparatus) using a micropipette puller (model P-97, Sutter Instrument Company). Electrodes were filled with 0.7 M KCL and 1.7 M K^+ citrate, then connected to the amplifier using 0.37 mm Teflon coated silver wire (Advent Research Materials); where the Teflon coating at the tip had been removed and coated with silver chloride to allow conductance. When inserted into an oocyte these electrodes gave a resistance of 1-2 MΩ; which allows sufficient current to pass rapidly into the oocyte to give fast voltage-clamping. A third electrode, E2, is connected to the bath via a platinum wire (Goodfellow) encased within an agar bridge, which acts to confirm that the bath is clamped and give an accurate record of membrane potential. The electrophysiology experiments were carried out at the University of Nottingham using a CA-1B amplifier (Dagan Instruments), which allows use of a protocol whereby the inside of the cell is held at “zero” (a virtual ground state compared to the bath) whilst the bath is voltage clamped. This results in much faster clamping speeds allowing the investigation of rapid changes in current as seen in VGSCs. All oocytes used needed to be of sufficient quality able to survive testing, as determined by a resting membrane potential more negative than -10 mV (though upwards of -15 mV was preferred) and a leakage current of below -150 nA when clamped to -70 mV (all voltages stated are relative to the virtual ground) (Figure 7.1).

Figure 7.1: The TEVC Experimental Design

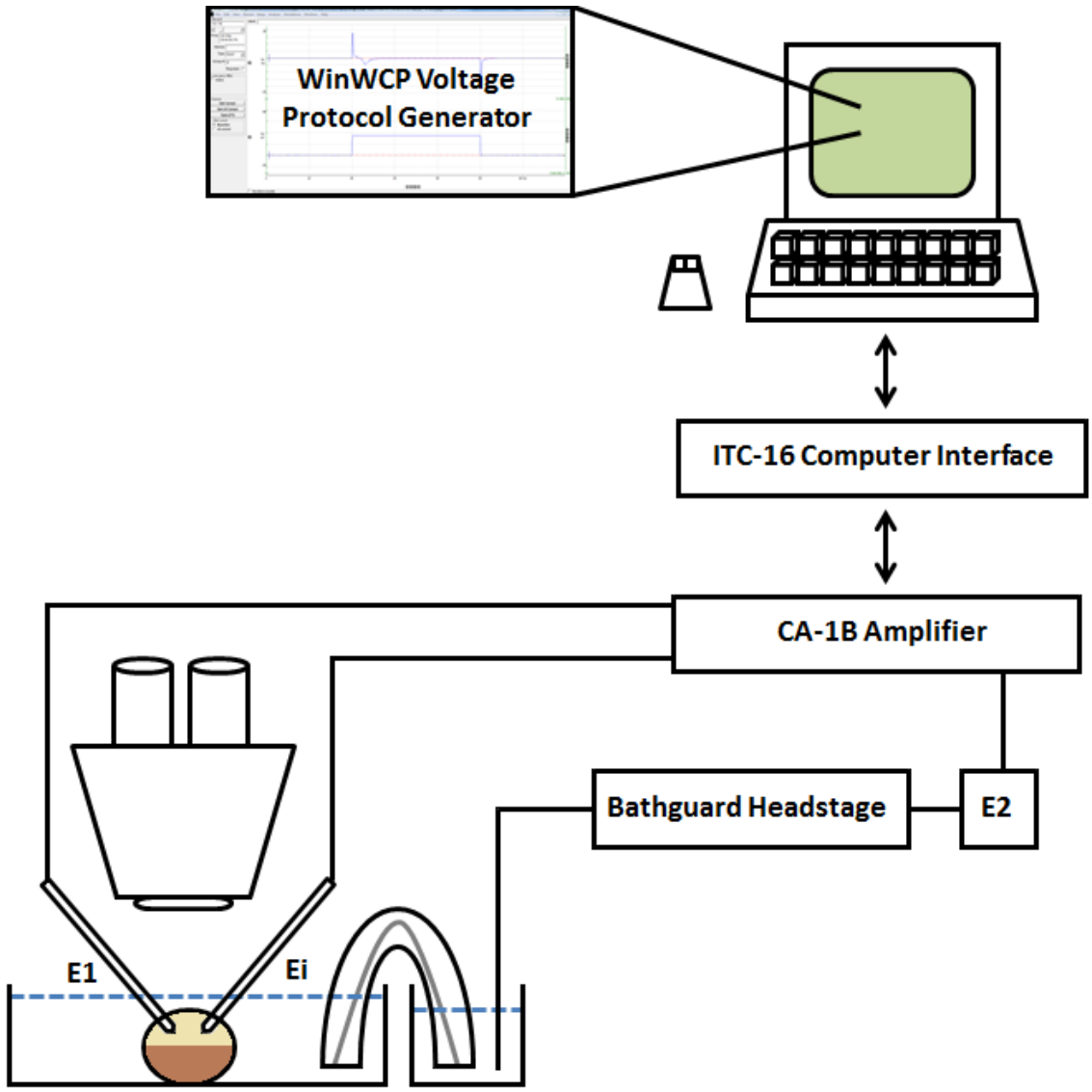

A representation of TEVC Electrophysiology as used in this study. The oocyte is placed in a disposable Petri dish containing Xenopus Ringer and impaled with two glass micro-electrodes, Ei and E1, which are in turn connected to an amplifier. An agar bridge in the Xenopus Ringer connect a third electrode, E2, to accurately confirm the oocyte membrane potential and that the bath is clamped during experiments. Ei and E1 are shielded by a grounded metal dividing plate, reducing coupling between the two electrodes. Voltage protocols are generated in Win-WCP and pass to the amplifier via an ITC-16 computer interface (Instrutech Corporation), which converts the digital signal to analogue. Signals from the amplifier are passed back to the computer via this interface, which then converts the analogue signal to digital, and results are stored on the computer hard drive.

Once clamped, the oocytes underwent a series of voltage protocols to investigate the activity of the VGSC they were expressing. All protocols were designed and recorded using the WinWCP programme (John Dempster, University of Strathclyde) and were developed at Nottingham University in the lab of Ian Duce and Ian Mellor (Usherwood et al., 2007; Usherwood et al., 2005). For each protocol, 4 leak-subtraction pulses per test potential were performed to counter any membrane leakage in the oocyte. Four different electrophysiological protocols were used:

Voltage Protocol 1

This protocol (Figure 7.2) allowed the study of activation and fast-inactivation of a VGSC in the presence and absence of a toxicant (Usherwood et al., 2005). The oocytes were clamped to -70 mV before the voltage was increased, with a 30 ms step depolarisation, to the test potential (V_T). Test potentials ranged from -65 mV to +45 mV and increased in 5mV increments.

Figure 7.2: Voltage Protocol 1

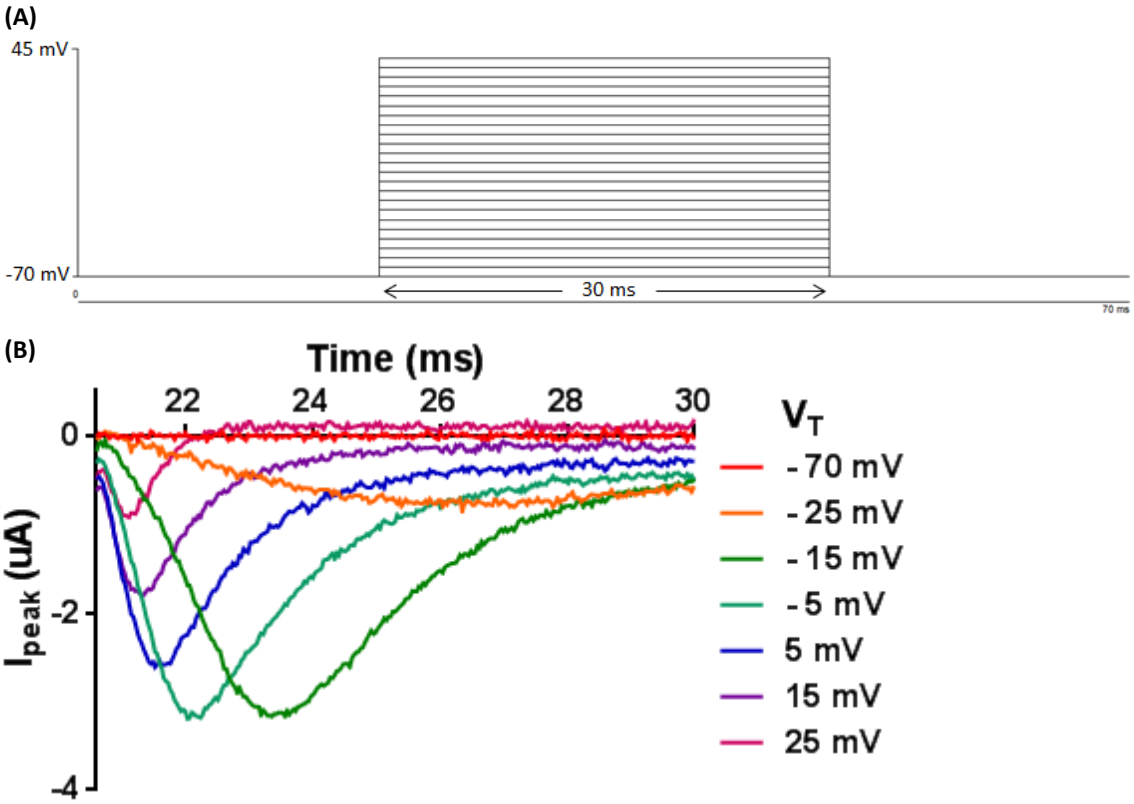

(A) A representation of Voltage Protocol 1 showing the baseline clamped potential of -70 mV, followed by a 30 ms step depolarisation from -70 to +45 mV in 5 mV increments. (B) Exemplar raw data resulting from the application of Voltage Protocol 1 on *X. laevis* oocytes expressing the *V. destructor* native VGSC.

Voltage Protocol 2

This protocol (Figure 7.3) allowed the study of steady state inactivation of a VGSC in the presence and absence of toxicants. Oocytes were clamped to -70 mV before the application of a 200 ms inactivation pre-pulse ($V_{T.inact}$). This pre-pulse ranged from -90 mV to -20mV and was increased in 5 mV increments. Following each pre-pulse, the cells were subjected to a V_T of -10 mV of 30 ms duration, this would cause immediate activation in a native VGSC. However, the extent of activation seen is dependent on the value of the pre-pulse potential, the more positive this potential, the more VGSCs would be in an inactivated state come V_T, and the smaller the resultant sodium current would be.

Figure 7.3: Voltage Protocol 2

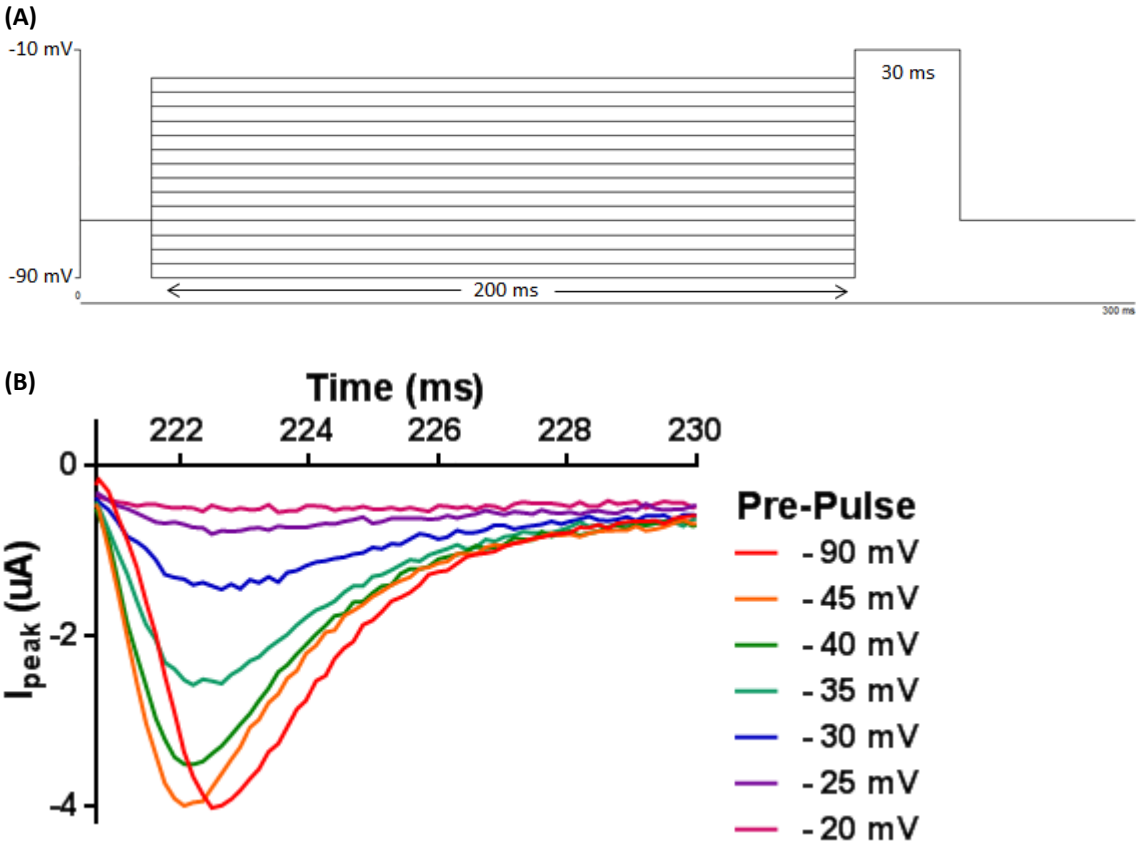

(A) A representation of Voltage Protocol 2 showing the baseline clamped potential of -70 mV, followed by the 200 ms step depolarisation from -90 to -20 mV in 5 mV increments. A 30 ms test pulse at -10 mV at the end of the protocol was designed to investigate VGSC inactivation. (B) Exemplar raw data resulting from the application of Voltage Protocol 2 on *X. laevis* oocytes expressing the *V. destructor* native VGSC. Current shown is that recorded during the 30 ms V_T of -10 mV following the stated pre-pulse value.

Voltage Protocol 3

This protocol (Figure 7.4) allowed the study of a characteristic feature of VGSCs expressed in oocytes and treated with pyrethroids, known as the tail current. Tail currents are the observable manifestation of the action of pyrethroids, when they slow channel inactivation/deactivation (Vais et al., 2001). Oocytes were clamped to -70 mV before the application of 100 0 mV conditioning pulses of 5 ms duration, each at a frequency of 66 Hz. Between each conditioning pulse there was a 10 ms interval, allowing time for any recovery of VGSCs from open (at 0 mV) to closed-resting state (at -70 mV). Because pyrethroids bind preferentially to the open confirmation of arthropod VGSCs (Vais et al., 2000a), binding of these insecticides to the VGSC is encouraged during this pre-conditioning step. Following the pre-conditioning pulses, a single 12 second repolarisation pulse of -110 mV was applied, a voltage step that should induce VGSCs into an inactivated then deactivated state (Figure 18). During this repolarisation pulse, the VGSCs which have undergone modification by pyrethroid insecticides will show a delay in closing, and a residual current peak will be observed (Figure 28). The amplitude and duration of any residual current can then be measured to give a value for the percentage modification of a VGSC by a pyrethroid insecticide (Usherwood et al., 2007; Vais et al., 2001).

Figure 7.4: Voltage Protocol 3

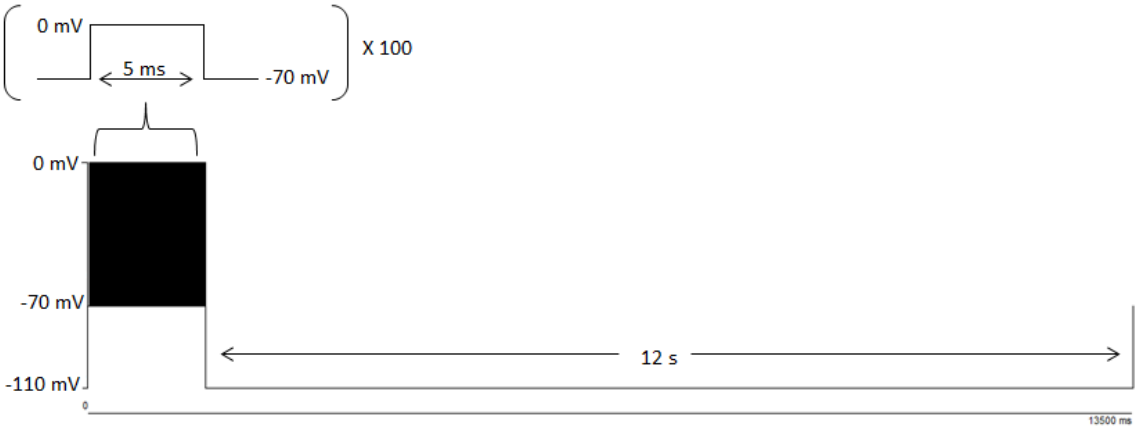

A representation of Voltage Protocol 3 showing the baseline clamped potential of -70 mV followed by 100 5 ms pre-conditioning pulses to 0 mV. A 12 second repolarisation pulse to -110 mV at the end was designed to investigate VGSC inactivation/deactivation.

Voltage Protocol 4

This protocol (Figure 7.5) allowed the study of the block of arthropod VGSCs caused by Tetrodotoxin (TTX). Oocytes were clamped to -70 mV before the voltage was increased to -10 mV for a single 35 ms step depolarisation. This protocol was repeated 25 times.

Figure 7.5: Voltage Protocol 4

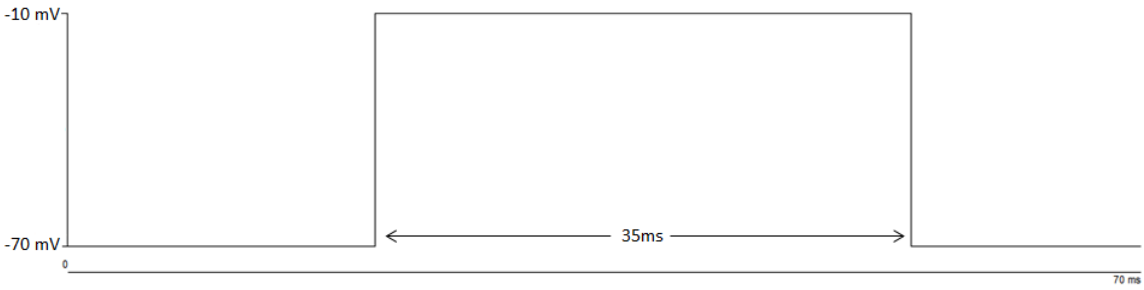

A representation of Voltage Protocol 4 showing the baseline clamped potential of -70 mV followed by a single 35 ms test depolarisation step to -10 mV.

7.2.8 Application of Toxicants to VGSCs Expressed in Oocytes

TTX is a potent neurotoxin known to block mammalian and insect VGSCs and as such can be used to confirm that it is expressed VGSCs that are responsible for any observed voltage-dependent current fluctuations in *X. laevis* oocytes (Agnew et al., 1980; Catterall, 2000, 2012; Feng et al., 1995; O'Dowd and Aldrich, 1988). To this end a final bath concentration of 2 µM TTX (dissolved in nuclease-free water) was applied to the oocytes which had been injected with cRNA encoding arthropod VGSCs after 12 repeats of Voltage Protocol 4. All pyrethroid toxicants were dissolved in dimethyl-sulphoxide (DMSO) to make 10^{-2} M working stocks prior to application. The final bath concentration of DMSO did not exceed 1% of the total volume, which previous studies (Burton, 2012; Usherwood et al., 2007) have shown has no effect on the arthropod VGSCs. This was confirmed in the current study (data not shown). The pyrethroids deltamethrin, flumethrin , permethrin and tau-fluvalinate were each all added to the bath in concentrations ranging from 1 nM to 10 µM. All toxicants and DMSO were added to the bath in 2 µl volumes by pipetting, actives were allowed to diffuse through the bath for 10 minutes, during which time their circulation was aided by gentle blowing across the bath, before commencement of the voltage protocols.

7.2.9 Data analysis of TEVC Recordings

All data analyses and graph plotting was done using GraphPad Prism 6 (GraphPad Software) available at: https://www.graphpad.com/

Following Voltage Protocol 1 (Section 7.2.7) the amplitude of the current recorded at each voltage step was plotted against the test potential to give a current-voltage relationship for the activation of the expressed VGSCs. Following leak-current subtraction (in Win WCP), current peak data was baseline corrected using the mean current amplitude of the first three test-potentials were no VGSCs were activated. Baseline corrected data was then transformed by -1 and normalised, then transformed back to negative values. This processing accounted for differences in current amplitude that were due to different VGSC expression levels between oocytes. The mean and standard error of the mean (SEM) for each current peak was calculated at each test potential, then fitted using a modified Boltzmann equation (Equation 1) to give a current-voltage relationship curve. This allowed the determination of the half-activation potential ($V_{50.act}$), the voltage at which half the VGSCs in the cell can be considered to be active, and the reversal potential (V_{rev}), the voltage at which there is no net movement of sodium ions across the membrane.

Equation 1:

$$I_{peak} = G_{max}((V_T - V_{rev})/(1+\exp((V_T - V_{50.act})/k))$$

Where I_{peak} is the peak sodium current elicited by the step depolarisation test potential (V_T), G_{max} is the maximum sodium ion conductance, V_{rev} is the reversal potential, $V_{50.act}$ is the test potential that would give a half maximum I_{peak}, and *k* is the slope factor in mV.

Recordings from Voltage Protocol 1 also enabled the fitting of a normalised conductance-voltage relationship. Maximum conductance (G_{max}) and reversal-potential (V_{rev}) values for baseline corrected current peak data from each cell were calculated using Equation 1. The normalised conductance (G/G_{max}) for each value of V_T was then calculated from baseline corrected data for each cell using Equation 2.

Equation 2:

$G/G_{max} = (I_{peak}/(V_T-V_{rev}))/G_{max}$

Where I_{peak} is the peak sodium current elicited by the step depolarisation test potential (V_T), G is the conductance at V_T, G_{max} is the maximum sodium ion conductance, and V_{rev} is the reversal potential.

The mean and SEM of these data was taken, giving the mean normalised conductance (G/G_{max}) for each V_T. These values were then fitted using Equation 3, a Boltzmann sigmoidal, to give a normalised conductance-voltage relationship curve and a calculation of $V_{50.act}$ based on conductance.

Equation 3:

$G/G_{max} = B+(Top-B)/(1+exp((V_{50.act}-V_T)/k))$

Normalised conductance (G/G_{max}) is given a function of the depolarising step test potential (V_T), normalised conductance varies from a minimum (B) value to a maximal Top value, $V_{50.act}$ is the half-activation potential (at which 50% of the channels would be activated), and k is the slope factor in mV.

Following Voltage Protocol 2 (Section 7.2.7) the amplitude of the current recorded following each $V_{T.inact}$ (I_{peak}) was divided by the maximal peak current elicited for the series of -10 mV V_T pulses (I_{max}), to give the normalised current for steady-state inactivation of the expressed VGSCs. Following leak-current subtraction (in Win WCP), I_{peak} data was transformed and normalised, to account for differences in current amplitude due to different levels of VGSC expression in different oocytes. Normalised current (I_{peak}/I_{max}) was plotted against each $V_{T.inact}$, then fitted using a Boltzmann equation (Equation 4). This allowed calculation of the half-inactivation voltage, the voltage at which half the VGSCs in a cell could be considered inactivated ($V_{50.inact}$).

Equation 4:

$I_{peak}/I_{max} = B+(Top-B)/(1+exp((V_{50.inact}-V_{T.inact})/k))$

Normalised current flow (I_{peak}/I_{max}) is given a function of inactivating pre-pulse ($V_{T.inact}$), where I_{peak} is the peak sodium current given by a single $V_{T.inact}$ pre-pulse, and I_{max} is the maximum peak current elicited by a series of V_T pulses. Normalised current varies from a minimum (B) value to a maximal Top value, where $V_{50.inact}$ is the half-inactivation potential (at which 50% of the channels would be inactivated), and k is the slope factor in mV.

In more recent studies (Burton, 2012; Burton et al., 2011; Usherwood et al., 2007) Equation 5 has been used to analyse the tail current area by determining the integral modification (M_i) of a VGSC in the presence and absence of a pyrethroid. This takes into account, not only the peak current elicited during a tail current, but also the duration of the depolarisation event (Usherwood et al., 2007). Following leak-current subtraction (in Win WCP), current peak data obtained by application of Voltage Protocol 3 (Section 7.2.7) was transformed by -1 and early data points (corresponding to duration of the pre-conditioning pulses) were excluded. The area under the curve (AUC) of transformed data was calculated, including only those peaks above the baseline. AUC data were then re-transformed by -1 to give the value $I_{tail.integral}$ (a multiplication of the negative peak amplitude of the tail current by the time the peak remains negative). Following this processing the tail current data was fitted to Equation 5 to give the M_i value for that cell and pyrethroid concentration. These values were pooled to calculate mean and SEM M_i data for test pyrethroids.

Equation 5:

$$M_i = ((I_{tail.integral} /(V_T-V_{rev}))/G_{max})x100$$

Integral modification (M_i) is given a function of $I_{tail.integral}$ (a multiplication of the negative peak amplitude of the tail current by the time the peak remains negative) divided by the depolarising step test potential (V_T) minus the reversal potential of the cell in the absence of any toxicant (V_{rev}). Divided by the maximum conductance of the cell (G_{max}), again in the absence of any toxicant. In this case, V_T is -110 mV. Data is multiplied by 100 to give a percentage value.

7.3 Results

7.3.1 *Varroa 13-5* and *para 13-5* VGSC Mutagenesis and Expression

D. melanogaster para 13-5 mutants C933A/G/V were successfully made into cRNA transcripts and were injected into *X. laevis* oocytes, as was the native *D. melanogaster para 13-5*. As data for the C933A mutant has already been published (Usherwood et al., 2007), and as this is not a native residue in *V. destructor* mites or ticks, this mutant was abandoned. Of the two remaining *D. melanogaster para 13-5* mutants, C933G has shown expression in *X. laevis* oocytes but this was intermittent and poor, and the C933V mutant failed to express, most likely due to oocyte quality at the time. In the

past, the native *V. destructor 13-5* VGSC has suffered badly from random mutagenesis in *E. coli*, and has proven difficult to maintain in both Stratagene's XL1 Blue and XL10 Gold ultracompetent cells (Joel González-Cabrera personal communication). Perhaps not surprisingly, given the difficulties maintaining native *V. destructor 13-5*, only the *V. destructor 13-5* G933V mutant was obtained, and correct clones were only obtained through transformation into Invitrogen's MAX Efficiency® Stbl2™ competent cells followed by colony PCR (Section 4.10 and 4.11). However, this was successfully made into a cRNA transcript and injected into *X. laevis* oocytes, as was the native *V. destructor 13-5*, for testing using TEVC Electrophysiology; both the native *V. destructor 13-5* VGSC and the *V. destructor 13-5* G933V mutant showed expression in *X. laevis* oocytes, as did the native *D. melanogaster para 13-5* VGSC when co-expressed with *Tip E* (Feng et al., 1995; Warmke et al., 1997). These three constructs allowed investigation into potential differences in pyrethroid binding between insect and acarine channels, particularly involving residue 933, and so were taken forward for use in TEVC experiments.

7.3.2 Characterisation of Arthropod VGSCs

7.3.2.1 Activation

Mean values (along with SEMs) for $V_{50.act}$ and V_{rev} for arthropod VGSCs in the absence of any toxicant, calculated using Equations 1,2 and 3, are listed in Table 7.13. Current-voltage relationships for these VGSCs and conductance-voltage relationships are shown in Figure 7.6.

Table 7.13: Values of $V_{50.act}$ and V_{rev} for Arthropod VGSCs in the Absence of Any Toxicant

VGSC Source	$V_{50.act}$ (mV)	V_{rev} (mV)	(n)
D. melanogaster para	-29.33 ± 0.32	174.70 ± 9.71	37
V. destructor Native	-17.98 ± 0.50	64.75 ± 2.10	32
V. destructor G933V Mutant	-18.26 ± 0.63	70.15 ± 3.24	27

Figure 7.6: Activation Relationships of Arthropod VGSCs

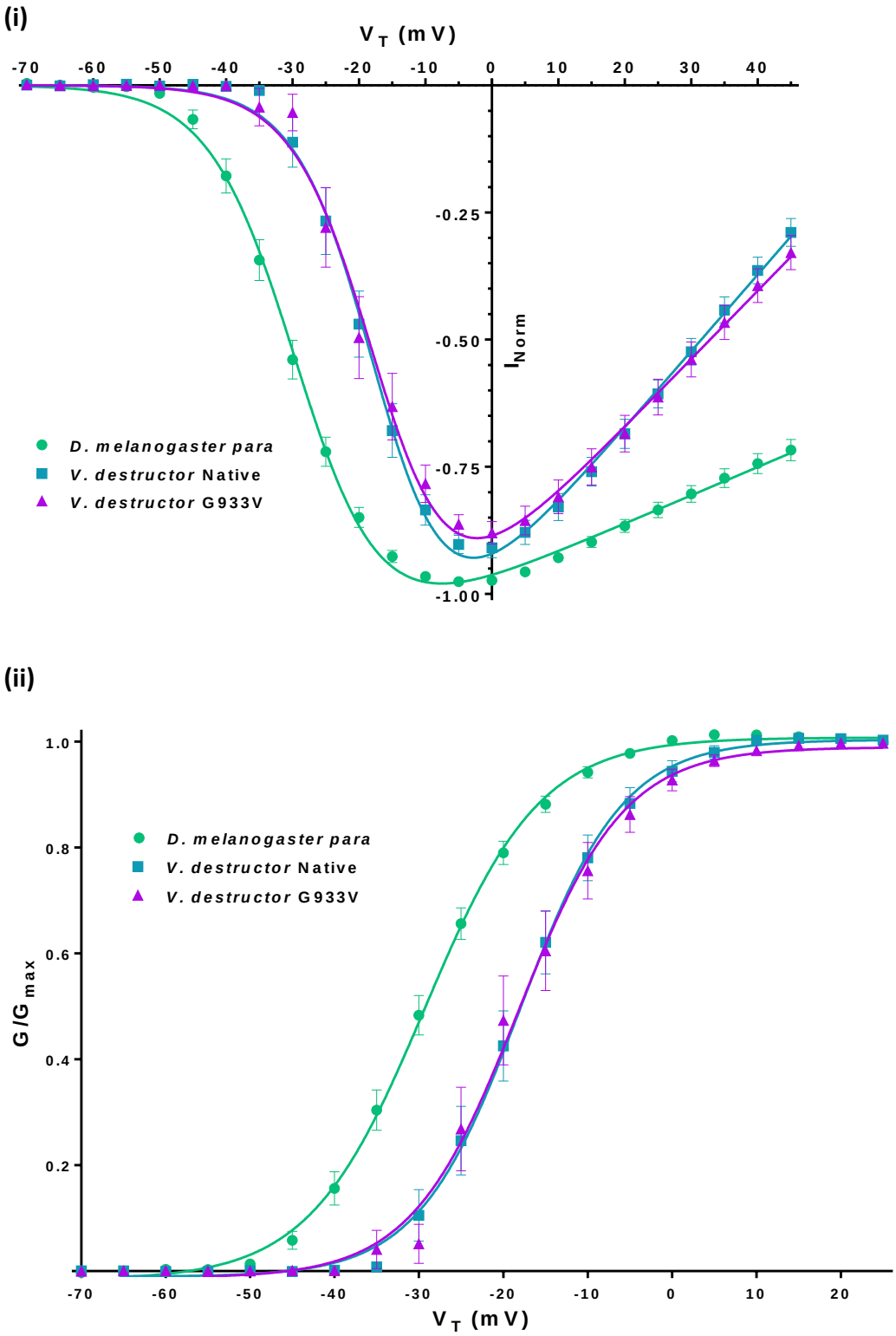

(i) Current-voltage relationships of arthropod VGSCs recorded using Voltage Protocol 1 (Section 7.2.7) and fitted using Equation 1 (Section 7.2.9). (ii) Conductance-voltage relationships of arthropod VGSCs recorded using Voltage Protocol 1 (Section 7.2.7) and fitted using Equations 1, 2 and 3 (Section 7.2.9).

7.3.2.2 Steady-State Inactivation

Mean values (along with SEMs) for $V_{50.inact}$ values for arthropod VGSCs in the absence of any toxicant, calculated using Equation 4, are listed in Table 7.14 and normalised current-voltage (pre-pulse) relationships for these VGSCs are shown in Figure 7.7.

Table 7.14: Values of $V_{50.inact}$ for Arthropod VGSCs in the Absence of Any Toxicant

VGSC Source	$V_{50.inact}$ (mV)	(n)
D. melanogaster para	-48.14 ± 0.18	38
V. destructor Native	-30.33 ± 0.86	40
V. destructor G933V Mutant	-28.61 ± 0.75	34

Figure 7.7: Steady-State Inactivation Relationships of Arthropod VGSCs

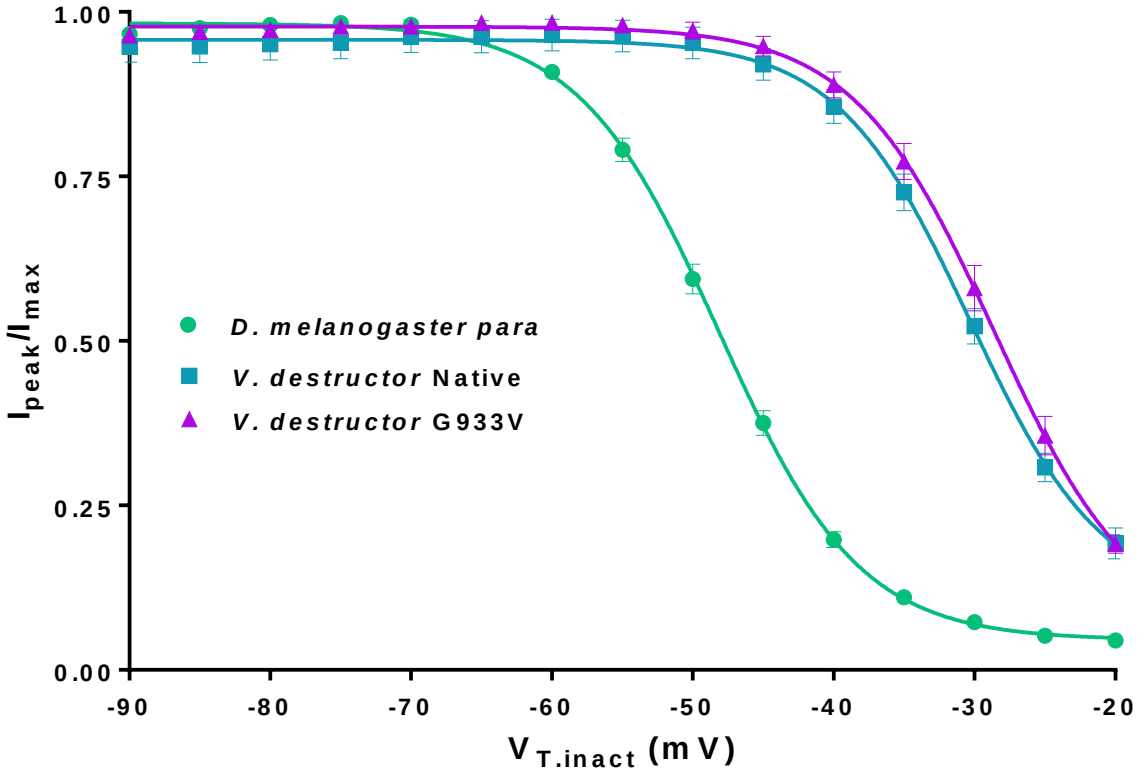

Voltage dependence of inactivation for arthropod VGSCs as recorded using Voltage Protocol 2 (Section 7.2.7) and fitted using Equation 4 (Section 7.2.9).

7.3.3 Effects of Pyrethroid on Arthropod VGSCs

Pyrethroids toxicants were applied to *X. laevis* oocytes (Section 7.2.8) to assess their effects on activation, steady-state inactivation, and their ability to induce tail currents.

7.3.3.1 Effects of Pyrethroids on Activation

Mean values (along with SEMs) for $V_{50.act}$ of arthropod VGSCs in the absence of any toxicant and in the presence of 100 nM of each pyrethroid, as calculated using Equations 1, 2, and 3, are listed in Table 7.15. Conductance-voltage relationships for these VGSCs are shown in Figure 7.8. These relationships show how the activation of each arthropod VGSC is affected by individual pyrethroid toxicants, with a shift to the left demonstrating that activation is occurring at a more negative voltage. Such a shift would be expected to correlate with increasing concentrations of a pyrethroid toxicant, their mode of action being previously demonstrated to involve stabilising arthropod VGSCs in the active conformation, thus more channels would be open and conductive at lower voltages (Vais et al., 1997).

Table 7.15: Values of $V_{50.act}$ for Arthropod VGSCs in the Absence of Any Toxicant and in the Presence of 100 nM Pyrethroid

VGSC Source	Pyrethroid Applied	$V_{50.act}$ (mV)	P-Value (Toxicant-Control)*	(n)
D. melanogaster	None	-29.33 ± 0.32	N/A	37
D. melanogaster	100 nM Deltamethrin	-37.58 ± 1.05	<0.05	7
D. melanogaster	100 nM Flumethrin	-37.57 ± 1.23	<0.05	9
D. melanogaster	100 nM Permethrin	-35.57 ± 0.84	<0.05	6
D. melanogaster	100 nM Tau-Fluvalinate	-32.05 ± 0.65	<0.05	8
V. destructor Native	None	-17.98 ± 0.50	N/A	32
V. destructor Native	100 nM Deltamethrin	-19.71 ± 0.87	<0.05	9
V. destructor Native	100 nM Flumethrin	-10.83 ± 1.22	<0.05	4
V. destructor Native	100 nM Permethrin	-21.13 ± 2.22	<0.05	6
V. destructor Native	100 nM Tau-Fluvalinate	-28.46 ± 1.13	<0.05	4
V. destructor G933V Mutant	None	-18.26 ± 0.63	N/A	27
V. destructor G933V Mutant	100 nM Deltamethrin	-7.99 ± 2.71	<0.05	6
V. destructor G933V Mutant	100 nM Flumethrin	-26.09 ± 0.57	<0.05	3
V. destructor G933V Mutant	100 nM Permethrin	-15.57 ± 4.14	<0.05	6
V. destructor G933V Mutant	100 nM Tau-Fluvalinate	-26.90 ± 1.73	<0.05	5

***P-Values were calculated using GraphPad Prism 6 by comparing conductance-voltage relationship curves using an extra sum-of-squares F test. Values of less than 0.05 demonstrate that for a given pyrethroid and VGSC the $V_{50.act}$ values generated by these curves in the absence or presence of pyrethroid were significantly different to one another.**

Figure 7.8: Conductance of Arthropod VGSCs Treated with Pyrethroid Toxicants

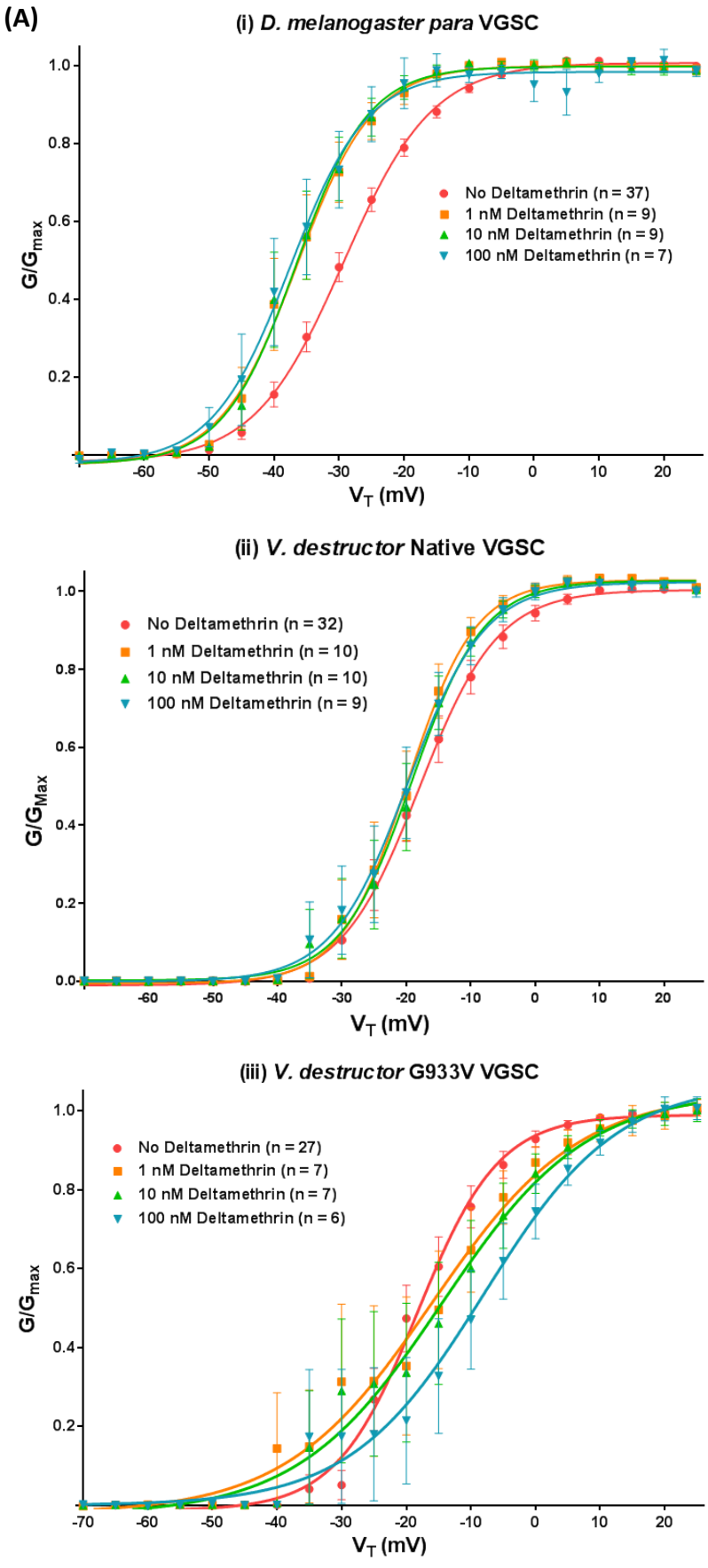

(B)

(i) *D. melanogaster para* VGSC

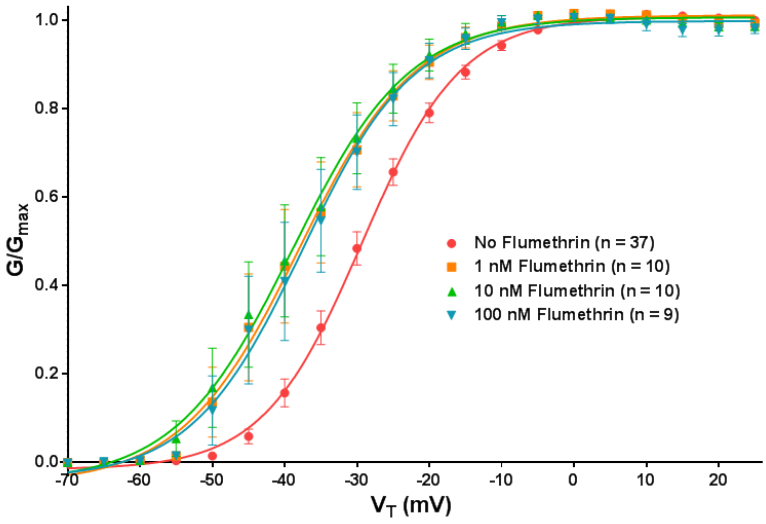

(ii) *V. destructor* Native VGSC

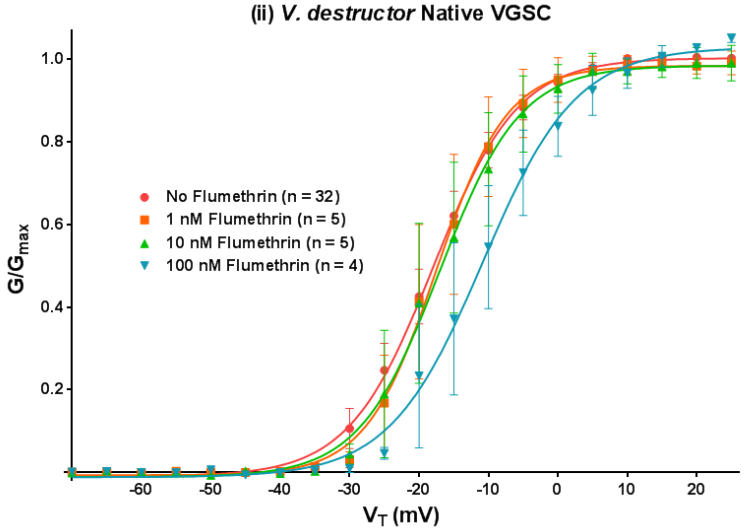

(iii) *V. destructor* G933V VGSC

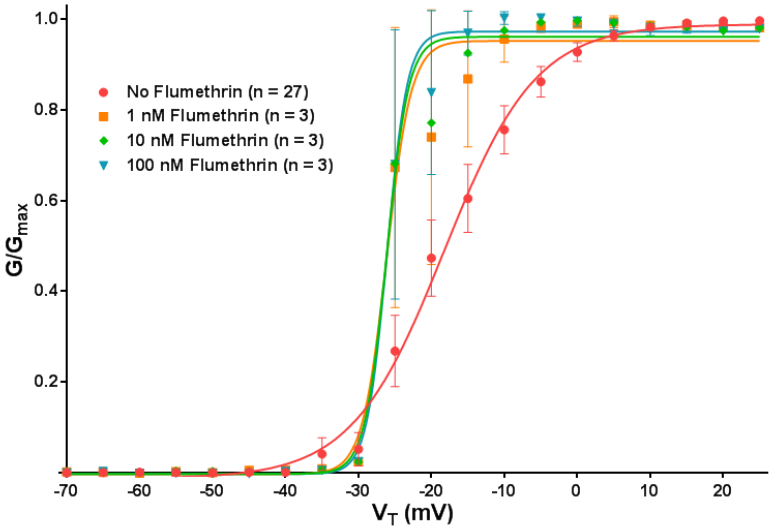

(C)

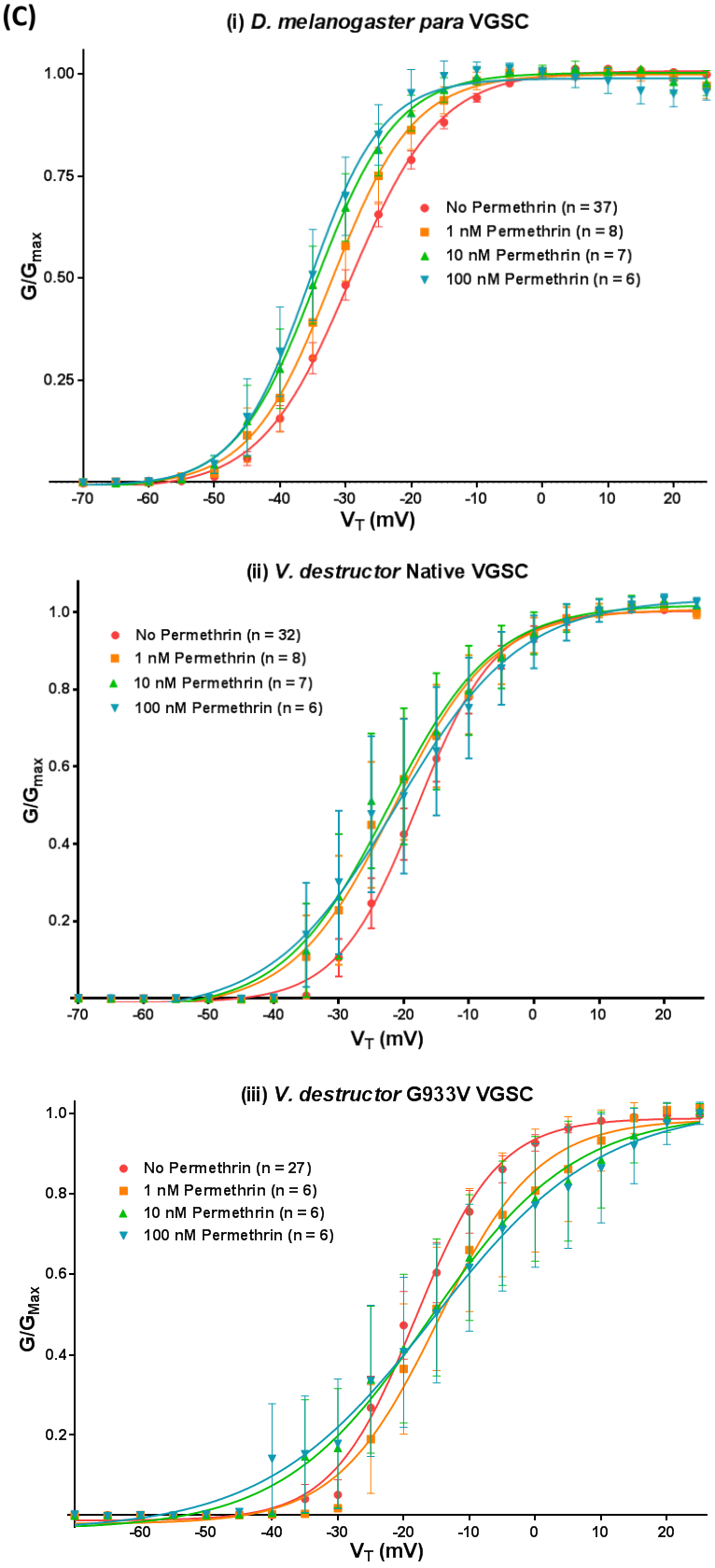
(i) D. melanogaster para VGSC
No Permethrin (n = 37)
1 nM Permethrin (n = 8)
10 nM Permethrin (n = 7)
100 nM Permethrin (n = 6)
G/Gmax
VT (mV)
(ii) V. destructor Native VGSC
No Permethrin (n = 32)
1 nM Permethrin (n = 8)
10 nM Permethrin (n = 7)
100 nM Permethrin (n = 6)
G/Gmax
VT (mV)
(iii) V. destructor G933V VGSC
No Permethrin (n = 27)
1 nM Permethrin (n = 6)
10 nM Permethrin (n = 6)
100 nM Permethrin (n = 6)
G/GMax
VT (mV)

(D)

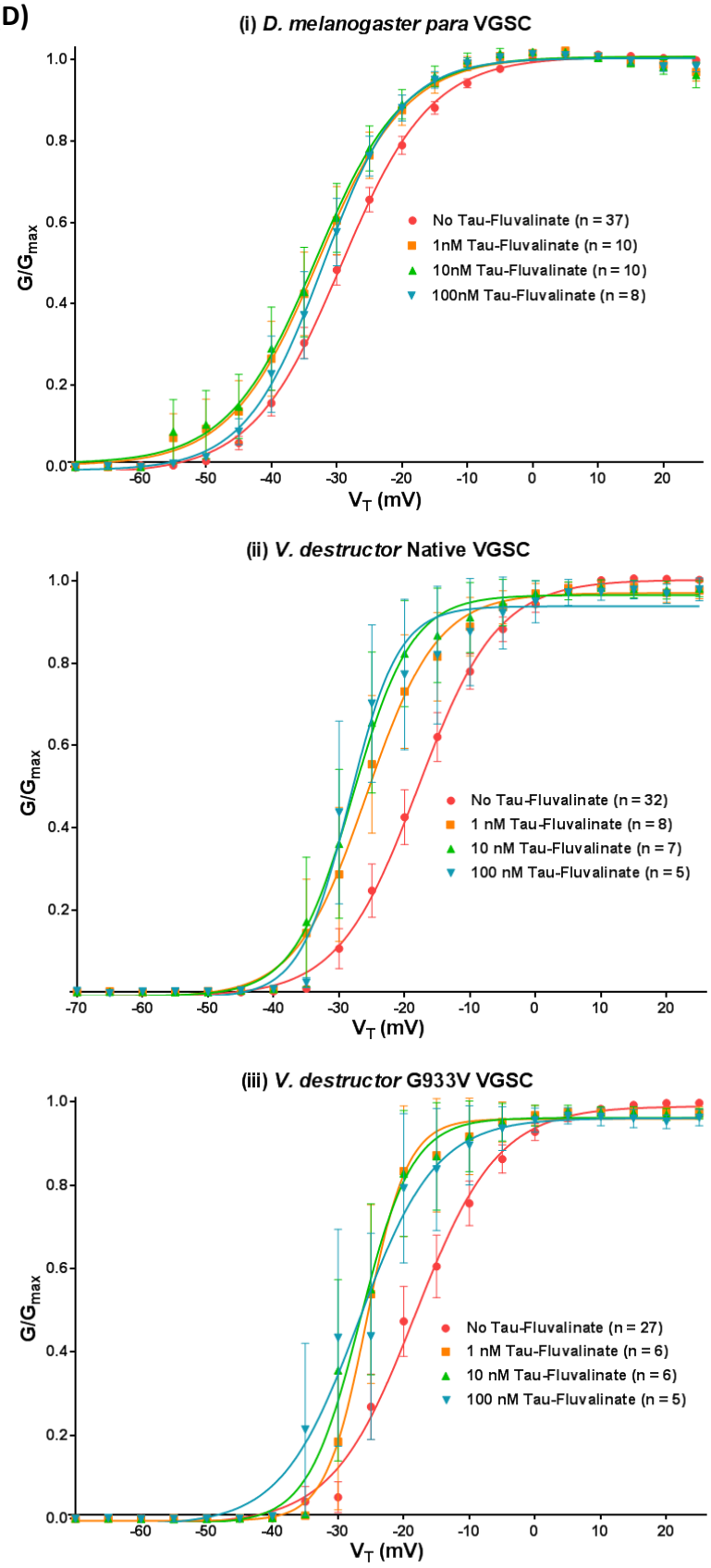

Conductance-voltage relationships of arthropod VGSCs recorded using Voltage Protocol 1 (Section 7.2.7) and plotted using Equations 1, 2 and 3 (Section 7.2.9) in the presence of no toxicant and (A) 1-100 nM Deltamethrin; (B) 1-100 nM Flumethrin; (C) 1-100 nM Permethrin; (D) 1-100 nM Tau-Fluvalinate.

7.3.3.2 Effects of Pyrethroid on Steady-State Inactivation

Mean values (along with SEMs) for $V_{50.inact}$ values for arthropod VGSCs in the absence of toxicant and in the presence of 100 nM of each pyrethroid, as calculated using Equations 4, are listed in Table 7.16 and normalised current-voltage (pre-pulse) relationships for these VGSCs are shown in Figure 7.9. These relationships show how the fast inactivation of each arthropod VGSC is affected by individual pyrethroid toxicants, with a shift to the right demonstrating that fast inactivation is occurring at a more positive voltage. This positive shift would be expected to occur in line with increasing pyrethroid concentration, as pyrethroids have been previously demonstrated to block arthropod VGSCs moving from an open to an "inactivated" closed state, meaning VGSCs would be promoted to the inactivated conformation at more positive V_T potentials following pyrethroid application. (Vais et al., 1997).

Table 7.16: Values of $V_{50.inact}$ for Arthropod VGSCs in the Absence of Any Toxicant and in the Presence of 100 nM Pyrethroid

VGSC Source	Pyrethroid Applied	$V_{50.inact}$ (mV)	P-Value (Toxicant-Control)*	(n)
D. melanogaster	None	-48.14 ± 0.18	N/A	38
D. melanogaster	100 nM Deltamethrin	-49.67 ± 0.32	<0.05	5
D. melanogaster	100 nM Flumethrin	-48.81 ± 0.57	0.20	3
D. melanogaster	100 nM Permethrin	-49.53 ± 0.37	<0.05	5
D. melanogaster	100 nM Tau-Fluvalinate	-48.63 ± 0.34	0.27	8
V. destructor Native	None	-30.33 ± 0.86	N/A	40
V. destructor Native	100 nM Deltamethrin	-36.32 ± 0.79	<0.05	10
V. destructor Native	100 nM Flumethrin	-29.80 ± 1.20	<0.05	9
V. destructor Native	100 nM Permethrin	-31.10 ± 0.80	0.44	10
V. destructor Native	100 nM Tau-Fluvalinate	-31.59 ± 1.18	0.22	10
V. destructor G933V Mutant	None	-28.61 ± 0.75	N/A	34
V. destructor G933V Mutant	100 nM Deltamethrin	-33.11 ± 0.99	<0.05	8
V. destructor G933V Mutant	100 nM Flumethrin	-27.57 ± 0.70	<0.05	5
V. destructor G933V Mutant	100 nM Permethrin	-33.91 ± 2.17	<0.05	10
V. destructor G933V Mutant	100 nM Tau-Fluvalinate	-28.72 ± 1.57	<0.05	10

***P-Values were calculated in GraphPad Prism 6 by comparing voltage dependence of inactivation curves using an extra sum-of-squares F test. Values of less than 0.05 demonstrate that for a given pyrethroid and VGSC the $V50_{.inact}$ values generated by these curves in the absence or presence of pyrethroid are significantly different to one another.**

Figure 7.9: Conductance of Arthropod VGSCs Treated with Pyrethroid Toxicants

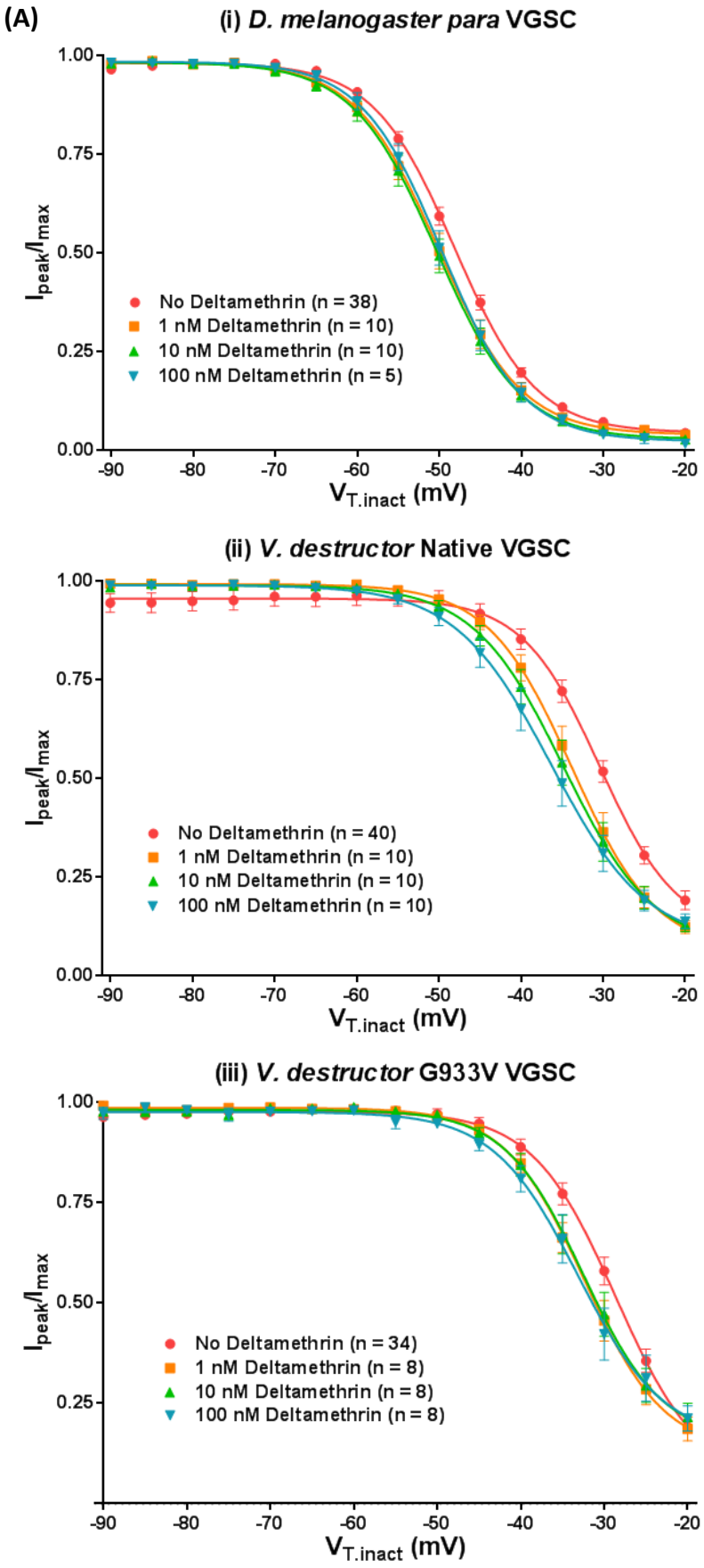

(B)

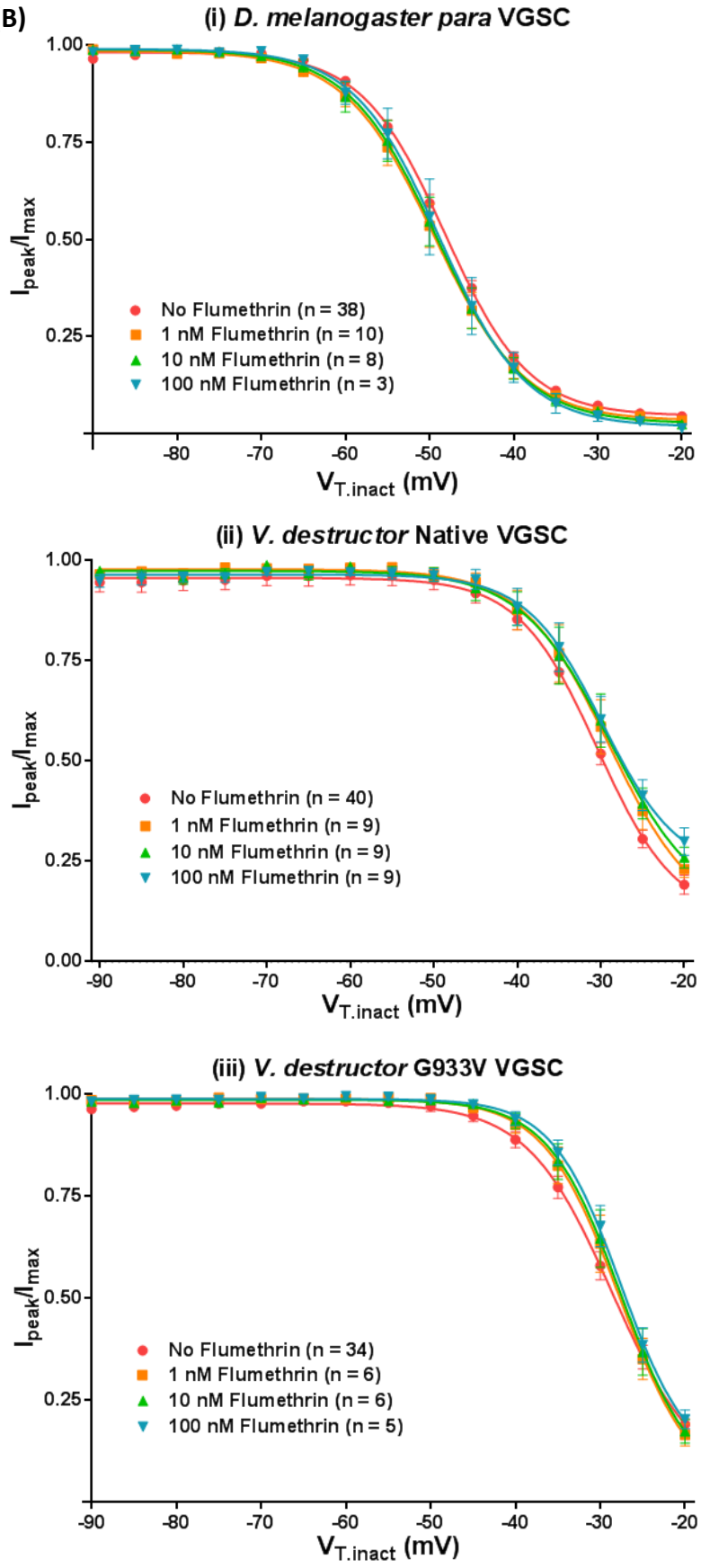
(i) D. melanogaster para VGSC
1.00
0.75
0.50
0.25
I_peak/I_max
No Flumethrin (n = 38)
1 nM Flumethrin (n = 10)
10 nM Flumethrin (n = 8)
100 nM Flumethrin (n = 3)
-80
-70
-60
-50
-40
-30
-20
V_T.inact (mV)
(ii) V. destructor Native VGSC
1.00
0.75
0.50
0.25
0.00
I_peak/I_max
No Flumethrin (n = 40)
1 nM Flumethrin (n = 9)
10 nM Flumethrin (n = 9)
100 nM Flumethrin (n = 9)
-90
-80
-70
-60
-50
-40
-30
-20
V_T.inact (mV)
(iii) V. destructor G933V VGSC
1.00
0.75
0.50
0.25
I_peak/I_max
No Flumethrin (n = 34)
1 nM Flumethrin (n = 6)
10 nM Flumethrin (n = 6)
100 nM Flumethrin (n = 5)
-90
-80
-70
-60
-50
-40
-30
-20
V_T.inact (mV)

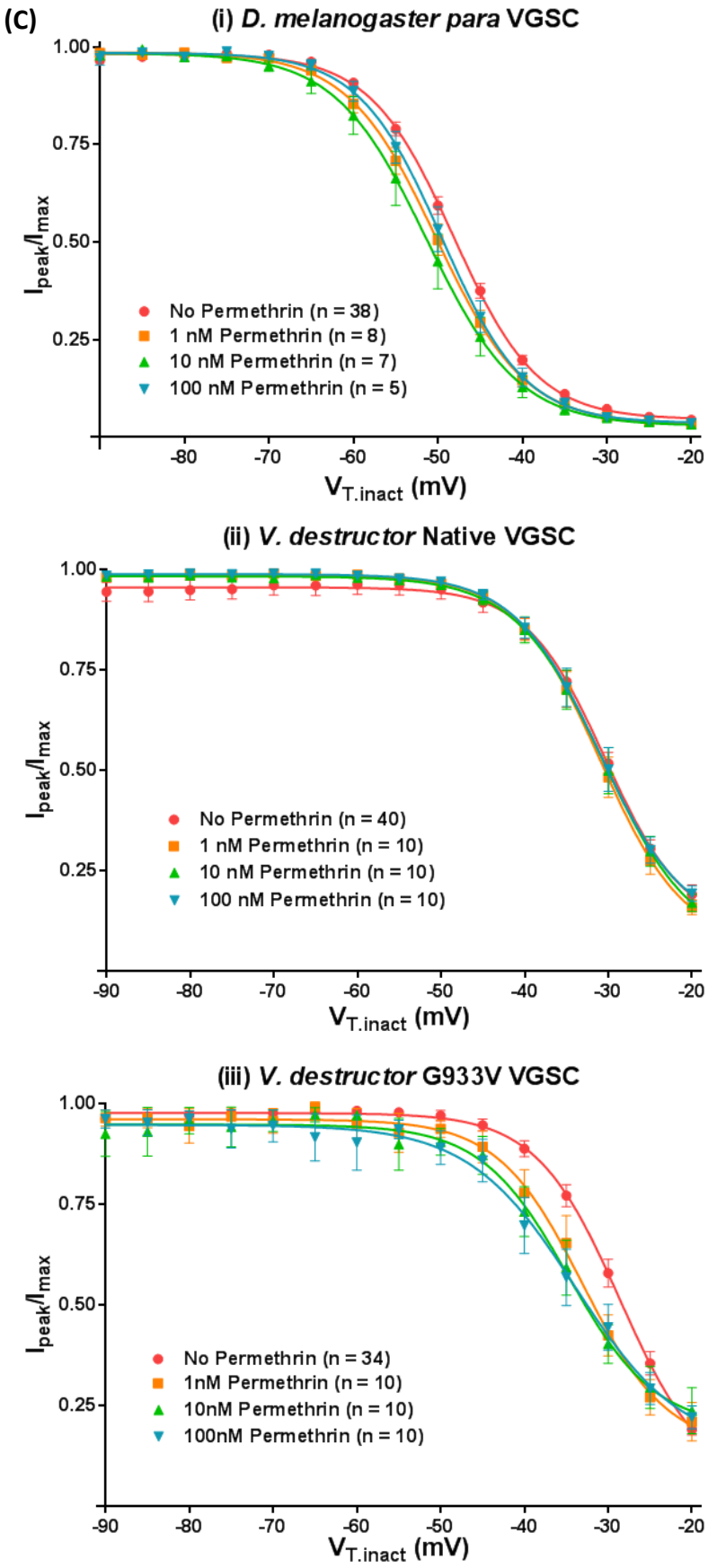
(C)
(i) D. melanogaster para VGSC
1.00
0.75
0.50
0.25
I_peak/I_max
No Permethrin (n = 38)
1 nM Permethrin (n = 8)
10 nM Permethrin (n = 7)
100 nM Permethrin (n = 5)
-80
-70
-60
-50
-40
-30
-20
V_T.inact (mV)
(ii) V. destructor Native VGSC
1.00
0.75
0.50
0.25
I_peak/I_max
No Permethrin (n = 40)
1 nM Permethrin (n = 10)
10 nM Permethrin (n = 10)
100 nM Permethrin (n = 10)
-90
-80
-70
-60
-50
-40
-30
-20
V_T.inact (mV)
(iii) V. destructor G933V VGSC
1.00
0.75
0.50
0.25
I_peak/I_max
No Permethrin (n = 34)
1nM Permethrin (n = 10)
10nM Permethrin (n = 10)
100nM Permethrin (n = 10)
-90
-80
-70
-60
-50
-40
-30
-20
V_T.inact (mV)

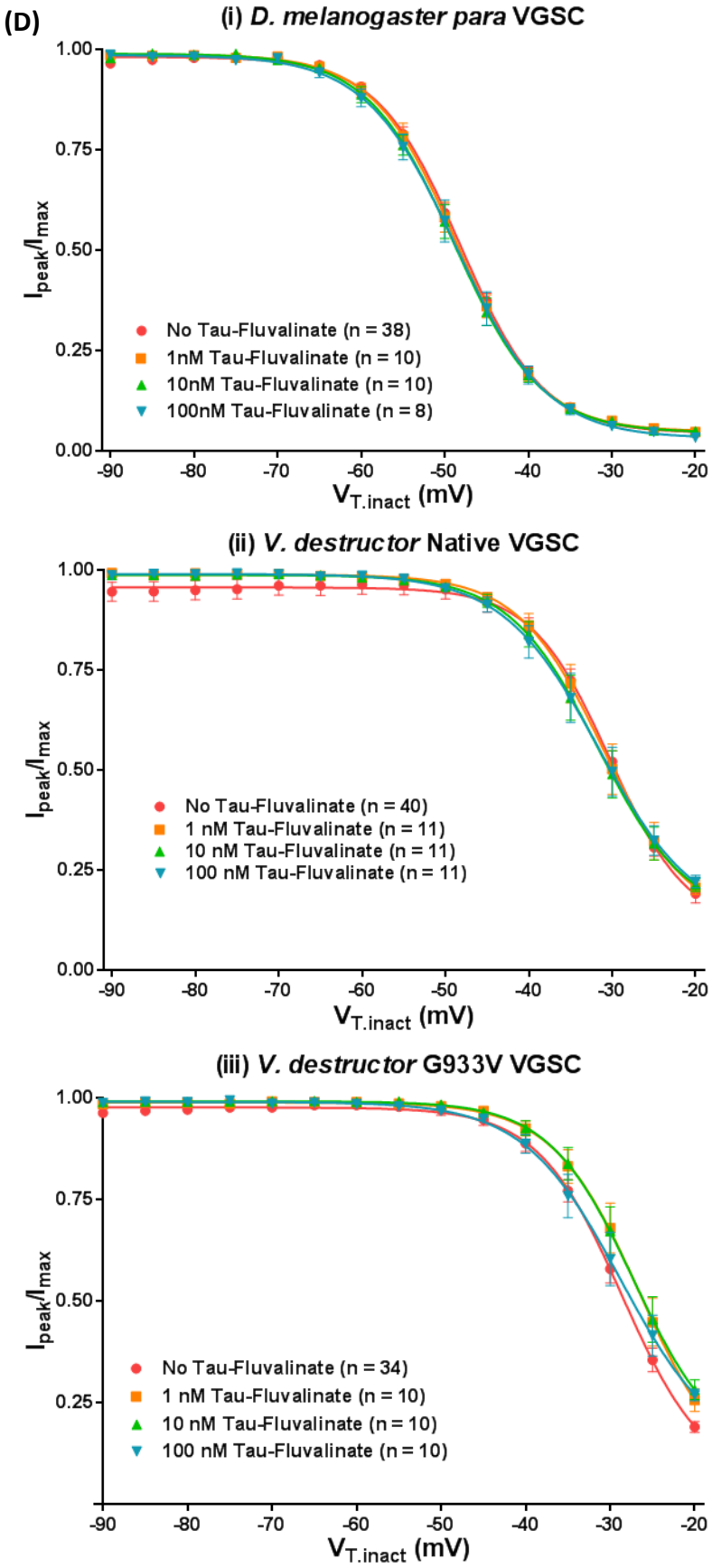

Stead-state inactivation relationships of arthropod VGSCs recorded using Voltage Protocol 2 (Section 7.2.7) and plotted using Equation 4 (Section 7.2.9) in the presence of no toxicant and (A) 1-100 nM Deltamethrin; (B) 1-100 nM Flumethrin; (C) 1-100 nM Permethrin; (D) 1-100 nM Tau-Fluvalinate.

7.3.3.3 Pyrethroid Induced Tail Currents

Tail currents allow the observation of action of pyrethroid insecticides, whereby they slow VGSC inactivation/deactivation, this can be translated into a percentage modification (M_i) of each type of arthropod VGSC by each pyrethroid toxicant, with levels of modification being previously shown to increase in line with pyrethroid concentration in native arthropod VGSCs (Vais et al., 2001). Mean values (along with SEMs) for M_i values for arthropod VGSCs in the absence of toxicant and in the presence of 100 nM or 1 μM of each pyrethroid, as calculated using Equations 4, are listed in Table 7.17 and shown in Figures 7.10 and 7.11 respectively.

Table 7.17: Values of M_i (%) for Arthropod VGSCs in the Presence of 100 nM and 1 µM of Pyrethroid Toxicant

VGSC Source	Pyrethroid	100 nM			1 uM		
		Mean Mi (%)	SEM	(n)	Mean Mi (%)	SEM	(n)
D. melanogaster para	Deltamethrin	142.23	89.58	9	487.85	307.58	6
D. melanogaster para	Flumethrin	192.69	64.12	10	401.54	223.13	7
D. melanogaster para	Permethrin	47.93	22.29	8	215.03	75.55	8
D. melanogaster para	Tau-Fluvalinate	108.03	52.94	10	392.27	163.38	7
V. destructor Native	Deltamethrin	4.79	1.23	10	99.01	31.78	10
V. destructor Native	Flumethrin	2.05	0.84	5	4.92	1.64	5
V. destructor Native	Permethrin	-0.076	0.15	9	2.46	1.35	9
V. destructor Native	Tau-Fluvalinate	21.91	11.05	8	253.14	57.55	8
V. destructor G933V	Deltamethrin	3.73	3.02	6	58.17	35.19	6
V. destructor G933V	Flumethrin	2.71	0.79	5	7.82	2.72	5
V. destructor G933V	Permethrin	0.17	0.21	8	1.68	0.73	8
V. destructor G933V	Tau-Fluvalinate	72.89	49.96	7	269.10	68.30	7

Mean M_i (%) response of a VGSC to pyrethroid pesticides at 100 nM and 1 µM concentrations. Values were calculated following Voltage Protocol 3 using Equation 5 (Section 7.2.9) in Graph Pad 6.

Figure 7.10: Integral Modification of Arthropod VGSCs Treated with 100 nM Pyrethroid Toxicant

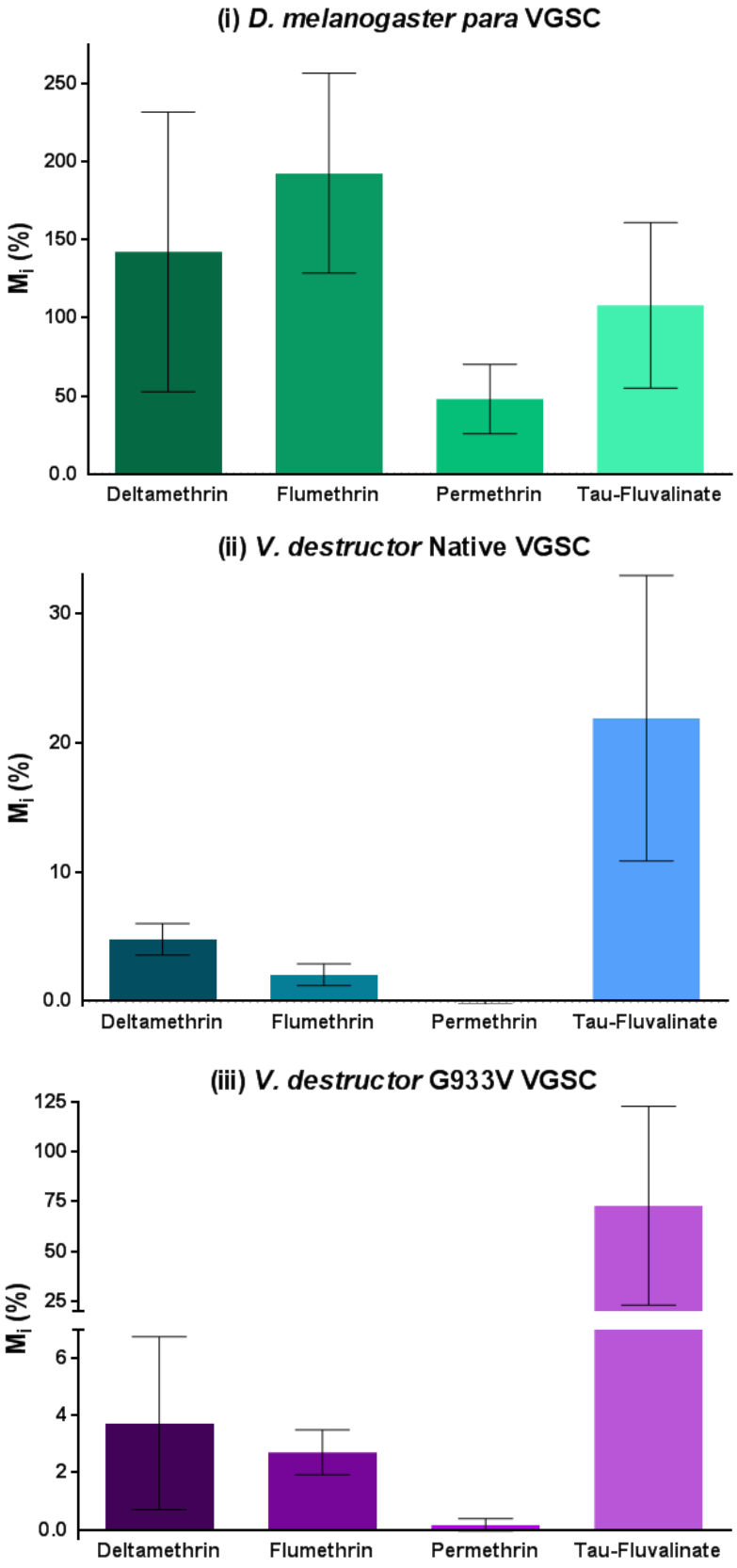

Mean M_i (%) response of a VGSC to 100 nM concentrations of pyrethroid pesticides. Values were calculated following Voltage Protocol 3 using Equation 5 (Section 7.2.9) in Graph Pad 6.

Figure 7.11: Integral Modification of Arthropod VGSCs Treated with 1 µM Pyrethroid Toxicant

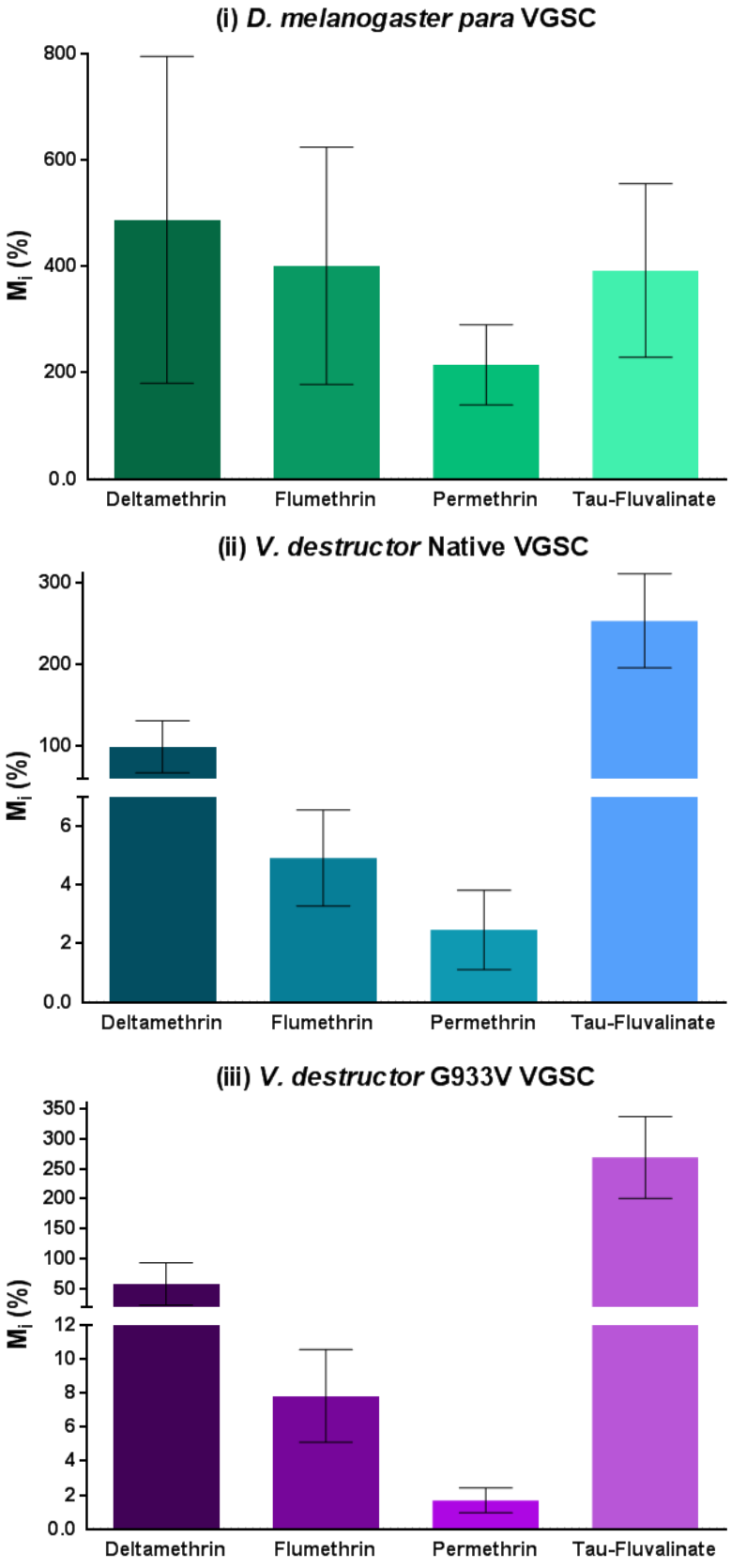

Mean M_i (%) response of a VGSC to 1 µM concentrations of pyrethroid pesticides. Values were calculated following Voltage Protocol 3 using Equation 5 (Section 7.2.9) in Graph Pad 6.

7.3.4 TTX Effects on D. melanogaster para and V. destructor VGSCs

Voltage Protocol 4 (Section 7.2.7) was used to measure the effects of 2 µM TTX applied to arthropod VGSCs (Section 7.2.8). Results of this experiment in the present study can be seen in Figure 7.12. The concentration of TTX delivered gave approximated a 50% block *of V. destructor* VGSCs and a complete block of the *D. melanogaster para* VGSC, as reported previously (Burton, 2012; Du et al., 2009a).

Figure 7.12: Results of an Application of 2 µM TTX on the *D. melanogaster para* and *V. destructor* Native and G933V Mutant VGSCs

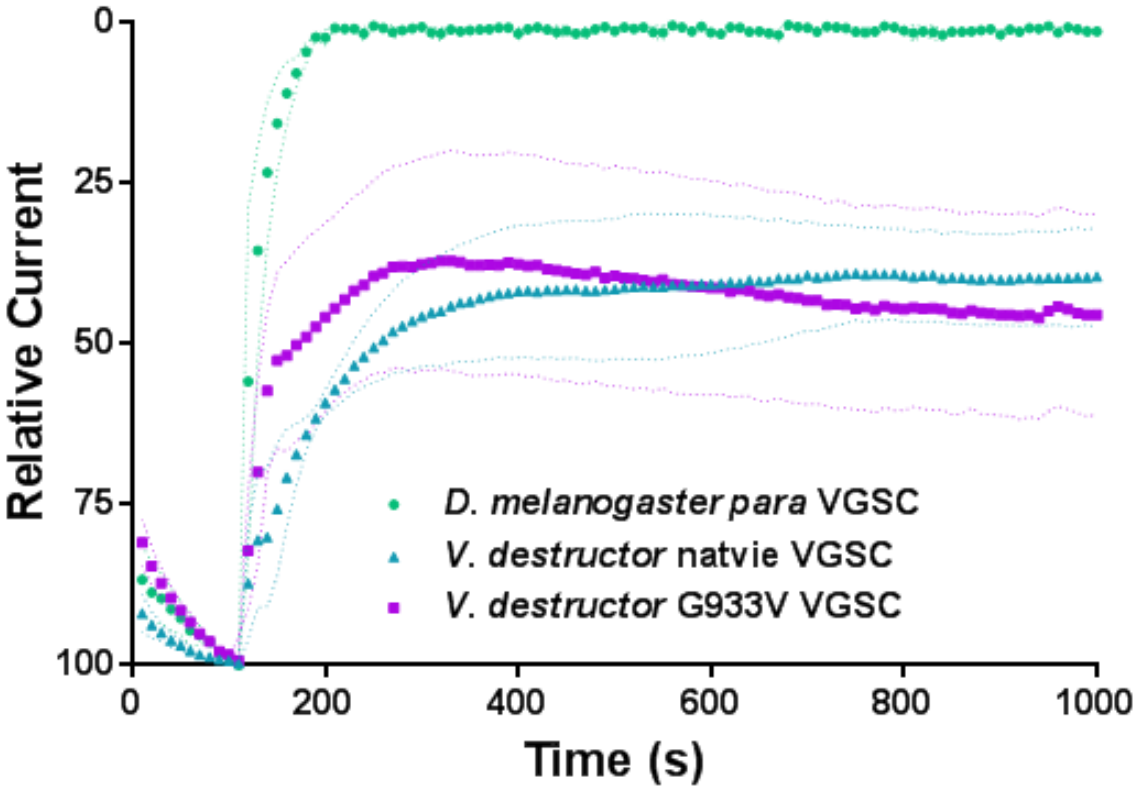

Inhibition of arthropod VGSCs by 2 µM TTX using Voltage Protocol 4. The mean response of a total number (n) of 3 cells for each VGSC type is shown along with 95% confidence intervals of the means (small dots).

7.4 Discussion

7.4.1 Activation of Arthropod VGSCs in the Absence of Any Toxicant

In the absence of any toxicant the *D. melanogaster para* channel $V_{50.act}$ value reported in this study of -29.33 ± 0.32 (n= 37) is lower than values previously reported for native versions of this VGSC (Burton et al., 2011; Usherwood et al., 2007; Usherwood et al., 2005; Vais et al., 2000a; Warmke et al., 1997). However, it is not significantly different to values reported for a *D. melanogaster para* VGSC containing the naturally-occurring mutation L932F (P>0.05 One-Way ANOVA with Dunnett post-test using Graph Pad 6), which should not induce major changes in the kinetic properties of the VGSC, amongst other mutant versions of this channel (Usherwood et al., 2007). Thus, the $V_{50.act}$ value obtained in this study for the native *D. melanogaster para* VGSC is likely representative of variation seen in this channel and is within expected parameters. Values of $V_{50.act}$ for the *V. destructor* native and G933V Mutant VGSCs in the absence of any toxicant were -17.98 ± 0.50 (n = 32) and -18.26 ± 0.63 (n = 27) respectively. These values were not expected to differ significantly from one another as the mutation incurred is naturally occurring and would not be expected to impact on channel gating due to its position within the VGSC (Jonsson et al., 2010; O'Reilly et al., 2006; Usherwood et al., 2007). Indeed both *V. destructor* VGSC $V_{50.act}$ values are not significantly different to one another, or to the value for the *V. destructor* native channel previously obtained by Du *et al* 2009 of -18.23 ± 3.33 (n = 5) (P>0.05 One-Way ANOVA with Dunnett post-test using Graph Pad 6). This strongly suggests that $V_{50.act}$ values for *V. destructor* VGSCs found in this study accurately represent values for these VGSCs when expressed in *X. laevis* oocytes. Interesting, this implies that the insect and acari VGSCs tested show distinct properties in terms of their kinetics of activation (Tables 7.13 and 7.14), and these values are in fact significantly different to one another (P<0.05 One-Way ANOVA with Dunnett post-test using Graph Pad 6). However, $V_{50.act}$ values obtained for *V. destructor* VGSCs in this study are statistically comparable to those previously reported for both native and mutant *D. melanogaster para* VGSCs (P<0.05 One-Way ANOVA with Dunnett post-test using Graph Pad 6) (Burton et al., 2011; Usherwood et al., 2005; Warmke et al., 1997). As $V_{50.act}$ values for *D. melanogaster para* VGSCs seem to show a

degree of variation in the literature, it is not prudent to suggest that they are truly distinct. Further experimentation may shed light on the nature of the variation seen in $V_{50.act}$ values for the *D. melanogaster para* native VGSC. For example, investigations as to whether Tip E co-expression plays a role, as unlike *D. melanogaster para* VGSCs, *V. destructor* VGSC expression in *X. laevis* oocytes is not enhanced by the co-expression of an auxiliary protein (Du et al., 2009a; Warmke et al., 1997).

7.4.2 Inactivation of Arthropod VGSCs in the Absence of Any Toxicant

In contrast, values of $V_{50.inact}$ for *D. melanogaster para* VGSCs in the absence of any toxicant are more comparable between experiments. The $V_{50.inact}$ value of -48.14 ± 0.18 (n = 38) reported in this study is not significantly different to that reported for the native *D. melanogaster para* VGSC in Burton *et al* 2011 and 2012 ($P>0.05$ One-Way ANOVA with Dunnett post-test using Graph Pad 6), and is comparable to those values reported in the literature (Usherwood et al., 2005; Vais et al., 2000b; Warmke et al., 1997). Values of $V_{50.inact}$ for the *V. destructor* native and G933V Mutant VGSCs in the absence of any toxicant were -30.33 ± 0.86 (n = 40) and 28.61 ± 0.75 (n = 34) respectively. Again, values were not expected to differ significantly from one another, due to the position of the G933V mutation within the channel (Jonsson et al., 2010; O'Reilly et al., 2006; Usherwood et al., 2007), and both *V. destructor* VGSC $V_{50.inact}$ values are not significantly different to one another; or to the value for the *V. destructor* native channel previously obtained by Du *et al* 2009 of -29.16 ± 1.72 (n = 5) ($P>0.05$ One-Way ANOVA with Dunnett post-test using Graph Pad 6). Thus, it is likely that the $V_{50.inact}$ values for *V. destructor* VGSCs found in this study also accurately represent values for these VGSCs. Unlike $V_{50.act}$ values obtained for *V. destructor* VGSCs, $V_{50.inact}$ values in this study are also statistically different to those previously reported for native *D. melanogaster para* VGSCs ($P<0.05$ One-Way ANOVA with Dunnett post-test using Graph Pad 6) (Burton et al., 2011; Usherwood et al., 2005; Warmke et al., 1997). The *V. destructor* VGSC $V_{50.inact}$ values in this study shift to the positive when compared to those for *D. melanogaster para* VGSCs, indicating that these VGSCs inactivate at a more positive potential, therefore these channels close at a higher membrane potential after activation. As pyrethroids are thought to bind preferentially

to open VGSCs, stabilising the "activated" state (Bloomquist, 1996; Soderlund and Bloomquist, 1989), this suggests that *V. destructor* VGSCs could be more susceptible to the effects of pyrethroids than *D. melanogaster para* VGSCs. The observed tendency towards inactivation at higher potentials would increase the probability of pyrethroid binding, as the time period during which VGSCs are open, or "activated", would be increased.

7.4.3 Activation of Arthropod VGSCs in the Presence of Pyrethroids

Analysis of $V_{50.act}$ values for VGSCs after exposure to 100 nM pyrethroid revealed a significant shift towards the positive for *V. destructor* native VGSCs treated with flumethrin and *V. destructor* G933V VGSCs treated with deltamethrin or permethrin (Figure 7.8) (Table 7.15). In contrast, in previous studies with the *D. melanogaster* native VGSC, $V_{50.act}$ values shifted towards the negative following pyrethroid application (Burton et al., 2011). As do all *D. melanogaster para* VGSCs tested with pyrethroids in the present study. This negative shift is in line with the theory that pyrethroids stabilise arthropod VGSCs in the "activated" open conformation, meaning more VGSCs are promoted to the open state at more negative V_T potentials following pyrethroid application. All other pyrethroids applied to both native and mutant *V. destructor* VGSCs produced a significant shift in the negative direction, as in line with previous work, and the conductance-voltage relationship graphs for those producing positive shifts show large errors (Figure 7.8). The reasons for this positive shift are currently unknown, but as pyrethroids tested were shown to modify the *V. destructor* VGSCs by application of Voltage Protocol 3 (Section 7.3.3.3) the reason behind this anomaly unlikely to be due to a lack of pyrethroid action on the VGSCs.

7.4.4 Inactivation of Arthropod VGSCs in the Presence of Pyrethroids

The proposed theory that *V. destructor* VGSCs could be more susceptible to the effects of pyrethroids than *D. melanogaster para* VGSCs, due to their tendency towards inactivation at higher membrane potentials, is supported by the response of arthropod VGSCs to pyrethroid toxicants in this study. Analysis of $V_{50.inact}$ values for VGSCs after

exposure to 100 nM pyrethroid revealed a significant shift towards more negative values for *D. melanogaster para* VGSCs treated with deltamethrin or permethrin, *V. destructor* native VGSCs treated with deltamethrin or flumethrin, and *V. destructor* G933V VGSCs treated with any pyrethroid. In prior studies with the *D. melanogaster* native VGSC, $V_{50.inact}$ values shifted towards the positive following pyrethroid application (Burton et al., 2011), as do other VGSCs tested with pyrethroids in the present study (Table 7.16) (Figure 7.9). Namely *D. melanogaster para* VGSCs treated with flumethrin or tau-fluvalinate, and *V. destructor* native VGSCs treated with permethrin or tau-fluvalinate. This positive shift is in line with the theory that pyrethroids block arthropod VGSCs moving from an open to an "inactivated" closed state, meaning VGSCs would only be promoted to the inactivated closed conformation at more positive V_T potentials following pyrethroid application. The theoretic cycling of the VGSC between states is shown in Figure 3.5 (Replicated in Figure 7.13 below).

Figure 7.13: The Four States of the VGSC

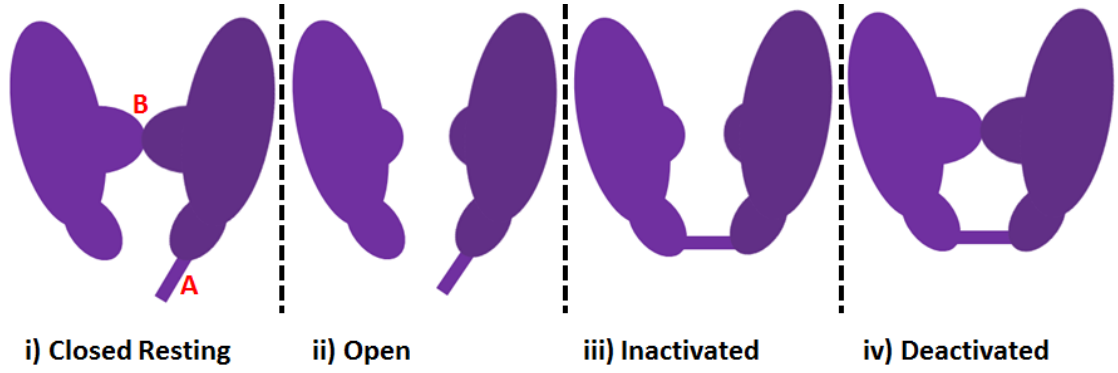

A diagrammatic representation of the four states of the VGSC: i) Closed resting, ii) Open, iii) Inactivated, iv) Deactivated. Where A) indicates the inactivation gate and B) indicates the activation gate. During Voltage Protocol 2 net VGSC movement from an open to an inactivated state is measured.

Pyrethroids bind preferentially to open forms of the arthropod VGSC, and are known to inhibit deactivation (Bloomquist, 1996). However, their effects on inactivation, and the movement of the inactivation gate, are primarily investigated using Voltage Protocol 2. It could be that pyrethroids play a varied role in this fast inactivation, or do not affect it at all, and variations seen in $V_{50.inact}$ values following their application in this study are due to experimental variation. Though significant, the shifts are small, with the largest being around 6 mV (*V. destructor* native VGSC tested with

deltamethrin) (Table 7.16). This is much lower than the 17 to 20 mV shift range seen when comparing *D. melanogaster* para VGSCs to *V. destructor* VGSCs in the absence of any toxicant (Table 7.14) (Figure 7.7). Further investigation of this property of pyrethroids could be of interest following the current study, especially given the shifts in $V_{50.inact}$ seen between the insect and acari VGSCs tested in the present work in the absence of any toxicant. It may be that this property is not important for pyrethroid insecticidal action.

7.4.5 Pyrethroid Induced Tail Currents at Arthropod VGSCs

Tail currents allow the observation of action of pyrethroid insecticides, whereby they slow VGSC inactivation/deactivation (Vais et al., 2001). In the present study, tail currents were recorded to give the M_i (%) of a VGSC in the presence and absence of a pyrethroid toxicant. This figure takes into account not only the peak current elicited during a tail current but also the duration of it (Usherwood et al., 2007). Previous studies have shown that tail currents recorded for pyrethroids acting on insect VGSCs stay below a defined zero current baseline (Burton et al., 2011; Du et al., 2006; Liu et al., 2006; Tan et al., 2002; Usherwood et al., 2007; Usherwood et al., 2005; Vais et al., 2001; Vais et al., 2000b). This point, set at VH = -70 mV, marks a zero point for the calculation of the area under the curve required to give the M_i (%) for a VGSC. In the present study, while *D. melanogaster para* VGSCs followed this pattern, tail currents recorded for the pyrethroids deltamethrin, flumethrin and tau-fluvalinate rose above the current recorded at VH = -70 mV for both native and mutant *V. destructor* VGSCs (Figure 7.14). This tail-current rise tended to increase with pyrethroid concentration and was not present in the absence of toxicant. This phenomenon suggests a different pyrethroid response in acarine VGSCs compared to insects, and presented a problem in analysis by acting to artificially reduce the M_i (%) value recorded for these VGSCs. If the baseline for *V. destructor* VGSCs was set at VH = -70 mV this effect would be enhanced. Therefore, in this study, the baseline from which the area under the curve was calculated for *V. destructor* VGSCs was set at the end of the recording, at approximately 13.45 seconds.

Figure 7.14: Raw Data Showing Tail Currents from Arthropod VGSCs

(A) VGSC Tail Currents in the Absence of Toxicant

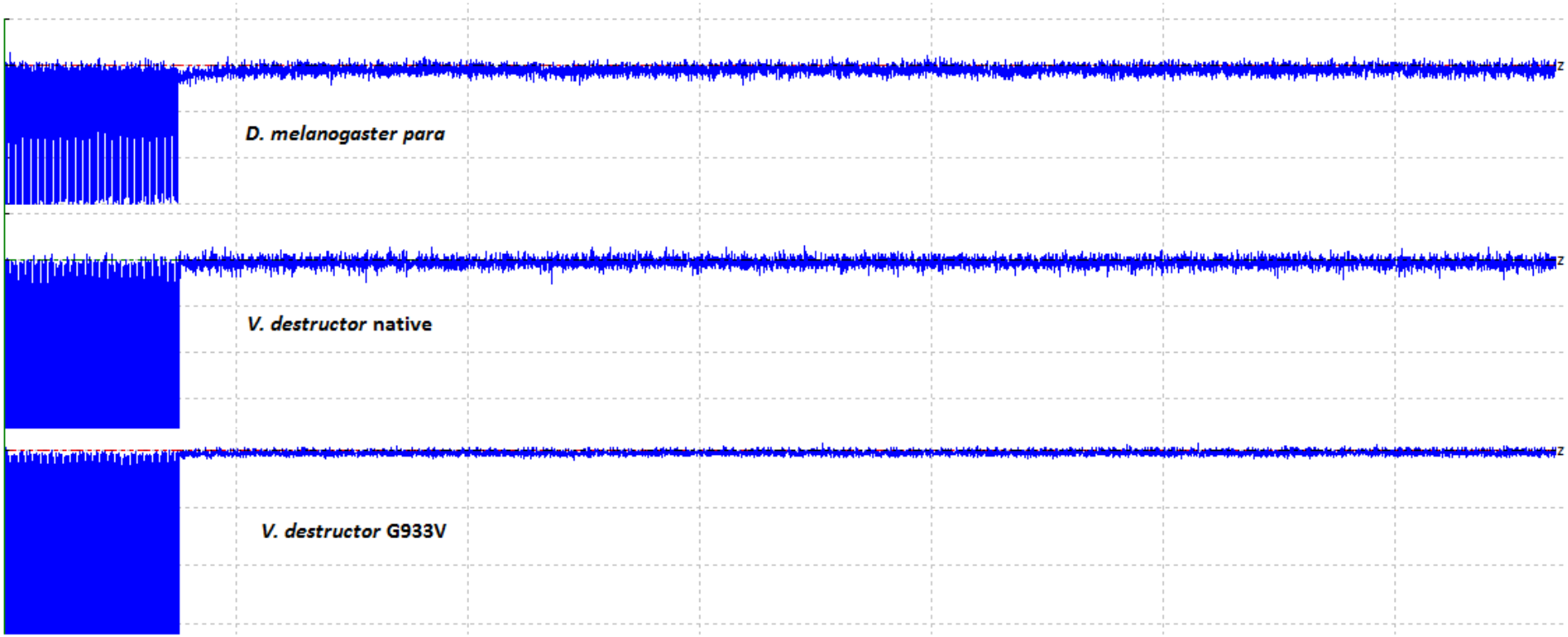

(B) *D. melanogaster para* VGSC Tail Currents with 100 nM Pyrethroid

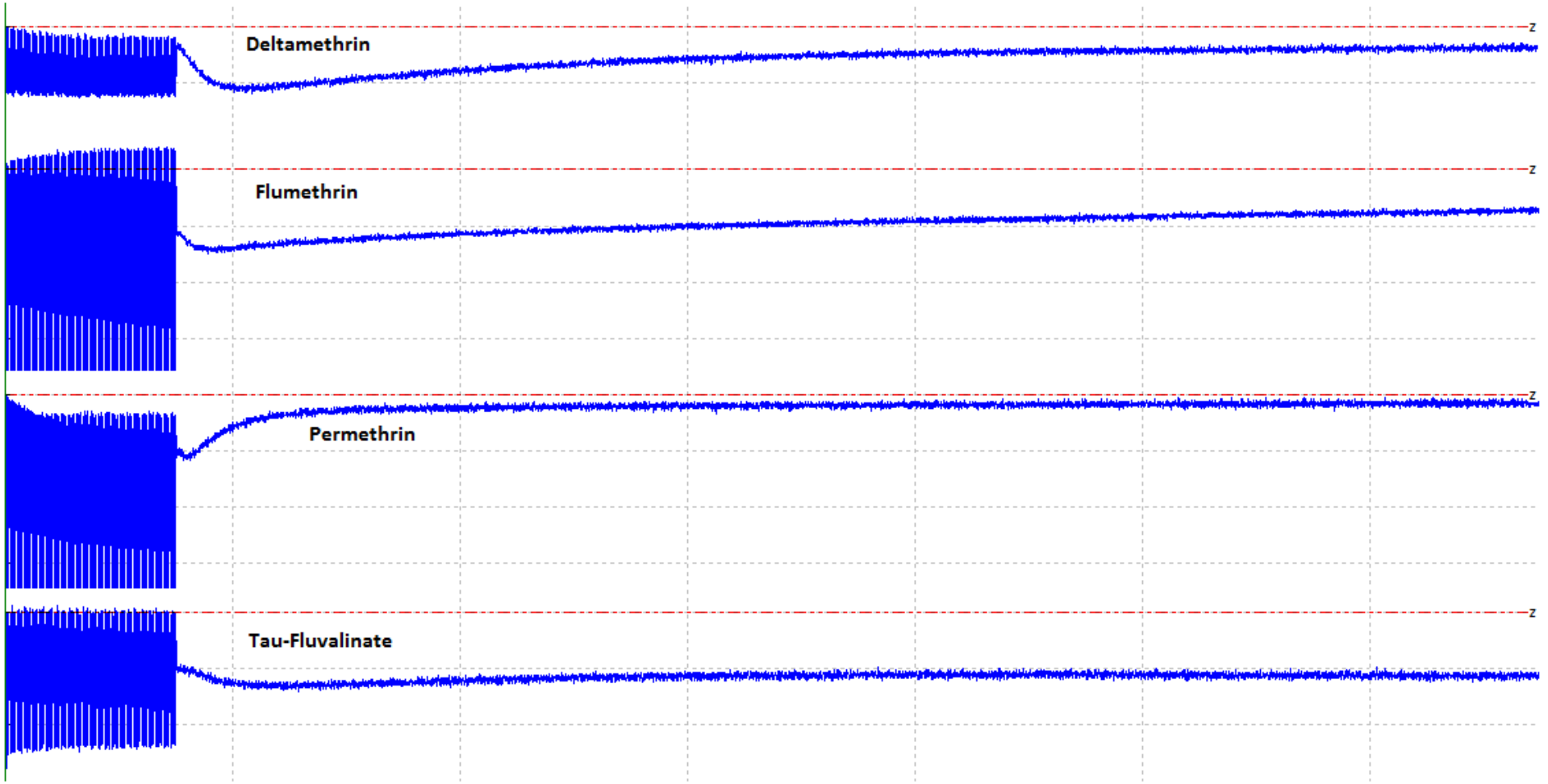

(C) *V. destructor* native VGSC Tail Currents with 100 nM Pyrethroid

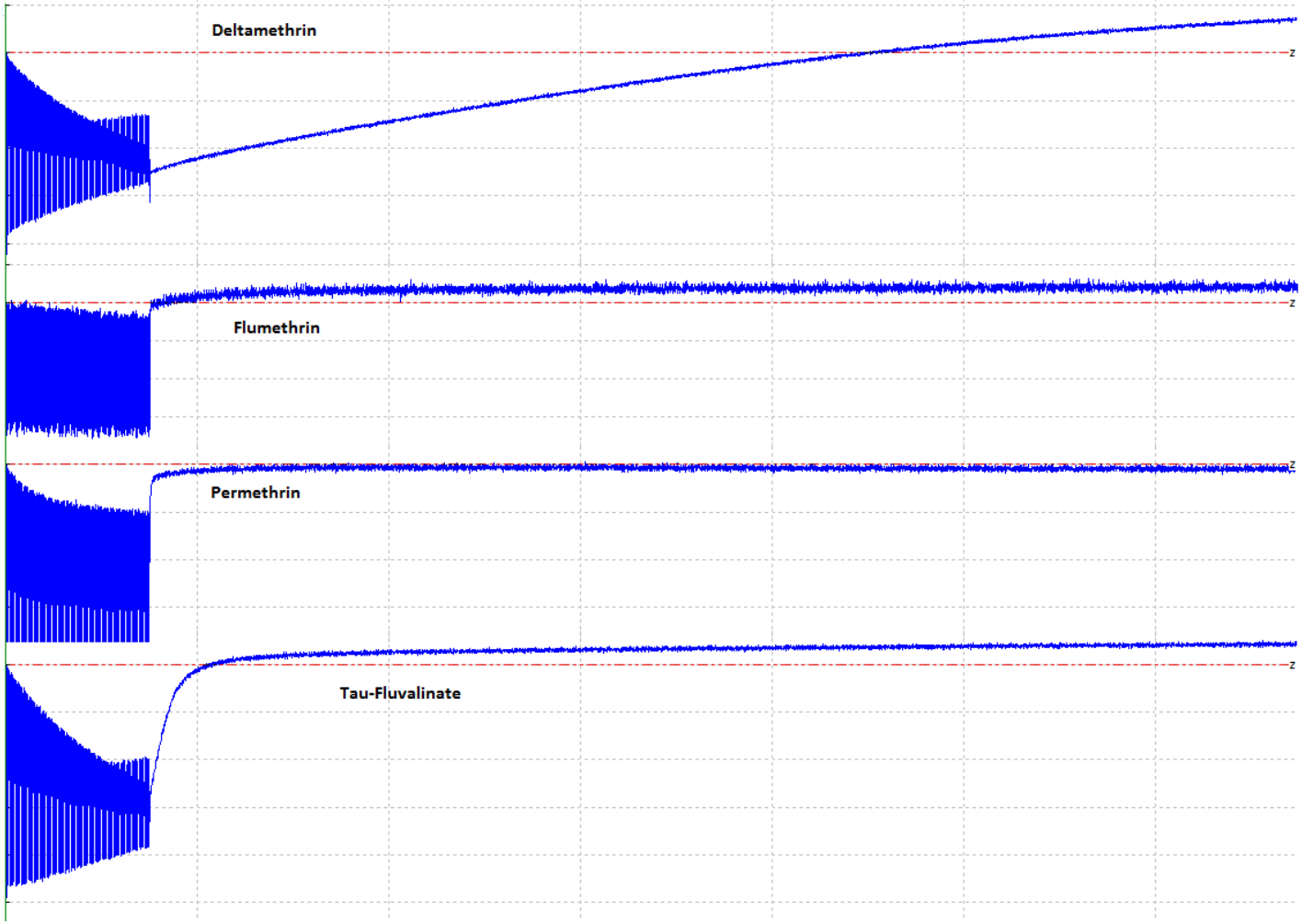

(D) *V. destructor* G933V VGSC Tail Currents with 100 nM Pyrethroid

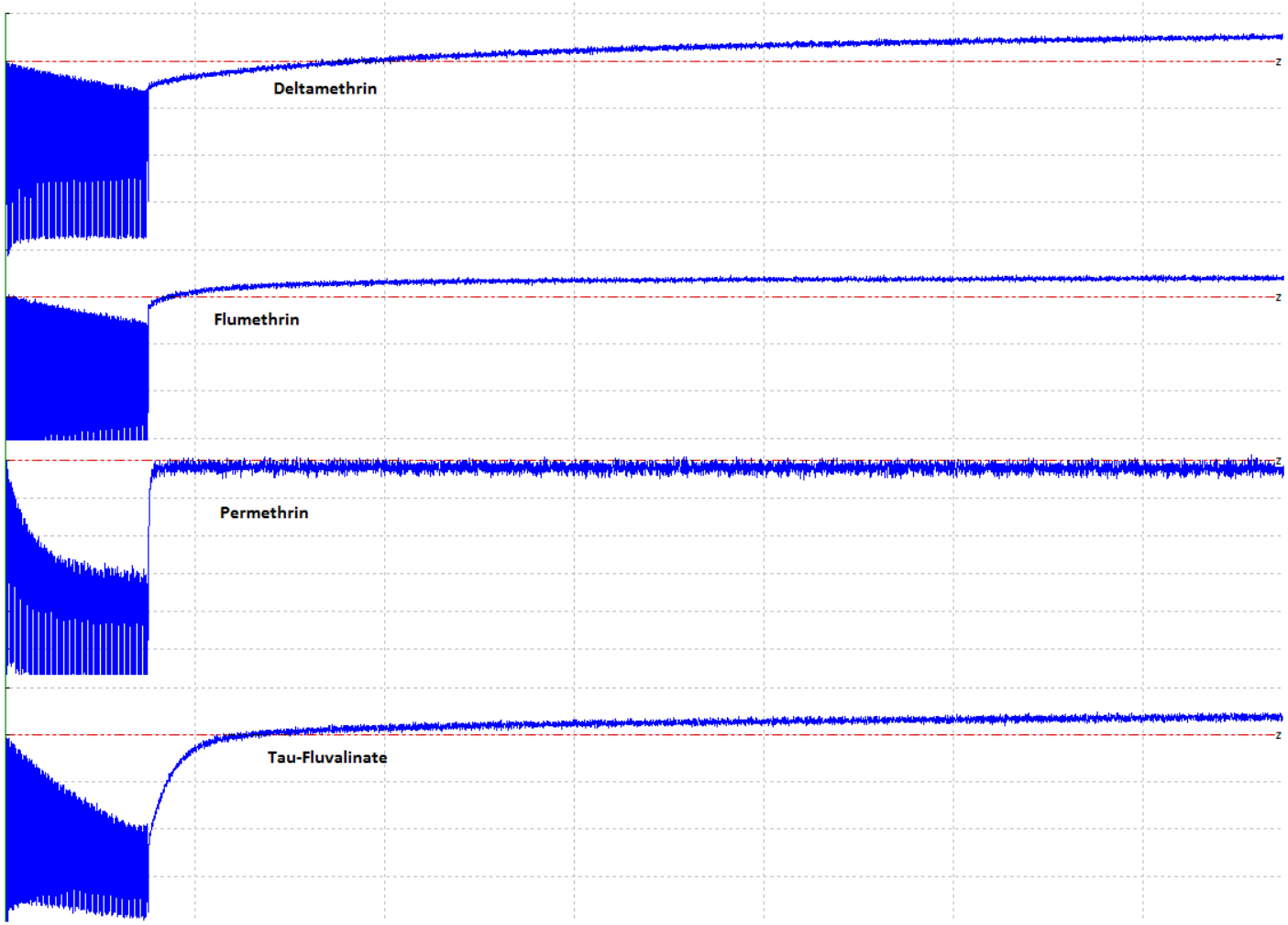

Example tail currents (A) In the absence of toxicant and in the presence of 100 nM pyrethroid for (B) *D. melanogaster para*, (C) *V. destructor* native and (D) *V. destructor* G933V VGSCs. Channels were expressed in *X. laevis* oocytes and exposed to pyrethroid toxicant (Section 7.2.8) before the application of Voltage Protocols 1, 2 and 3 (Section 7.2.7). Data shown was extracted from WinWCP following Voltage Protocol 3 (John Dempster, University of Strathclyde) and illustrates tail-current rise above the Time ≈ 0 baseline seen in *V. destructor* VGSCs (red line).

Pyrethroids with suggested selective acaricidal activity differ from other pyrethroids by having large halogenated substituents in their acidic moiety (Figure 7.15). According to the model proposed by O'Reilly *et al* 2014, pyrethroids with these larger moieties could be accommodated in acarine channels, such as the *V. destructor* native VGSC, which have a smaller glycine at position 933, but not so well by insect channels, such as the *M. domestica* VGSC, which has a larger cysteine residue in this position, nor by the mutated *V. destructor* G933V VGSC. This result is supported by the findings of Jonsson *et al* 2010, that R. microplus cattle ticks resistant to flumethrin but not to cypermethrin carried the G933V mutation in their VGSCs.

Figure 7.15: Pyrethroids Used in Electrophysiological Studies of Arthropod VGSCs

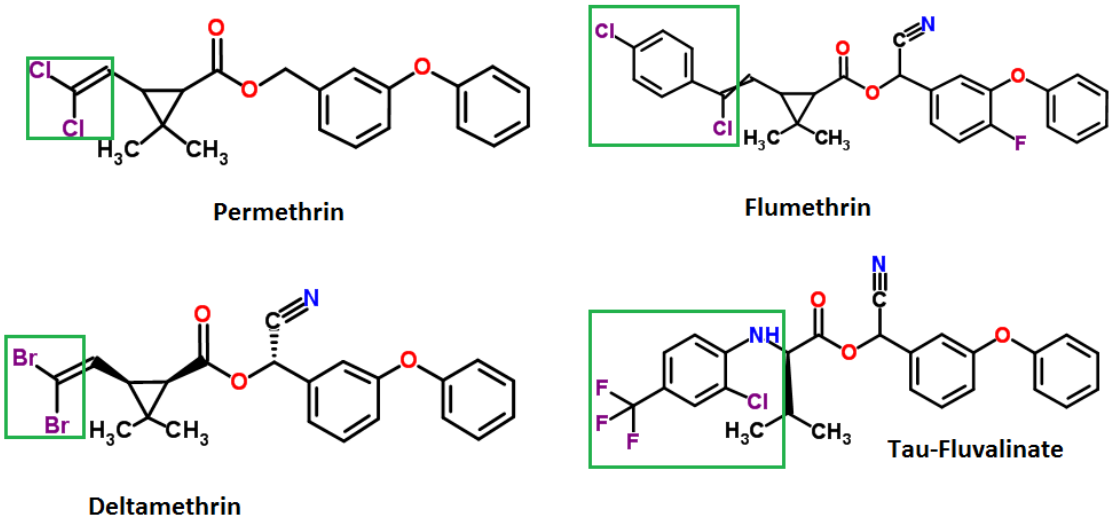

Permethrin, Flumethrin, Deltamethrin and Tau-Fluvalinate shown as examples of pyrethroids with relatively large and small acidic moieties. Areas of interest within the acidic portion are highlighted by green boxes. All pyrethroid structures are from ChemSpider 2016.

If the O'Reilly *et al* 2014 model were to hold true, we would expect both flumethrin and tau-fluvalinate to show reduced activity at the *D. melanogaster para* and the *V. destructor* G933V mutant VGSCs compared the *V. destructor* native VGSC. To this end, comparisons of VGSC M_i (%) were made to see if VGSCs from different species responded significantly differently to each of the pyrethroids tested (Table 7.17). The only significant result found was that for permethrin; where the *D. melanogaster para* VGSC showed significantly greater modification in response to permethrin application than either the *V. destructor* native or the *V. destructor* G933V VGSCs. This was true at

both 100 nM and 1 µM permethrin (P<0.05 One-way ANOVA with Dunnett post-test using Graph Pad 6), a finding which does not support the model proposed by O'Reilly *et al* 2014. Furthermore, the fact that G933V was seen to be a selective resistance mutation to flumethrin in *R. microplus* (Jonsson et al., 2010) contradicts conclusions in this study. Even within species this work found that arthropod VGSC M_i (%) varied little between pyrethroids; in fact for *D. melanogaster para* VGSCs the mean M_i (%) response of a VGSC to one pyrethroid did not differ significantly in its response to any other at either 100 nM or 1 µM pyrethroid concentration (P>0.05 One-way ANOVA with Dunnett post-test using Graph Pad 6). For *V. destructor* native VGSCs only the mean M_i (%) response of VGSCs exposed to tau-fluvalinate differed significantly in their response to other pyrethroids. These VGSCs showed a greater M_i (%) than permethrin at 100 nM and at 1 µM pyrethroid concentrations, and deltamethrin and flumethrin at 1 µM concentrations only (P<0.05 One-way ANOVA with Dunnett post-test using Graph Pad 6). This result is similar to that for the *V. destructor* G933V VGSC, where only the mean M_i (%) response of VGSCs exposed to tau-fluvalinate differed significantly in their response to other pyrethroids, again giving a greater M_i (%), but this time only at 1 µM concentrations for all three other pyrethroids (P<0.05 One-way ANOVA with Dunnett post-test using Graph Pad 6). Clearly future work is needed before firm conclusions are drawn about the action of pyrethroids at insect versus acarine VGSCs. During testing, *X. laevis* oocytes injected with *V. destructor* VGSCs and exposed to deltamethrin frequently lost membrane clamp at pyrethroid concentrations high enough to induce a tail-current, suggesting an opening of the VGSCs triggered by the pyrethroid leading to irreversible current flow. However, the rise seen in deltamethrin tail currents at higher pyrethroid concentrations may mean that some of the effects of deltamethrin, and the other Type II pyrethroids tested, could be unrecorded and therefore their action underestimated. To combat this, any future work will involve a modified version of Voltage Protocol 3 that extends the hyperpolarising phase. This will allow observation of tail currents in *V. destructor* VGSCs to see if they eventually decline. Furthermore, now that the work in this study has established suitable pyrethroid concentrations to induce tail currents in *V. destructor* VGSCs, it would be sensible to test each oocyte with one concentration only per pyrethroid in future, as pre-bound pyrethroid could explain the rising tail currents

seen. Work should also be expanded to other Type I and Type II pyrethroids (Khambay and Jewess, 2005), as it is interesting to note that in this study only the Type II pyrethroids (those with α-cyano group at the α-benzylic position; Namely deltamethrin, flumethrin and tau-fluvalinate) produced the effects seen. Such work could inform discussion into the nature of pyrethroid binding at the arthropod VGSC, as the tail current rising above the baseline could suggest that type II pyrethroids bind for a longer period to acarine VGSCs than to those of insects. It will also be necessary to design an experiment to see if certain pyrethroids can bind at voltages during which the *V. destructor* VGSCs should be closed, another factor which could cause the observed tail currents. Finally, as it has been shown that pyrethroids can bind to other channels besides the VGSC (Casida et al., 1983), it would be interesting to use TEVC techniques to examine pyrethroid binding at different ion channels in acarine and insect species, to see if this explains differences in pyrethroid selectivity seen between species.

7.4.6 TTX Effects on Arthropod VGSCs

TTX has long been used as a means of confirming that an observed current in TEV electrophysiology is due to the expression of a VGSC. Though TTX has been shown to block the *D. melanogaster para* VGSC effectively in numerous studies (Burton, 2012; Feng et al., 1995; O'Dowd and Aldrich, 1988; Warmke et al., 1997), it is significantly less potent at the *V. destructor* VGSC (Du et al., 2009a). The concentration of TTX causing 50% response inhibition from VGSCs (the IC_{50}) was found to be around 0.2 nM for *D. melanogaster para* VGSCs co-expressed with *D. melanogaster TipE* (Feng et al., 1995). In contrast the IC_{50} for TTX was found to be 1.05 ± 0.28 μM for the native *V. destructor* VGSC and 1.45 ± 0.50 μM for a *V. destructor* VGSC lacking a region corresponding to optional exon b in *B. germanica* (Du et al., 2009a). As removal of this region did not significantly affect TTX binding at the *V. destructor* VGSC, the maximum possible concentration to gain a 50% block of the *V. destructor* VGSC can be estimated as ~1.95 μM. Thus, the application of TTX to a final bath concentration of 2 μM in the current study gave a full block of *D. melanogaster para* VGSC signals and approximately 50% block of *V. destructor* native and G933V mutant VGSC signals

(Figure 7.12). This is in keeping with the findings of Du *et al* 2009 with regards to the *V. destructor* VGSCs and of previous work by Warmke *et al* 1997 and Burton 2012 (for example) with regards to the *D. melanogaster para* VGSC.

8 Pyrethroid Bioassays of Acarine Species and *M. domestica*

8.1 Chapter Introduction and Aims

Comparison of the *D. melanogaster* para and *V. destructor* VGSCs expressed in oocytes using electrophysiological methods showed that, although there was a significance difference in the response of these channels to permethrin, there was no significant difference in the sensitivity of the insect and mite channels to pyrethroids with large-halogenated groups (Section 7.4.5). This chapter aims to test whether similar sensitivities to these compounds are found in whole insects/acari using contact bioassays. Four ticks (*A. americanum*, *I. ricinus*, *R. sanguineous* and *D. variabilis*), a representative insect (*M. domestica*) and the mite, *V. destructor* were tested using the same 4 pyrethroids used in electrophysiological studies in Chapter 7: Permethrin, deltamethrin, flumethrin and tau-fluvalinate.

8.2 Chapter Specific Methods

8.2.1 Arthropods

A. americanum, *D. variabilis, I. ricinus*, *R. sanguineous*, *M. domestica*, and *V. destructor* were sourced as described in Section 4.1. The *V. destructor* were collected from adult bees rather than capped worker bee brood combs as in previous studies (Kamler et al., 2016; Kanga et al., 2010), due to a lack of availability of brood combs. Samples for bioassay where taken from storage boxes; for the ticks this was done within a heated frame to prevent escape of individuals and for *M. domestica* this was done under carbon dioxide, with flies treated a maximum of two times with an incapacitating dose. *V. destructor* were taken from the field at the hive site (The Honey Farm, Imkerei Ullmann, Erlensee, Germany), with the being mites being removed from captured adult bees using a soft paint brush, and placed immediately into the treatment vials.

8.2.2 Contact Bioassays

A glass vial technique (Plapp et al., 1987) was used to measure the response of adult arthropods to insecticides in the laboratory. The tests were done in 25 ml volume glass scintillation vials, which were coated with a solution of insecticide in 0.25 ml acetone and rolled gently on their sides using a commercial roller until the acetone evaporated leaving an even coating of dried insecticide on the vial's inner surface. Vials were prepared a maximum of one day before use. To estimate the toxicity of the pyrethroids, increasing doses were used along with two controls; a blank vial with no coating and a vial coated in 0.25 ml acetone only. All species were tested with the same pyrethroid concentrations at five-fold dilutions, except for *I. ricinus*, which was tested using ten-fold dilutions (see Table 48). Five adult arthropods were placed into each vial and the vials were closed with plastic caps containing small air holes. The vials were then incubated according to species; *A. americanum*, *D. variabilis, I. ricinus*, *M. domestica* and *V. destructor* were kept in the dark at 85% humidity and 21°C, and *R. sanguineus* in the dark at ambient room conditions (approx. 40-60% humidity and 21°C). Pyrethroid effects were observed at 2, 4, 6, 24 and 48 hours after exposure depending on the species. The exact experimental test conditions were established from range-finding trials. These were performed once for all tick species, with one replicate per pyrethroid concentration. Raw-data are detailed in Section 10.4 Appendix 4. For *V. destructor* the range-finding trials used a comparatively reduced number of doses, due to a lack of mites. Raw-data from these trials is also detailed in Section 10.4 Appendix 4. Each experimental test was replicated a minimum of 3 times. Concentrations used and recording times for these experiments are shown in Table 8.1. At each observation stage individuals unable to move when subjected to a stimulus (heat or carbon dioxide for tick species, or tapping of the vial for *V. destructor* or *M. domestica*), were considered dead, those with unusual or minimal movement compared to control individuals (and thus unable to infect a host animal) were considered to show a knockdown effect.

Table 8.1: Concentrations and Recording Times for Pyrethroid Contact Bioassays

Species	Concentrations Used (ppm)	Recording Times (Hours)
M. domestica	1650, 330, 66, 13.2, 2.64, 0.528, 0.1056, 0.02112	2, 4, 6, 24
D. variabilis	1650, 330, 66, 13.2, 2.64, 0.528, 0.1056, 0.02112	4, 24, 48
R. Sanguineus	1650, 330, 66, 13.2, 2.64, 0.528, 0.1056, 0.02112	4, 24, 48
I. ricinus	1650, 165, 16.5, 1.65, 0.165, 0.0165, 0.00165, 0.000165	4, 24, 48

8.2.3 Statistical Analysis

The data obtained from the bioassays were subjected to probit analysis (Finney, 1947), using counts of dead or knockdown individuals, for each insecticide and assessment time, allowing a comparison of EC_{50} values (the dose required to affect 50% of individuals). This allowed comparisons between the tick species with those for, *M. domestica*. Models were fitted using the probit analysis implementation in GenStat for Windows 18th Edition (VSN International, Hemel Hempstead, UK; www.vsni.co.uk), assuming an underlying binomial distribution for the counts and a logit link function and relating the proportion affected to the log 10 transformed pyrethroid doses (ppm). Because there was limited information available for responses between the extreme responses of 0% and 100% of individuals being affected, a common slope parameter was assumed for each assessment time for each insecticide. These analyses provided estimates of the EC_{50} values for each species, together with standard errors (using Fieller's theorem), on the log 10 dose scale, from which 95% confidence limits were constructed on the log 10 dose scale. EC_{50} values and associated 95% confidence limits were then back-transformed to the raw dose scale. A further logistic regression analysis (also implemented in GenStat for Windows 18th Edition) provided a parameterisation of the fitted probit model, allowing a direct assessment of the difference in the logit intercept parameter (effectively the logit transformation of the proportion affected at a log 10 dose of zero) for each tick species relative to *M. domestica*. A two sided z-test of these differences identified where the intercept parameter (and hence EC_{50} value) for each species was significantly different ($p < 0.05$)

from that for *M. domestica* (a more negative intercept value being associated with a larger EC_{50} value, a more positive intercept value being associated with a smaller EC_{50} value than that of *M. domestica*). Observed proportions of affected individuals and the fitted probit curves were plotted on the log 10 dose scale, illustrating the parallel nature of the fitted curves on this scale as a consequence of assuming a common slope parameter.

8.3 Results

8.3.1 Range Finding Trials

Initial range-finding trials were done with tick species *A. americanum*, *D. variabilis, I. ricinus*, and *R. sanguineus* using ten-fold dilutions for each pyrethroid and starting at a concentration equivalent to 1 g/Ha (or 1650 ppm). It was concluded that five-fold dilutions would be the best, with some of the lower concentrations not being needed. The exception to this was for *I. ricinus*, where it was found that clear results were produced using a ten-fold dilution factor. This was probably due to the smaller body mass of *I. ricinus*, compared to the other species tested. Range finding trials were not possible for *M. domestica* because not enough flies were available, but since it has a mass comparable to the larger tick species, five-fold dilutions were assumed to be suitable. For *V. destructor* only range-finding trials were possible, due to limited availability of mites. The results of range-finding trials can be found in Section 10.4 Appendix 4.

8.3.2 Insect and Acari Comparative Contact Bioassays

Replicated bioassays were carried out with the ticks *D. variabilis, I. ricinus* and *R. sanguineus*, and the insect *M. domestica*. *A. americanum* could not be used due to lack of availability. The EC_{50} values, along with their lower and upper 95% CIs, are shown below, after 4 Hours pyrethroid exposure in Table 8.2 and after 24 hours pyrethroid exposure in Table 8.3. The EC_{50} values and their respective CIs are also presented as histograms in Figure 8.1 and as dose response curves in Section 10.5 Appendix 5.

Table 8.2: EC_{50}s for Pyrethroids (ppm) After 4 Hours Exposure

Species	Pyrethroid	EC_{50} (ppm)	Lower 95% CI	Upper 95% CI
M. domestica	Deltamethrin	0.24	0.14	0.39
D. variabilis	Deltamethrin	11.83*	8.44	15.89
R. Sanguineus	Deltamethrin	2.37*	1.69	3.18
I. ricinus	Deltamethrin	1.13*	0.67	1.60
M. domestica	Flumethrin	5.90	3.34	10.42
D. variabilis	Flumethrin	21.38*	12.13	37.75
R. Sanguineus	Flumethrin	1.06*	0.60	1.87
I. ricinus	Flumethrin	1.78*	0.91	3.45
M. domestica	Permethrin	1.30	0.80	2.10
D. variabilis	Permethrin	425.70*	274.20	670.20
R. Sanguineus	Permethrin	29.50*	18.40	47.30
I. ricinus	Permethrin	7.80*	4.20	13.80
M. domestica	Tau-Fluvalinate	5.90	3.71	9.40
D. variabilis	Tau-Fluvalinate	208.50*	132.14	324.30
R. Sanguineus	Tau-Fluvalinate	6.60	4.17	10.50
I. ricinus	Tau-Fluvalinate	5.20	2.74	9.90

*** = Significantly different to the *M. domestica* EC_{50} value for the same pyrethroid. As determined by a two sided z-test of these differences which identified where the intercept parameter for each species (and therefore EC_{50}) was significantly different ($P<0.05$) from that for *M. domestica* (Section 10.5 Appendix 5).**

Table 8.3: EC_{50}s for Pyrethroids (ppm) After 24 Hours Exposure

Species	Pyrethroid	EC_{50} (ppm)	Lower 95% CI	Upper 95% CI
M. domestica	Deltamethrin	0.24	0.15	0.37
D. variabilis	Deltamethrin	11.54*	7.79	16.73
R. Sanguineus	Deltamethrin	2.31*	1.56	3.35
I. ricinus	Deltamethrin	0.17	0.12	0.26
M. domestica	Flumethrin	1.18	0.74	1.88
D. variabilis	Flumethrin	0.08*	0.05	0.11
R. Sanguineus	Flumethrin	0.12*	0.08	0.18
I. ricinus	Flumethrin	0.14*	0.09	0.21
M. domestica	Permethrin	1.20	0.70	2.10
D. variabilis	Permethrin	318.20*	183.20	557.60
R. Sanguineus	Permethrin	3.80*	2.20	6.70
I. ricinus	Permethrin	0.70	0.40	1.40
M. domestica	Tau-Fluvalinate	5.90	3.53	9.90
D. variabilis	Tau-Fluvalinate	50.71*	30.53	84.00
R. Sanguineus	Tau-Fluvalinate	6.59	3.94	11.00
I. ricinus	Tau-Fluvalinate	3.15	1.72	5.90

*** = Significantly different to the *M. domestica* EC_{50} value for the same pyrethroid. As determined by a two sided z-test of these differences which identified where the intercept parameter for each species (and therefore EC_{50}) was significantly different ($P<0.05$) from that for *M. domestica* (Section 10.5 Appendix 5).**

Figure 8.1: EC_{50} Values of Pyrethroids (ppm) for Acarine Species and *M. domestica* after 4 and 24 Hours Exposure

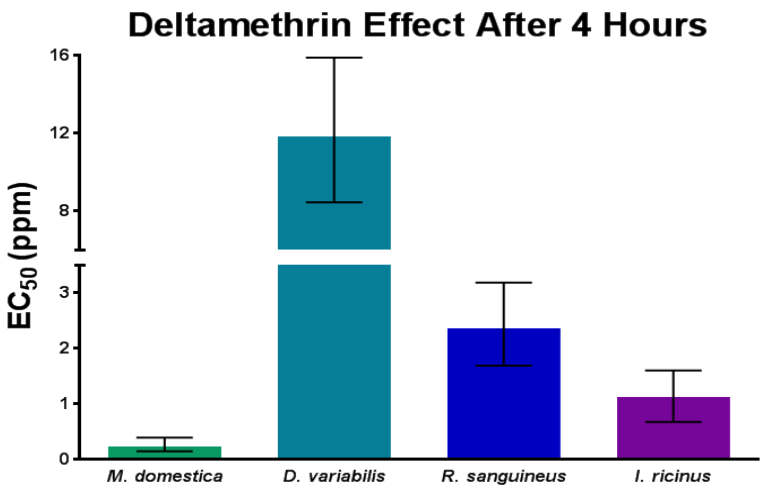

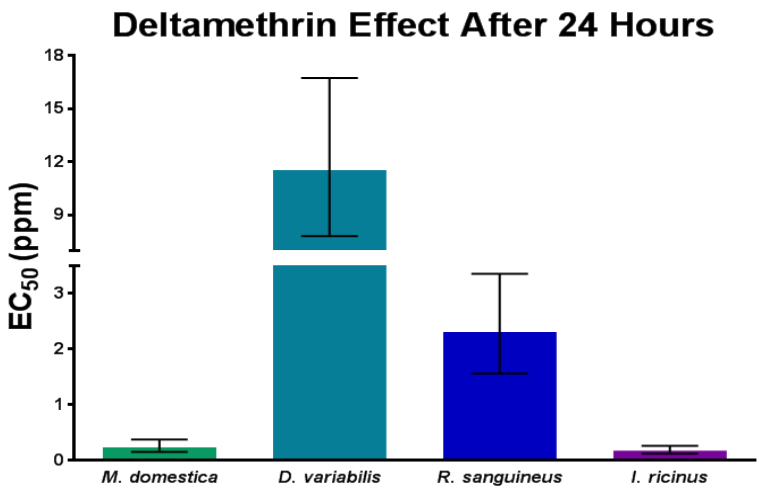

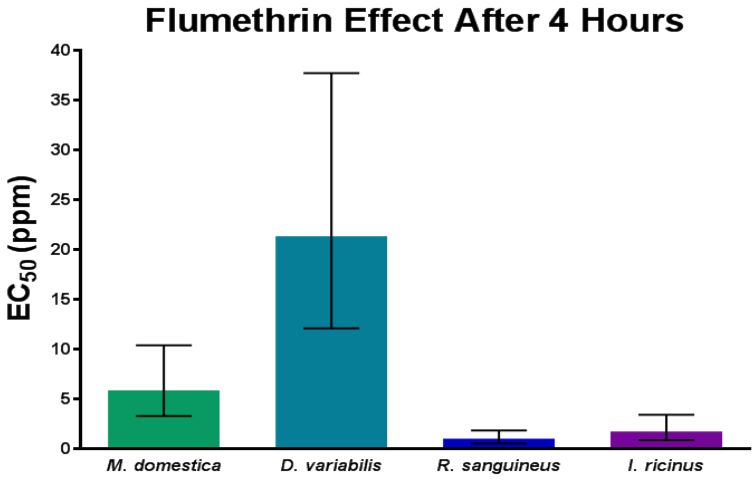

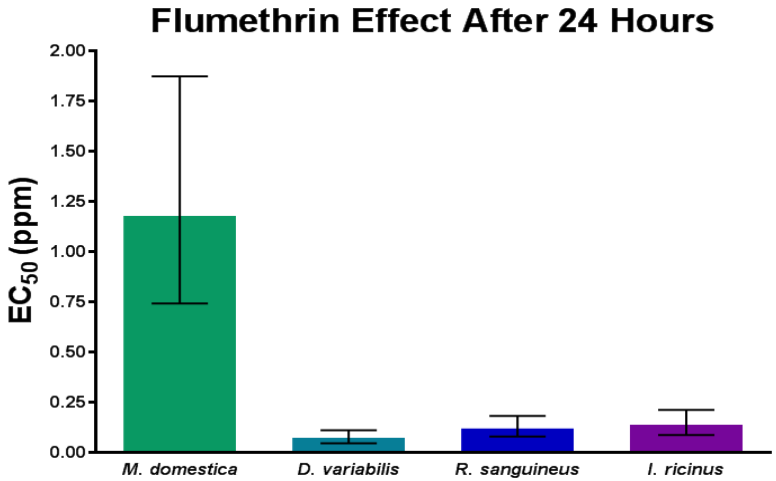

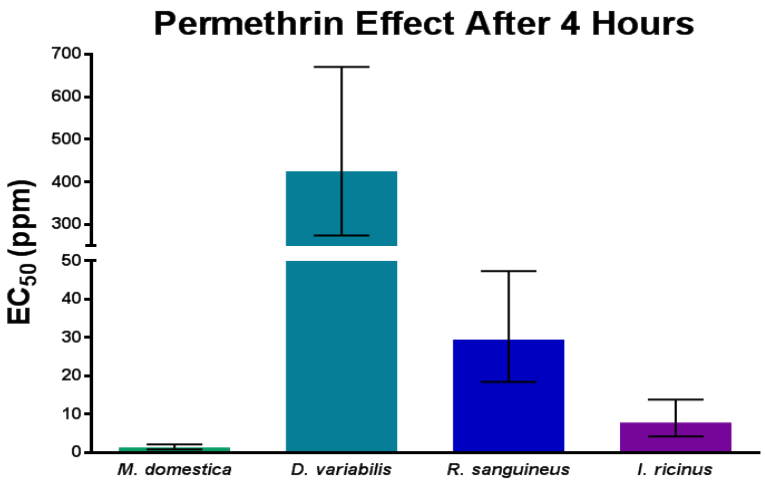
Permethrin Effect After 4 Hours
EC50 (ppm)
700
600
500
400
300
50
40
30
20
10
0
M. domestica
D. variabilis
R. sanguineus
I. ricinus

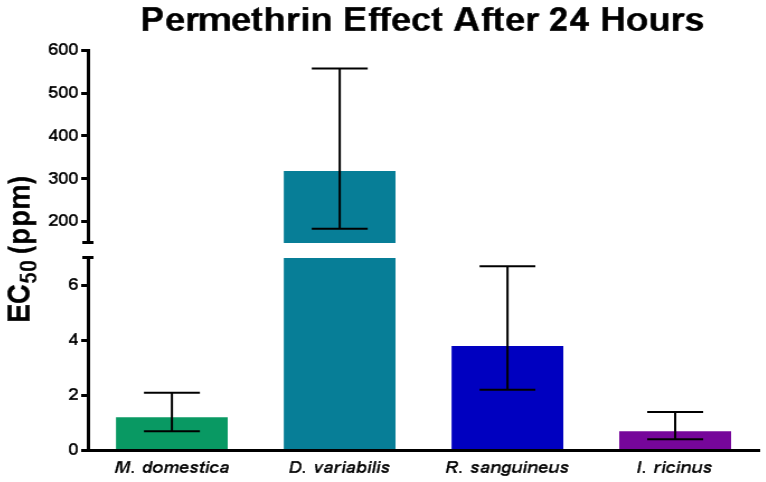
Permethrin Effect After 24 Hours
EC50 (ppm)
600
500
400
300
200
6
4
2
0
M. domestica
D. variabilis
R. sanguineus
I. ricinus

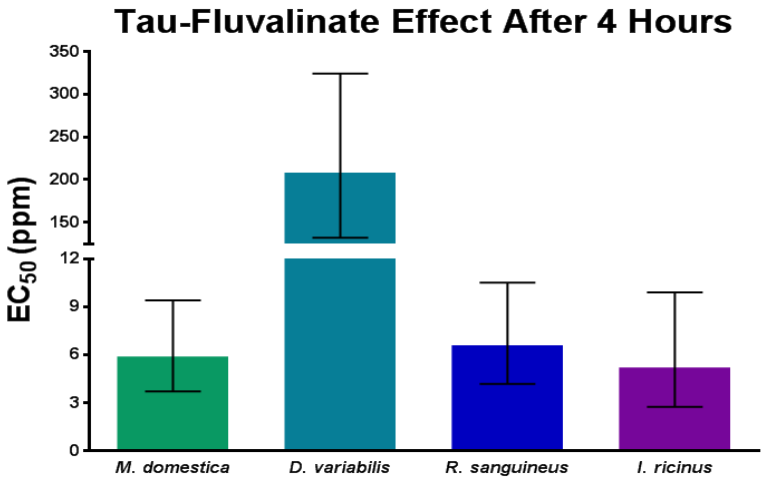
Tau-Fluvalinate Effect After 4 Hours
EC50 (ppm)
350
300
250
200
150
12
9
6
3
0
M. domestica
D. variabilis
R. sanguineus
I. ricinus

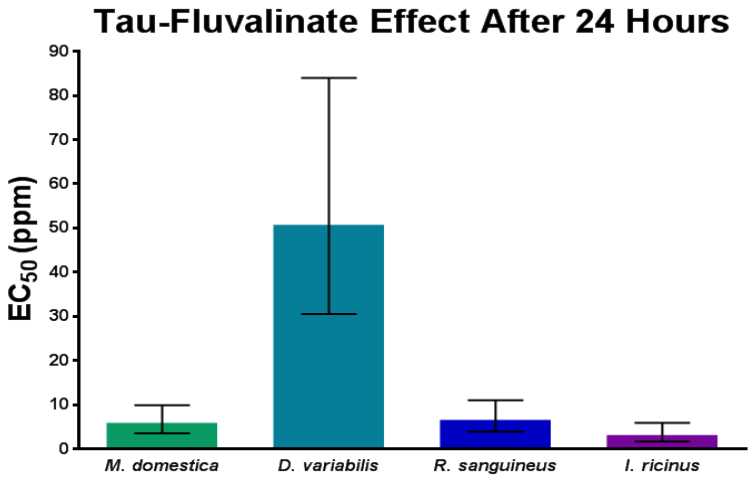
Tau-Fluvalinate Effect After 24 Hours
EC50 (ppm)
90
80
70
60
50
40
30
20
10
0
M. domestica
D. variabilis
R. sanguineus
I. ricinus

8.4 Discussion

8.4.1 *V. destructor* Bioassay Range-Finding Trials

At the time the trials were carried out control mortality in acetone-treated and blank vials was high, possibly due to fluctuations in humidity or to the age of the mites. Other successful studies used mites taken from the brood comb (Kamler et al., 2016; Kanga et al., 2010) rather than from adult bees as for the present study, and this may have affected mite health and survival during the bioassays. Because of concerns over mite survival, a scoring method for determining affected vs unaffected mites was used that involved observation through the glass of the vials. However, this may have led to wrong estimates of the number of affected/dead mites and the more robust method of Kanga *et al* 2010 and Kamler *et al* 2016, which involved tipping mites out and observing their motility, would have been more appropriate. As a further complication, the pyrethroid resistance status of the available mites was not known and so the results could have been skewed by the presence of pyrethroid resistance. These factors combined means that in this study it is not possible to draw any conclusions from the bioassays on *V. destructor*. It is the intention that improved studies will be carried out by Bayer Crop Science when a larger number of wild-type mites from brood combs are available. This will allow an expansion of the range of concentrations used, and improvements in control mortality and scoring methods, so that the determination of EC_{50} values for test pyrethroids against *V. destructor* will be possible.

8.4.2 Insect and Acari Comparative Contact Bioassays

Pyrethroids used in bioassays are shown in Figure 7.15 (Section 7.4.5) and are replicated in Figure 8.2.

Figure 8.2: Pyrethroids Used in Electrophysiological Studies of Arthropod VGSCs

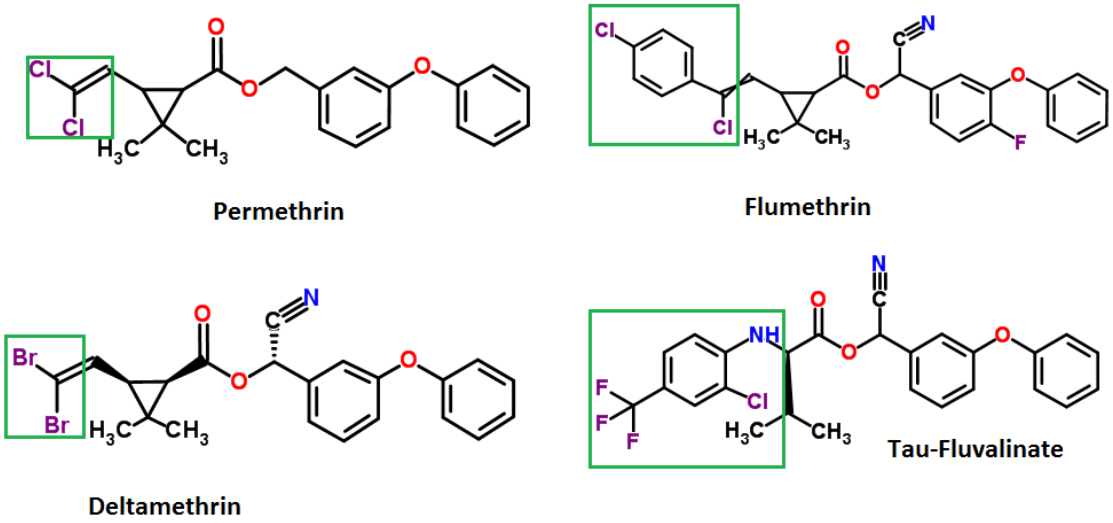

Permethrin, Flumethrin, Deltamethrin and Tau-Fluvalinate shown as examples of pyrethroids with relatively large and small acidic moieties. Areas of interest within the acidic portion are highlighted by green boxes. All pyrethroid structures are from ChemSpider 2016.

Both Deltamethrin and Permethrin have smaller halogenated substituents in their acidic moiety. Pyrethroids with suggested selective acaricidal activity differ from other pyrethroids by having large halogenated substituents in their acidic moiety. According to the model proposed by O'Reilly *et al* 2014, pyrethroids with these larger moieties could be accommodated in acarine channels, such as the tick channels tested in the contact bioassays above, which have a smaller glycine at position 933, but not by insect channels, such as the *M. domestica* channel, which has a larger cysteine residue in this position. If this model were to hold true, we would expect neither deltamethrin nor permethrin to show selective acaricidal activity, as they have comparatively smaller acidic moieties. This appears to be the case here, where both pyrethroids show no greater potency for acarine species compared to *M. domestica*. In fact, both deltamethrin and permethrin show a statistically significantly greater effect on *M. domestica* compared to *D. variabilis* and *R. sanguineus* ($P<0.05$ two-sided z-test) (Table 8.3).

Interestingly, the effects of these two pyrethroids varies between tick species. When compared to *D. variabilis* at 24 hours, deltamethrin has a ~5 fold greater effect on *R. sanguineus* and a ~67 fold greater effect on *I. ricinus*, while permethrin has a ~83 fold

greater effect on *R. sanguineus* and a ~455 fold greater effect on *I. ricinus* (Table 8.3). These differences in efficacy could be due to a number of complex differences between the tick species tested; such as body mass, metabolic processes, cuticle composition, and symbiont presence or absence. Further investigations are merited into the reasons behind the significantly more pronounced effects that these pyrethroids have on *I. ricinus* and *R. sanguineus* compared to *D. variabilis*, as this may aid development of more effective tick control.

Pyrethroids with larger acidic moieties used in comparative bioassays were flumethrin and tau-fluvalinate (Figure 8.2). According to the model proposed by O'Reilly *et al* 2014, both of these pyrethroids would show selective acaricidal activity. After 4 hours exposure to flumethrin, the EC_{50} value for *D. variabilis* was significantly higher than that for *M. domestica* ($P<0.05$ two-sided z-test), implying that more of this pyrethroid would be required to kill or knockdown this tick species compared to *M. domestica*. However, for *R. sanguineus* and *I. ricinus* the EC_{50} values were significantly lower ($P<0.05$ two-sided z-test) than that for *M. domestica*, implying that less of this pyrethroid would be required to kill or knockdown the acari tested compared to *M. domestica* (Table 8.2). After 24 hours exposure to flumethrin, the EC_{50} values for all acarine species tested were significantly lower than that for *M. domestica* ($P<0.05$ two-sided z-test), implying that less of this pyrethroid would be required to kill or knockdown the tick species tested compared to *M. domestica* (Table 8.3). Thus results with flumethrin after 24 hours support the O'Reilly model that pyrethroids with larger halogenated groups in their acidic moieties show increased acaricidal selectivity. However, results after 4 hours show that this pyrethroid was significantly slower to act on *D. variabilis* compared to the other tick species and to *M. domestica* ($P<0.05$ two-sided z-test). As *D. variabilis* is an important disease vector species fast action of acaricidal compounds to cause a knockdown or kill effect on this species are critical, to prevent the spread of disease to humans and other animals (Deplazes et al., 2016; Service, 2012). It is currently unclear what may slow the action of flumethrin on this species, but investigations into this mechanism represent useful future work.

After 4 hours exposure to tau-fluvalinate, the EC_{50} value for *D. variabilis* was significantly higher than that for *M. domestica* ($P<0.05$ two-sided z-test), implying that more of this pyrethroid would be required to kill or knockdown this tick species compared to *M. domestica* (Table 8.2). After 24 hours of tau-fluvalinate exposure, the EC_{50} values for all acarine species had reduced; however, the EC_{50} value for *D. variabilis* still significantly higher than that for *M. domestica* by ~9 fold (Table 8.3) ($P<0.05$ two-sided z-test). The EC_{50} values for *R. sanguineus* and *I. ricinus* are not significantly different to that for *M. domestica* after both 4 and 24 hours exposure (Figure 8.1) ($P>0.05$ two-sided z-test). So although tau-fluvalinate has a comparatively larger halogenated moiety (Figure 8.2) it does not appear to show greater acarine over insect selectivity, at least in those species tested in this study. This suggests that the model proposed my O'Reilly *et al* 2014 does not completely cover the complexity involved in pyrethroid selectivity. Further bioassays involving more individuals and more species would be required to confirm this, but in conclusion, results here suggest that acaricidal selectivity is complex and dependent on more than the target protein; it is possible that metabolic or structural mechanisms combine with target-site differences to pay a role in selectivity. Further investigations into the reasons behind pesticide specificity should be undertaken to look into differences in the exoskeletal structure and metabolic processes between species before the O'Reilley *et al* 2014 model of pyrethroid selectivity at the arthropod VGSC involving residue 933 can be confirmed or denied.

9 General Discussion and Future Directions

This chapter summarises the main findings of this thesis and suggested future work to build on these discoveries is outlined.

9.1 Acarine VGSCs and Pyrethroid Resistance

Chapter 5 demonstrated that acarine species show high levels of conservation in the amino-acid sequence of the membrane spanning domains of their VGSCs, including the putative pyrethroid binding site proposed by O'Reilly *et al* 2006. Similarly, there is conservation between the acarine channels and those of the insect *M. domestica*. However, subtle sequence differences were found between individuals that could affect pyrethroid toxicity and specificity. Specifically, this work identified two mutations conferring amino acid substitutions in the VGSC of ticks. One, V1010F, found in *R. microplus*, is in a position not reported previously to be involved in resistance and the other, F1538L, found in *R. sanguineus*, is in the same position as F1538I, previously shown to be associated with pyrethroid resistance in pollen beetles. Both warrant further investigation regarding their influence over VGSC sensitivity using electrophysiological methods.

Alongside F1538L, *R. sanguineus* ticks were found to also have the L925I substitution, which has been confirmed to be responsible for pyrethroid resistance (Morin et al., 2002; Rinkevich et al., 2013; Usherwood et al., 2007) and G933V, suspected to confer selective pyrethroid resistance (Jonsson et al., 2010). In one individual tick (RST3), G933V and F1538L were found heterozygously on opposite alleles, as seen previously for G933V and L925I in *R. microplus* ticks resistant to flumethrin but not cypermethrin (Jonsson et al., 2010). The model proposed by O'Reilly *et al* 2014 predicts that G933V would give resistance to pyrethroids like flumethrin, with comparatively large halogenated groups, but not to permethrin, with comparatively small halogenated groups (Figure 29). Thus, if the model were correct, then G933V/F1538L ticks would not be resistant to permethrin, unless F1538L alone gives target site resistance. This has been suggested for pollen beetles with heterozygous F1538L (Wrzesinska et al.,

2014). Alternatively, metabolic resistance could also be involved and such resistance has been characterised previously in *R. sanguineus* (Miller et al., 2001). It would be useful to gather more *R. sanguineus* samples from the same geographical area to examine the phenotypic and genotypic causes of any resistance in more detail.

9.2 Chimeric VGSCs

Chapter 6 described attempts to create chimeric *R. microplus*/*D. melanogaster* VGSC constructs for functional studies. Although none of the attempts were totally successful, the creation of *Chimeras L2*/*L4* and *Chimera LC* constructs highlighted possible alternative exon usage in the *R. microplus* (Parkhurst) VGSC comparable to that seen in other arthropods (Figure 15). Firstly, alternative exon usage in an area which encodes optional exon b in other arthropods (Dong et al., 2014; Loughney et al., 1989), a region suspected to be involved in the modulation of current flow, because removal of this exon increases peak current of *B. germanica* and *V. destructor* VGSCs (Du et al., 2009a; Song et al., 2004). Secondly, alternative exon usage in an area which encodes mutually exclusive exons k/l in other arthropods, a variable region found in several animal species, including the acari *V. destructor* (Dong et al., 2014; Lee et al., 2002). This area is interesting because it has been shown to modulates the generation of a persistent current in the *D. melanogaster para* channel, with channels containing exon l showing greater persistent currents (so maintaining the open state for longer) than those containing exon k (Lin et al., 2009). All chimeric constructs created in the present study show a slightly greater level of similarity to exon l in the *D. melanogaster para* VGSC (Figure 15). However, *Chimera LC* shows less similarity to exon l than do *Chimeras L2*/*L4*, therefore *Chimera LC* could represent an "exon k" type variant in *R. microplus*. This is interesting given that *D. melanogaster para* VGSCs expressing the k exon variation have been reported to be 24 times less sensitive to the pyrethroid deltamethrin than those expressing the l exon variation (Burton, 2012). Further examination of *R. microplus* exon usage would help clarify the potential importance of alternative splicing in this species with regards to pyrethroid resistance and VGSC properties.

9.3 Electrophysiology with Arthropod VGSCs

Chapter 7 reports the first use of electrophysiological to determine the effects of pyrethroids on *V. destructor* VGSCs. Although the results do not support the prediction of the model by O'Reilly *et al* 2014, that pyrethroids with large halogenated moieties (flumethrin and tau-fluvalinate) should show increased selectivity for the *V. destructor* native VGSC, when compared to the *V. destructor* G933V or *D. melanogaster para* VGSCs, they do offer novel information. The substitution G933V does not appear to give selective resistance to flumethrin or tau-fluvalinate, as was reported in Australian *R. microplus* ticks (Jonsson et al., 2010), but this needs to be confirmed by more electrophysiological testing, particularly given the rising ail currents seen with Type II pyrethroids and *V. destructor* VGSCs (Figure 28). This phenomenon prevents firm conclusions being drawn from the recordings because the inward current baseline and the end point of tail currents cannot be determined. However, it hints at important information regarding the binding capacity of pyrethroids to acarine VGSCs compared to those from insects. The unexpected results from the *V. destructor* VGSCs needs to be further investigated, using different experimental conditions, to see if there really is a fundamental difference in the functioning of acarine VGSCs compared with those from insects, which have been much more widely studied.

9.4 Contact Bioassays with Arthropods

As with permethrin resistance found in *R. sanguineus* in Chapter 5 and the electrophysiological studies in Chapter 7, the contact bioassays reported in Chapter 8, suggest that the model proposed by O'Reilly *et al* 2014 does not completely cover the complexity involved in pyrethroid selectivity between acarine and insect species. In particular tau-fluvalinate, a pyrethroid with a larger halogenated group (Figure 29), did not show the increased acaricidal specificity that the model would predict. All tick species tested were sequenced in this thesis (Chapter 5) and were confirmed to have similar sequences across membrane-spanning domains of their VGSCs, including the potential pyrethroid binding areas (Du et al., 2013; O'Reilly et al., 2006) and to have a G at position 933 (O'Reilly et al., 2014) (Section 10.2 Appendix 2). This suggests that

other factors besides selectivity at the VGSC, could be contributing to the action of pyrethroids on whole arthropods, notably metabolic or structural mechanisms. This possibility is supported by observations within tick species, that *D. reticulatus* is relatively insensitive to permethrin, deltamethrin and tau-fluvalinate, compared to *R. sanguineus* and *I. ricinus*. This is of particular interest as this tick was not relatively more resistant to Flumethrin. Further bioassays are needed to look into possible differences in exoskeletal structure and hence uptake of the pyrethroids, and into metabolic differences between species.

9.5 Future Directions

As a result of the findings in this thesis, the following future work is proposed:

1. Results from the sequencing of the VGSC form *R. sanguineus* ticks resistant to pyrethroids were limited due to a lack of individuals. More samples could be taken from the same geographical area, so the extent of the resistance can be accurately assessed and management strategies imposed. Furthermore, testing of individuals for resistance to a pyrethroid with a comparatively large halogenated group, such as flumethrin, and one with a comparatively small halogenated group, such as permethrin, would enable further investigation of the model of pyrethroid selectivity proposed by O'Reilly *et al* 2014. The one or two individuals carrying G933V examined in this study are not sufficient to confirm or reject the hypothesis proposed for the role of residue 933 in pyrethroid selectivity

2. Future work on the chimeric *R. microplus*/*D. melanogaster* VGSC constructs made in Chapter 6 might produce a functional channel. One option to deliver this would be moving the chimeric VGSC (and *X. laevis* Beta-globin sequences) to different bacterial expression vectors to attempt to stabilise the construct in *E. coli*. Another option is to move these regions to an insect expression vector and attempt expression in insect cells, using patch-clamp electrophysiology to monitor expression levels.

3. As exon variation can affect pyrethroid action at the *R. microplus* VGSC (Burton, 2012; Lin et al., 2009), it would be interesting to investigate the use of the alternative exons found in this study in *R. microplus*, looking at different developmental stages and tissue types. This could inform targeting of tick control strategies.

4. Investigation of the suspected *R. microplus* exon "l" and "k" sequences using electrophysiological methods might be accomplished by inserting these separately in place of the same region in the *D. melanogaster para* or *V. destructor* VGSC and then testing for pyrethroid selectivity

5. Chapter 7 showed rise tail currents for *V. destructor* VGSCs (Figure 27). This phenomenon warrants further investigation so that firm conclusions can be drawn regarding pyrethroid interactions at these channels. Initial advanced investigations have shown that testing each oocyte with Voltage Protocols 1-3 (Section 7.2.7) prior to pyrethroid application, then applying 10 μM pyrethroid and running Voltage Protocol 3 only, removes the rise in tail currents previously seen. This methodology with therefore be employed to attempt to measure the M_i for pyrethroids at 10 μM concentrations (Figure 9.1).

Figure 9.1: Tail-Currents in Native *V. destructor* VGSCs Resulting from Modified Protocol Application

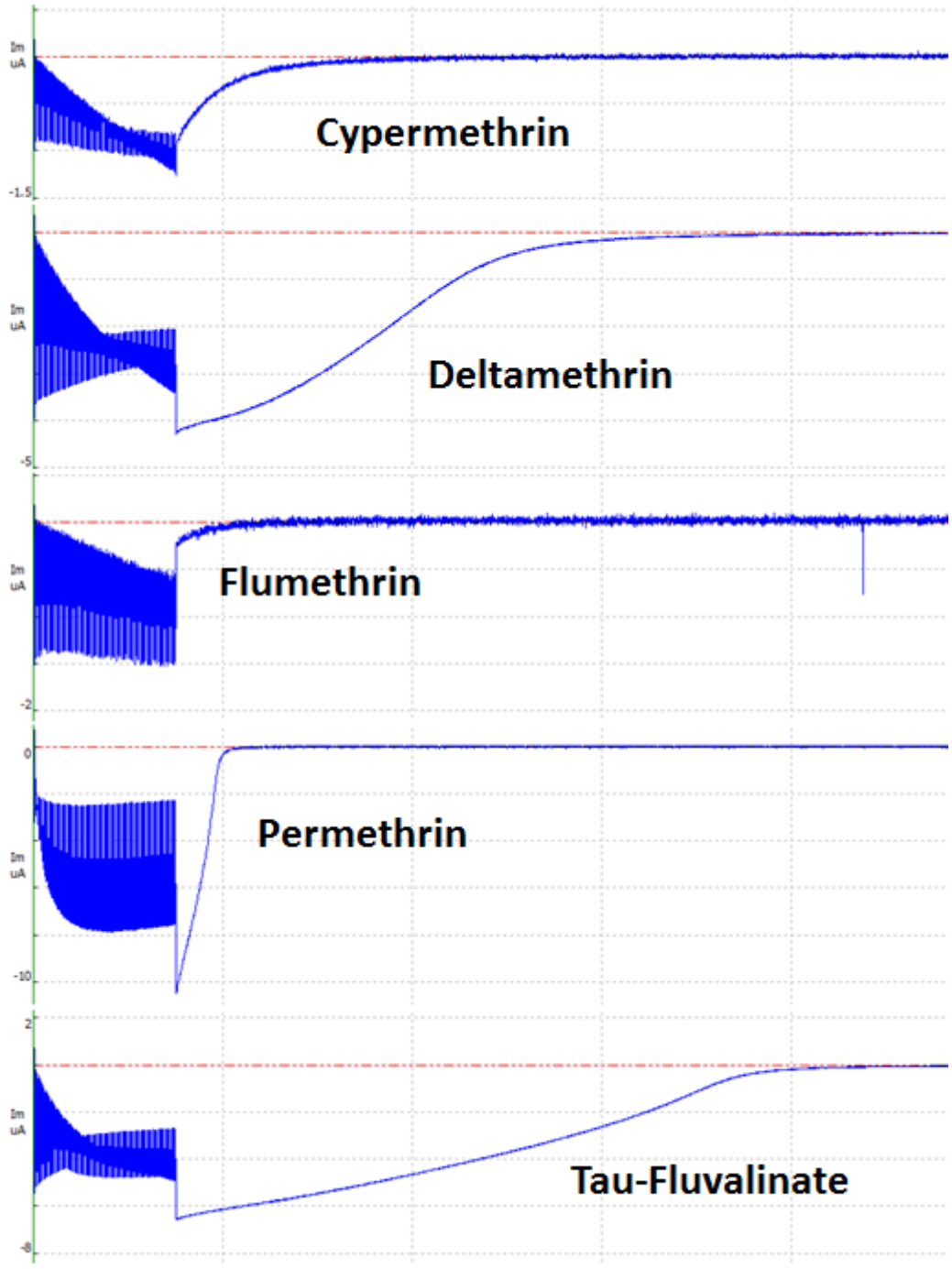

Example tail currents in the presence of 10 µM pyrethroid for *V. destructor* native VGSCs. Channels were expressed in *X. laevis* oocytes and exposed to pyrethroid toxicant (Section 7.2.8) before the application of Voltage Protocol 3only (Section 7.2.7). Data shown was extracted from WinWCP (John Dempster, University of Strathclyde) and illustrates the removal of the tail-current rise above the Time ≈ 0 baseline previously seen in *V. destructor* VGSCs (red line).

6. TEVC electrophysiology experiments in Chapter 7 did not conclusively prove or discount the proposal by O'Reilley *et al* 2014, that differences in the amino acid residue at position 933 in the VGSC of arthropods could determine pyrethroid selectivity for insects or acari. Therefore, the technique of genome editing using the CRISPR/Cas9 system could be used to replace the cysteine at residue 933 in the *D. melanogaster* VGSC with a glycine, as found at position 933 in most acarine VGSCs (Cong et al., 2013). If the resultant mutant *D. melanogaster* were found to have increased sensitivity to pyrethroids with large halogenated groups when compared to flies with native VGSCs, this would help to confirm the model put forward by O'Reilley *et al* 2014 that this residue leads to acari having greater susceptibility to these compounds.

7. The bioassays reported in Chapter 8 produced interesting results regarding pyrethroid specificity both between acarine and insect species and within the acari. However, these were limited in their scope and should be extended to more replicates, with each species and more types of pyrethroids.

8. Bioassays in Chapter 8 showed differences in the effectiveness of different pyrethroids, not just between insects and acari, but between different tick species. Interestingly, work in Chapter 6 showed that *R. microplus* has variable exon k/l usage within its VGSC, a region which has been linked to the modulation of persistent current in the *D. melanogaster para* channel, with channels containing exon l showing greater persistent currents and susceptibility to pyrethroids (Burton, 2012; Lin et al., 2009). Therefore, further work examining the amino acids in the region corresponding to exon k/l in those ticks tested in Chapter could determine if any differences in the sequence present, or in the expression level of exon variants, would account for the differences in pyrethroid activity seen between tick species. Such differences could then be further examined using TEVC electrophysiology and could inform pyrethroid use against these tick species.

Overall, the work reported here has looked at the interactions of VGSCs from insects and acari using bioassays, cloning/sequencing and electrophysiology. Each has provided valuable and interesting preliminary data, but each approach has its own drawbacks, and further optimisation is required to draw the results together. This could then offer ideas for the selective control of acari, an area of great importance in the field.

10 Appendices

10.1 Appendix 1

The *R. microplus* VGSC as sequenced from in this study following cDNA PCR amplification.

The sequence spans from the 5’ end of the channel before Domain I past the end of the protein coding sequence and into the 3’ UTR.

Membrane-spanning segments and the domains to which they belong are indicated by blue bars, these were estimated using information from the *V. destructor* mite channel as sequenced by Wang *et al* 2003.

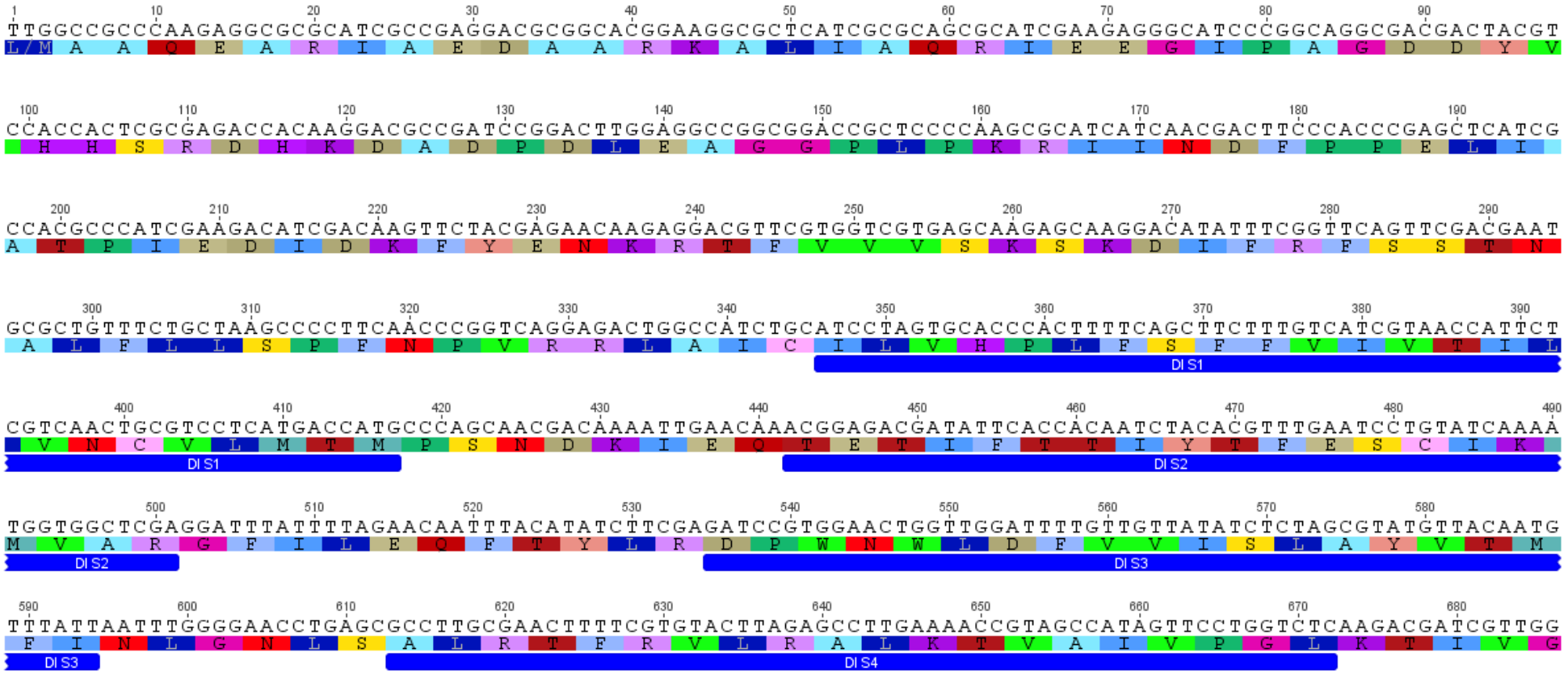
DI S1
DI S1
DI S2
DI S2
DI S3
DI S3
DI S4

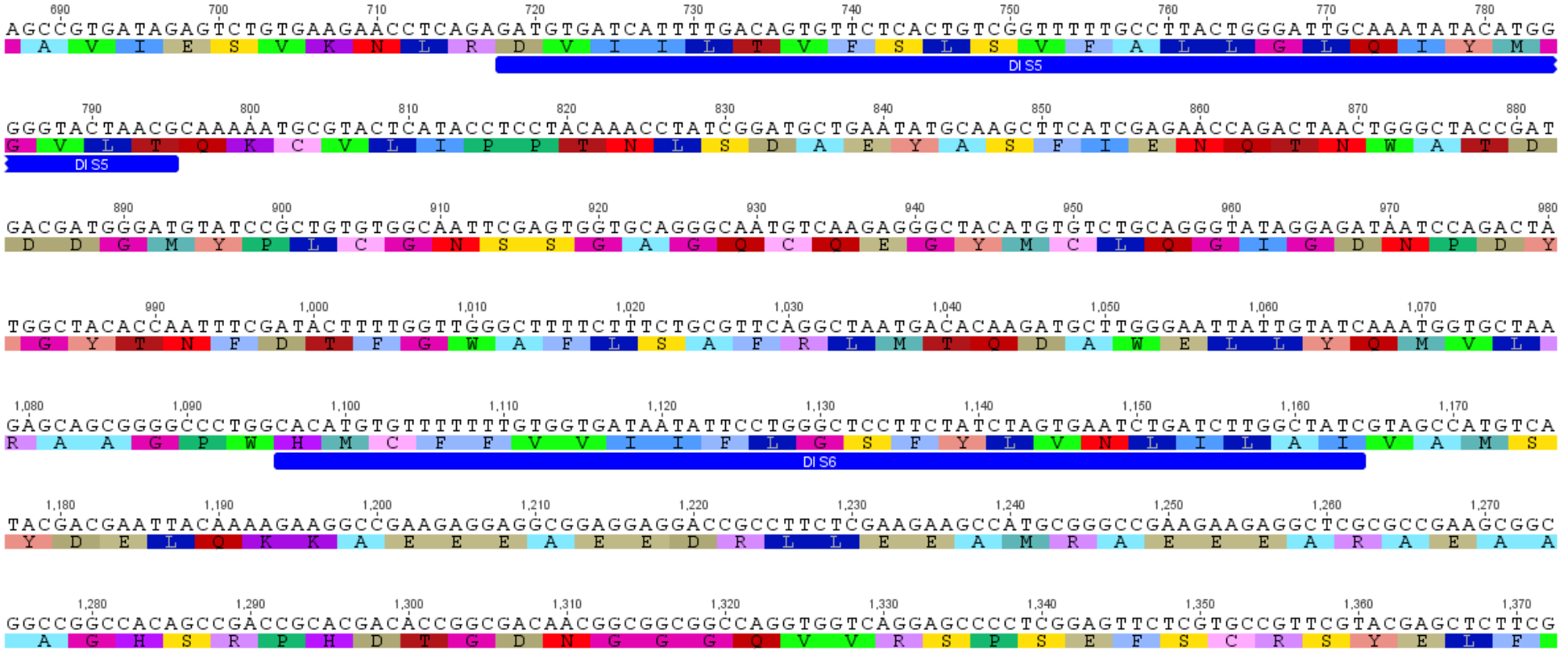
690 700 710 720 730 740 750 760 770 780
AGCCGTGATAGAGTCTGTGAAGAACCTCAGAGATGTGATCATTTTGACAGTGTTCTCACTGTCGGTTTTTGCCTTACTGGGATTGCAAATATACATGG
A V I E S V K N L R D V I I L T V F S L S V F A L L G L Q I Y M
DI S5
790 800 810 820 830 840 850 860 870 880
GGGTACTAACGCAAAAATGCGTACTCATACCTCCTACAAACCTATCGGATGCTGAATATGCAAGCTTCATCGAGAACCAGACTAACTGGGCTACCGAT
G V L T Q K C V L I P P T N L S D A E Y A S F I E N Q T N W A T D
DI S5
890 900 910 920 930 940 950 960 970 980
GACGATGGGATGTATCCGCTGTGTGGCAATTCGAGTGGTGCAGGGCAATGTCAAGAGGGCTACATGTGTCTGCAGGGTATAGGAGATAATCCAGACTA
D D G M Y P L C G N S S G A G Q C Q E G Y M C L Q G I G D N P D Y
990 1,000 1,010 1,020 1,030 1,040 1,050 1,060 1,070
TGGCTACACCAATTTCGATACTTTTGGTTGGGCTTTTCTTTCTGCGTTCAGGCTAATGACACAAGATGCTTGGGAATTATTGTATCAAATGGTGCTAA
G Y T N F D T F G W A F L S A F R L M T Q D A W E L L Y Q M V L
1,080 1,090 1,100 1,110 1,120 1,130 1,140 1,150 1,160 1,170
GAGCAGCGGGGCCCTGGCACATGTGTTTTTTTGTGGTGATAATATTCCTGGGCTCCTTCTATCTAGTGAATCTGATCTTGGCTATCGTAGCCATGTCA
R A A G P W H M C F F V V I I F L G S F Y L V N L I L A I V A M S
DI S6
1,180 1,190 1,200 1,210 1,220 1,230 1,240 1,250 1,260 1,270
TACGACGAATTACAAAAGAAGGCCGAAGAGGAGGCGGAGGAGGACCGCCTTCTCGAAGAAGCCATGCGGGCCGAAGAAGAGGCTCGCGCCGAAGCGGC
Y D E L Q K K A E E E A E E D R L L E E A M R A E E E A R A E A A
1,280 1,290 1,300 1,310 1,320 1,330 1,340 1,350 1,360 1,370
GGCCGGCCACAGCCGACCGCACGACACCGGCGACAACGGCGGCGGCCAGGTGGTCAGGAGCCCCTCGGAGTTCTCGTGCCGTTCGTACGAGCTCTTCG
A G H S R P H D T G D N G G G Q V V R S P S E F S C R S Y E L F

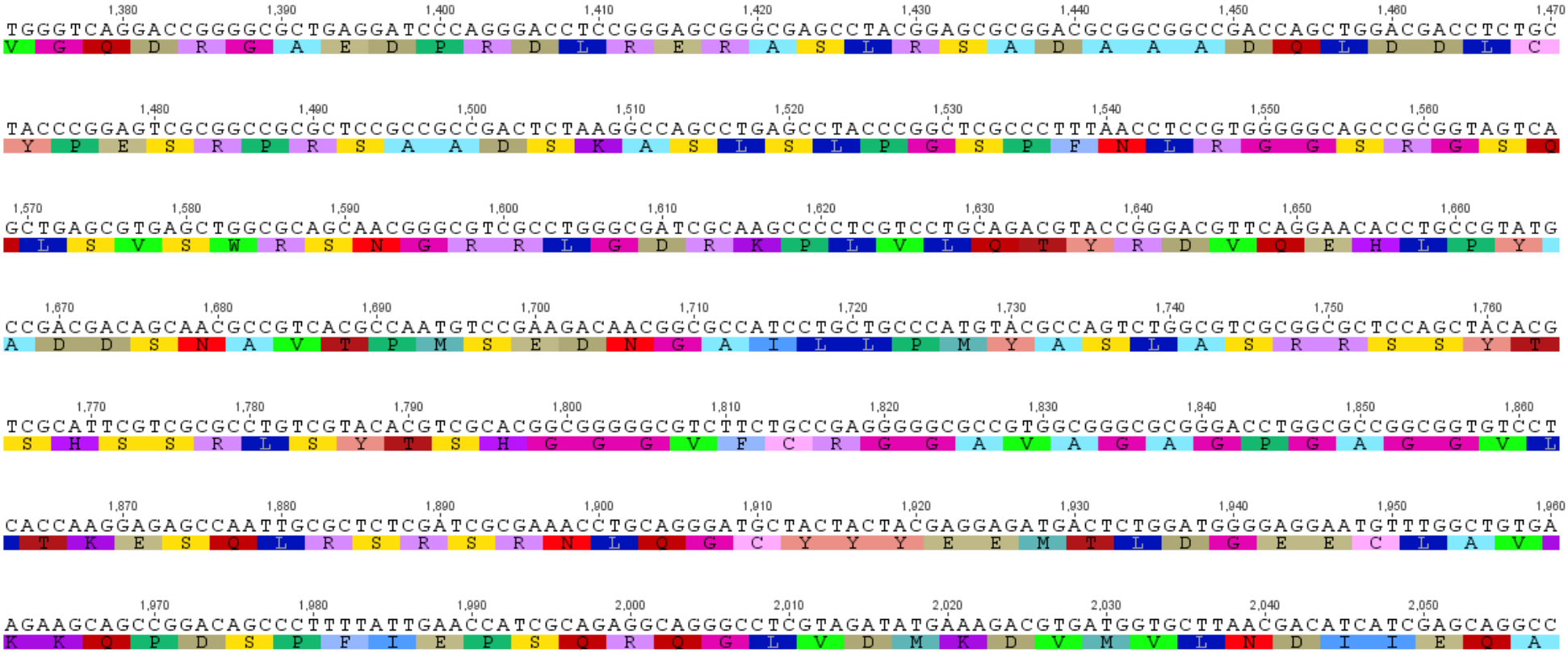
1,380 1,390 1,400 1,410 1,420 1,430 1,440 1,450 1,460 1,470
TGGGTCAGGACCGGGGCGCTGAGGATCCCAGGGACCTCCGGGAGCGGGCGAGCCTACGGAGCGCGGACGCGGCGGCCGACCAGCTGGACGACCTCTGC
V G Q D R G A E D P R D L R E R A S L R S A D A A A D Q L D D L C
1,480 1,490 1,500 1,510 1,520 1,530 1,540 1,550 1,560
TACCCGGAGTCGCGGCCGCGCTCCGCCGCCGACTCTAAGGCCAGCCTGAGCCTACCCGGCTCGCCCTTTAACCTCCGTGGGGGCAGCCGCGGTAGTCA
Y P E S R P R S A A D S K A S L S L P G S P F N L R G G S R G S Q
1,570 1,580 1,590 1,600 1,610 1,620 1,630 1,640 1,650 1,660
GCTGAGCGTGAGCTGGCGCAGCAACGGGCGTCGCCTGGGCGATCGCAAGCCCCTCGTCCTGCAGACGTACCGGGACGTTCAGGAACACCTGCCGTATG
L S V S W R S N G R R L G D R K P L V L Q T Y R D V Q E H L P Y
1,670 1,680 1,690 1,700 1,710 1,720 1,730 1,740 1,750 1,760
CCGACGACAGCAACGCCGTCACGCCAATGTCCGAAGACAACGGCGCCATCCTGCTGCCCATGTACGCCAGTCTGGCGTCGCGGCGCTCCAGCTACACG
A D D S N A V T P M S E D N G A I L L P M Y A S L A S R R S S Y T
1,770 1,780 1,790 1,800 1,810 1,820 1,830 1,840 1,850 1,860
TCGCATTCGTCGCGCCTGTCGTACACGTCGCACGGCGGGGGCGTCTTCTGCCGAGGGGGCGCCGTGGCGGGCGCGGGACCTGGCGCCGGCGGTGTCCT
S H S S R L S Y T S H G G G V F C R G G A V A G A G P G A G G V L
1,870 1,880 1,890 1,900 1,910 1,920 1,930 1,940 1,950 1,960
CACCAAGGAGAGCCAATTGCGCTCTCGATCGCGAAACCTGCAGGGATGCTACTACTACGAGGAGATGACTCTGGATGGGGAGGAATGTTTGGCTGTGA
T K E S Q L R S R S R N L Q G C Y Y Y E E M T L D G E E C L A V
1,970 1,980 1,990 2,000 2,010 2,020 2,030 2,040 2,050
AGAAGCAGCCGGACAGCCCTTTTATTGAACCATCGCAGAGGCAGGGCCTCGTAGATATGAAAGACGTGATGGTGCTTAACGACATCATCGAGCAGGCC
K K Q P D S P F I E P S Q R Q G L V D M K D V M V L N D I I E Q A

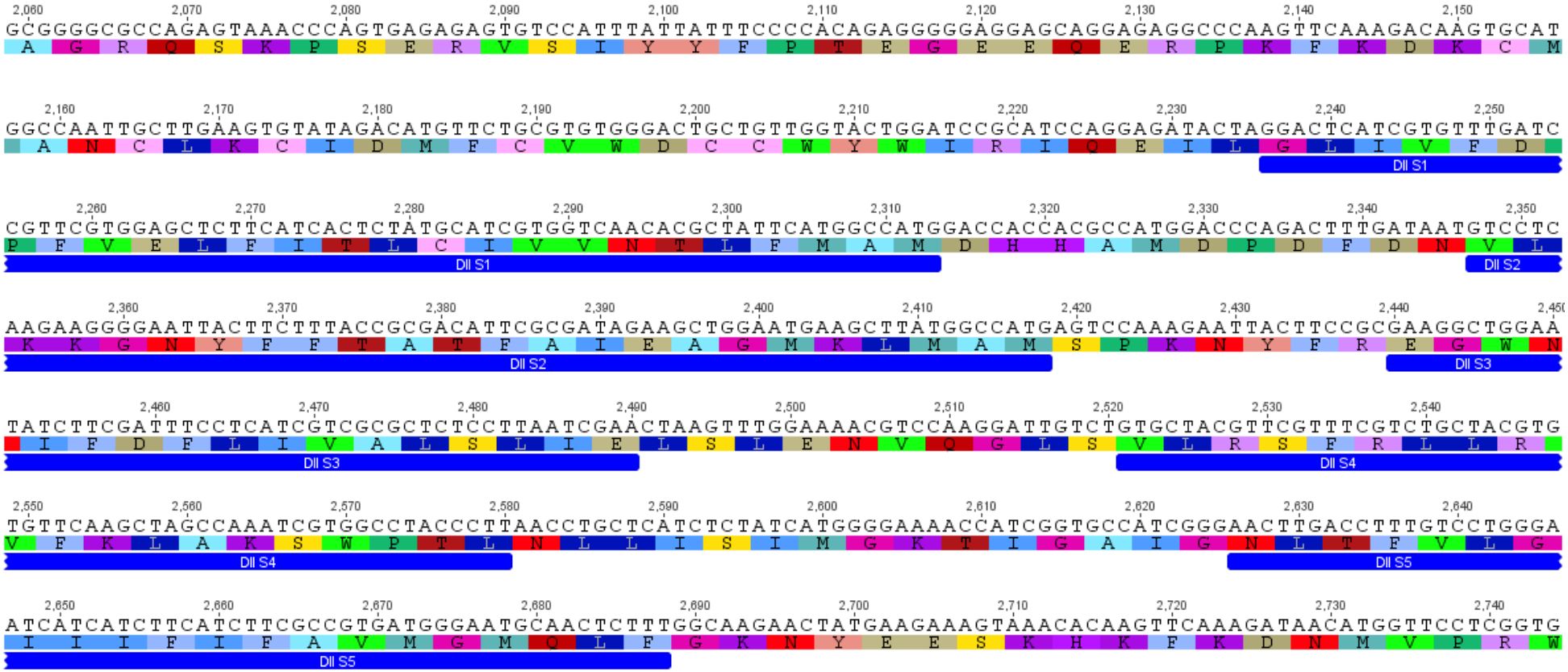
2,060 2,070 2,080 2,090 2,100 2,110 2,120 2,130 2,140 2,150
GCGGGGCGCCAGAGTAAACCCAGTGAGAGAGTGTCCATTTATTATTTCCCCACAGAGGGGGAGGAGCAGGAGAGGCCCAAGTTCAAAGACAAGTGCAT
A G R Q S K P S E R V S I Y Y F P T E G E E Q E R P K F K D K C M
2,160 2,170 2,180 2,190 2,200 2,210 2,220 2,230 2,240 2,250
GGCCAATTGCTTGAAGTGTATAGACATGTTCTGCGTGTGGGACTGCTGTTGGTACTGGATCCGCATCCAGGAGATACTAGGACTCATCGTGTTTGATC
A N C L K C I D M F C V W D C C W Y W I R I Q E I L G L I V F D
Dll S1
2,260 2,270 2,280 2,290 2,300 2,310 2,320 2,330 2,340 2,350
CGTTCGTGGAGCTCTTCATCACTCTATGCATCGTGGTCAACACGCTATTCATGGCCATGGACCACCACGCCATGGACCCAGACTTTGATAATGTCCTC
P F V E L F I T L C I V V N T L F M A M D H H A M D P D F D N V L
Dll S1
Dll S2
2,360 2,370 2,380 2,390 2,400 2,410 2,420 2,430 2,440 2,450
AAGAAGGGGAATTACTTCTTTACCGCGACATTCGCGATAGAAGCTGGAATGAAGCTTATGGCCATGAGTCCAAAGAATTACTTCCGCGAAGGCTGGAA
K K G N Y F F T A T F A I E A G M K L M A M S P K N Y F R E G W N
Dll S2
Dll S3
2,460 2,470 2,480 2,490 2,500 2,510 2,520 2,530 2,540
TATCTTCGATTTCCTCATCGTCGCGCTCTCCTTAATCGAACTAAGTTTGGAAAACGTCCAAGGATTGTCTGTGCTACGTTCGTTTCGTCTGCTACGTG
I F D F L I V A L S L I E L S L E N V Q G L S V L R S F R L L R
Dll S3
Dll S4
2,550 2,560 2,570 2,580 2,590 2,600 2,610 2,620 2,630 2,640
TGTTCAAGCTAGCCAAATCGTGGCCTACCCTTAACCTGCTCATCTCTATCATGGGGAAAACCATCGGTGCCATCGGGAACTTGACCTTTGTCCTGGGA
V F K L A K S W P T L N L L I S I M G K T I G A I G N L T F V L G
Dll S4
Dll S5
2,650 2,660 2,670 2,680 2,690 2,700 2,710 2,720 2,730 2,740
ATCATCATCTTCATCTTCGCCGTGATGGGAATGCAACTCTTTGGCAAGAACTATGAAGAAAGTAAACACAAGTTCAAAGATAACATGGTTCCTCGGTG
I I I F I F A V M G M Q L F G K N Y E E S K H K F K D N M V P R W
Dll S5

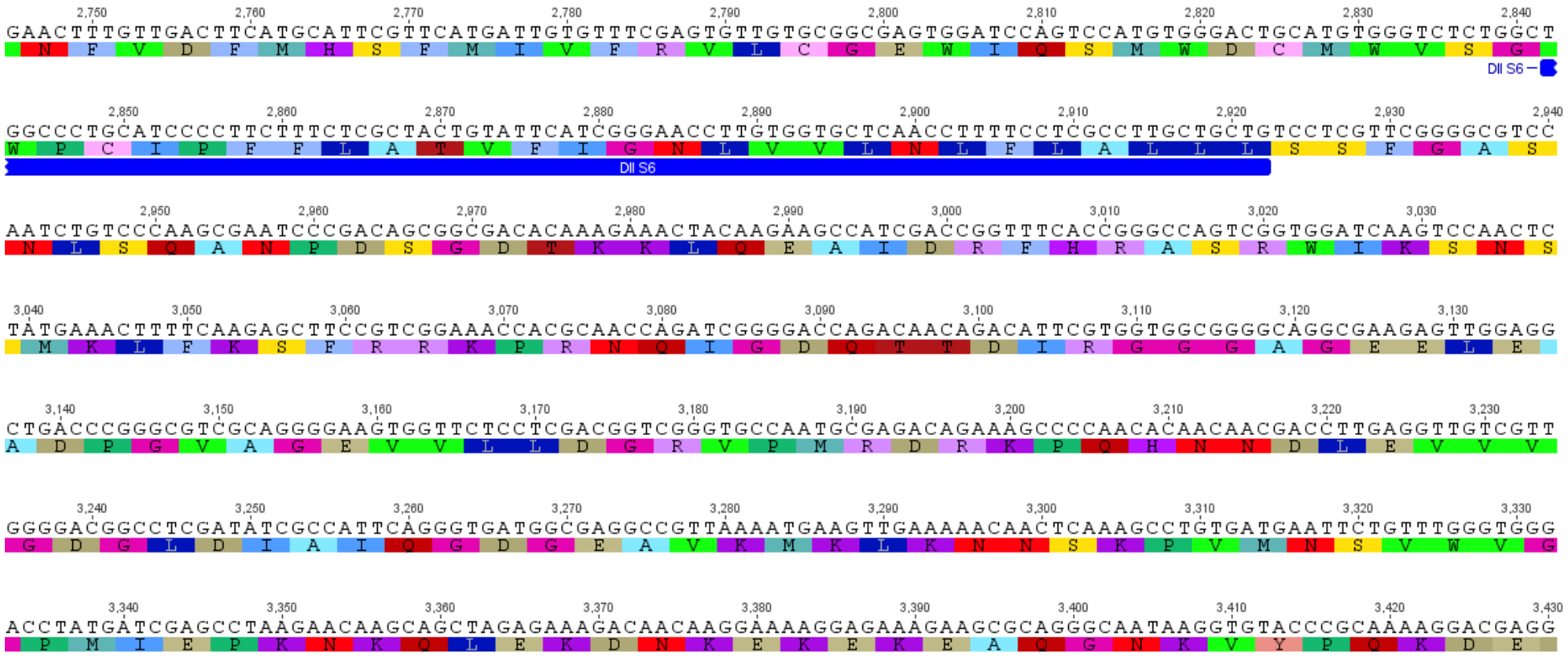
2,750 2,760 2,770 2,780 2,790 2,800 2,810 2,820 2,830 2,840
GAACTTTGTTGACTTCATGCATTCGTTCATGATTGTGTTTCGAGTGTTGTGCGGCGAGTGGATCCAGTCCATGTGGGACTGCATGTGGGTCTCTGGCT
N F V D F M H S F M I V F R V L C G E W I Q S M W D C M W V S G
DII S6
2,850 2,860 2,870 2,880 2,890 2,900 2,910 2,920 2,930 2,940
GGCCCTGCATCCCCTTCTTTCTCGCTACTGTATTCATCGGGAACCTTGTGGTGCTCAACCTTTTCCTCGCCTTGCTGCTGTCCTCGTTCGGGGCGTCC
W P C I P F F L A T V F I G N L V V L N L F L A L L L S S F G A S
DII S6
2,950 2,960 2,970 2,980 2,990 3,000 3,010 3,020 3,030
AATCTGTCCCAAGCGAATCCCGACAGCGGCGACACAAAGAAACTACAAGAAGCCATCGACCGGTTTCACCGGGCCAGTCGGTGGATCAAGTCCAACTC
N L S Q A N P D S G D T K K L Q E A I D R F H R A S R W I K S N S
3,040 3,050 3,060 3,070 3,080 3,090 3,100 3,110 3,120 3,130
TATGAAACTTTTCAAGAGCTTCCGTCGGAAACCACGCAACCAGATCGGGGACCAGACAACAGACATTCGTGGTGGCGGGGCAGGCGAAGAGTTGGAGG
M K L F K S F R R K P R N Q I G D Q T T D I R G G G A G E E L E
3,140 3,150 3,160 3,170 3,180 3,190 3,200 3,210 3,220 3,230
CTGACCCGGGCGTCGCAGGGGAAGTGGTTCTCCTCGACGGTCGGGTGCCAATGCGAGACAGAAAGCCCCAACACAACAACGACCTTGAGGTTGTCGTT
A D P G V A G E V V L L D G R V P M R D R K P Q H N N D L E V V V
3,240 3,250 3,260 3,270 3,280 3,290 3,300 3,310 3,320 3,330
GGGGACGGCCTCGATATCGCCATTCAGGGTGATGGCGAGGCCGTTAAAATGAAGTTGAAAAACAACTCAAAGCCTGTGATGAATTCTGTTTGGGTGGG
G D G L D I A I Q G D G E A V K M K L K N N S K P V M N S V W V G
3,340 3,350 3,360 3,370 3,380 3,390 3,400 3,410 3,420 3,430
ACCTATGATCGAGCCTAAGAACAAGCAGCTAGAGAAAGACAACAAGGAAAAGGAGAAAGAAGCGCAGGGCAATAAGGTGTACCCGCAAAAGGACGAGG
P M I E P K N K Q L E K D N K E K E K E A Q G N K V Y P Q K D E

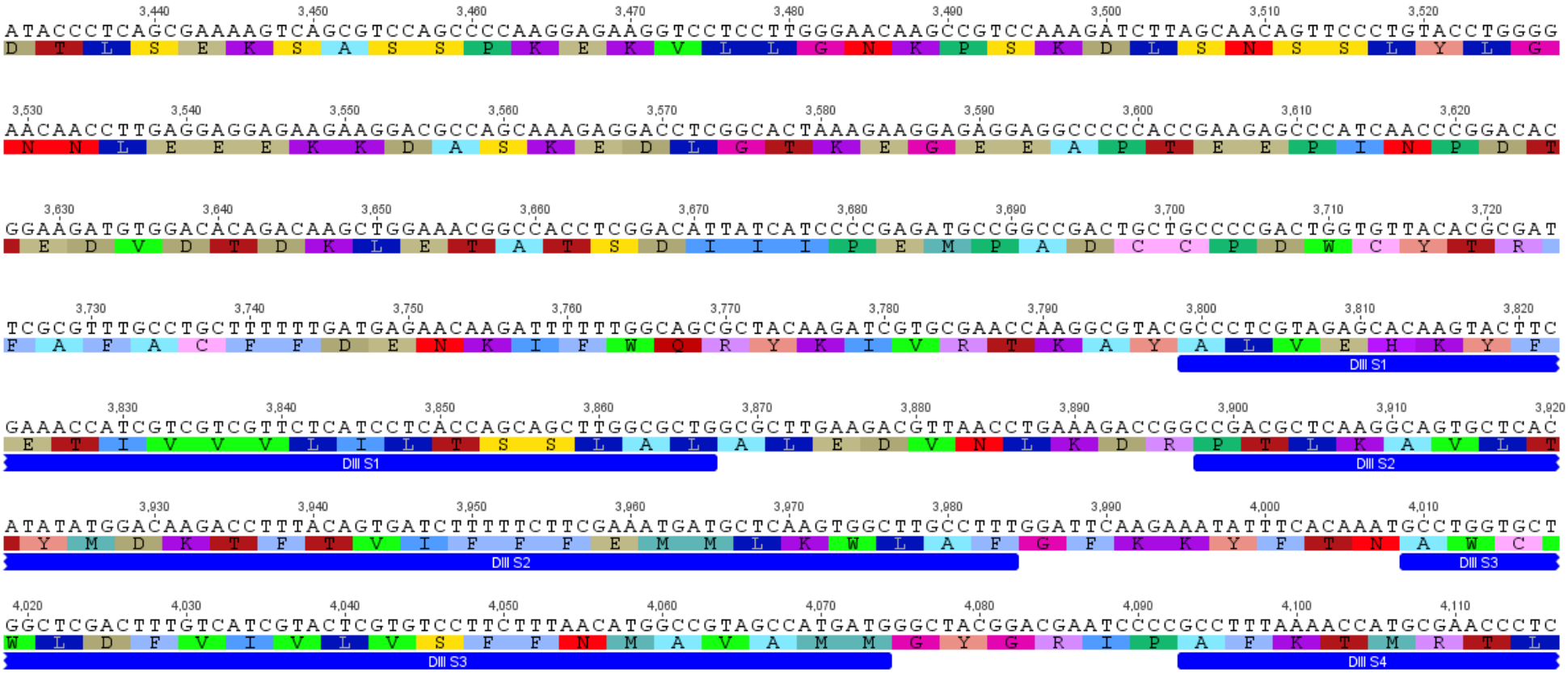
3,440 3,450 3,460 3,470 3,480 3,490 3,500 3,510 3,520
ATACCCTCAGCGAAAAGTCAGCGTCCAGCCCCAAGGAGAAGGTCCTCCTTGGGAACAAGCCGTCCAAAGATCTTAGCAACAGTTCCCTGTACCTGGGG
D T L S E K S A S S P K E K V L L G N K P S K D L S N S S L Y L G
3,530 3,540 3,550 3,560 3,570 3,580 3,590 3,600 3,610 3,620
AACAACCTTGAGGAGGAGAAGAAGGACGCCAGCAAAGAGGACCTCGGCACTAAAGAAGGAGAGGAGGCCCCCACCGAAGAGCCCATCAACCCGGACAC
N N L E E E K K D A S K E D L G T K E G E E A P T E E P I N P D T
3,630 3,640 3,650 3,660 3,670 3,680 3,690 3,700 3,710 3,720
GGAAGATGTGGACACAGACAAGCTGGAAACGGCCACCTCGGACATTATCATCCCCGAGATGCCGGCCGACTGCTGCCCCGACTGGTGTTACACGCGAT
E D V D T D K L E T A T S D I I I P E M P A D C C P D W C Y T R
3,730 3,740 3,750 3,760 3,770 3,780 3,790 3,800 3,810 3,820
TCGCGTTTGCCTGCTTTTTTGATGAGAACAAGATTTTTTGGCAGCGCTACAAGATCGTGCGAACCAAGGCGTACGCCCTCGTAGAGCACAAGTACTTC
F A F A C F F D E N K I F W Q R Y K I V R T K A Y A L V E H K Y F
DIII S1
3,830 3,840 3,850 3,860 3,870 3,880 3,890 3,900 3,910 3,920
GAAACCATCGTCGTCGTTCTCATCCTCACCAGCAGCTTGGCGCTGGCGCTTGAAGACGTTAACCTGAAAGACCGGCCGACGCTCAAGGCAGTGCTCAC
E T I V V V L I L T S S L A L A L E D V N L K D R P T L K A V L T
DIII S1
DIII S2
3,930 3,940 3,950 3,960 3,970 3,980 3,990 4,000 4,010
ATATATGGACAAGACCTTTACAGTGATCTTTTTCTTCGAAATGATGCTCAAGTGGCTTGCCTTTGGATTCAAGAAATATTTCACAAATGCCTGGTGCT
Y M D K T F T V I F F F E M M L K W L A F G F K K Y F T N A W C
DIII S2
DIII S3
4,020 4,030 4,040 4,050 4,060 4,070 4,080 4,090 4,100 4,110
GGCTCGACTTTGTCATCGTACTCGTGTCCTTCTTTAACATGGCCGTAGCCATGATGGGCTACGGACGAATCCCCGCCTTTAAAACCATGCGAACCCTC
W L D F V I V L V S F F N M A V A M M G Y G R I P A F K T M R T L
DIII S3
DIII S4

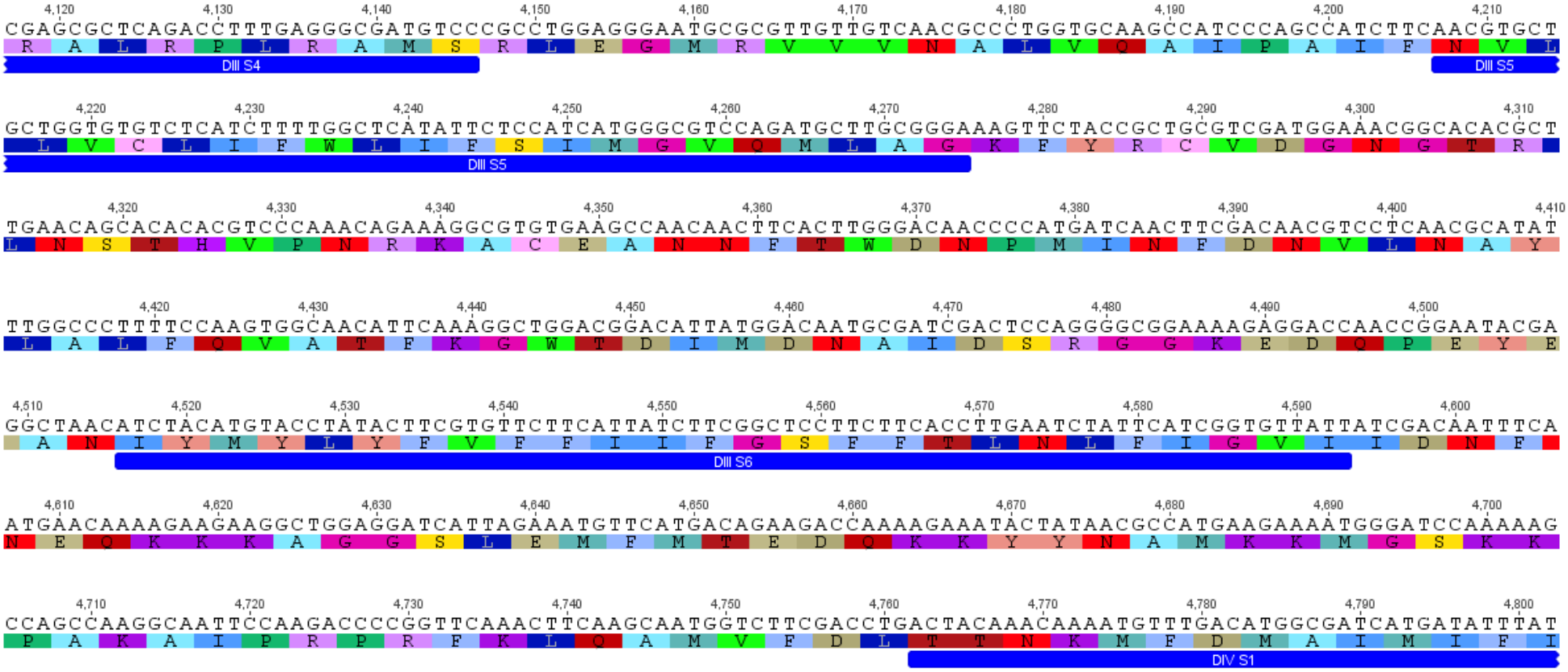
4,120 4,130 4,140 4,150 4,160 4,170 4,180 4,190 4,200 4,210
CGAGCGCTCAGACCTTTGAGGGCGATGTCCCGCCTGGAGGGAATGCGCGTTGTTGTCAACGCCCTGGTGCAAGCCATCCCAGCCATCTTCAACGTGCT
R A L R P L R A M S R L E G M R V V V N A L V Q A I P A I F N V L
DIII S4
DIII S5
4,220 4,230 4,240 4,250 4,260 4,270 4,280 4,290 4,300 4,310
GCTGGTGTGTCTCATCTTTTGGCTCATATTCTCCATCATGGGCGTCCAGATGCTTGCGGGAAAGTTCTACCGCTGCGTCGATGGAAACGGCACACGCT
L V C L I F W L I F S I M G V Q M L A G K F Y R C V D G N G T R
DIII S5
4,320 4,330 4,340 4,350 4,360 4,370 4,380 4,390 4,400 4,410
TGAACAGCACACACGTCCCAAACAGAAAGGCGTGTGAAGCCAACAACTTCACTTGGGACAACCCCATGATCAACTTCGACAACGTCCTCAACGCATAT
L N S T H V P N R K A C E A N N F T W D N P M I N F D N V L N A Y
4,420 4,430 4,440 4,450 4,460 4,470 4,480 4,490 4,500
TTGGCCCTTTTCCAAGTGGCAACATTCAAAGGCTGGACGGACATTATGGACAATGCGATCGACTCCAGGGGCGGAAAAGAGGACCAACCGGAATACGA
L A L F Q V A T F K G W T D I M D N A I D S R G G K E D Q P E Y E
4,510 4,520 4,530 4,540 4,550 4,560 4,570 4,580 4,590 4,600
GGCTAACATCTACATGTACCTATACTTCGTGTTCTTCATTATCTTCGGCTCCTTCTTCACCTTGAATCTATTCATCGGTGTTATTATCGACAATTTCA
A N I Y M Y L Y F V F F I I F G S F F T L N L F I G V I I D N F
DIII S6
4,610 4,620 4,630 4,640 4,650 4,660 4,670 4,680 4,690 4,700
ATGAACAAAAGAAGAAGGCTGGAGGATCATTAGAAATGTTCATGACAGAAGACCAAAAGAAATACTATAACGCCATGAAGAAAATGGGATCCAAAAAG
N E Q K K K A G G S L E M F M T E D Q K K Y Y N A M K K M G S K K
4,710 4,720 4,730 4,740 4,750 4,760 4,770 4,780 4,790 4,800
CCAGCCAAGGCAATTCCAAGACCCCGGTTCAAACTTCAAGCAATGGTCTTCGACCTGACTACAAACAAAATGTTTGACATGGCGATCATGATATTTAT
P A K A I P R P R F K L Q A M V F D L T T N K M F D M A I M I F I
DIV S1

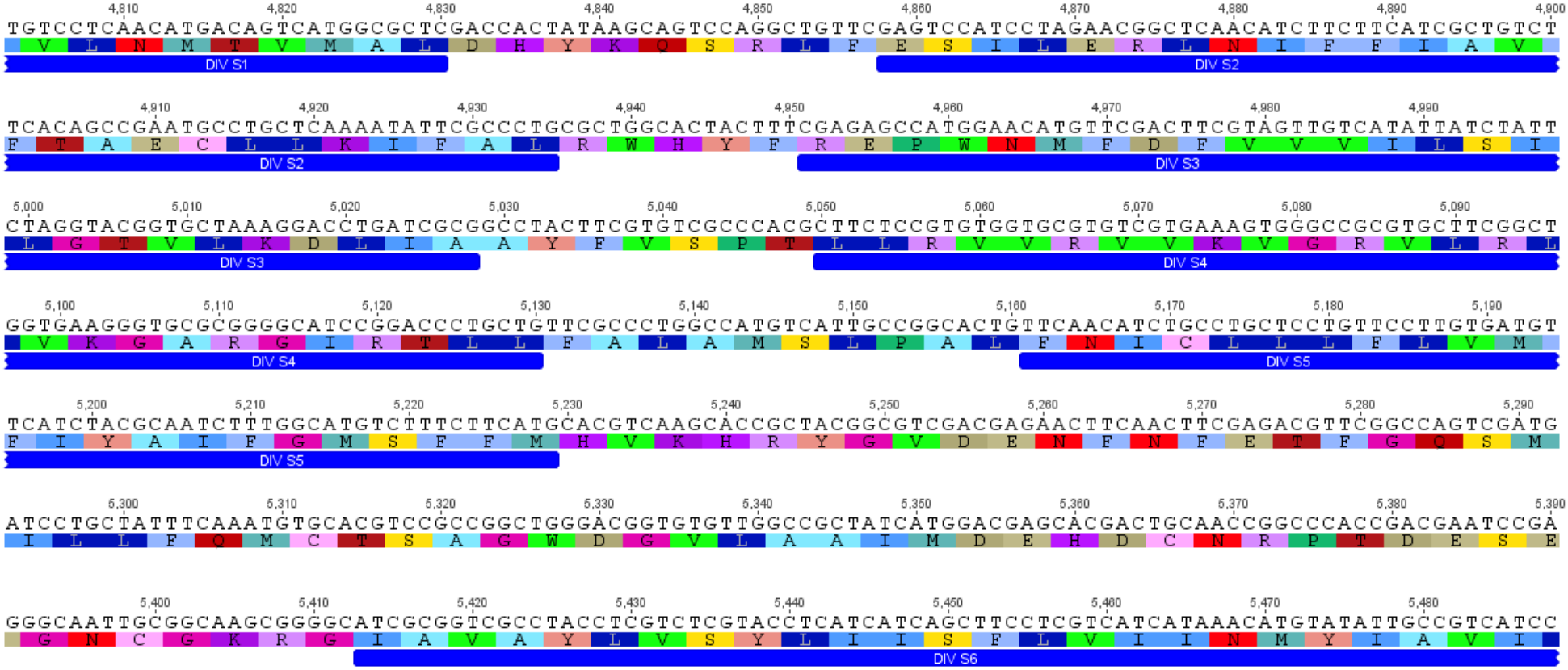
4,810 4,820 4,830 4,840 4,850 4,860 4,870 4,880 4,890 4,900
TGTCCTCAACATGACAGTCATGGCGCTCGACCACTATAAGCAGTCCAGGCTGTTCGAGTCCATCCTAGAACGGCTCAACATCTTCTTCATCGCTGTCT
V L N M T V M A L D H Y K Q S R L F E S I L E R L N I F F I A V
DIV S1
DIV S2
4,910 4,920 4,930 4,940 4,950 4,960 4,970 4,980 4,990
TCACAGCCGAATGCCTGCTCAAAATATTCGCCCTGCGCTGGCACTACTTTCGAGAGCCATGGAACATGTTCGACTTCGTAGTTGTCATATTATCTATT
F T A E C L L K I F A L R W H Y F R E P W N M F D F V V V I L S I
DIV S2
DIV S3
5,000 5,010 5,020 5,030 5,040 5,050 5,060 5,070 5,080 5,090
CTAGGTACGGTGCTAAAGGACCTGATCGCGGCCTACTTCGTGTCGCCCACGCTTCTCCGTGTGGTGCGTGTCGTGAAAGTGGGCCGCGTGCTTCGGCT
L G T V L K D L I A A Y F V S P T L L R V V R V V K V G R V L R L
DIV S3
DIV S4
5,100 5,110 5,120 5,130 5,140 5,150 5,160 5,170 5,180 5,190
GGTGAAGGGTGCGCGGGGCATCCGGACCCTGCTGTTCGCCCTGGCCATGTCATTGCCGGCACTGTTCAACATCTGCCTGCTCCTGTTCCTTGTGATGT
V K G A R G I R T L L F A L A M S L P A L F N I C L L L F L V M
DIV S4
DIV S5
5,200 5,210 5,220 5,230 5,240 5,250 5,260 5,270 5,280 5,290
TCATCTACGCAATCTTTGGCATGTCTTTCTTCATGCACGTCAAGCACCGCTACGGCGTCGACGAGAACTTCAACTTCGAGACGTTCGGCCAGTCGATG
F I Y A I F G M S F F M H V K H R Y G V D E N F N F E T F G Q S M
DIV S5
5,300 5,310 5,320 5,330 5,340 5,350 5,360 5,370 5,380 5,390
ATCCTGCTATTTCAAATGTGCACGTCCGCCGGCTGGGACGGTGTGTTGGCCGCTATCATGGACGAGCACGACTGCAACCGGCCCACCGACGAATCCGA
I L L F Q M C T S A G W D G V L A A I M D E H D C N R P T D E S E
5,400 5,410 5,420 5,430 5,440 5,450 5,460 5,470 5,480
GGGCAATTGCGGCAAGCGGGGCATCGCGGTCGCCTACCTCGTCTCGTACCTCATCATCAGCTTCCTCGTCATCATAAACATGTATATTGCCGTCATCC
G N C G K R G I A V A Y L V S Y L I I S F L V I I N M Y I A V I
DIV S6

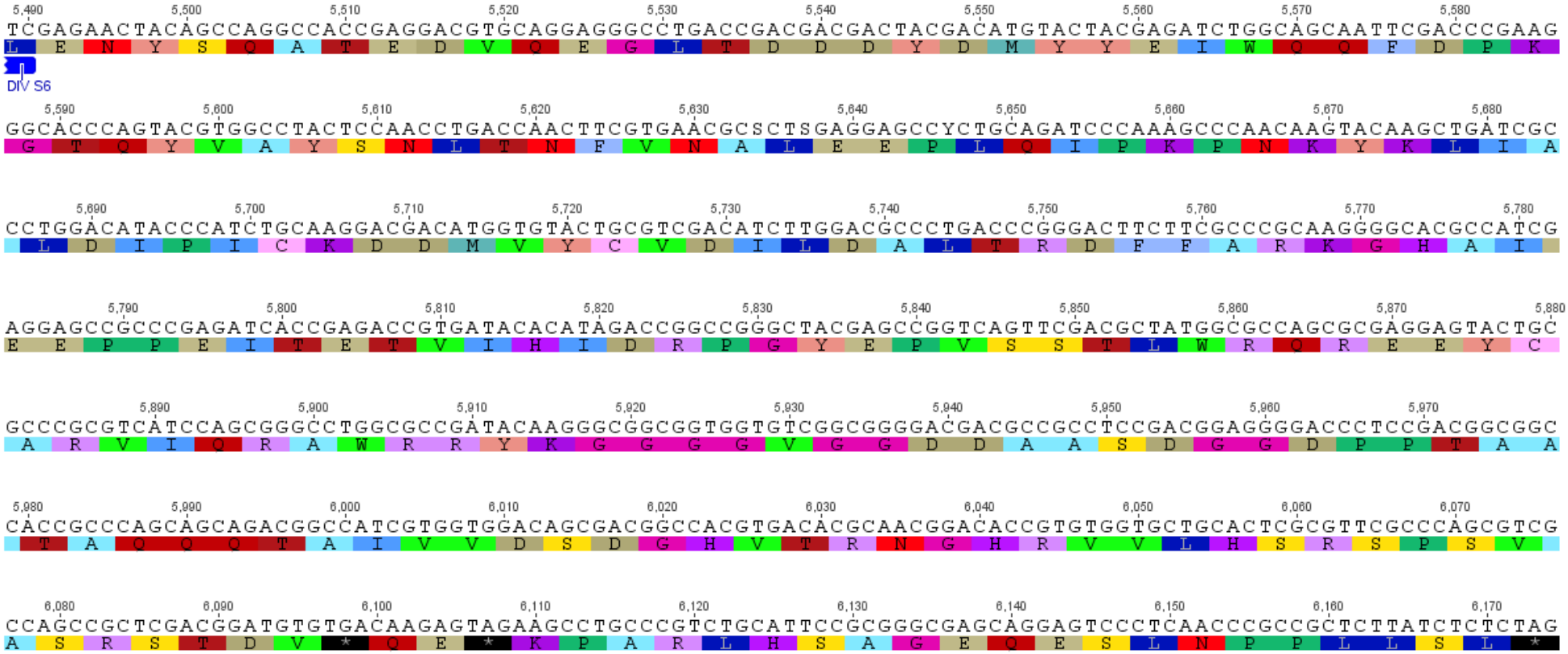
5,490 5,500 5,510 5,520 5,530 5,540 5,550 5,560 5,570 5,580
TCGAGAACTACAGCCAGGCCACCGAGGACGTGCAGGAGGGCCTGACCGACGACGACTACGACATGTACTACGAGATCTGGCAGCAATTCGACCCGAAG
L E N Y S Q A T E D V Q E G L T D D D Y D M Y Y E I W Q Q F D P K
DIV S6
5,590 5,600 5,610 5,620 5,630 5,640 5,650 5,660 5,670 5,680
GGCACCCAGTACGTGGCCTACTCCAACCTGACCAACTTCGTGAACGCSCTSGAGGAGCCYCTGCAGATCCCAAAGCCCAACAAGTACAAGCTGATCGC
G T Q Y V A Y S N L T N F V N A L E E P L Q I P K P N K Y K L I A
5,690 5,700 5,710 5,720 5,730 5,740 5,750 5,760 5,770 5,780
CCTGGACATACCCATCTGCAAGGACGACATGGTGTACTGCGTCGACATCTTGGACGCCCTGACCCGGGACTTCTTCGCCCGCAAGGGGCACGCCATCG
L D I P I C K D D M V Y C V D I L D A L T R D F F A R K G H A I
5,790 5,800 5,810 5,820 5,830 5,840 5,850 5,860 5,870 5,880
AGGAGCCGCCCGAGATCACCGAGACCGTGATACACATAGACCGGCCGGGCTACGAGCCGGTCAGTTCGACGCTATGGCGCCAGCGCGAGGAGTACTGC
E E P P E I T E T V I H I D R P G Y E P V S S T L W R Q R E E Y C
5,890 5,900 5,910 5,920 5,930 5,940 5,950 5,960 5,970
GCCCGCGTCATCCAGCGGGCCTGGCGCCGATACAAGGGCGGCGGTGGTGTCGGCGGGGACGACGCCGCCTCCGACGGAGGGGACCCTCCGACGGCGGC
A R V I Q R A W R R Y K G G G G V G G D D A A S D G G D P P T A A
5,980 5,990 6,000 6,010 6,020 6,030 6,040 6,050 6,060 6,070
CACCGCCCAGCAGCAGACGGCCATCGTGGTGGACAGCGACGGCCACGTGACACGCAACGGACACCGTGTGGTGCTGCACTCGCGTTCGCCCAGCGTCG
T A Q Q Q T A I V V D S D G H V T R N G H R V V L H S R S P S V
6,080 6,090 6,100 6,110 6,120 6,130 6,140 6,150 6,160 6,170
CCAGCCGCTCGACGGATGTGTGACAAGAGTAGAAGCCTGCCCGTCTGCATTCCGCGGGCGAGCAGGAGTCCCTCAACCCGCCGCTCTTATCTCTCTAG
A S R S T D V * Q E * K P A R L H S A G E Q E S L N P P L L S L *

10.2 Appendix 2

The VGSC domain-spanning regions from *A. americanum*, *A. hebraeum*, *D. gallinae*, *D. reticulatus*, D. *variabilis*, *I. ricinus*, *P. ovis* and *R. sanguineus* as sequenced from in this study following cDNA PCR amplification.

Membrane-spanning segments and the domains to which they belong are indicated by blue bars, these were estimated using information from the *V. destructor* mite channel as sequenced by Wang *et al* 2003.

***A. americanum* Domain I**

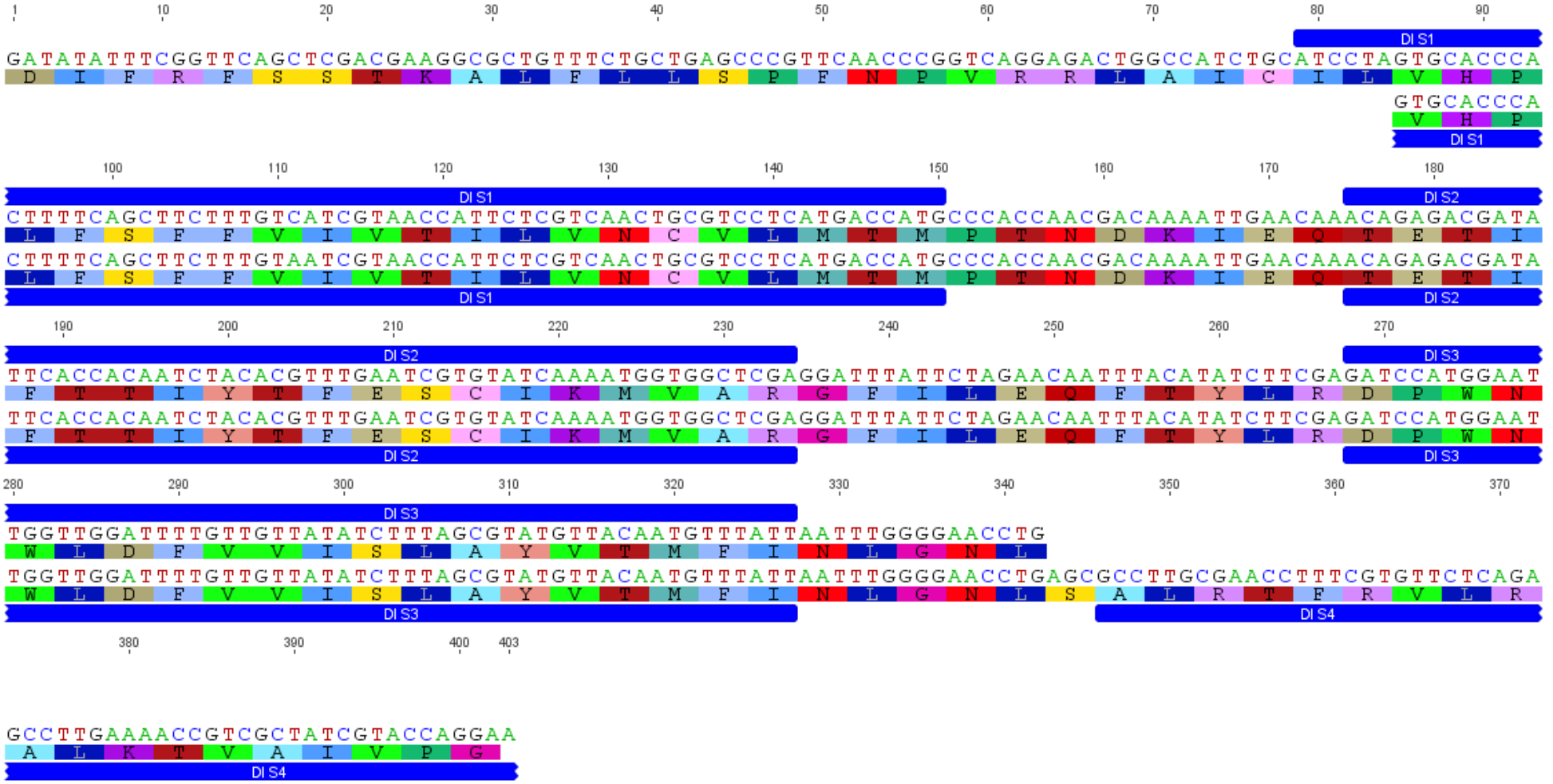

***A. americanum* Domain II**

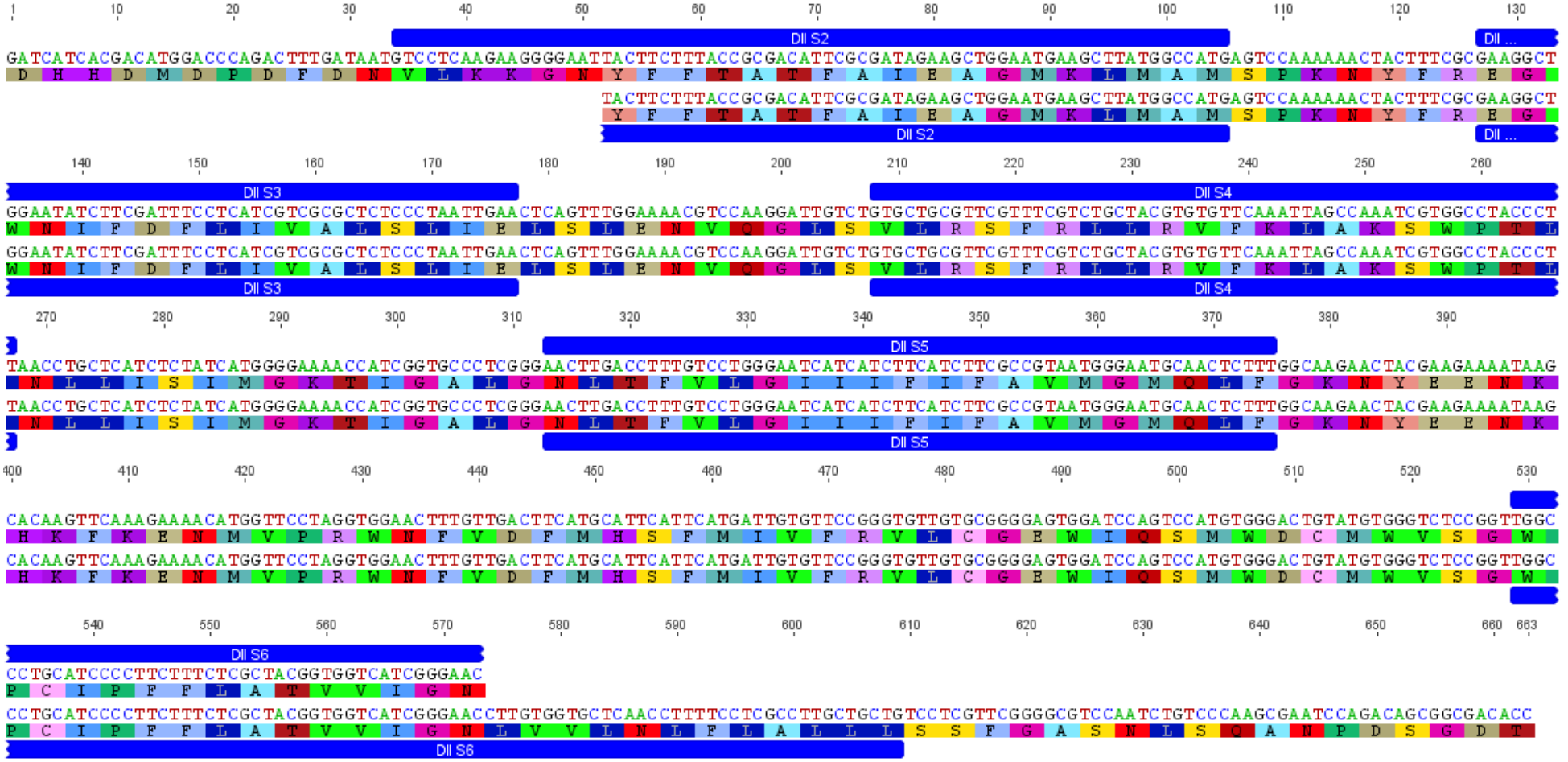

***A. americanum* Domain III**

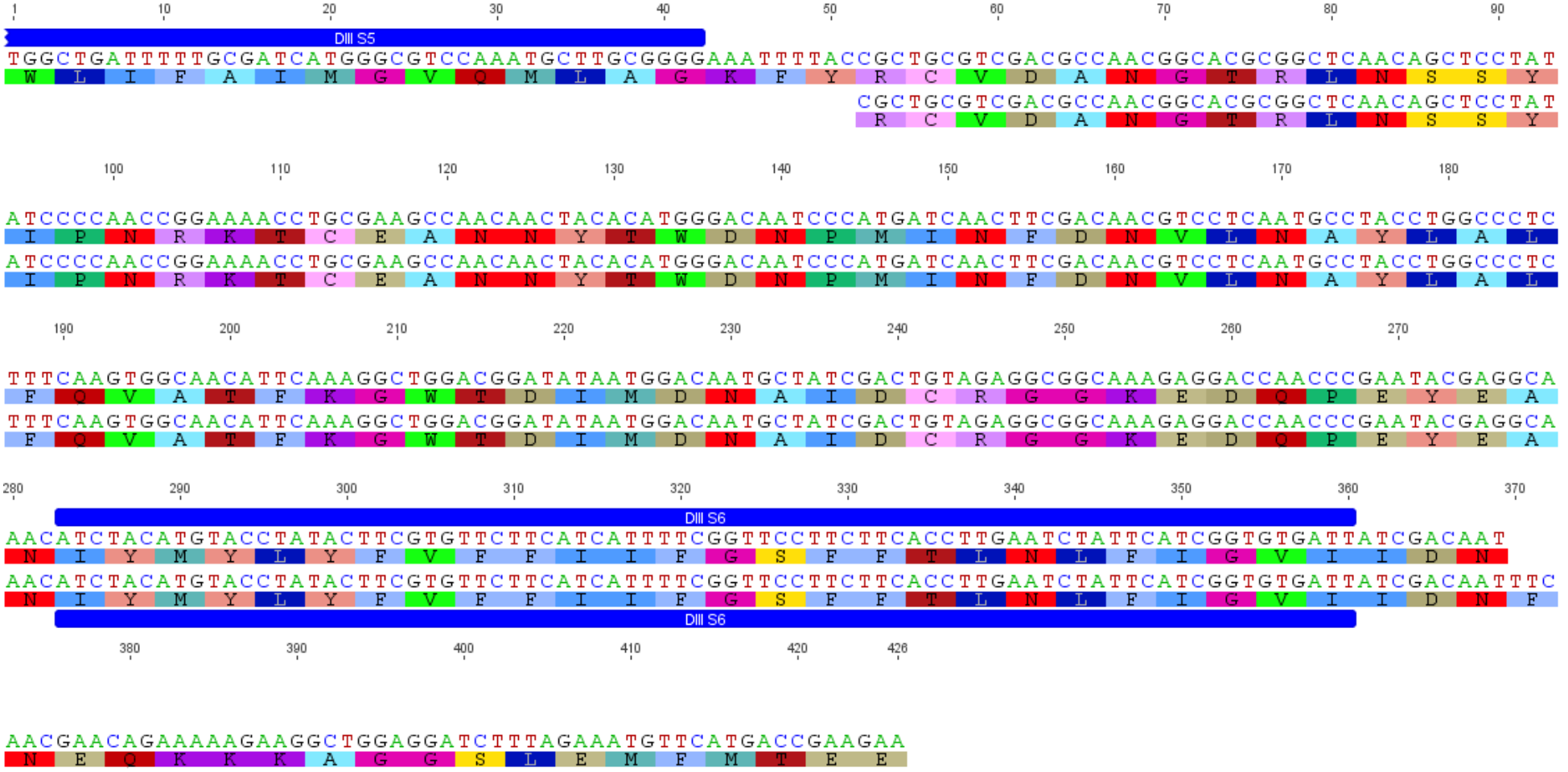

***A. americanum* DIV**

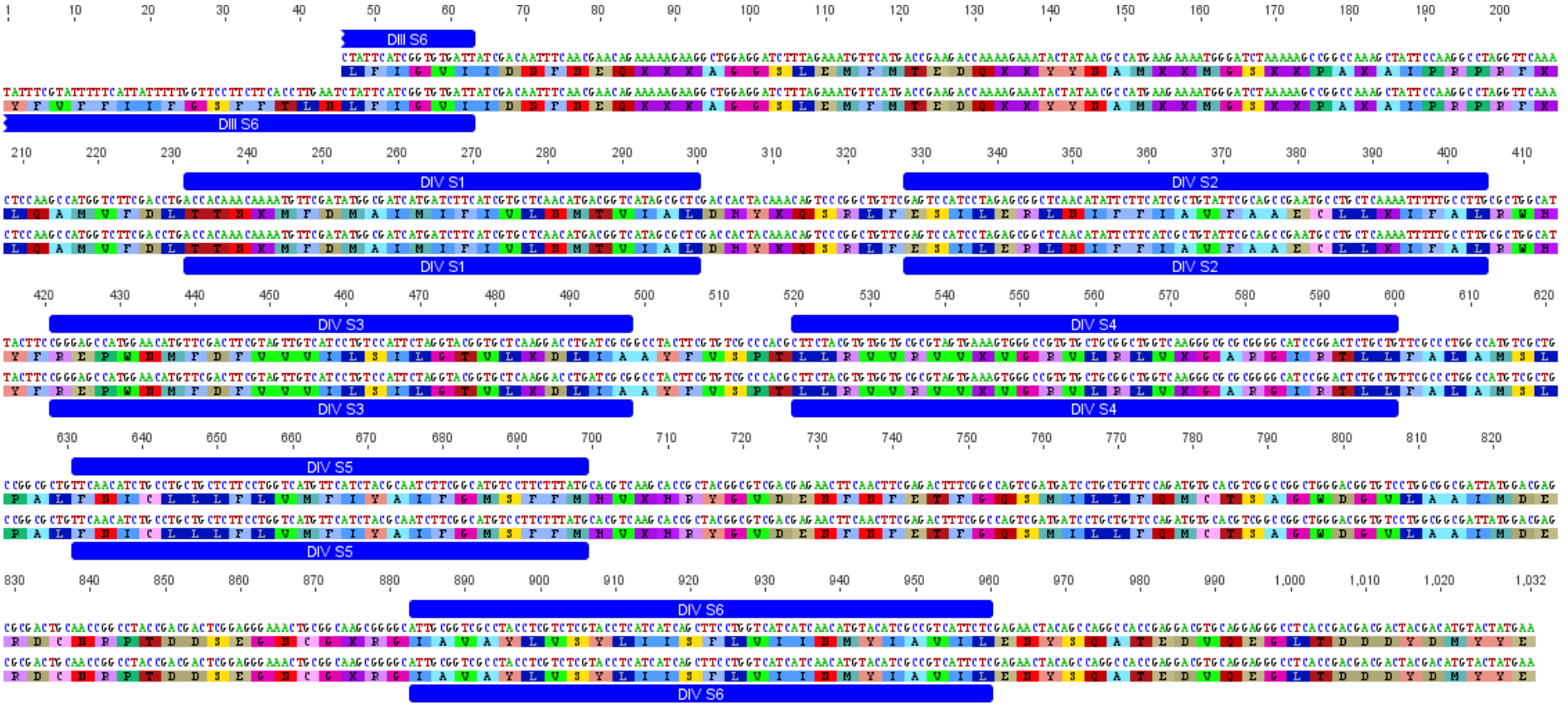

***A. hebraeum* DI**

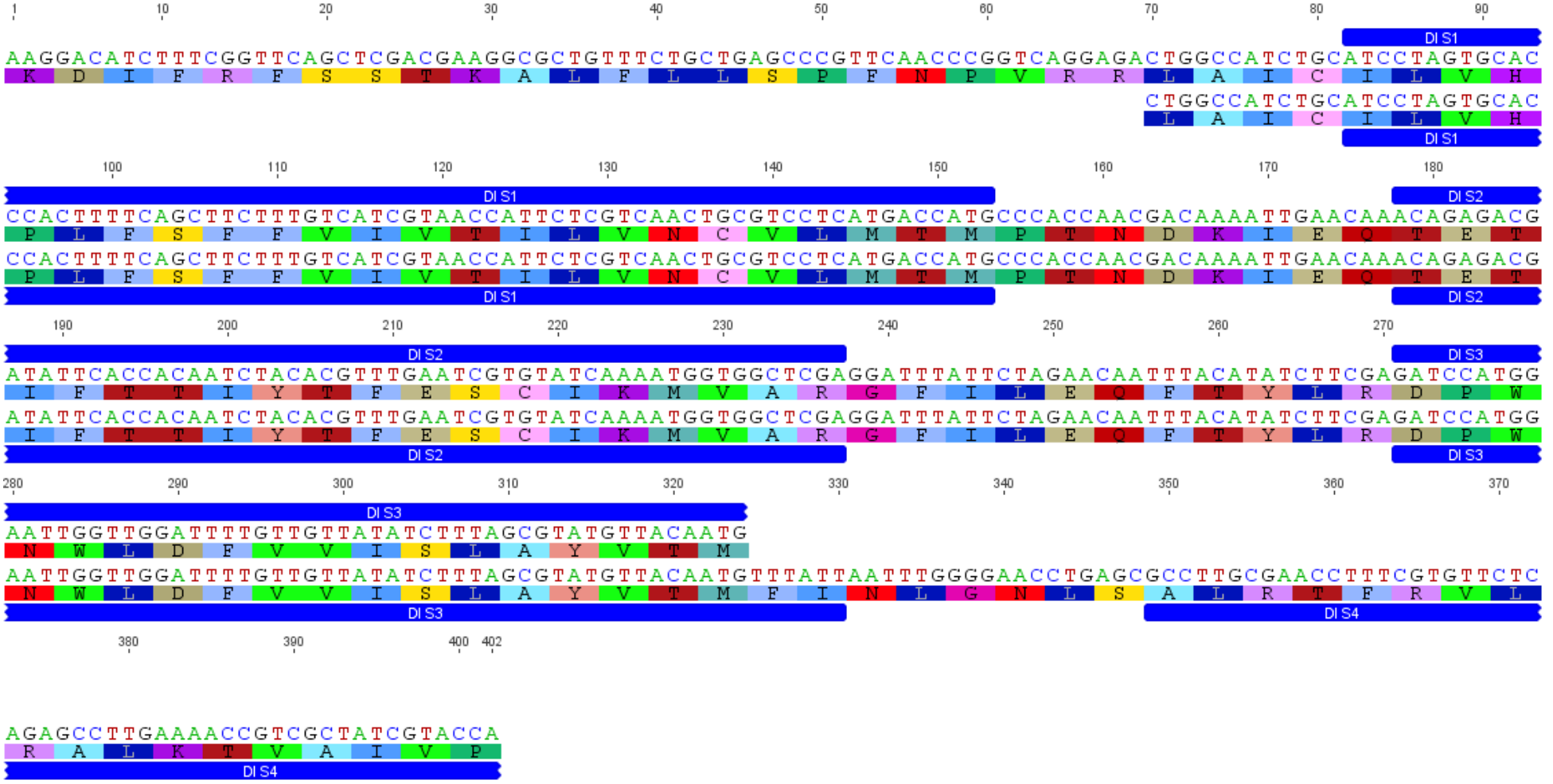

***A. hebraeum* DII**

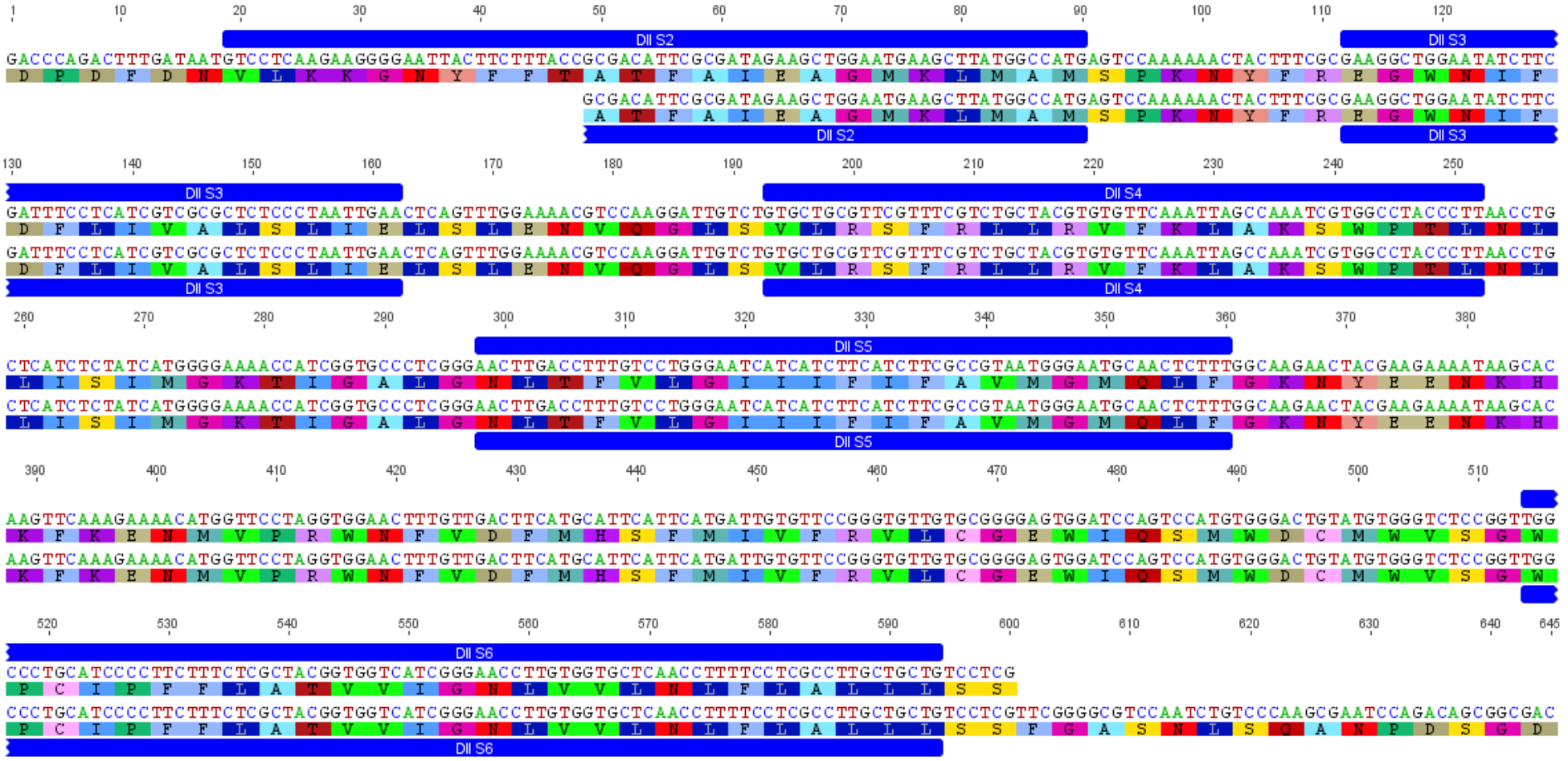

***A. hebraeum* DIII**

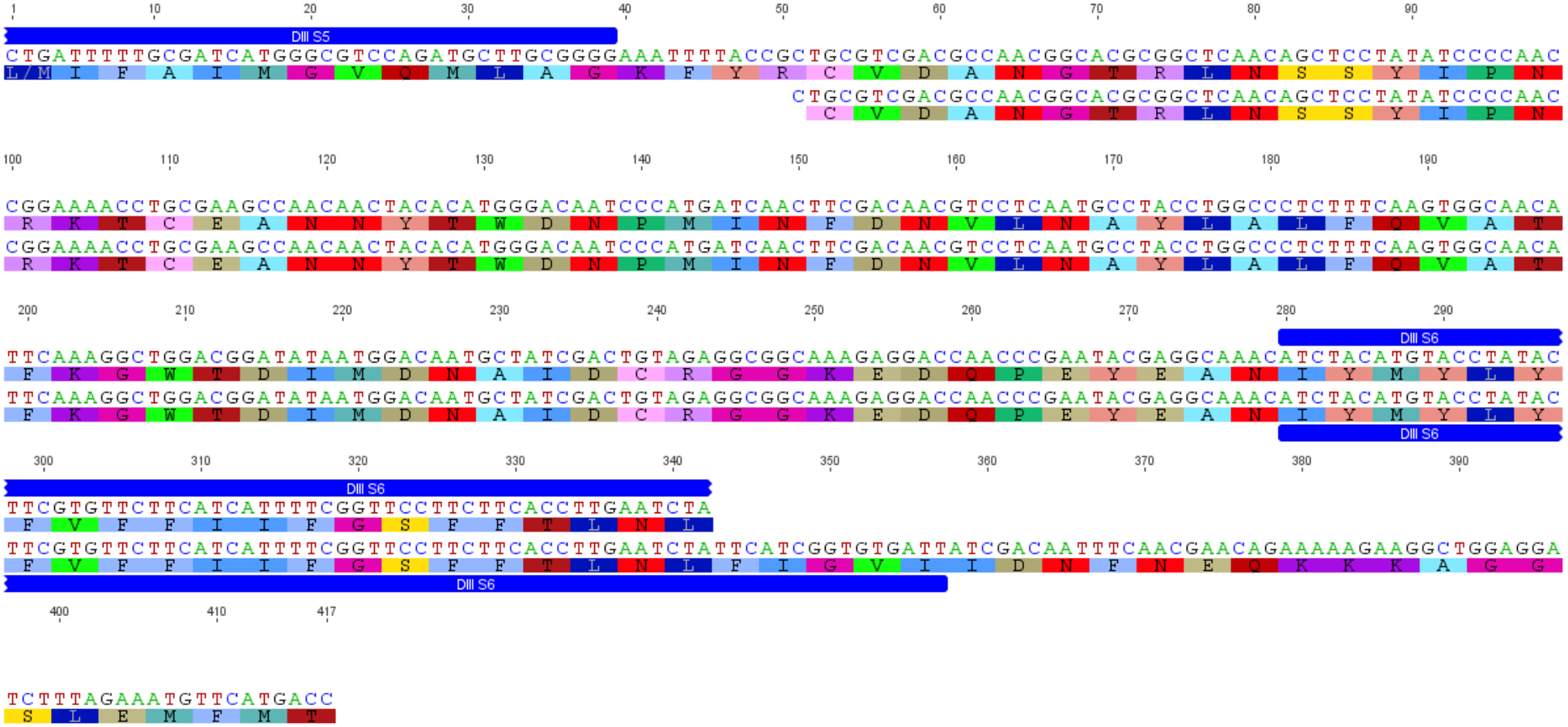

***A. hebraeum* DIV**

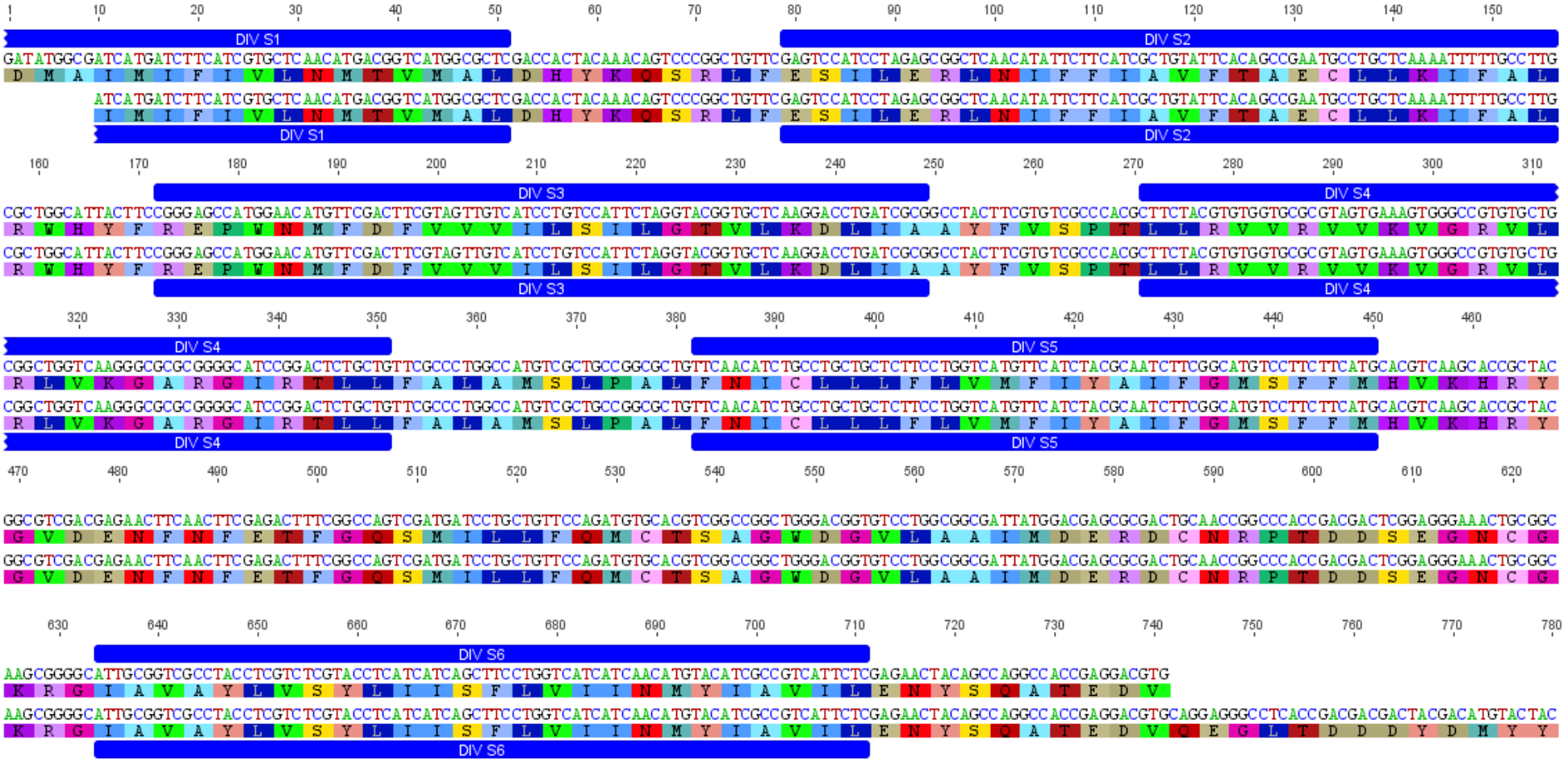

***D. gallinae* DI**

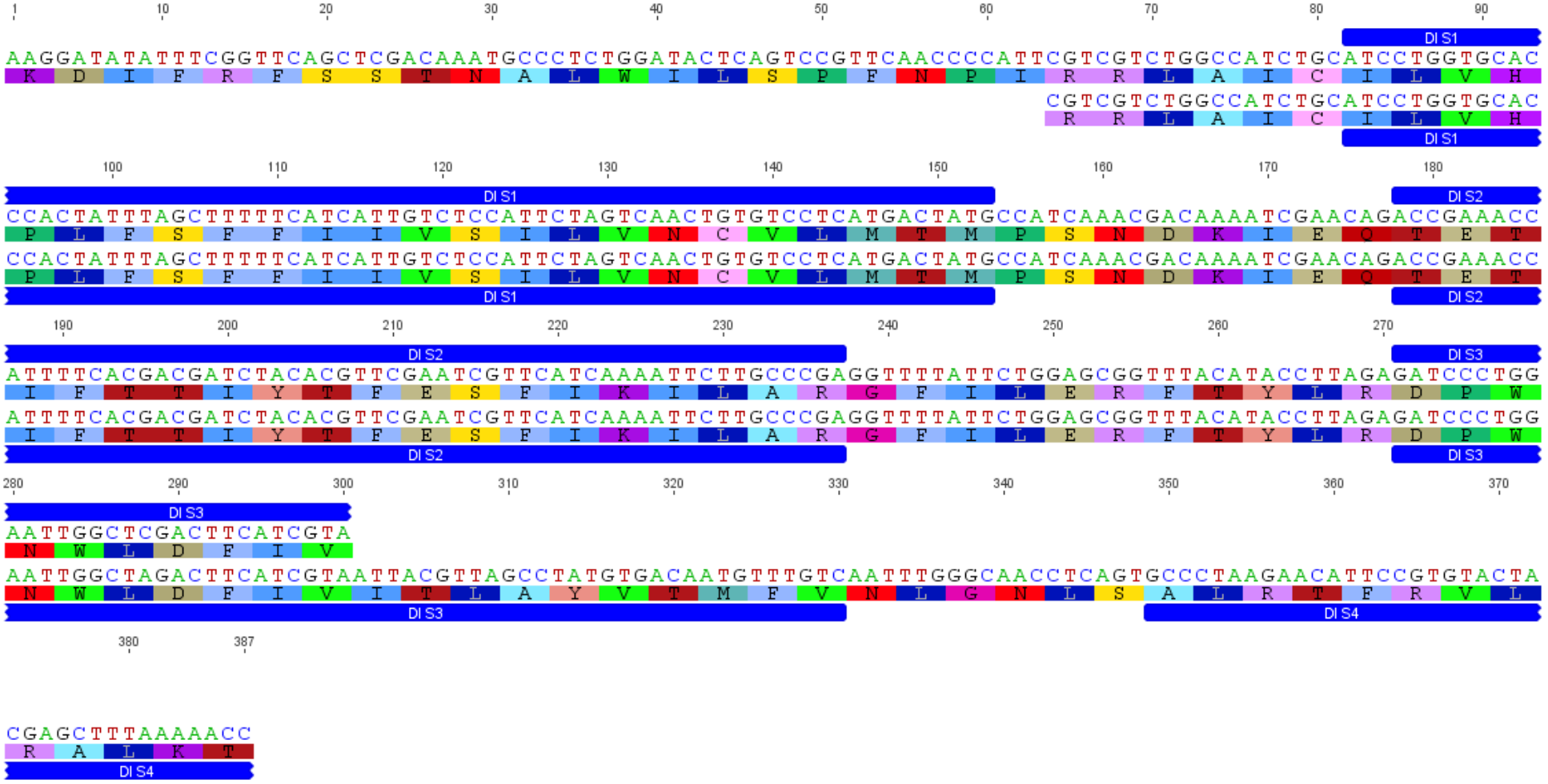

***D. gallinae* DII**

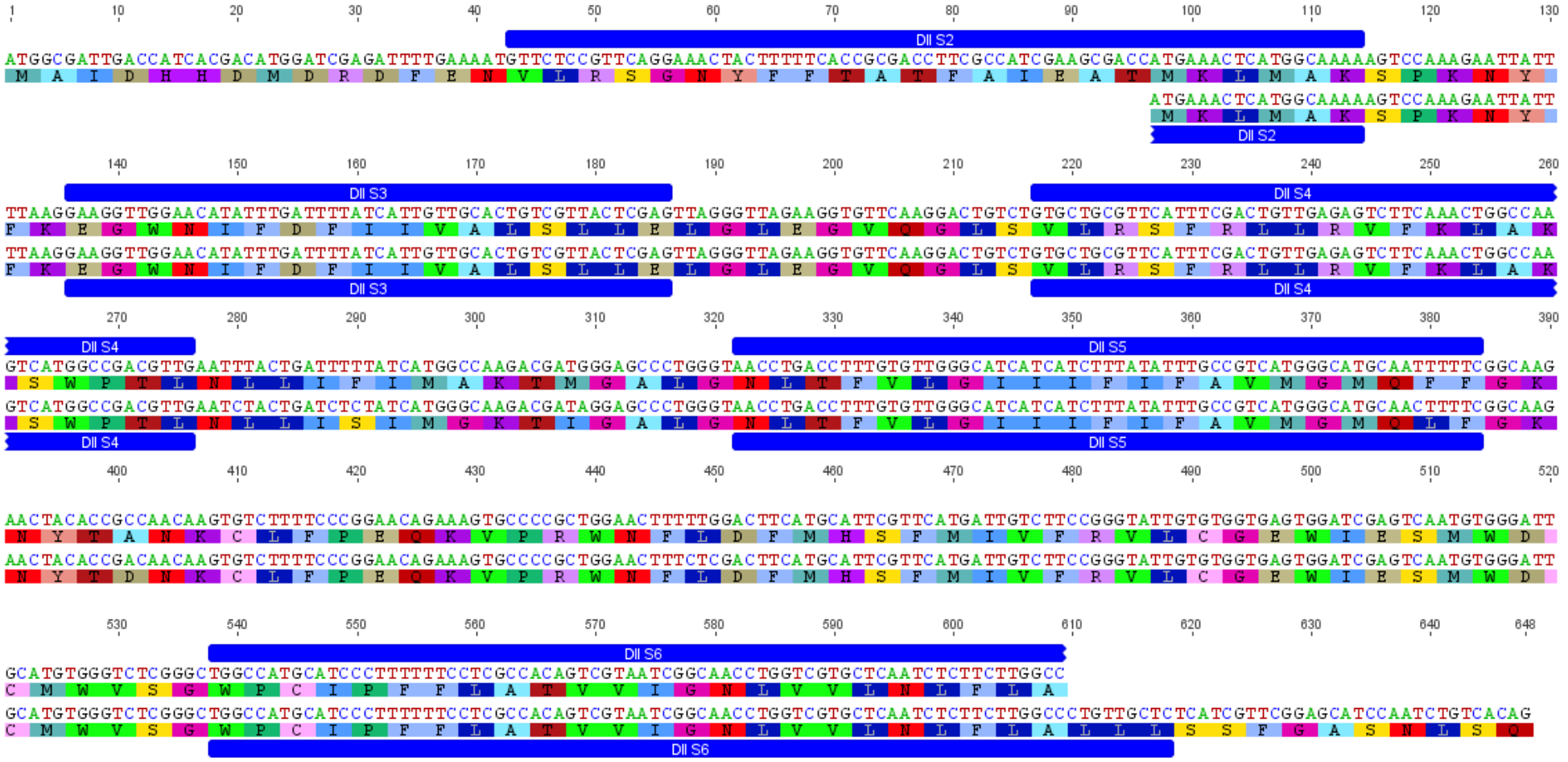

***D. gallinae* DIII**

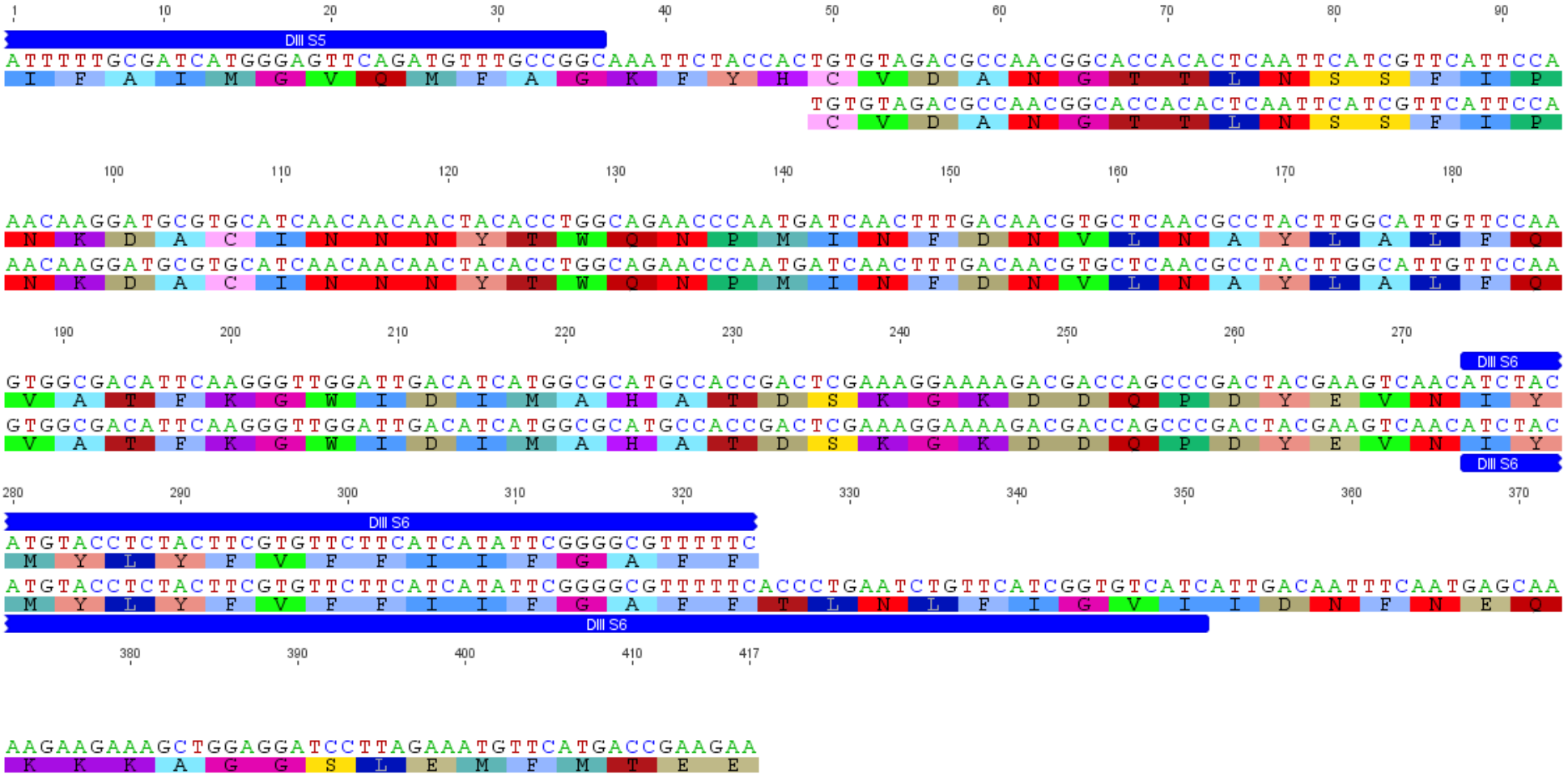

***D. gallinae* DIV**

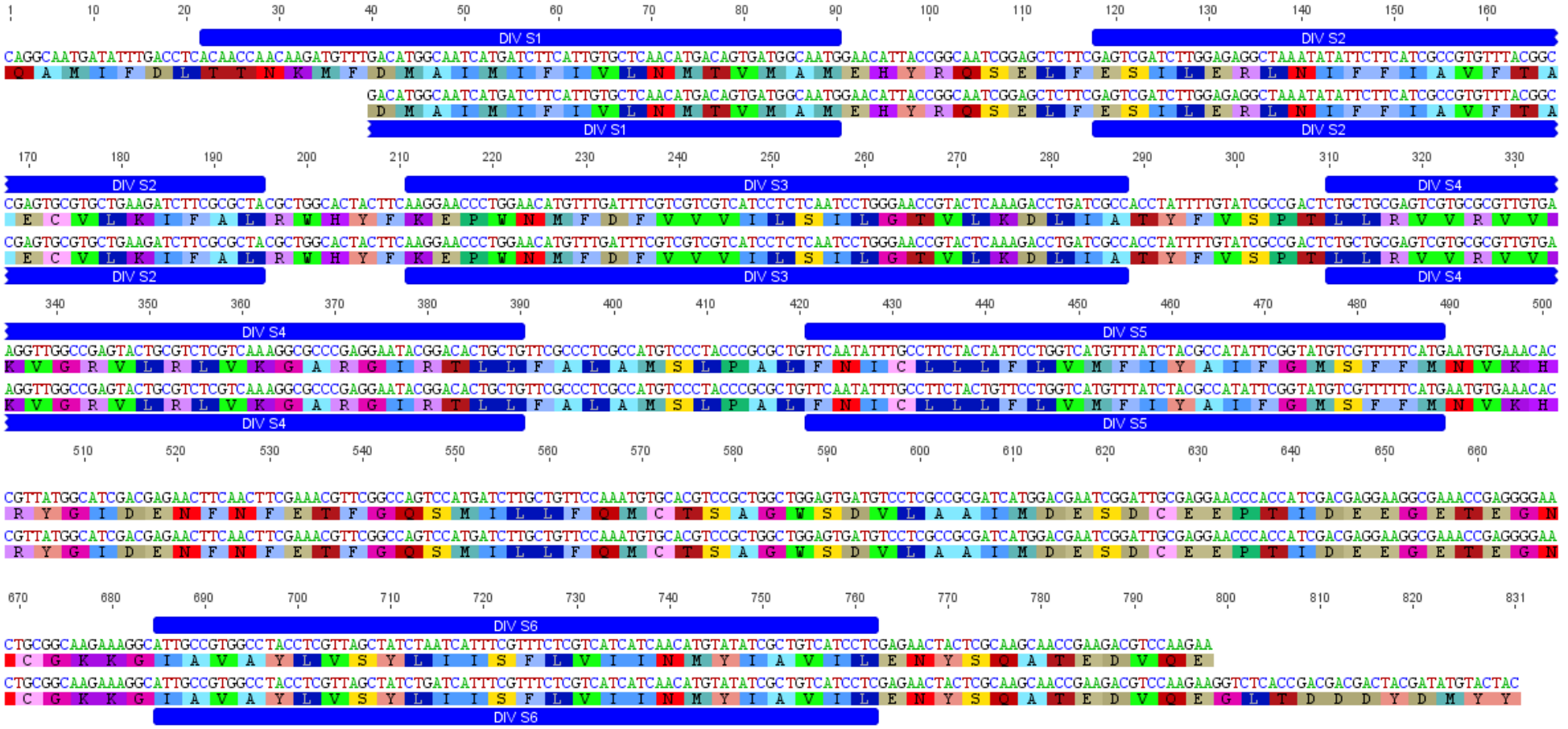

***D. reticulatus* DI**

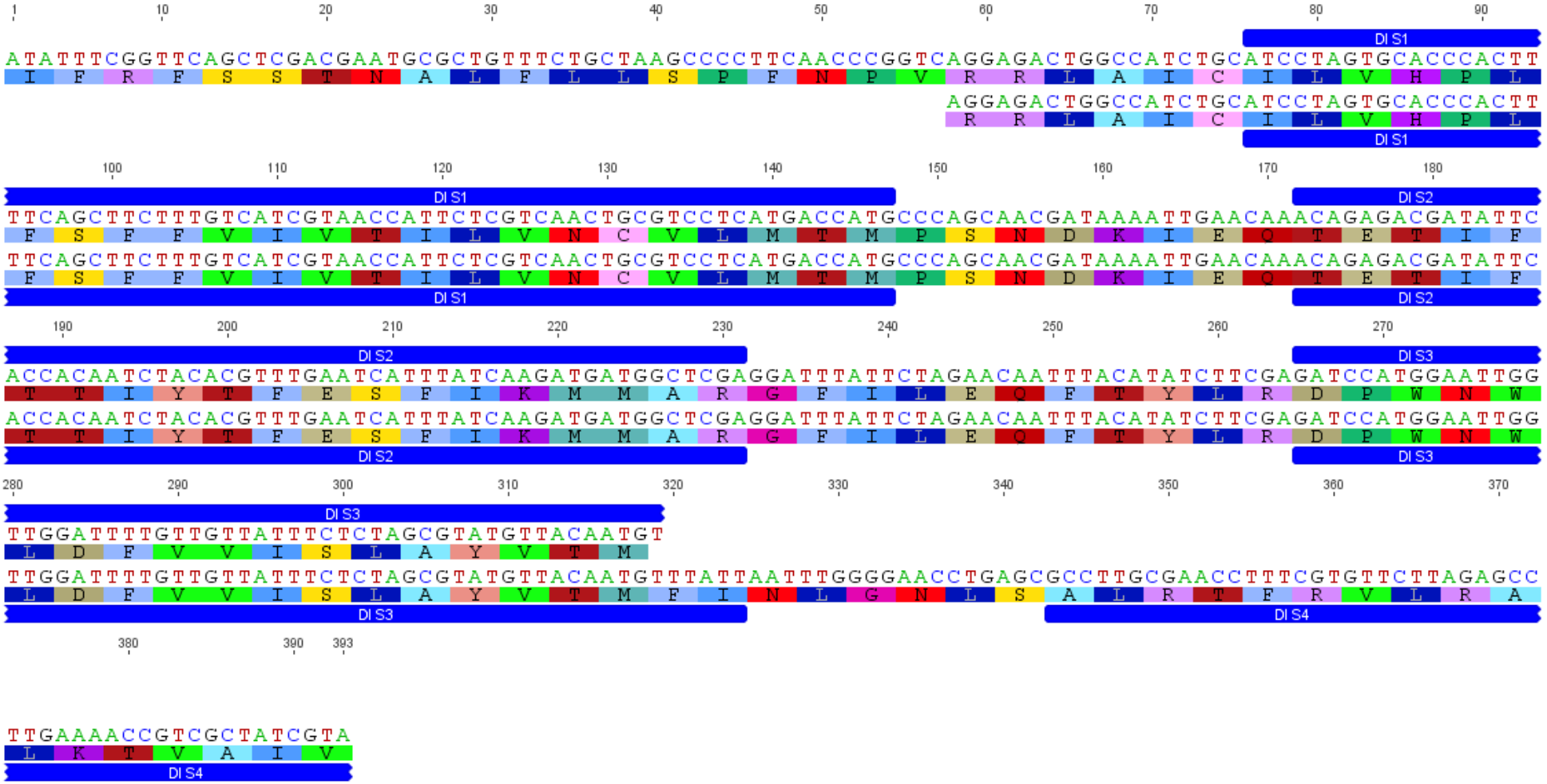

***D. reticulatus* DII**

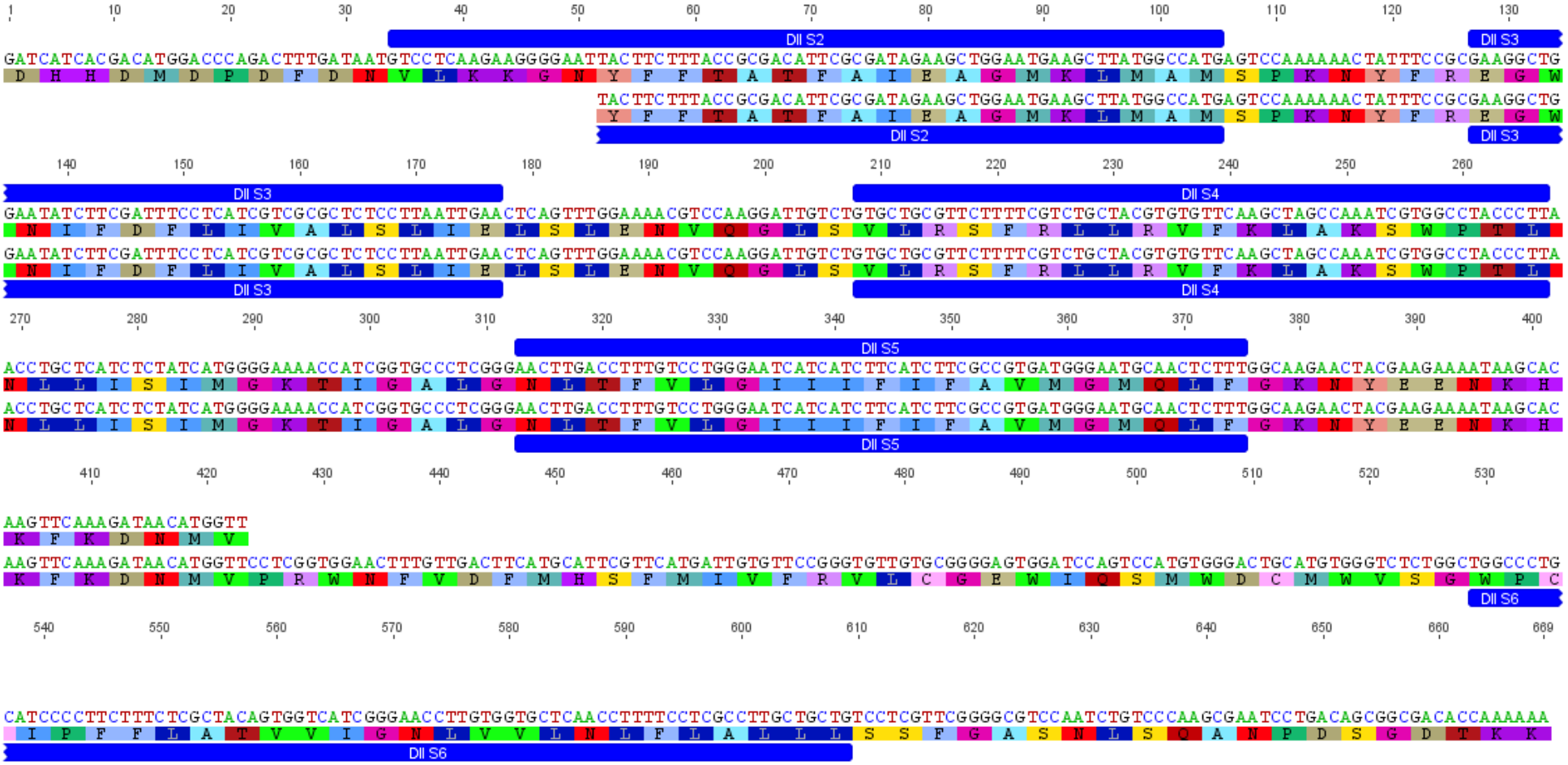

***D. reticulatus* DIII**

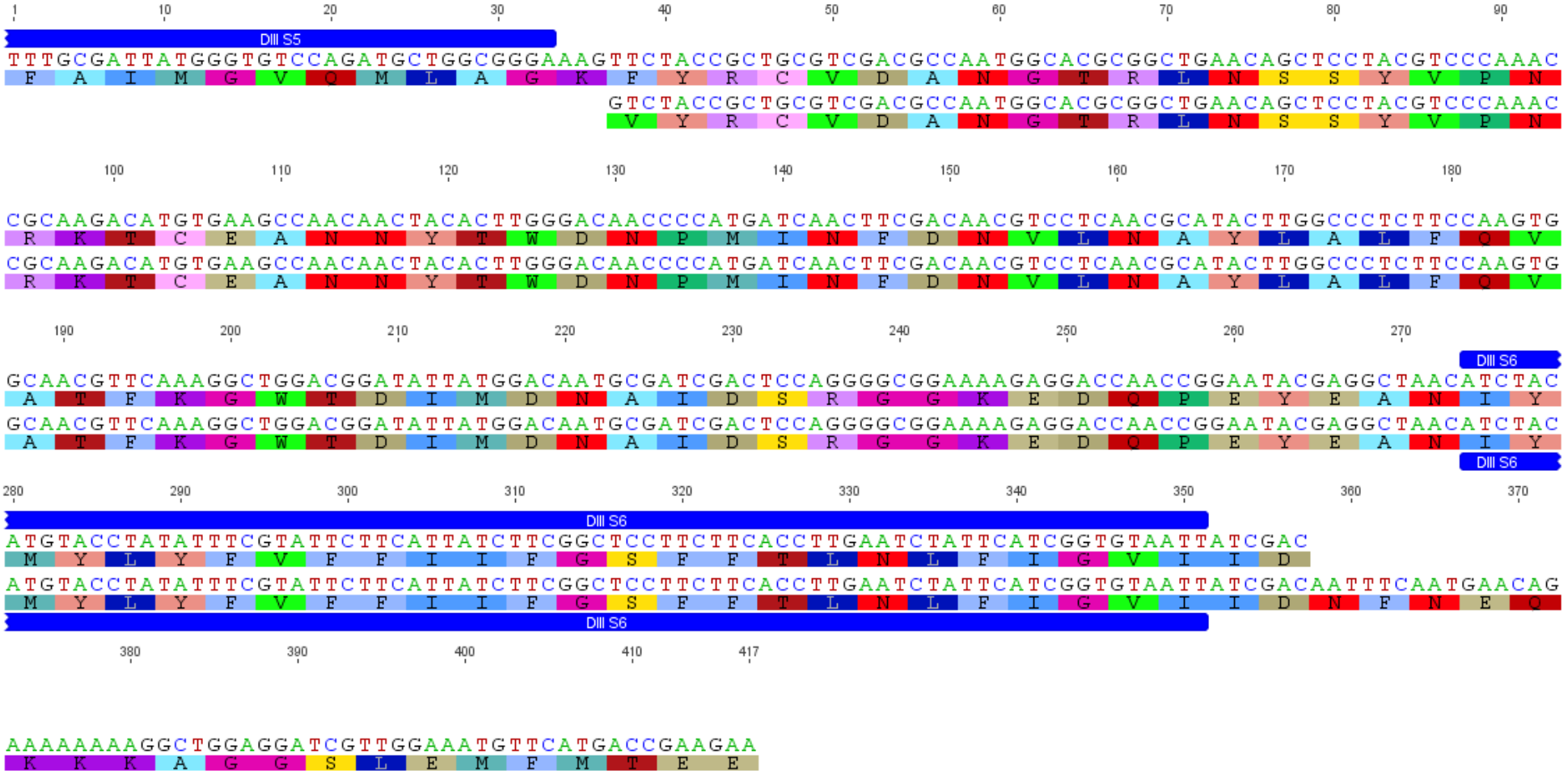

***D. reticulatus* DIV**

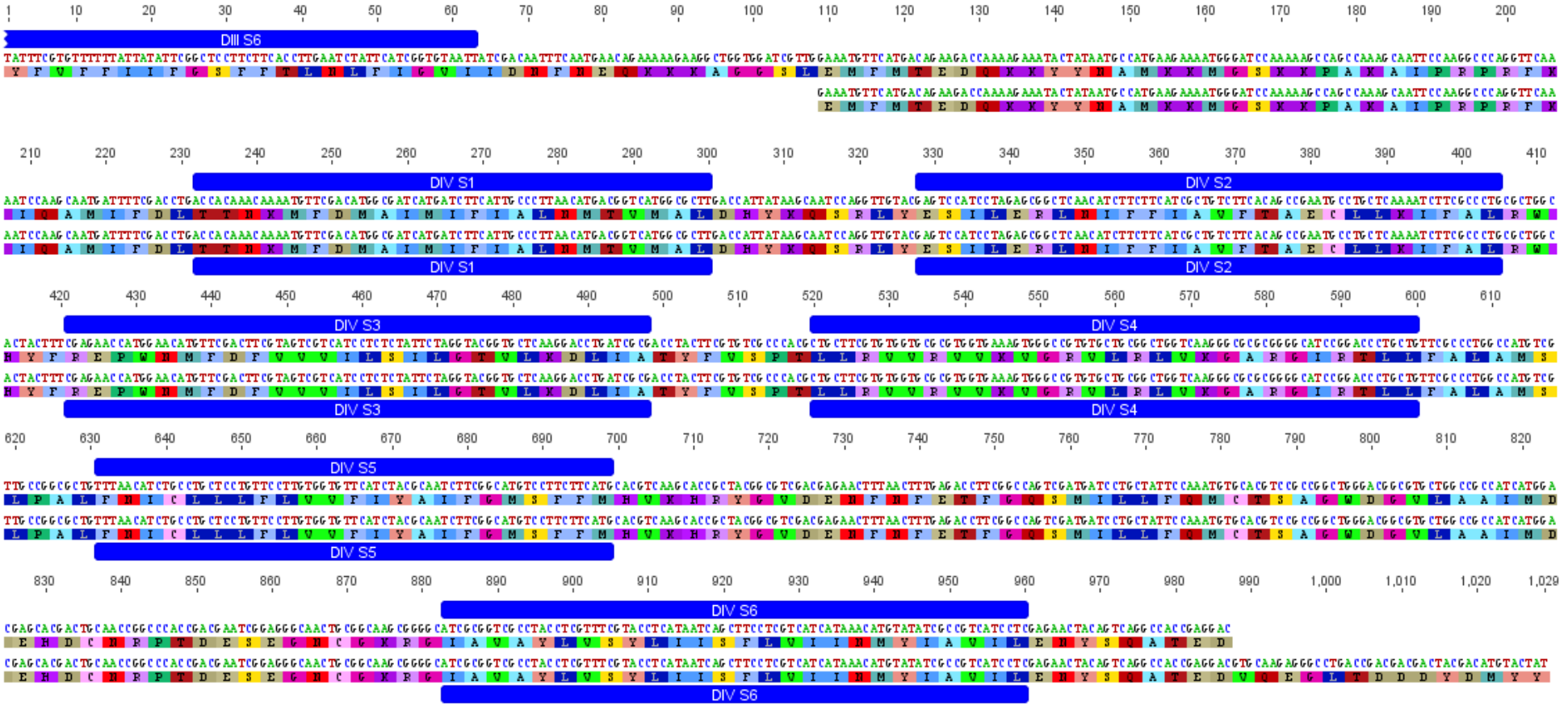

***D. variabilis* DI**

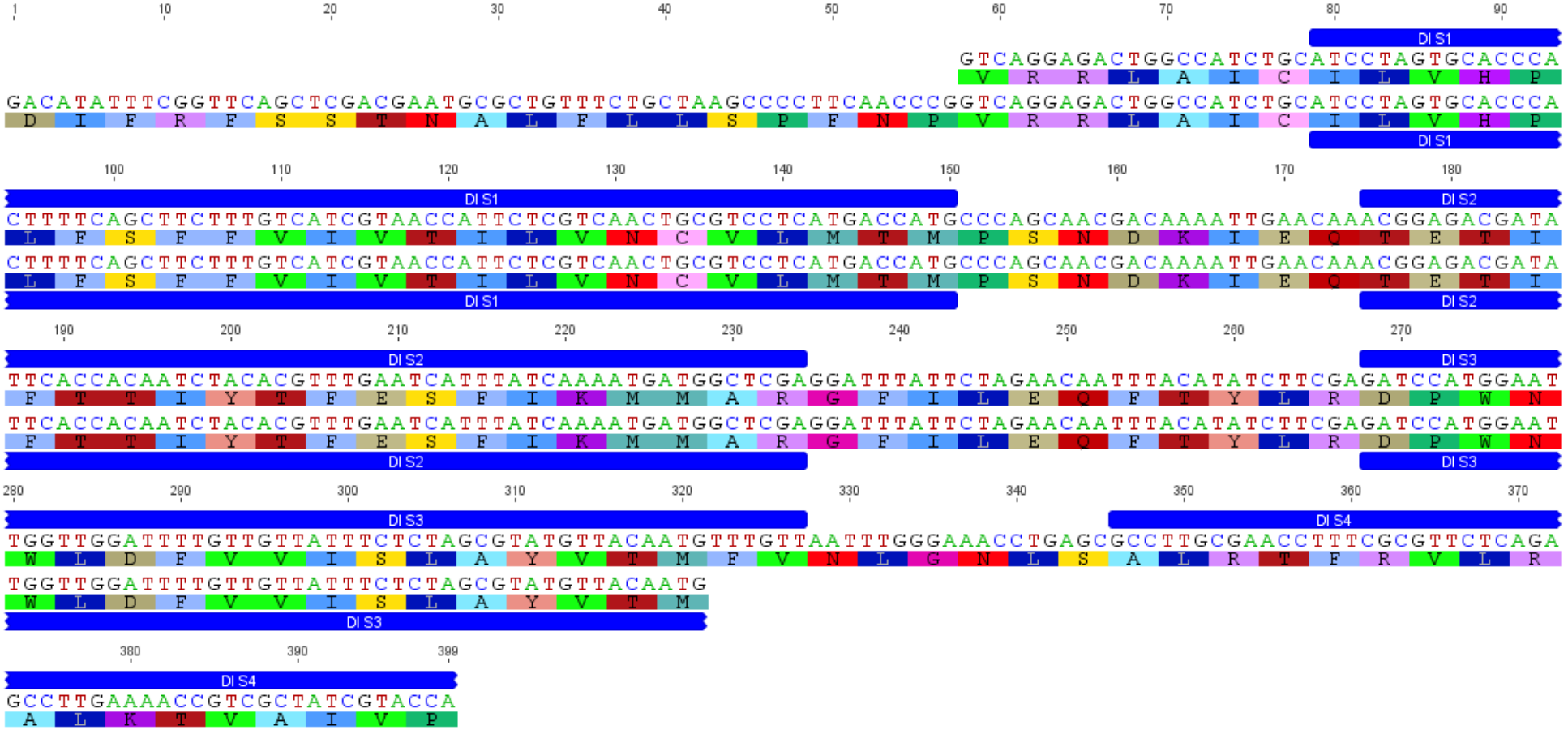

***D. variabilis* DII**

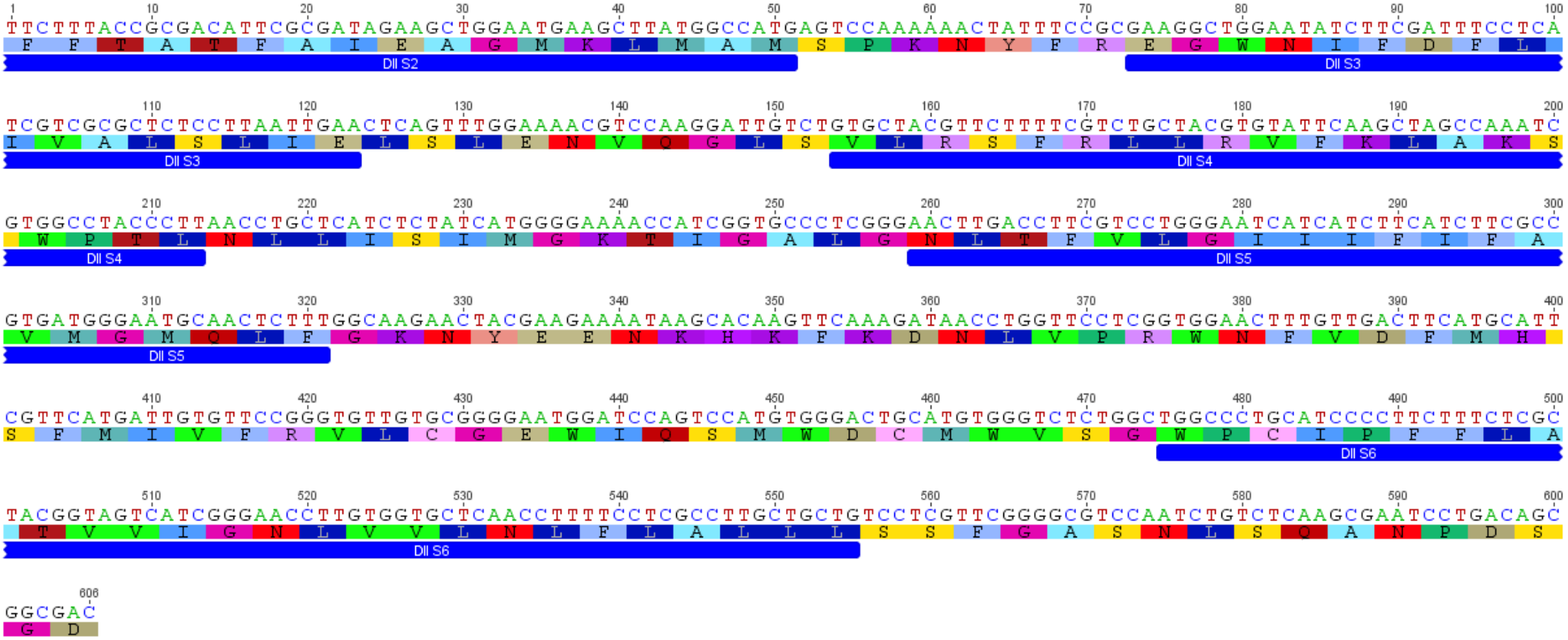

***D. variabilis* DIII**

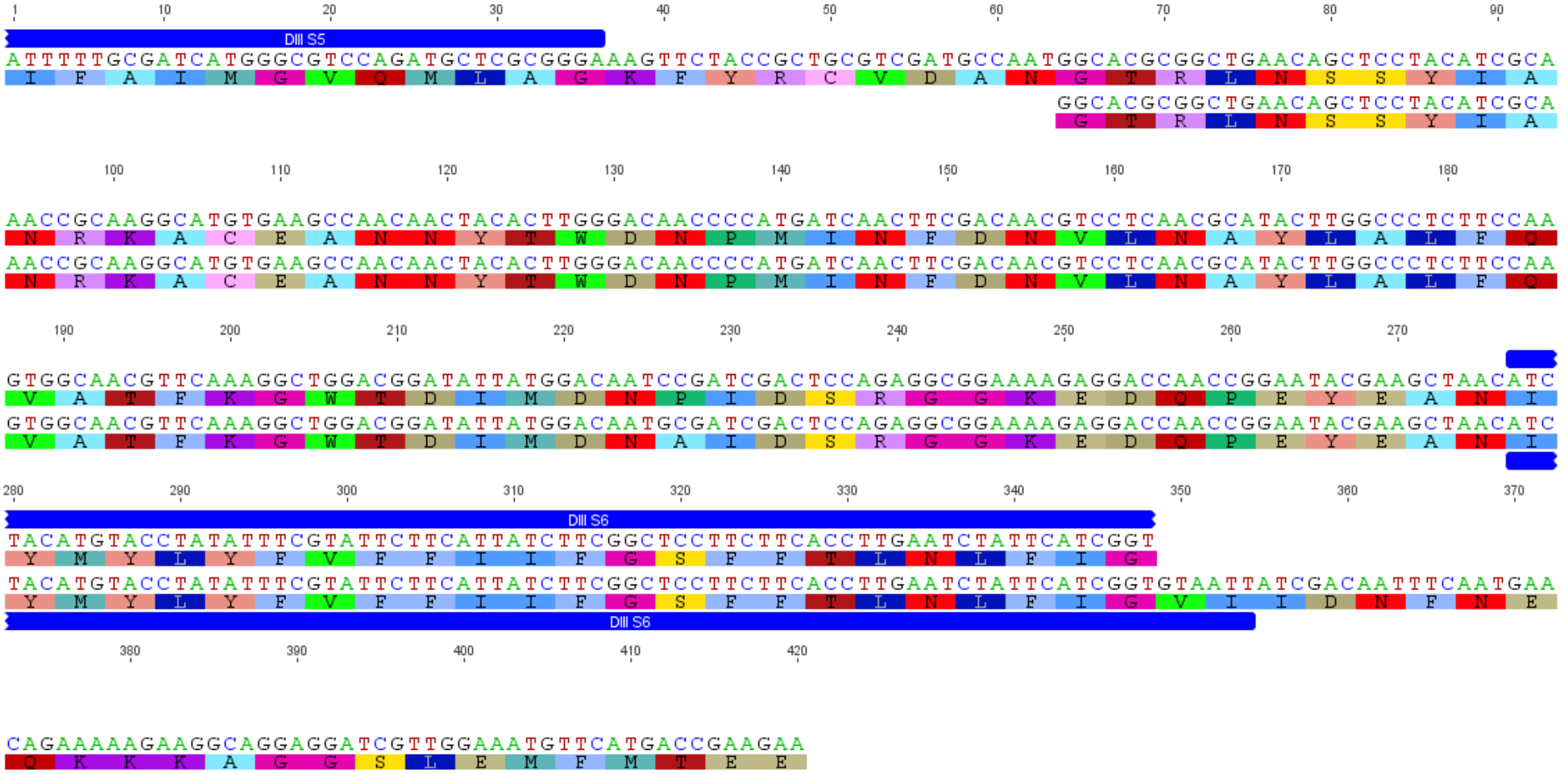

***D. variabilis* DIV**

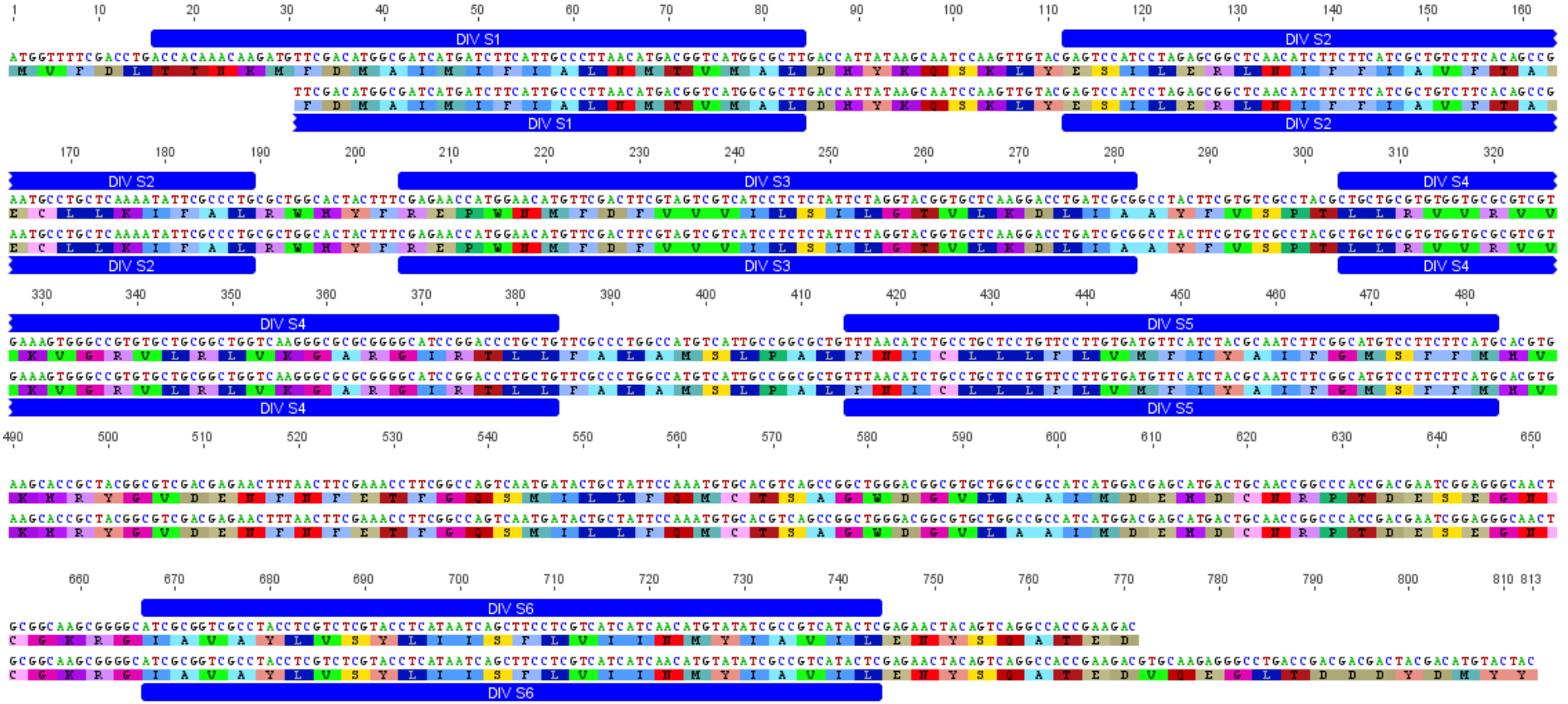

***I. ricinus* DI**

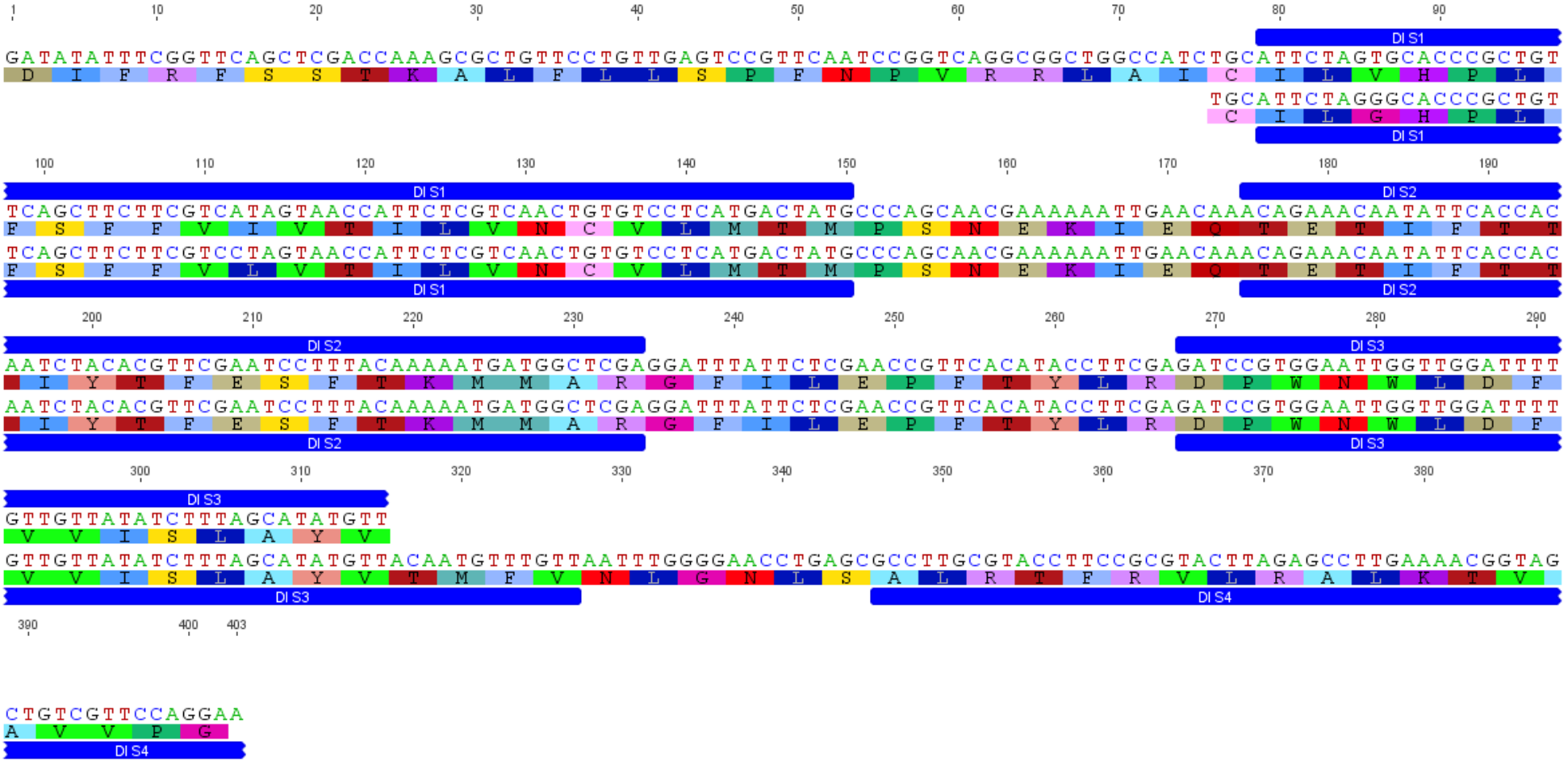

***I. ricinus* DII**

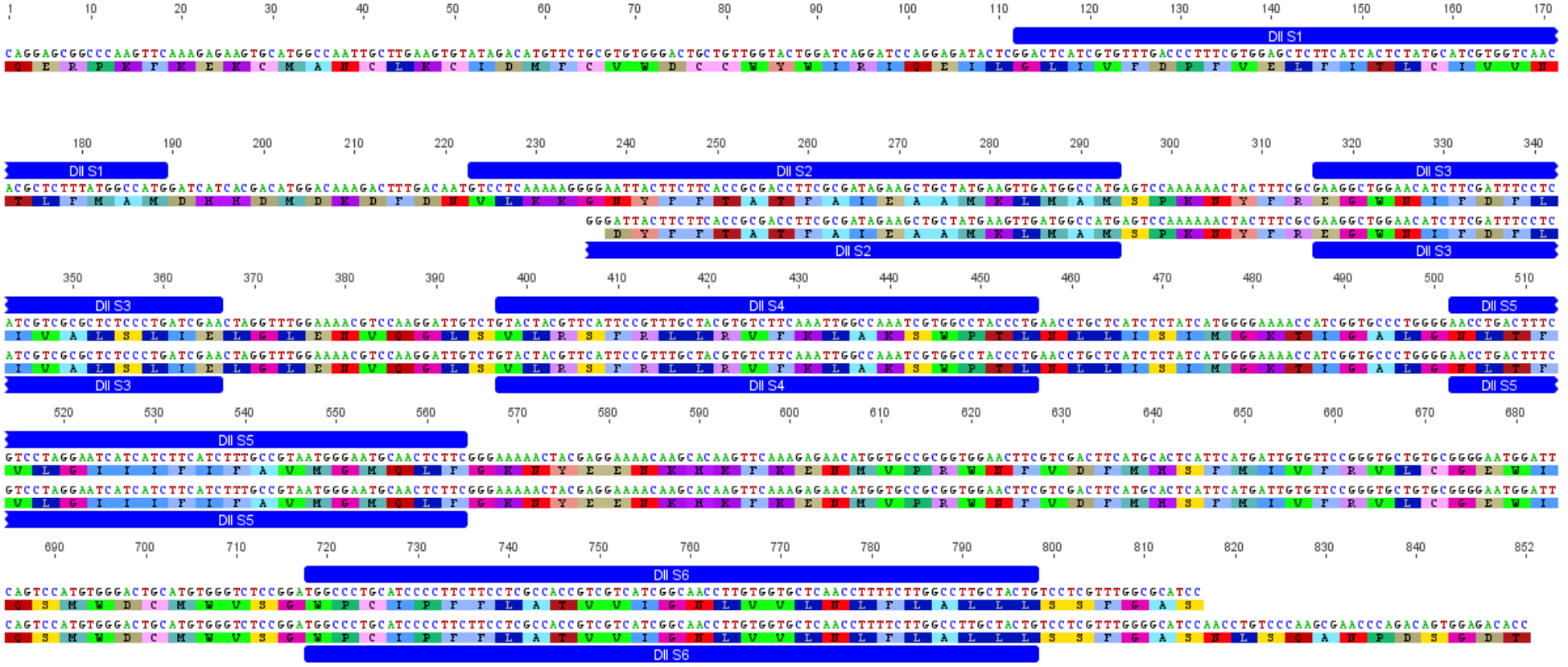

***I. ricinus* DIII**

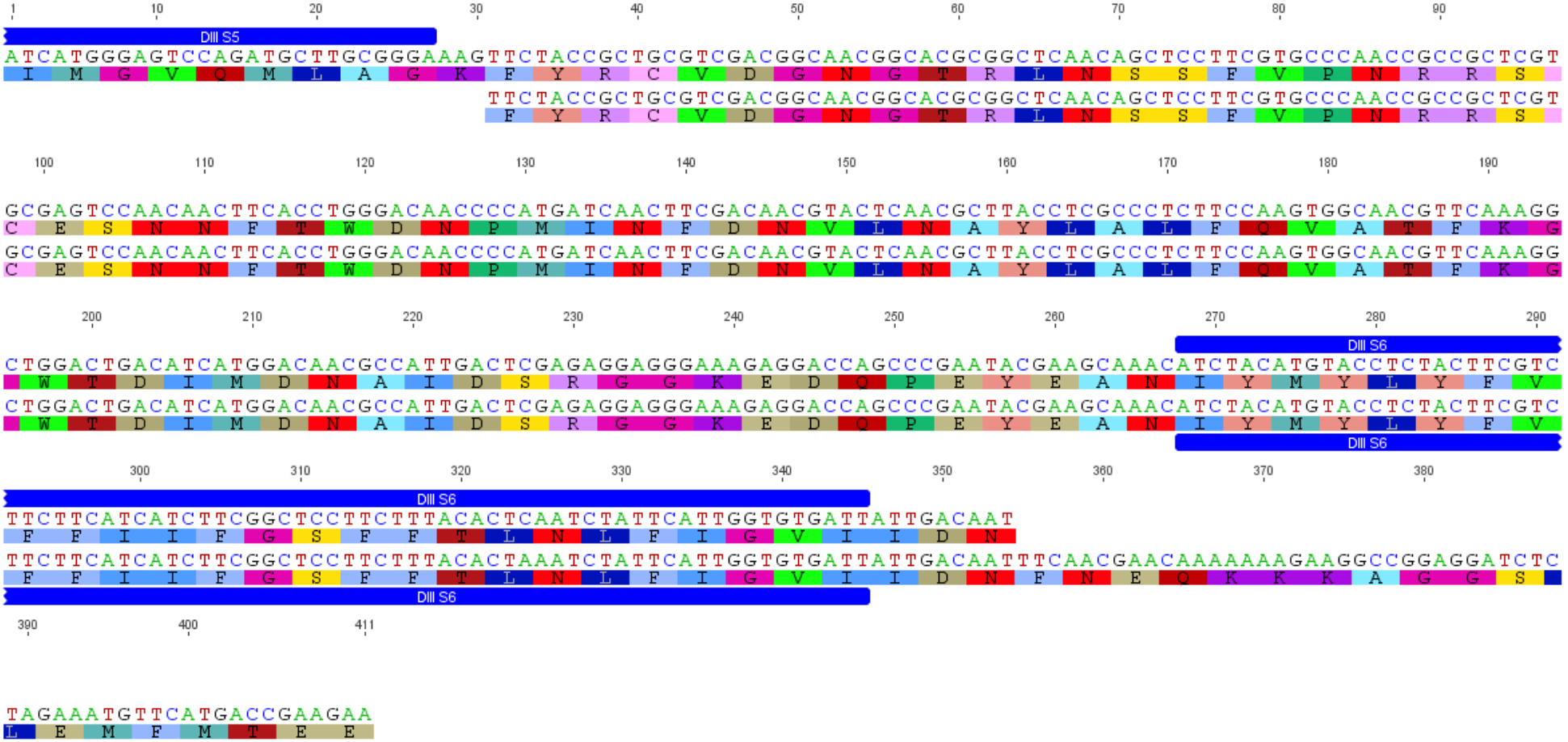

***I. ricinus* DIV**

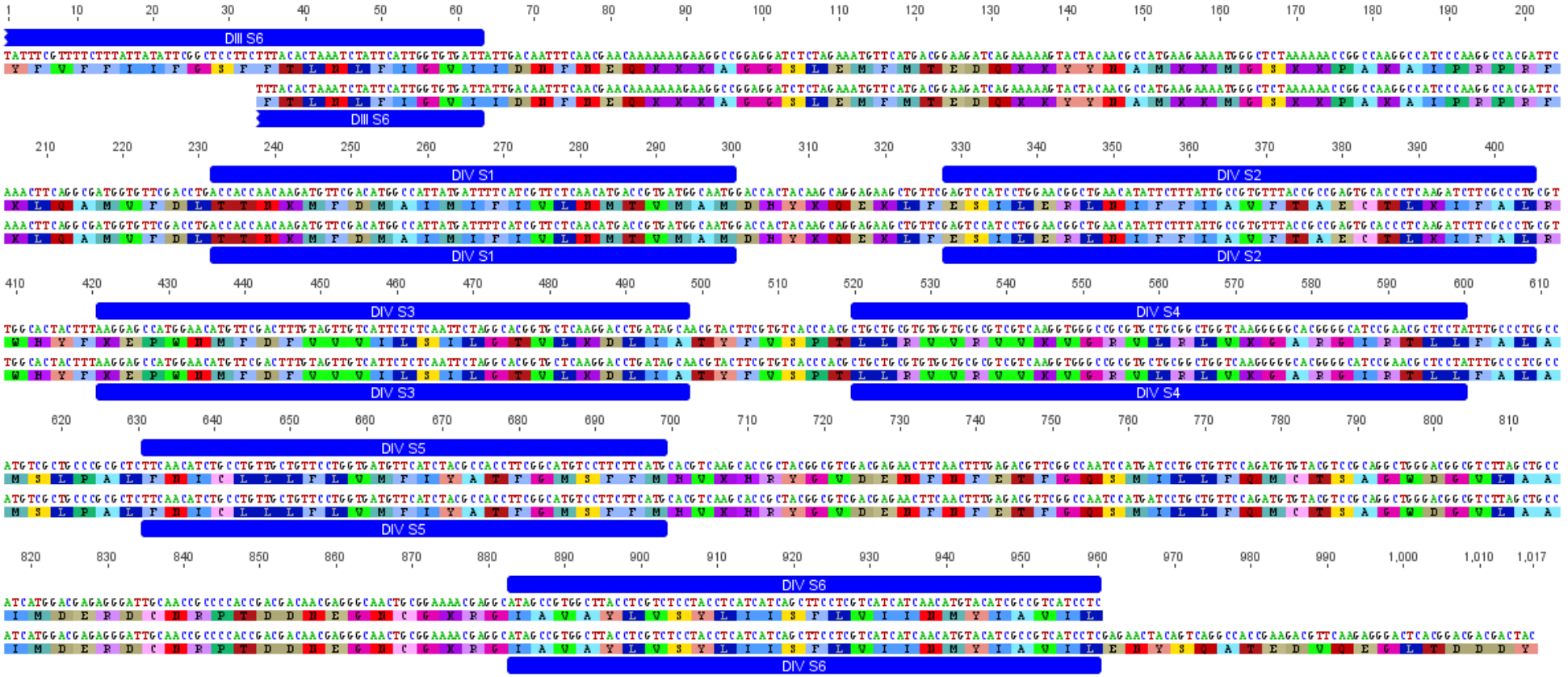

***P. ovis* DII**

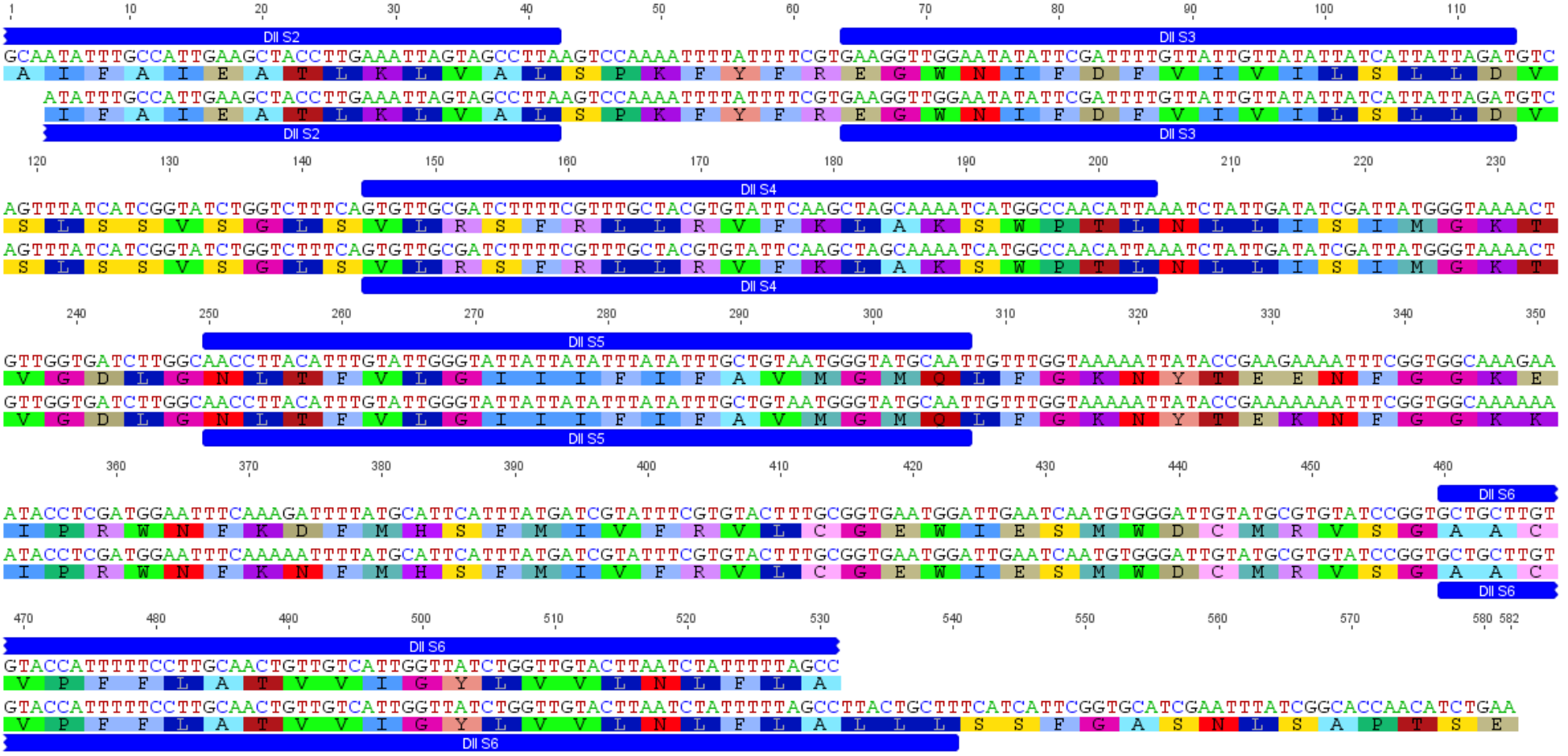

***P. ovis* DIII**

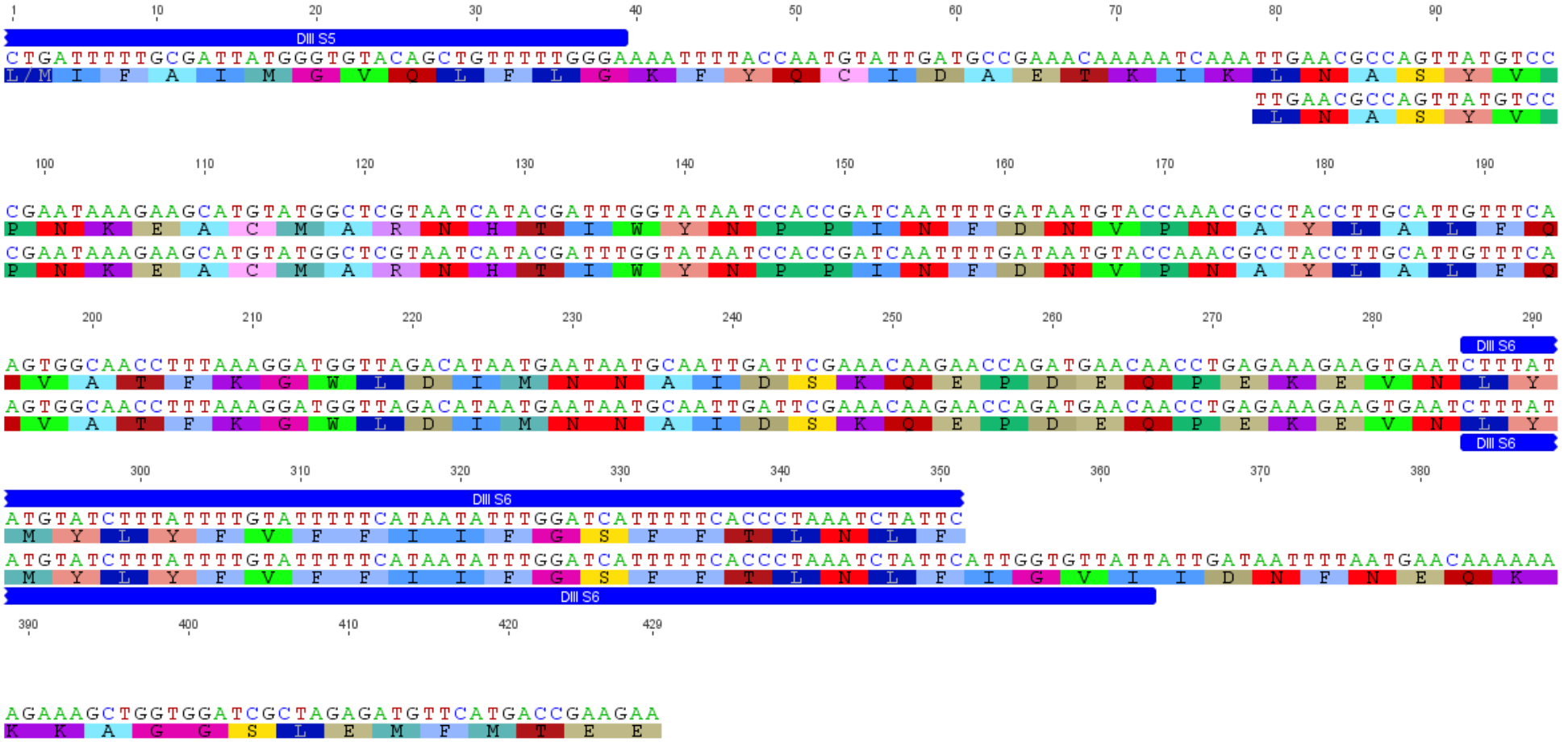

***P. ovis* DIV**

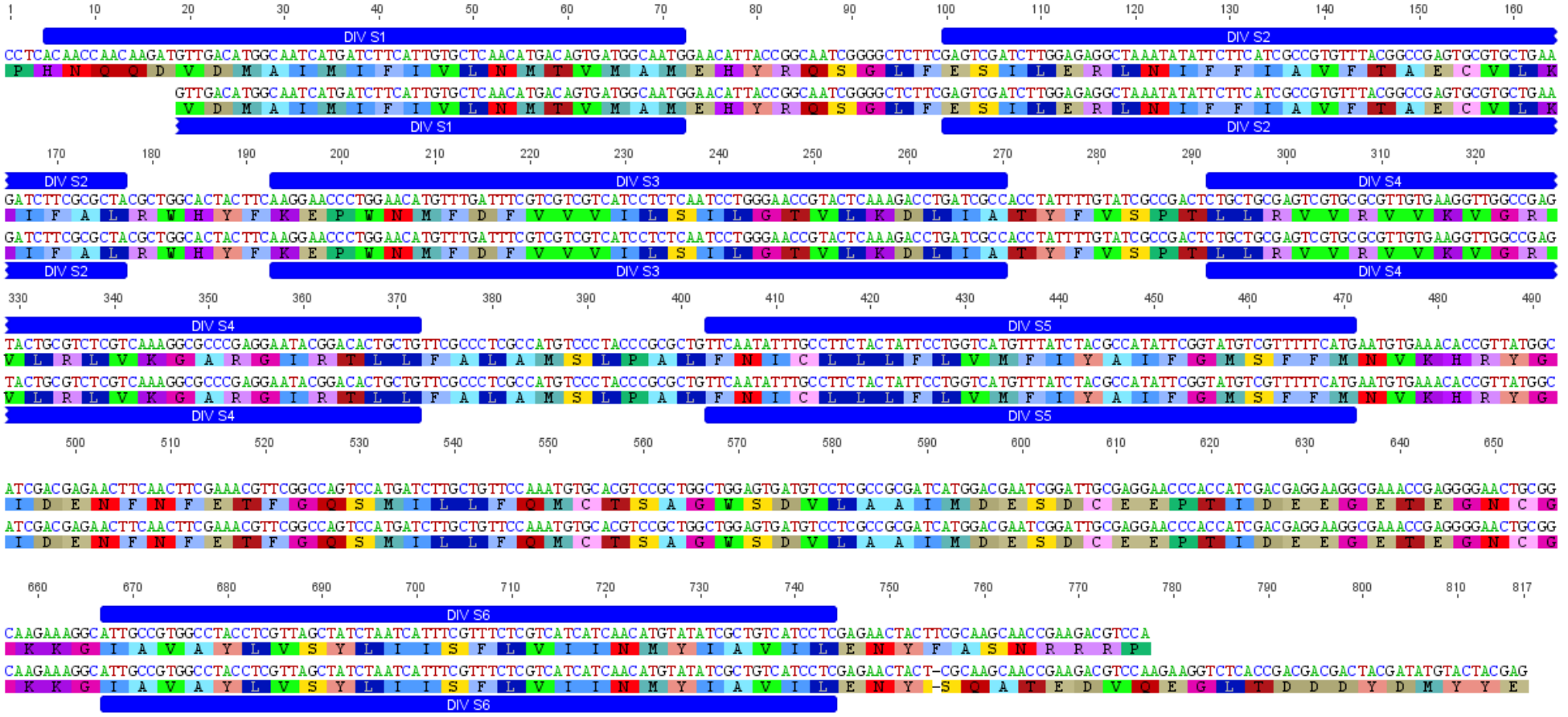

***R. sanguineus* DI**

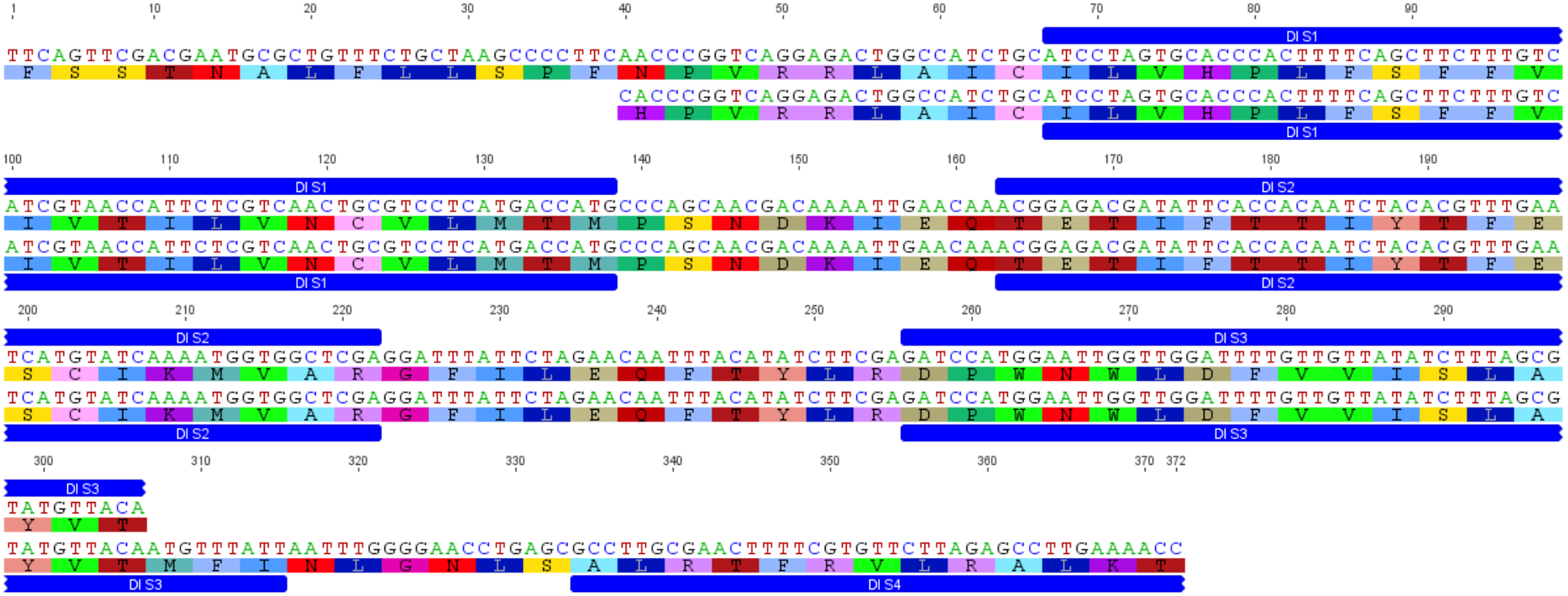

***R. sanguineus* DII**

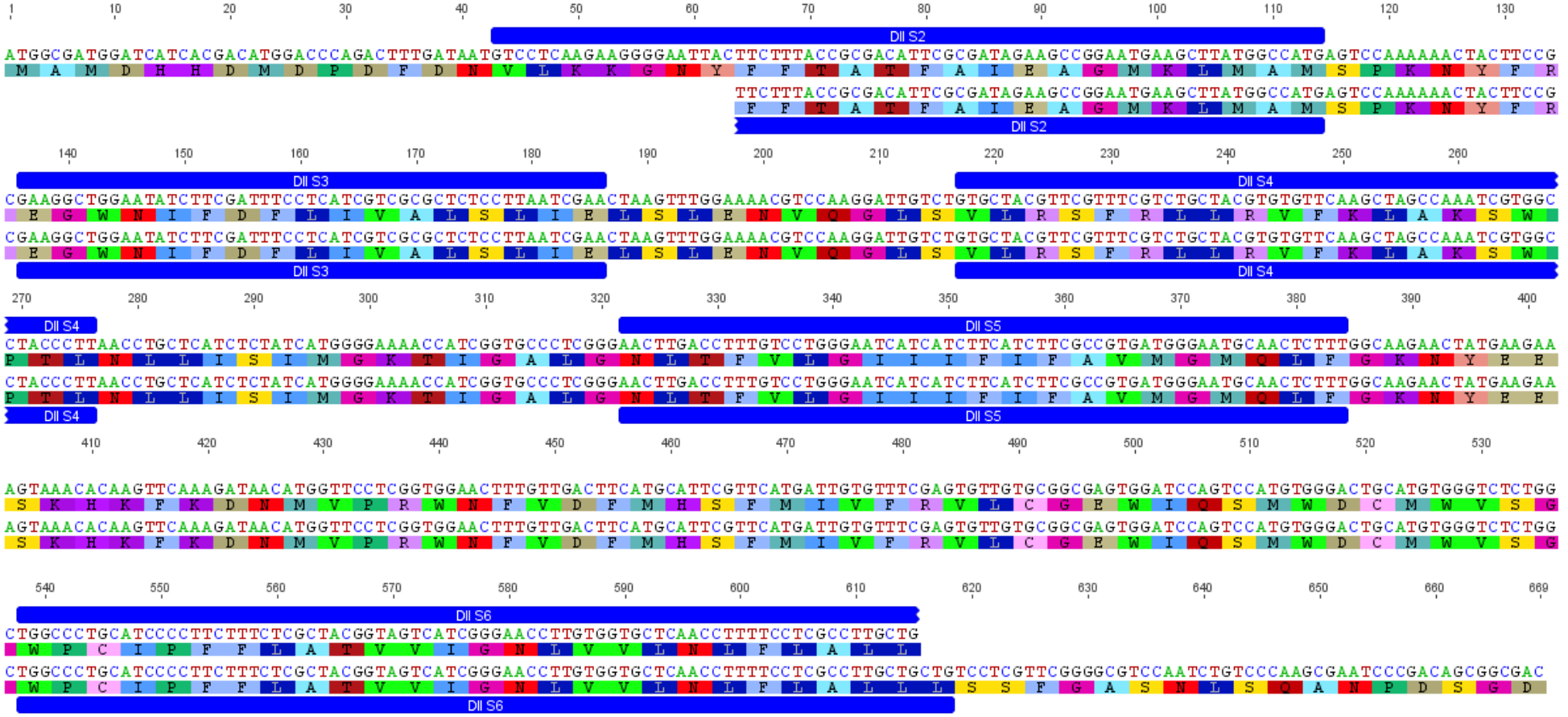

***R. sanguineus* DIII**

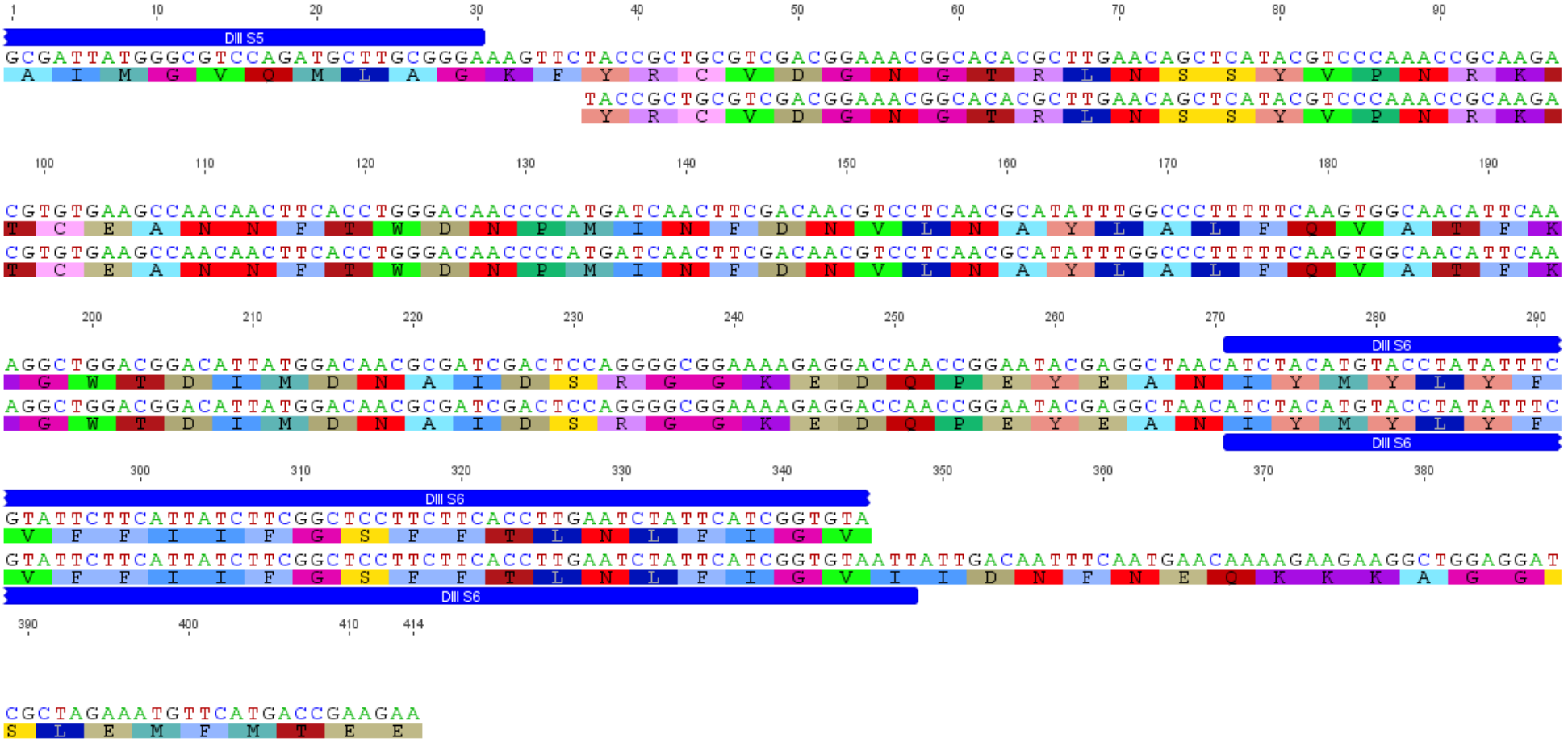

***R. sanguineus* DIV**

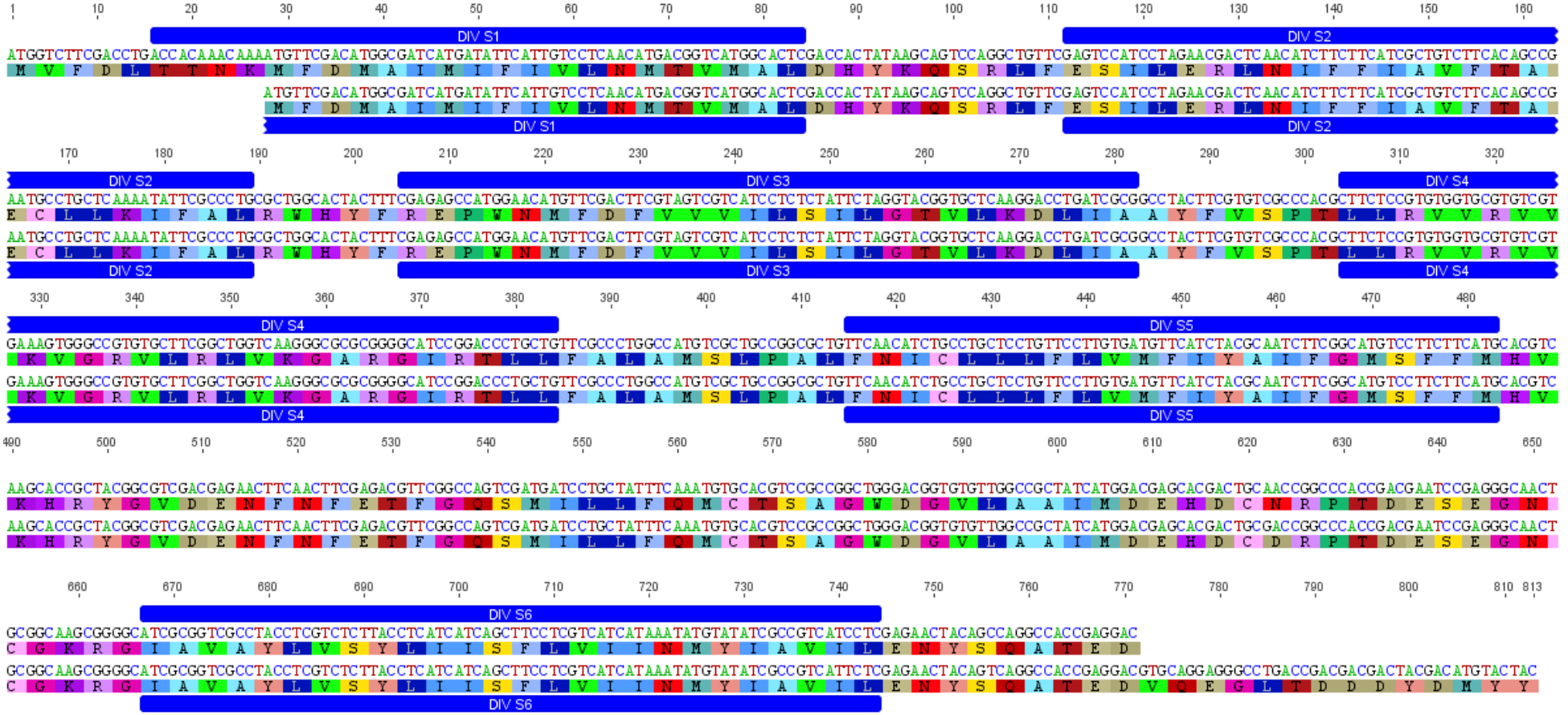

10.3 Appendix 3

The chimeric *R. microplus* and *D. melanogaster para* VGSC constructs *Chimera L2/L4* and *Chimera LC* in the expression vector pGH19 (Warmke *et al*., 1997). The construct includes the 5' and 3' untranslated *X. laevis* beta-globin sequences, indicated by purple bars, to stabilize heterologous cRNA expressed in *X. laevis* oocytes (Liu *et al*., 1996). Membrane-spanning segments and the domains to which they belong are indicated by blue bars, and were estimated using information from the *V. destructor* mite channel, as sequenced by Wang *et al* 2003. The 5' and 3' flanking *D. melanogaster para* regions are indicated by pale green bars, and the *R. microplus* VGSC domain-spanning insert is indicated by a pink bar. The position of a NotI restriction site in the native *R. microplus* channel is shown by a bright green bar, this site was removed by site directed mutagenesis to allow plasmid linearization for cRNA transcript preparation. The position of the stop codon in *Chimera LC* is indicated by a black bar.

Chimera L2/L4

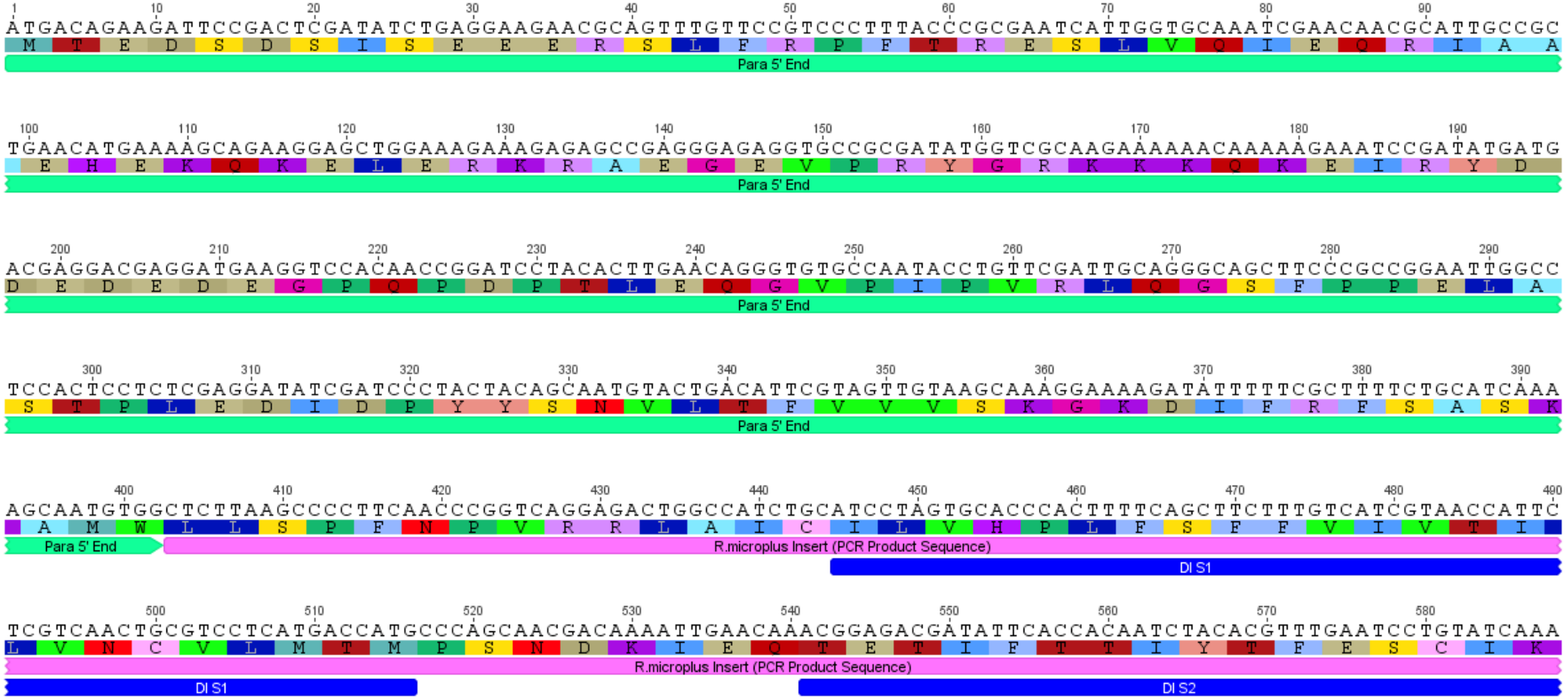

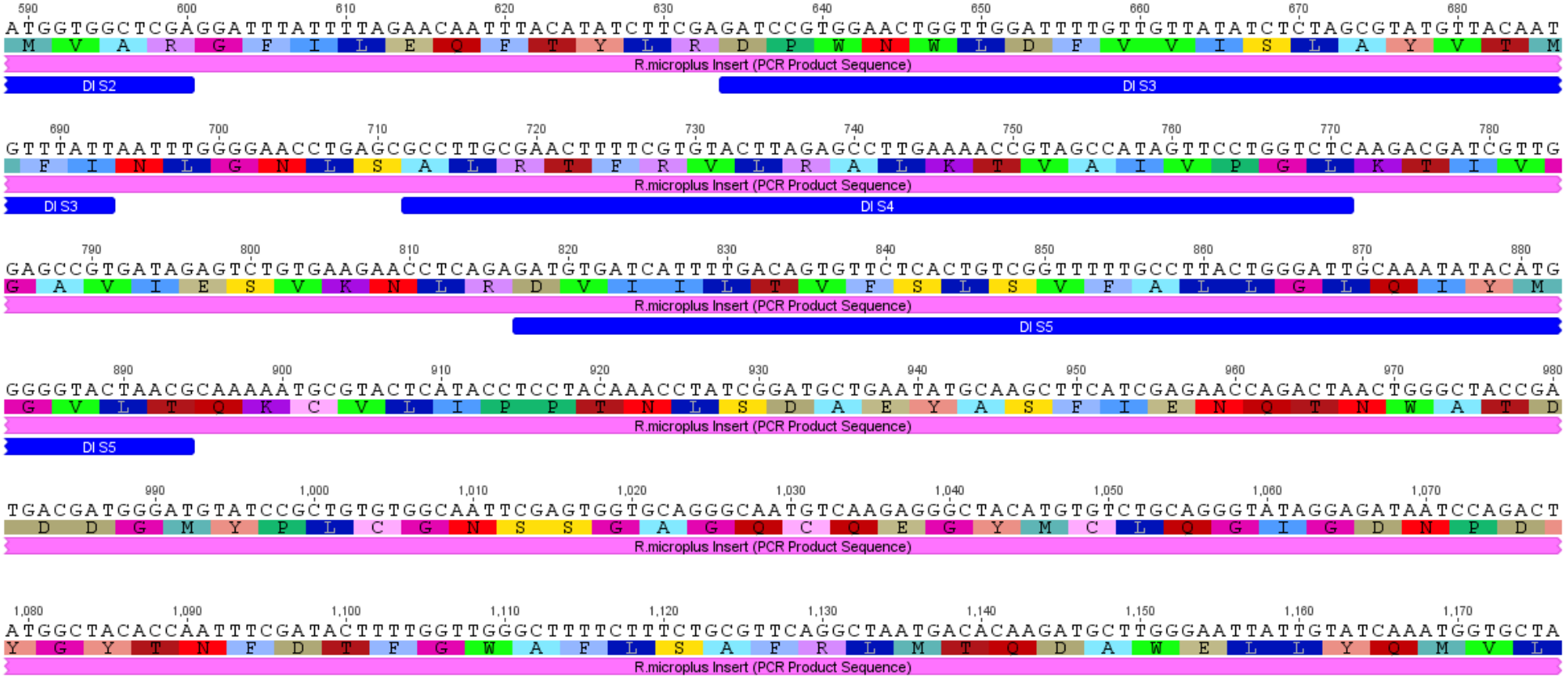
590 600 610 620 630 640 650 660 670 680
ATGGTGGCTCGAGGATTTATTTTAGAACAATTTACATATCTTCGAGATCCGTGGAACTGGTTGGATTTTGTTGTTATATCTCTAGCGTATGTTACAAT
M V A R G F I L E Q F T Y L R D P W N W L D F V V I S L A Y V T M
R.microplus Insert (PCR Product Sequence)
DI S2
DI S3
690 700 710 720 730 740 750 760 770 780
GTTTATTAATTTGGGGAACCTGAGCGCCTTGCGAACTTTTCGTGTACTTAGAGCCTTGAAAACCGTAGCCATAGTTCCTGGTCTCAAGACGATCGTTG
F I N L G N L S A L R T F R V L R A L K T V A I V P G L K T I V
R.microplus Insert (PCR Product Sequence)
DI S3
DI S4
790 800 810 820 830 840 850 860 870 880
GAGCCGTGATAGAGTCTGTGAAGAACCTCAGAGATGTGATCATTTTGACAGTGTTCTCACTGTCGGTTTTTGCCTTACTGGGATTGCAAATATACATG
G A V I E S V K N L R D V I I L T V F S L S V F A L L G L Q I Y M
R.microplus Insert (PCR Product Sequence)
DI S5
890 900 910 920 930 940 950 960 970 980
GGGGTACTAACGCAAAAATGCGTACTCATACCTCCTACAAACCTATCGGATGCTGAATATGCAAGCTTCATCGAGAACCAGACTAACTGGGCTACCGA
G V L T Q K C V L I P P T N L S D A E Y A S F I E N Q T N W A T D
R.microplus Insert (PCR Product Sequence)
DI S5
990 1,000 1,010 1,020 1,030 1,040 1,050 1,060 1,070
TGACGATGGGATGTATCCGCTGTGTGGCAATTCGAGTGGTGCAGGGCAATGTCAAGAGGGCTACATGTGTCTGCAGGGTATAGGAGATAATCCAGACT
D D G M Y P L C G N S S G A G Q C Q E G Y M C L Q G I G D N P D
R.microplus Insert (PCR Product Sequence)
1,080 1,090 1,100 1,110 1,120 1,130 1,140 1,150 1,160 1,170
ATGGCTACACCAATTTCGATACTTTTGGTTGGGCTTTTCTTTCTGCGTTCAGGCTAATGACACAAGATGCTTGGGAATTATTGTATCAAATGGTGCTA
Y G Y T N F D T F G W A F L S A F R L M T Q D A W E L L Y Q M V L
R.microplus Insert (PCR Product Sequence)

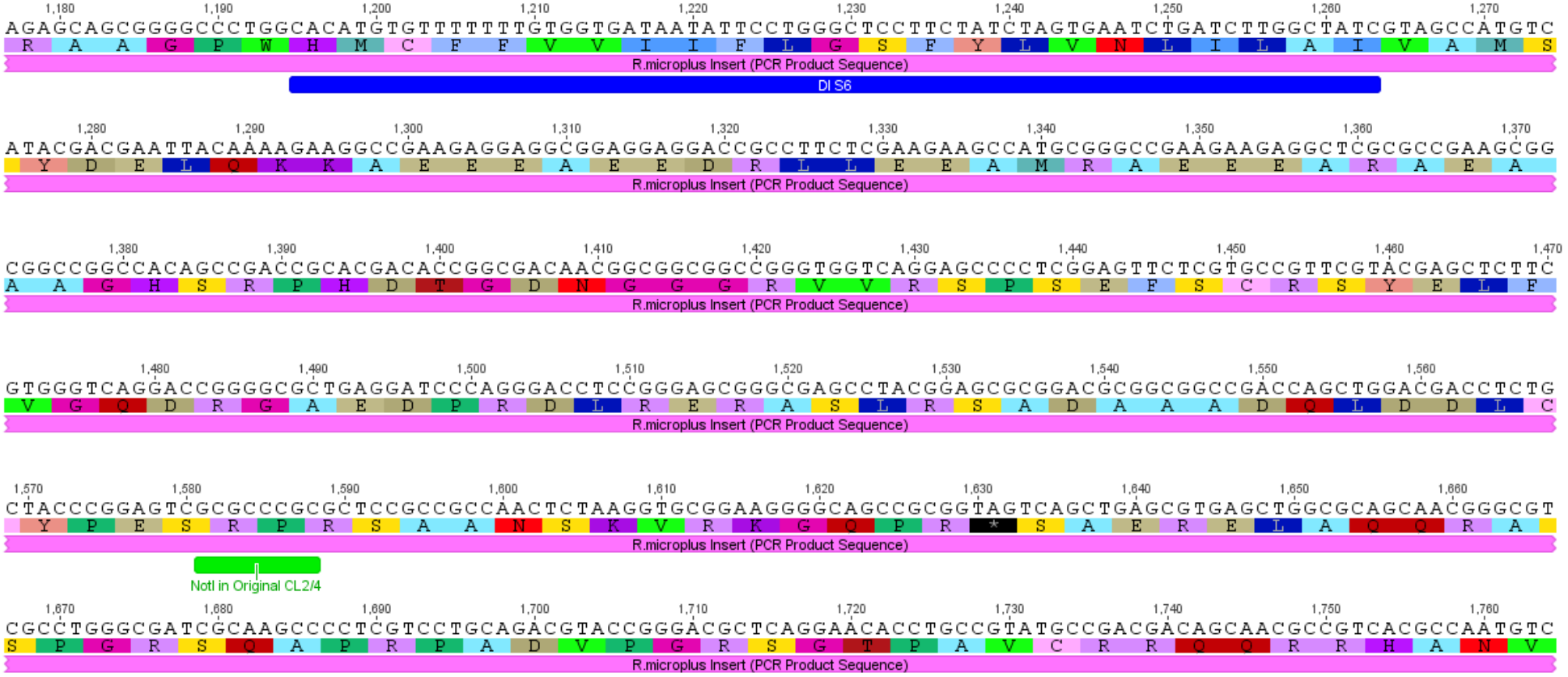
1,180 1,190 1,200 1,210 1,220 1,230 1,240 1,250 1,260 1,270
AGAGCAGCGGGGCCCTGGCACATGTGTTTTTTTGTGGTGATAATATTCCTGGGCTCCTTCTATCTAGTGAATCTGATCTTGGCTATCGTAGCCATGTC
R A A G P W H M C F F V V I I F L G S F Y L V N L I L A I V A M S
R.microplus Insert (PCR Product Sequence)
DI S6
1,280 1,290 1,300 1,310 1,320 1,330 1,340 1,350 1,360 1,370
ATACGACGAATTACAAAAGAAGGCCGAAGAGGAGGCGGAGGAGGACCGCCTTCTCGAAGAAGCCATGCGGGCCGAAGAAGAGGCTCGCGCCGAAGCGG
Y D E L Q K K A E E E A E E D R L L E E A M R A E E E A R A E A
R.microplus Insert (PCR Product Sequence)
1,380 1,390 1,400 1,410 1,420 1,430 1,440 1,450 1,460 1,470
CGGCCGGCCACAGCCGACCGCACGACACCGGCGACAACGGCGGCGGCCGGGTGGTCAGGAGCCCCTCGGAGTTCTCGTGCCGTTCGTACGAGCTCTTC
A A G H S R P H D T G D N G G G R V V R S P S E F S C R S Y E L F
R.microplus Insert (PCR Product Sequence)
1,480 1,490 1,500 1,510 1,520 1,530 1,540 1,550 1,560
GTGGGTCAGGACCGGGGCGCTGAGGATCCCAGGGACCTCCGGGAGCGGGCGAGCCTACGGAGCGCGGACGCGGCGGCCGACCAGCTGGACGACCTCTG
V G Q D R G A E D P R D L R E R A S L R S A D A A A D Q L D D L C
R.microplus Insert (PCR Product Sequence)
1,570 1,580 1,590 1,600 1,610 1,620 1,630 1,640 1,650 1,660
CTACCCGGAGTCGCGCCCGCGCTCCGCCGCCAACTCTAAGGTGCGGAAGGGGCAGCCGCGGTAGTCAGCTGAGCGTGAGCTGGCGCAGCAACGGGCGT
Y P E S R P R S A A N S K V R K G Q P R * S A E R E L A Q Q R A
R.microplus Insert (PCR Product Sequence)
NotI in Original CL2/4
1,670 1,680 1,690 1,700 1,710 1,720 1,730 1,740 1,750 1,760
CGCCTGGGCGATCGCAAGCCCCTCGTCCTGCAGACGTACCGGGACGCTCAGGAACACCTGCCGTATGCCGACGACAGCAACGCCGTCACGCCAATGTC
S P G R S Q A P R P A D V P G R S G T P A V C R R Q Q R R H A N V
R.microplus Insert (PCR Product Sequence)

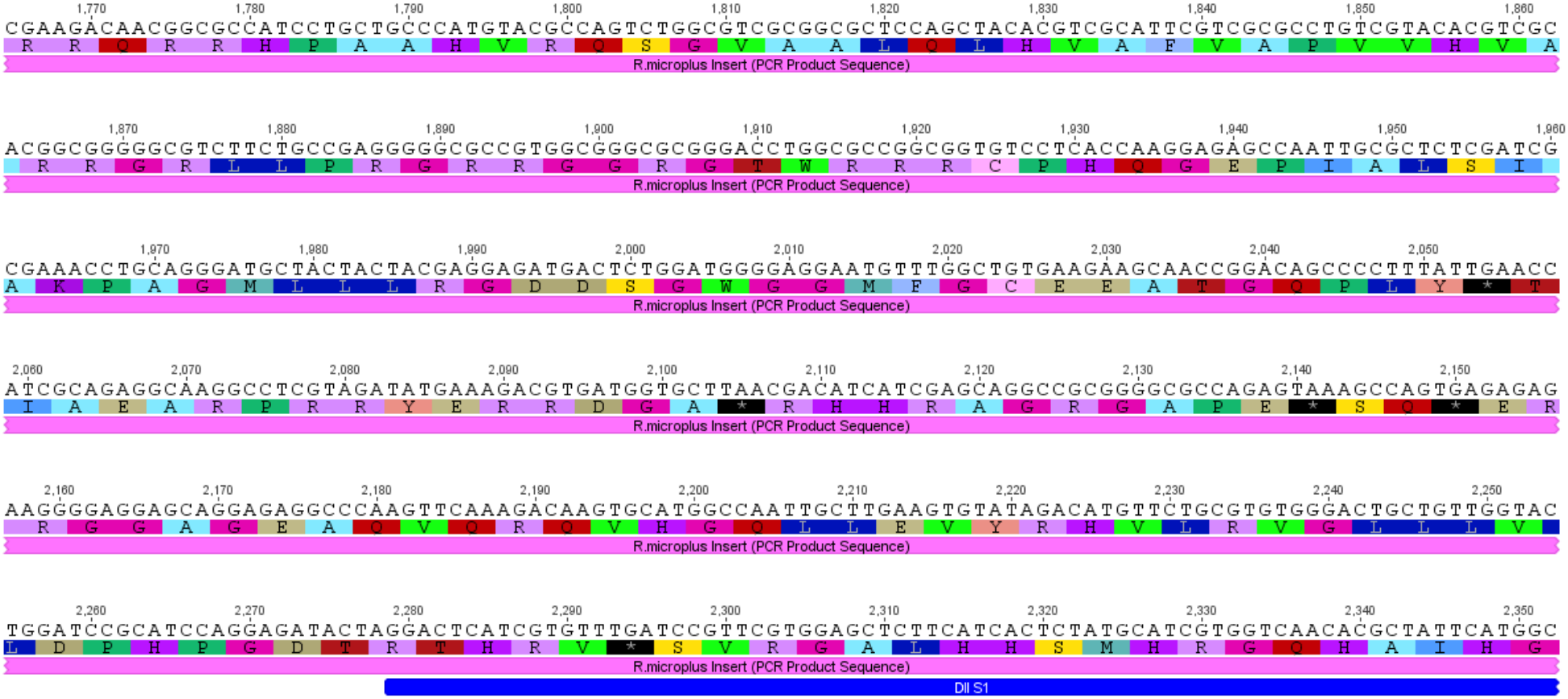
1,770 1,780 1,790 1,800 1,810 1,820 1,830 1,840 1,850 1,860
CGAAGACAACGGCGCCATCCTGCTGCCCATGTACGCCAGTCTGGCGTCGCGGCGCTCCAGCTACACGTCGCATTCGTCGCGCCTGTCGTACACGTCGC
R R Q R R H P A A H V R Q S G V A A L Q L H V A F V A P V V H V A
R.microplus Insert (PCR Product Sequence)
1,870 1,880 1,890 1,900 1,910 1,920 1,930 1,940 1,950 1,960
ACGGCGGGGGCGTCTTCTGCCGAGGGGGCGCCGTGGCGGGCGCGGGACCTGGCGCCGGCGGTGTCCTCACCAAGGAGAGCCAATTGCGCTCTCGATCG
R R G R L L P R G R R G G R G T W R R R C P H Q G E P I A L S I
R.microplus Insert (PCR Product Sequence)
1,970 1,980 1,990 2,000 2,010 2,020 2,030 2,040 2,050
CGAAACCTGCAGGGATGCTACTACTACGAGGAGATGACTCTGGATGGGGAGGAATGTTTGGCTGTGAAGAAGCAACCGGACAGCCCCTTTATTGAACC
A K P A G M L L L R G D D S G W G G M F G C E E A T G Q P L Y * T
R.microplus Insert (PCR Product Sequence)
2,060 2,070 2,080 2,090 2,100 2,110 2,120 2,130 2,140 2,150
ATCGCAGAGGCAAGGCCTCGTAGATATGAAAGACGTGATGGTGCTTAACGACATCATCGAGCAGGCCGCGGGGCGCCAGAGTAAAGCCAGTGAGAGAG
I A E A R P R R Y E R R D G A * R H H R A G R G A P E * S Q * E R
R.microplus Insert (PCR Product Sequence)
2,160 2,170 2,180 2,190 2,200 2,210 2,220 2,230 2,240 2,250
AAGGGGAGGAGCAGGAGAGGCCCAAGTTCAAAGACAAGTGCATGGCCAATTGCTTGAAGTGTATAGACATGTTCTGCGTGTGGGACTGCTGTTGGTAC
R G G A G E A Q V Q R Q V H G Q L L E V Y R H V L R V G L L L V
R.microplus Insert (PCR Product Sequence)
2,260 2,270 2,280 2,290 2,300 2,310 2,320 2,330 2,340 2,350
TGGATCCGCATCCAGGAGATACTAGGACTCATCGTGTTTGATCCGTTCGTGGAGCTCTTCATCACTCTATGCATCGTGGTCAACACGCTATTCATGGC
L D P H P G D T R T H R V * S V R G A L H H S M H R G Q H A I H G
R.microplus Insert (PCR Product Sequence)
DII S1

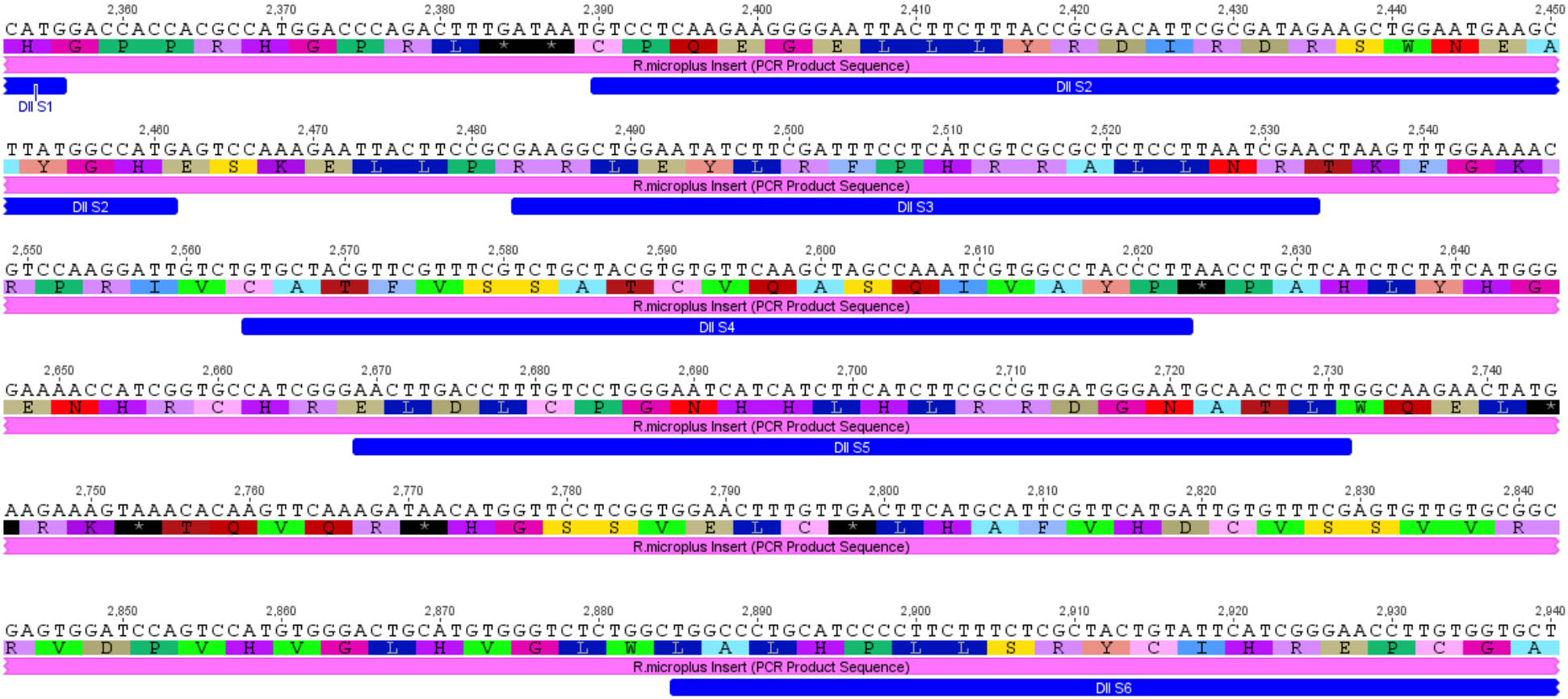
2,360 2,370 2,380 2,390 2,400 2,410 2,420 2,430 2,440 2,450
CATGGACCACCACGCCATGGACCCAGACTTTGATAATGTCCTCAAGAAGGGGAATTACTTCTTTACCGCGACATTCGCGATAGAAGCTGGAATGAAGC
H G P P R H G P R L * * C P Q E G E L L L Y R D I R D R S W N E A
R.microplus Insert (PCR Product Sequence)
DII S1
DII S2
2,460 2,470 2,480 2,490 2,500 2,510 2,520 2,530 2,540
TTATGGCCATGAGTCCAAAGAATTACTTCCGCGAAGGCTGGAATATCTTCGATTTCCTCATCGTCGCGCTCTCCTTAATCGAACTAAGTTTGGAAAAC
Y G H E S K E L L P R R L E Y L R F P H R R A L L N R T K F G K
R.microplus Insert (PCR Product Sequence)
DII S2
DII S3
2,550 2,560 2,570 2,580 2,590 2,600 2,610 2,620 2,630 2,640
GTCCAAGGATTGTCTGTGCTACGTTCGTTTCGTCTGCTACGTGTGTTCAAGCTAGCCAAATCGTGGCCTACCCTTAACCTGCTCATCTCTATCATGGG
R P R I V C A T F V S S A T C V Q A S Q I V A Y P * P A H L Y H G
R.microplus Insert (PCR Product Sequence)
DII S4
2,650 2,660 2,670 2,680 2,690 2,700 2,710 2,720 2,730 2,740
GAAAACCATCGGTGCCATCGGGAACTTGACCTTTGTCCTGGGAATCATCATCTTCATCTTCGCCGTGATGGGAATGCAACTCTTTGGCAAGAACTATG
E N H R C H R E L D L C P G N H H L H L R R D G N A T L W Q E L *
R.microplus Insert (PCR Product Sequence)
DII S5
2,750 2,760 2,770 2,780 2,790 2,800 2,810 2,820 2,830 2,840
AAGAAAGTAAACACAAGTTCAAAGATAACATGGTTCCTCGGTGGAACTTTGTTGACTTCATGCATTCGTTCATGATTGTGTTTCGAGTGTTGTGCGGC
R K * T Q V Q R * H G S S V E L C * L H A F V H D C V S S V V R
R.microplus Insert (PCR Product Sequence)
2,850 2,860 2,870 2,880 2,890 2,900 2,910 2,920 2,930 2,940
GAGTGGATCCAGTCCATGTGGGACTGCATGTGGGTCTCTGGCTGGCCCTGCATCCCCTTCTTTCTCGCTACTGTATTCATCGGGAACCTTGTGGTGCT
R V D P V H V G L H V G L W L A L H P L L S R Y C I H R E P C G A
R.microplus Insert (PCR Product Sequence)
DII S6

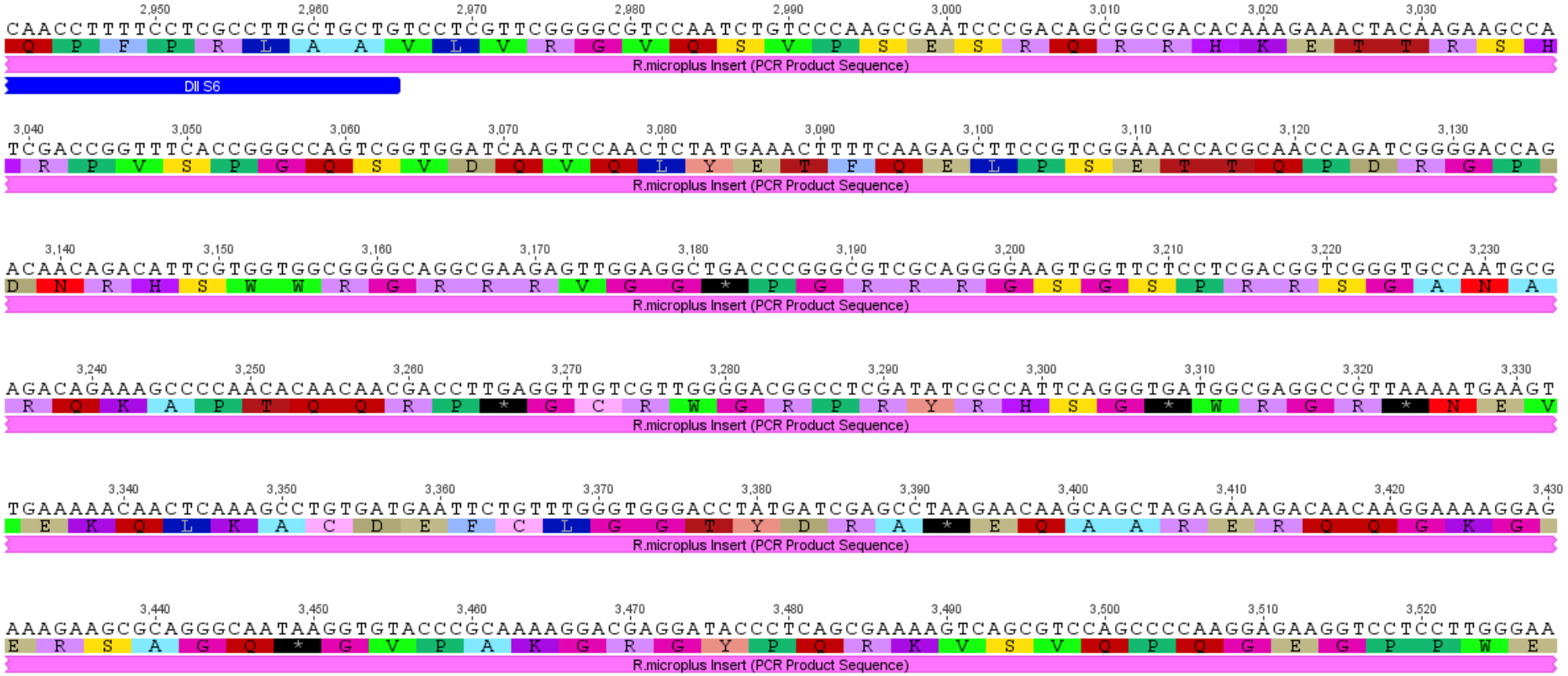
2,950 2,960 2,970 2,980 2,990 3,000 3,010 3,020 3,030
CAACCTTTTCCTCGCCTTGCTGCTGTCCTCGTTCGGGGCGTCCAATCTGTCCCAAGCGAATCCCGACAGCGGCGACACAAAGAAACTACAAGAAGCCA
Q P F P R L A A V L V R G V Q S V P S E S R Q R R H K E T T R S H
R.microplus Insert (PCR Product Sequence)
DII S6
3,040 3,050 3,060 3,070 3,080 3,090 3,100 3,110 3,120 3,130
TCGACCGGTTTCACCGGGCCAGTCGGTGGATCAAGTCCAACTCTATGAAACTTTTCAAGAGCTTCCGTCGGAAACCACGCAACCAGATCGGGGACCAG
R P V S P G Q S V D Q V Q L Y E T F Q E L P S E T T Q P D R G P
R.microplus Insert (PCR Product Sequence)
3,140 3,150 3,160 3,170 3,180 3,190 3,200 3,210 3,220 3,230
ACAACAGACATTCGTGGTGGCGGGGCAGGCGAAGAGTTGGAGGCTGACCCGGGCGTCGCAGGGGAAGTGGTTCTCCTCGACGGTCGGGTGCCAATGCG
D N R H S W W R G R R R V G G * P G R R R G S G S P R R S G A N A
R.microplus Insert (PCR Product Sequence)
3,240 3,250 3,260 3,270 3,280 3,290 3,300 3,310 3,320 3,330
AGACAGAAAGCCCCAACACAACAACGACCTTGAGGTTGTCGTTGGGGACGGCCTCGATATCGCCATTCAGGGTGATGGCGAGGCCGTTAAAATGAAGT
R Q K A P T Q Q R P * G C R W G R P R Y R H S G * W R G R * N E V
R.microplus Insert (PCR Product Sequence)
3,340 3,350 3,360 3,370 3,380 3,390 3,400 3,410 3,420 3,430
TGAAAAACAACTCAAAGCCTGTGATGAATTCTGTTTGGGTGGGACCTATGATCGAGCCTAAGAACAAGCAGCTAGAGAAAGACAACAAGGAAAAGGAG
E K Q L K A C D E F C L G G T Y D R A * E Q A A R E R Q Q G K G
R.microplus Insert (PCR Product Sequence)
3,440 3,450 3,460 3,470 3,480 3,490 3,500 3,510 3,520
AAAGAAGCGCAGGGCAATAAGGTGTACCCGCAAAAGGACGAGGATACCCTCAGCGAAAAGTCAGCGTCCAGCCCCAAGGAGAAGGTCCTCCTTGGGAA
E R S A G Q * G V P A K G R G Y P Q R K V S V Q P Q G E G P P W E
R.microplus Insert (PCR Product Sequence)

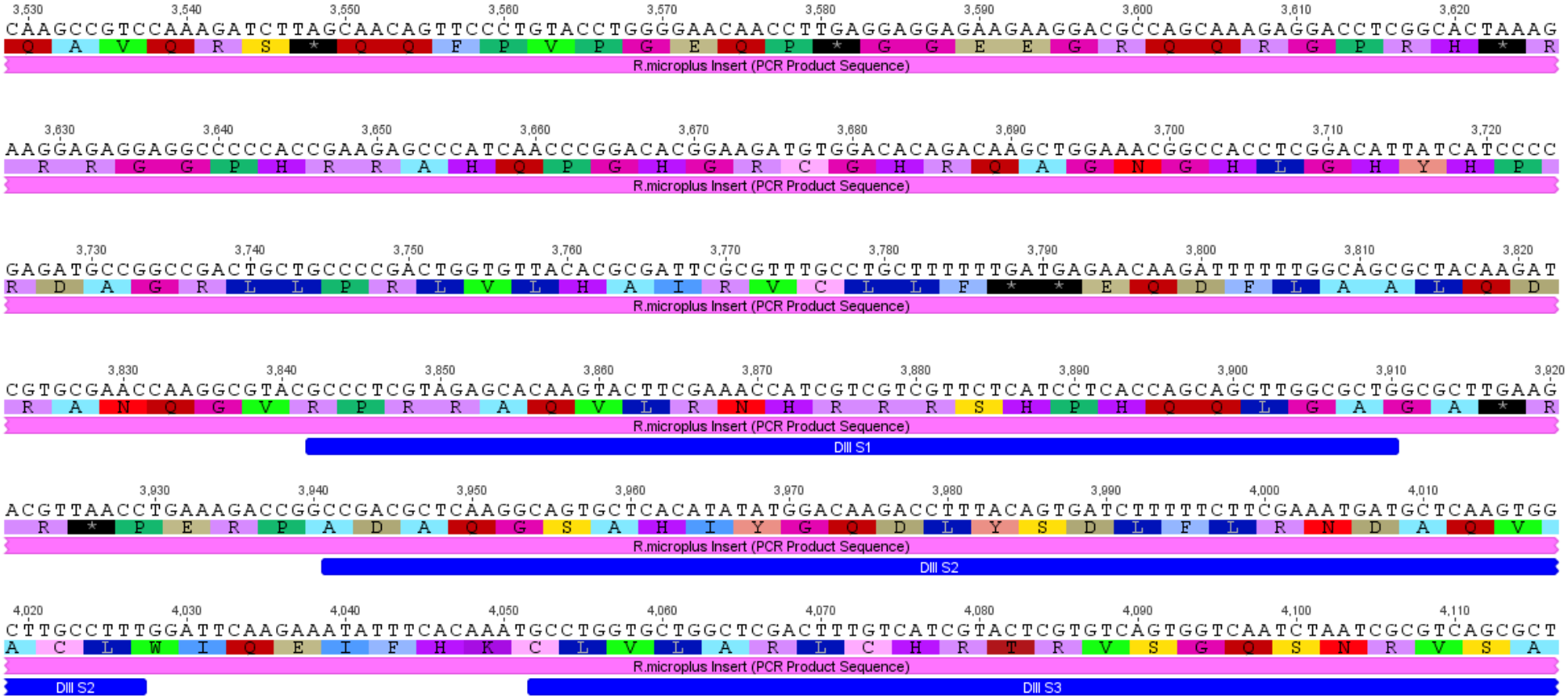
3,530 3,540 3,550 3,560 3,570 3,580 3,590 3,600 3,610 3,620
CAAGCCGTCCAAAGATCTTAGCAACAGTTCCCTGTACCTGGGGAACAACCTTGAGGAGGAGAAGAAGGACGCCAGCAAAGAGGACCTCGGCACTAAAG
Q A V Q R S * Q Q F P V P G E Q P * G G E E G R Q Q R G P R H * R
R.microplus Insert (PCR Product Sequence)
3,630 3,640 3,650 3,660 3,670 3,680 3,690 3,700 3,710 3,720
AAGGAGAGGAGGCCCCCACCGAAGAGCCCATCAACCCGGACACGGAAGATGTGGACACAGACAAGCTGGAAACGGCCACCTCGGACATTATCATCCCC
R R G G P H R R A H Q P G H G R C G H R Q A G N G H L G H Y H P
R.microplus Insert (PCR Product Sequence)
3,730 3,740 3,750 3,760 3,770 3,780 3,790 3,800 3,810 3,820
GAGATGCCGGCCGACTGCTGCCCCGACTGGTGTTACACGCGATTCGCGTTTGCCTGCTTTTTTGATGAGAACAAGATTTTTTGGCAGCGCTACAAGAT
R D A G R L L P R L V L H A I R V C L L F * * E Q D F L A A L Q D
R.microplus Insert (PCR Product Sequence)
3,830 3,840 3,850 3,860 3,870 3,880 3,890 3,900 3,910 3,920
CGTGCGAACCAAGGCGTACGCCCTCGTAGAGCACAAGTACTTCGAAACCATCGTCGTCGTTCTCATCCTCACCAGCAGCTTGGCGCTGGCGCTTGAAG
R A N Q G V R P R R A Q V L R N H R R R S H P H Q Q L G A G A * R
R.microplus Insert (PCR Product Sequence)
DIII S1
3,930 3,940 3,950 3,960 3,970 3,980 3,990 4,000 4,010
ACGTTAACCTGAAAGACCGGCCGACGCTCAAGGCAGTGCTCACATATATGGACAAGACCTTTACAGTGATCTTTTTCTTCGAAATGATGCTCAAGTGG
R * P E R P A D A Q G S A H I Y G Q D L Y S D L F L R N D A Q V
R.microplus Insert (PCR Product Sequence)
DIII S2
4,020 4,030 4,040 4,050 4,060 4,070 4,080 4,090 4,100 4,110
CTTGCCTTTGGATTCAAGAAATATTTCACAAATGCCTGGTGCTGGCTCGACTTTGTCATCGTACTCGTGTCAGTGGTCAATCTAATCGCGTCAGCGCT
A C L W I Q E I F H K C L V L A R L C H R T R V S G Q S N R V S A
R.microplus Insert (PCR Product Sequence)
DIII S2
DIII S3

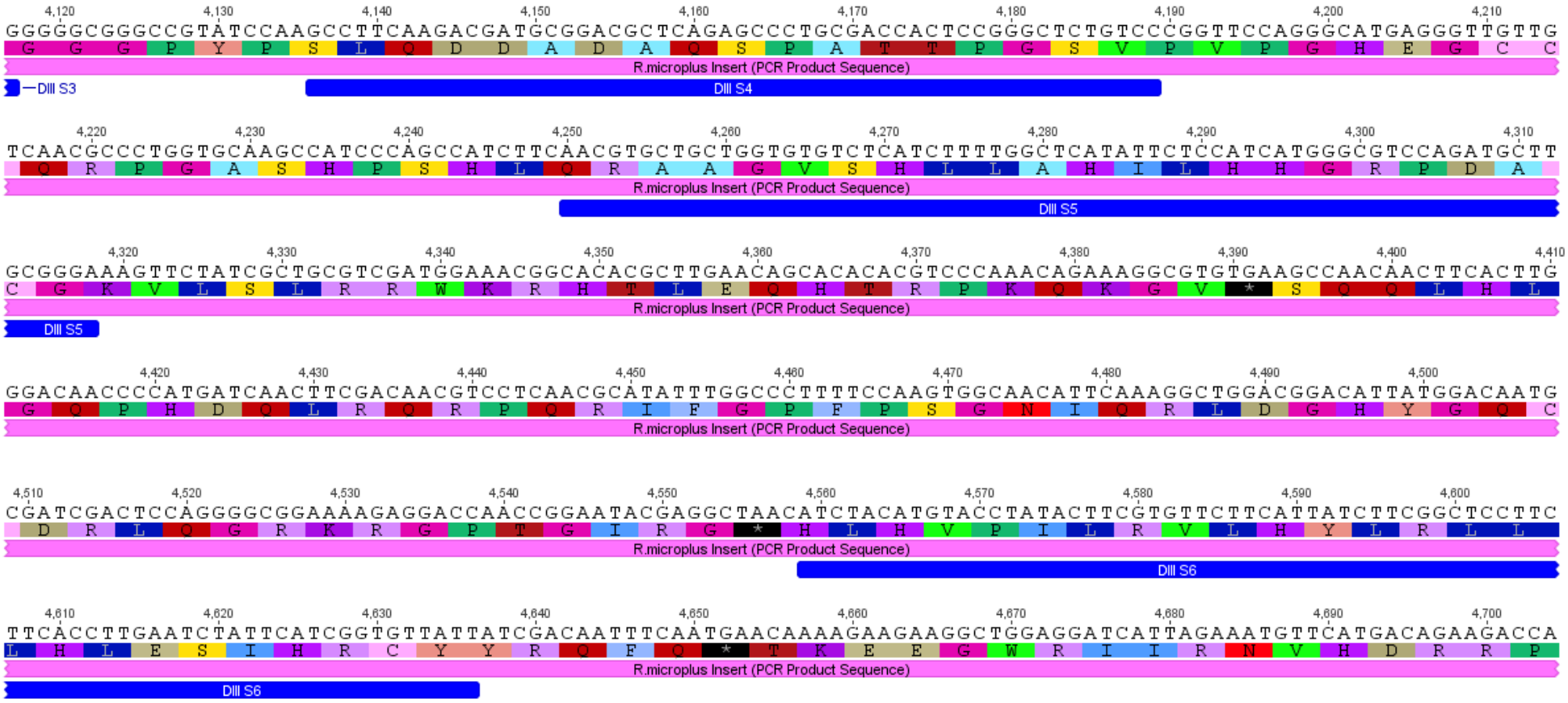
4,120 4,130 4,140 4,150 4,160 4,170 4,180 4,190 4,200 4,210
GGGGGCGGGCCGTATCCAAGCCTTCAAGACGATGCGGACGCTCAGAGCCCTGCGACCACTCCGGGCTCTGTCCCGGTTCCAGGGCATGAGGGTTGTTG
G G G P Y P S L Q D D A D A Q S P A T T P G S V P V P G H E G C C
R.microplus Insert (PCR Product Sequence)
DIII S3
DIII S4
4,220 4,230 4,240 4,250 4,260 4,270 4,280 4,290 4,300 4,310
TCAACGCCCTGGTGCAAGCCATCCCAGCCATCTTCAACGTGCTGCTGGTGTGTCTCATCTTTTGGCTCATATTCTCCATCATGGGCGTCCAGATGCTT
Q R P G A S H P S H L Q R A A G V S H L L A H I L H H G R P D A
R.microplus Insert (PCR Product Sequence)
DIII S5
4,320 4,330 4,340 4,350 4,360 4,370 4,380 4,390 4,400 4,410
GCGGGAAAGTTCTATCGCTGCGTCGATGGAAACGGCACACGCTTGAACAGCACACACGTCCCAAACAGAAAGGCGTGTGAAGCCAACAACTTCACTTG
C G K V L S L R R W K R H T L E Q H T R P K Q K G V * S Q Q L H L
R.microplus Insert (PCR Product Sequence)
DIII S5
4,420 4,430 4,440 4,450 4,460 4,470 4,480 4,490 4,500
GGACAACCCCATGATCAACTTCGACAACGTCCTCAACGCATATTTGGCCCTTTTCCAAGTGGCAACATTCAAAGGCTGGACGGACATTATGGACAATG
G Q P H D Q L R Q R P Q R I F G P F P S G N I Q R L D G H Y G Q C
R.microplus Insert (PCR Product Sequence)
4,510 4,520 4,530 4,540 4,550 4,560 4,570 4,580 4,590 4,600
CGATCGACTCCAGGGGCGGAAAAGAGGACCAACCGGAATACGAGGCTAACATCTACATGTACCTATACTTCGTGTTCTTCATTATCTTCGGCTCCTTC
D R L Q G R K R G P T G I R G * H L H V P I L R V L H Y L R L L
R.microplus Insert (PCR Product Sequence)
DIII S6
4,610 4,620 4,630 4,640 4,650 4,660 4,670 4,680 4,690 4,700
TTCACCTTGAATCTATTCATCGGTGTTATTATCGACAATTTCAATGAACAAAAGAAGAAGGCTGGAGGATCATTAGAAATGTTCATGACAGAAGACCA
L H L E S I H R C Y Y R Q F Q * T K E E G W R I I R N V H D R R P
R.microplus Insert (PCR Product Sequence)
DIII S6

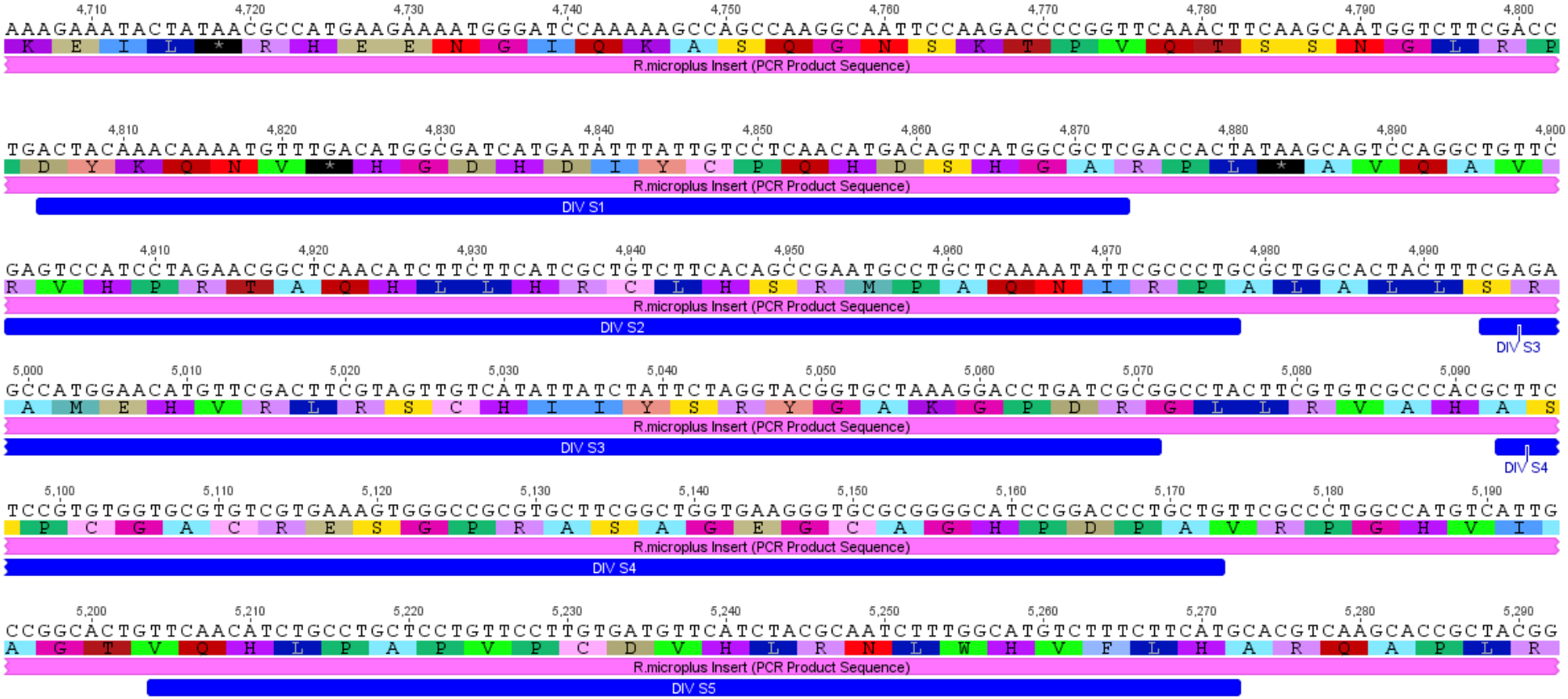
4,710 4,720 4,730 4,740 4,750 4,760 4,770 4,780 4,790 4,800
AAAGAAATACTATAACGCCATGAAGAAAATGGGATCCAAAAAGCCAGCCAAGGCAATTCCAAGACCCCGGTTCAAACTTCAAGCAATGGTCTTCGACC
K E I L * R H E E N G I Q K A S Q G N S K T P V Q T S S N G L R P
R.microplus Insert (PCR Product Sequence)
4,810 4,820 4,830 4,840 4,850 4,860 4,870 4,880 4,890 4,900
TGACTACAAACAAAATGTTTGACATGGCGATCATGATATTTATTGTCCTCAACATGACAGTCATGGCGCTCGACCACTATAAGCAGTCCAGGCTGTTC
D Y K Q N V * H G D H D I Y C P Q H D S H G A R P L * A V Q A V
R.microplus Insert (PCR Product Sequence)
DIV S1
4,910 4,920 4,930 4,940 4,950 4,960 4,970 4,980 4,990
GAGTCCATCCTAGAACGGCTCAACATCTTCTTCATCGCTGTCTTCACAGCCGAATGCCTGCTCAAAATATTCGCCCTGCGCTGGCACTACTTTCGAGA
R V H P R T A Q H L L H R C L H S R M P A Q N I R P A L A L L S R
R.microplus Insert (PCR Product Sequence)
DIV S2
DIV S3
5,000 5,010 5,020 5,030 5,040 5,050 5,060 5,070 5,080 5,090
GCCATGGAACATGTTCGACTTCGTAGTTGTCATATTATCTATTCTAGGTACGGTGCTAAAGGACCTGATCGCGGCCTACTTCGTGTCGCCCACGCTTC
A M E H V R L R S C H I I Y S R Y G A K G P D R G L L R V A H A S
R.microplus Insert (PCR Product Sequence)
DIV S3
DIV S4
5,100 5,110 5,120 5,130 5,140 5,150 5,160 5,170 5,180 5,190
TCCGTGTGGTGCGTGTCGTGAAAGTGGGCCGCGTGCTTCGGCTGGTGAAGGGTGCGCGGGGCATCCGGACCCTGCTGTTCGCCCTGGCCATGTCATTG
P C G A C R E S G P R A S A G E G C A G H P D P A V R P G H V I
R.microplus Insert (PCR Product Sequence)
DIV S4
5,200 5,210 5,220 5,230 5,240 5,250 5,260 5,270 5,280 5,290
CCGGCACTGTTCAACATCTGCCTGCTCCTGTTCCTTGTGATGTTCATCTACGCAATCTTTGGCATGTCTTTCTTCATGCACGTCAAGCACCGCTACGG
A G T V Q H L P A P V P C D V H L R N L W H V F L H A R Q A P L R
R.microplus Insert (PCR Product Sequence)
DIV S5

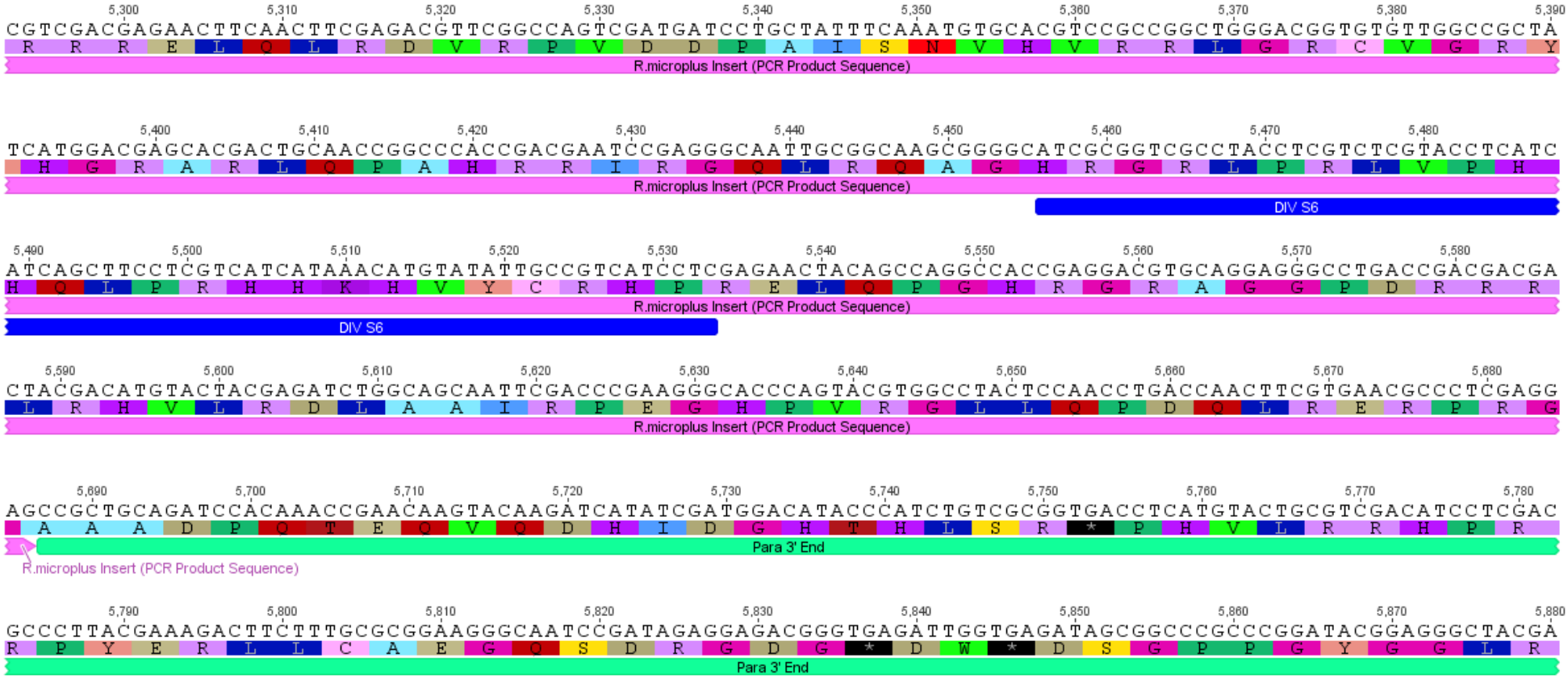
5,300 5,310 5,320 5,330 5,340 5,350 5,360 5,370 5,380 5,390
CGTCGACGAGAACTTCAACTTCGAGACGTTCGGCCAGTCGATGATCCTGCTATTTCAAATGTGCACGTCCGCCGGCTGGGACGGTGTGTTGGCCGCTA
R R R E L Q L R D V R P V D D P A I S N V H V R R L G R C V G R Y
R.microplus Insert (PCR Product Sequence)
5,400 5,410 5,420 5,430 5,440 5,450 5,460 5,470 5,480
TCATGGACGAGCACGACTGCAACCGGCCCACCGACGAATCCGAGGGCAATTGCGGCAAGCGGGGCATCGCGGTCGCCTACCTCGTCTCGTACCTCATC
H G R A R L Q P A H R R I R G Q L R Q A G H R G R L P R L V P H
R.microplus Insert (PCR Product Sequence)
DIV S6
5,490 5,500 5,510 5,520 5,530 5,540 5,550 5,560 5,570 5,580
ATCAGCTTCCTCGTCATCATAAACATGTATATTGCCGTCATCCTCGAGAACTACAGCCAGGCCACCGAGGACGTGCAGGAGGCCTGACCGACGACGA
H Q L P R H H K H V Y C R H P R E L Q P G H R G R A G G P D R R R
R.microplus Insert (PCR Product Sequence)
DIV S6
5,590 5,600 5,610 5,620 5,630 5,640 5,650 5,660 5,670 5,680
CTACGACATGTACTACGAGATCTGGCAGCAATTCGACCCGAAGGGCACCCAGTACGTGGCCTACTCCAACCTGACCAACTTCGTGAACGCCCTCGAGG
L R H V L R D L A A I R P E G H P V R G L L Q P D Q L R E R P R G
R.microplus Insert (PCR Product Sequence)
5,690 5,700 5,710 5,720 5,730 5,740 5,750 5,760 5,770 5,780
AGCCGCTGCAGATCCACAAACCGAACAAGTACAAGATCATATCGATGGACATACCCATCTGTCGCGGTGACCTCATGTACTGCGTCGACATCCTCGAC
A A A D P Q T E Q V Q D H I D G H T H L S R * P H V L R R H P R
Para 3' End
R.microplus Insert (PCR Product Sequence)
5,790 5,800 5,810 5,820 5,830 5,840 5,850 5,860 5,870 5,880
GCCCTTACGAAAGACTTCTTTGCGCGGAAGGGCAATCCGATAGAGGAGACGGGTGAGATTGGTGAGATAGCGGCCCGCCCGGATACGGAGGGCTACGA
R P Y E R L L C A E G Q S D R G D G * D W * D S G P P G Y G G L R
Para 3' End

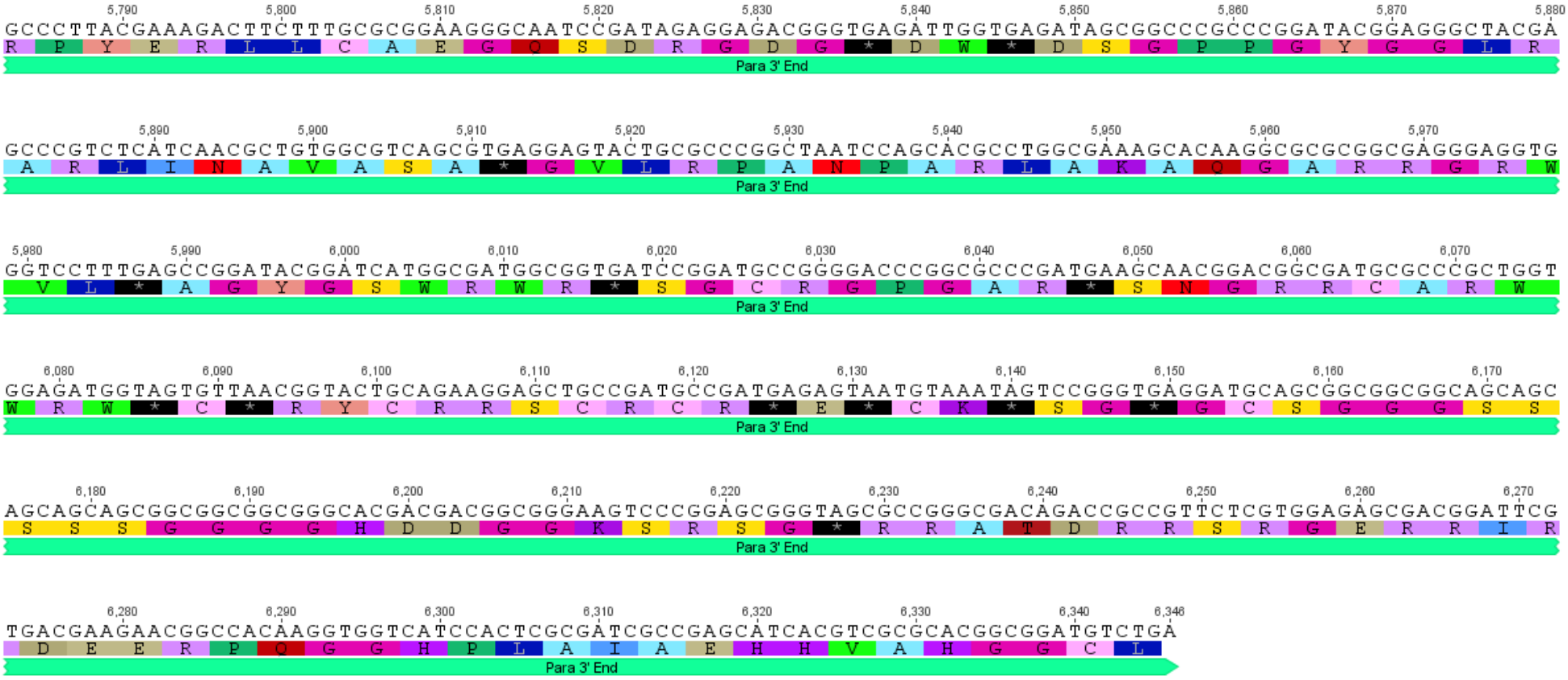
5,790 5,800 5,810 5,820 5,830 5,840 5,850 5,860 5,870 5,880
GCCCTTACGAAAGACTTCTTTGCGCGGAAGGGCAATCCGATAGAGGAGACGGGTGAGATTGGTGAGATAGCGGCCCGCCCCGGATACGGAGGGCTACGA
R P Y E R L L C A E G Q S D R G D G * D W * D S G P P G Y G G L R
Para 3' End
5,890 5,900 5,910 5,920 5,930 5,940 5,950 5,960 5,970
GCCCGTCTCATCAACGCTGTGGCGTCAGCGTGAGGAGTACTGCGCCCGGCTAATCCAGCACGCCTGGCGAAAGCACAAGGCGCGCGGCGAGGGAGGTG
A R L I N A V A S A * G V L R P A N P A R L A K A Q G A R R G R W
Para 3' End
5,980 5,990 6,000 6,010 6,020 6,030 6,040 6,050 6,060 6,070
GGTCCTTTGAGCCGGATACGGATCATGGCGATGGCGGTGATCCGGATGCCGGGGACCCGGCGCCCGATGAAGCAACGGACGGCGATGCGCCCGCTGGT
V L * A G Y G S W R W R * S G C R G P G A R * S N G R R C A R W
Para 3' End
6,080 6,090 6,100 6,110 6,120 6,130 6,140 6,150 6,160 6,170
GGAGATGGTAGTGTTAACGGTACTGCAGAAGGAGCTGCCGATGCCGATGAGAGTAATGTAAATAGTCCGGGTGAGGATGCAGCGGCGGCGGCAGCAGC
W R W * C * R Y C R R S C R C R * E * C K * S G * G C S G G G S S
Para 3' End
6,180 6,190 6,200 6,210 6,220 6,230 6,240 6,250 6,260 6,270
AGCAGCAGCGGCGGCGGCGGGCACGACGACGGCGGGAAGTCCCGGAGCGGGTAGCGCCGGGCGACAGACCGCCGTTCTCGTGGAGAGCGACGGATTCG
S S S G G G G H D D G G K S R S G * R R A T D R R S R G E R R I R
Para 3' End
6,280 6,290 6,300 6,310 6,320 6,330 6,340 6,346
TGACGAAGAACGGCCACAAGGTGGTCATCCACTCGCGATCGCCGAGCATCACGTCGCGCACGGCGGATGTCTGA
D E E R P Q G G H P L A I A E H H V A H G G C L
Para 3' End

Chimera LC

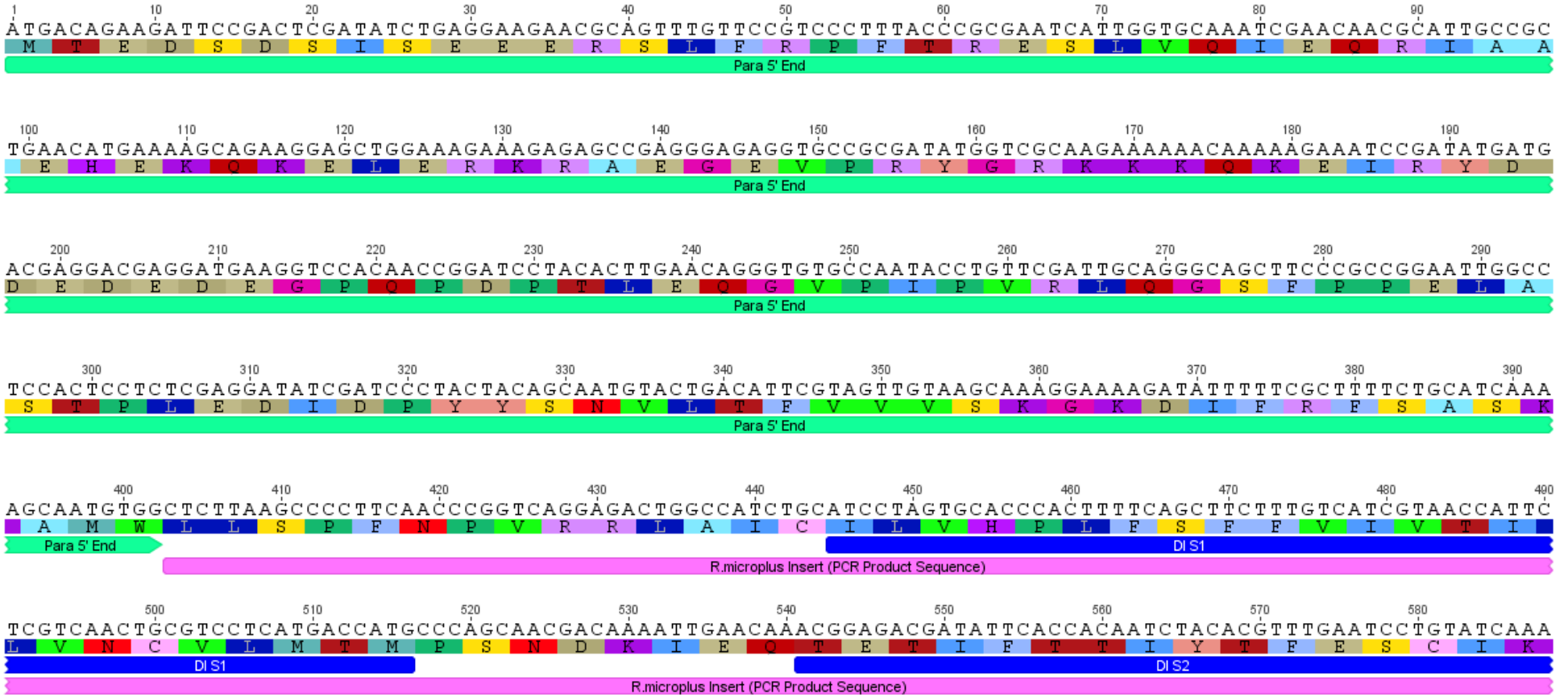
Para 5' End
Para 5' End
Para 5' End
Para 5' End
Para 5' End
DI S1
R.microplus Insert (PCR Product Sequence)
DI S1
DI S2
R.microplus Insert (PCR Product Sequence)

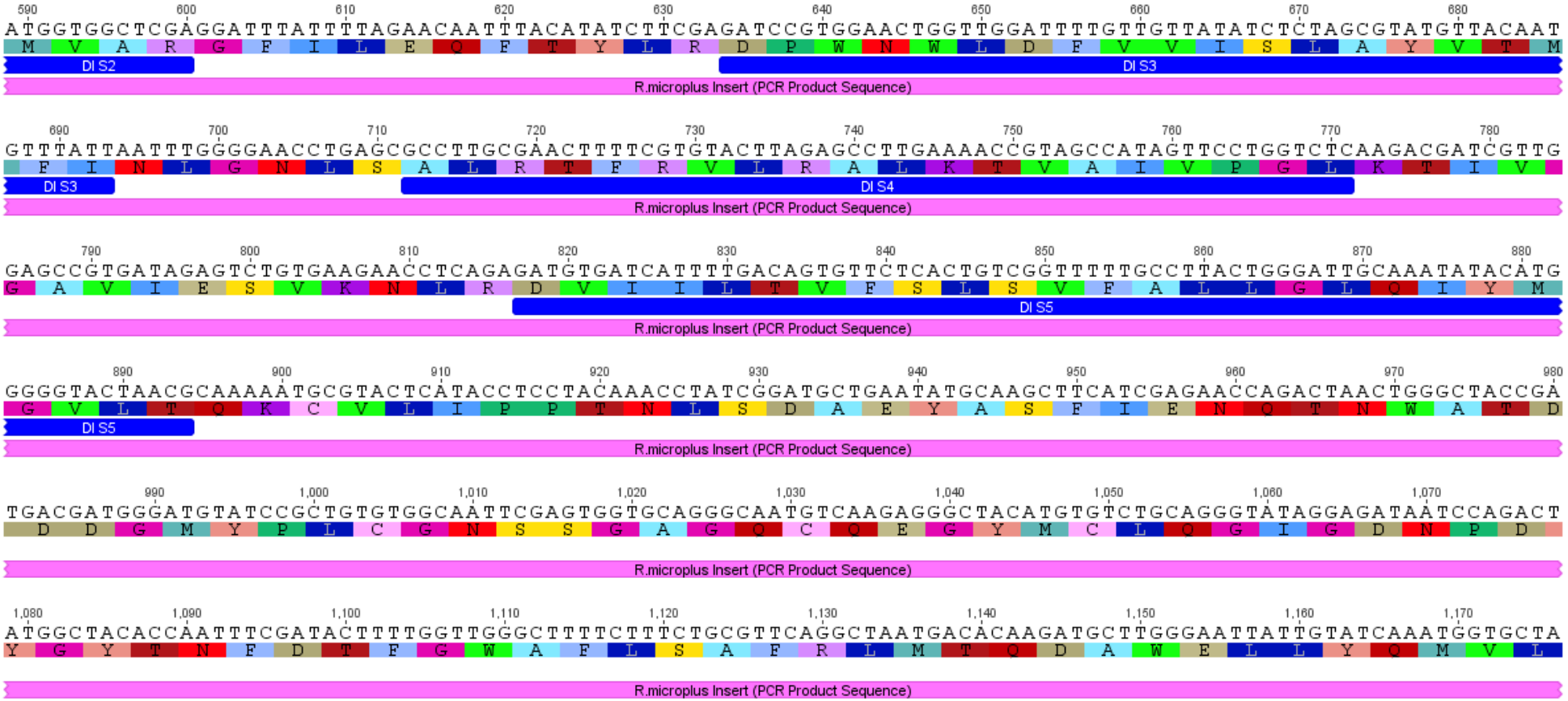
590 600 610 620 630 640 650 660 670 680
ATGGTGGCTCGAGGATTTATTTTAGAACAATTTACATATCTTCGAGATCCGTGGAACTGGTTGGATTTTGTTGTTATATCTCTAGCGTATGTTACAAT
M V A R G F I L E Q F T Y L R D P W N W L D F V V I S L A Y V T M
DI S2
DI S3
R.microplus Insert (PCR Product Sequence)
690 700 710 720 730 740 750 760 770 780
GTTTATTAATTTGGGGAACCTGAGCGCCTTGCGAACTTTTCGTGTACTTAGAGCCTTGAAAACCGTAGCCATAGTTCCTGGTCTCAAGACGATCGTTG
F I N L G N L S A L R T F R V L R A L K T V A I V P G L K T I V
DI S3
DI S4
R.microplus Insert (PCR Product Sequence)
790 800 810 820 830 840 850 860 870 880
GAGCCGTGATAGAGTCTGTGAAGAACCTCAGAGATGTGATCATTTTGACAGTGTTCTCACTGTCGGTTTTTGCCTTACTGGGATTGCAAATATACATG
G A V I E S V K N L R D V I I L T V F S L S V F A L L G L Q I Y M
DI S5
R.microplus Insert (PCR Product Sequence)
890 900 910 920 930 940 950 960 970 980
GGGGTACTAACGCAAAAATGCGTACTCATACCTCCTACAAACCTATCGGATGCTGAATATGCAAGCTTCATCGAGAACCAGACTAACTGGGCTACCGA
G V L T Q K C V L I P P T N L S D A E Y A S F I E N Q T N W A T D
DI S5
R.microplus Insert (PCR Product Sequence)
990 1,000 1,010 1,020 1,030 1,040 1,050 1,060 1,070
TGACGATGGGATGTATCCGCTGTGTGGCAATTCGAGTGGTGCAGGGCAATGTCAAGAGGGCTACATGTGTCTGCAGGGTATAGGAGATAATCCAGACT
D D G M Y P L C G N S S G A G Q C Q E G Y M C L Q G I G D N P D
R.microplus Insert (PCR Product Sequence)
1,080 1,090 1,100 1,110 1,120 1,130 1,140 1,150 1,160 1,170
ATGGCTACACCAATTTCGATACTTTTGGTTGGGCTTTTCTTTCTGCGTTCAGGCTAATGACACAAGATGCTTGGGAATTATTGTATCAAATGGTGCTA
Y G Y T N F D T F G W A F L S A F R L M T Q D A W E L L Y Q M V L
R.microplus Insert (PCR Product Sequence)

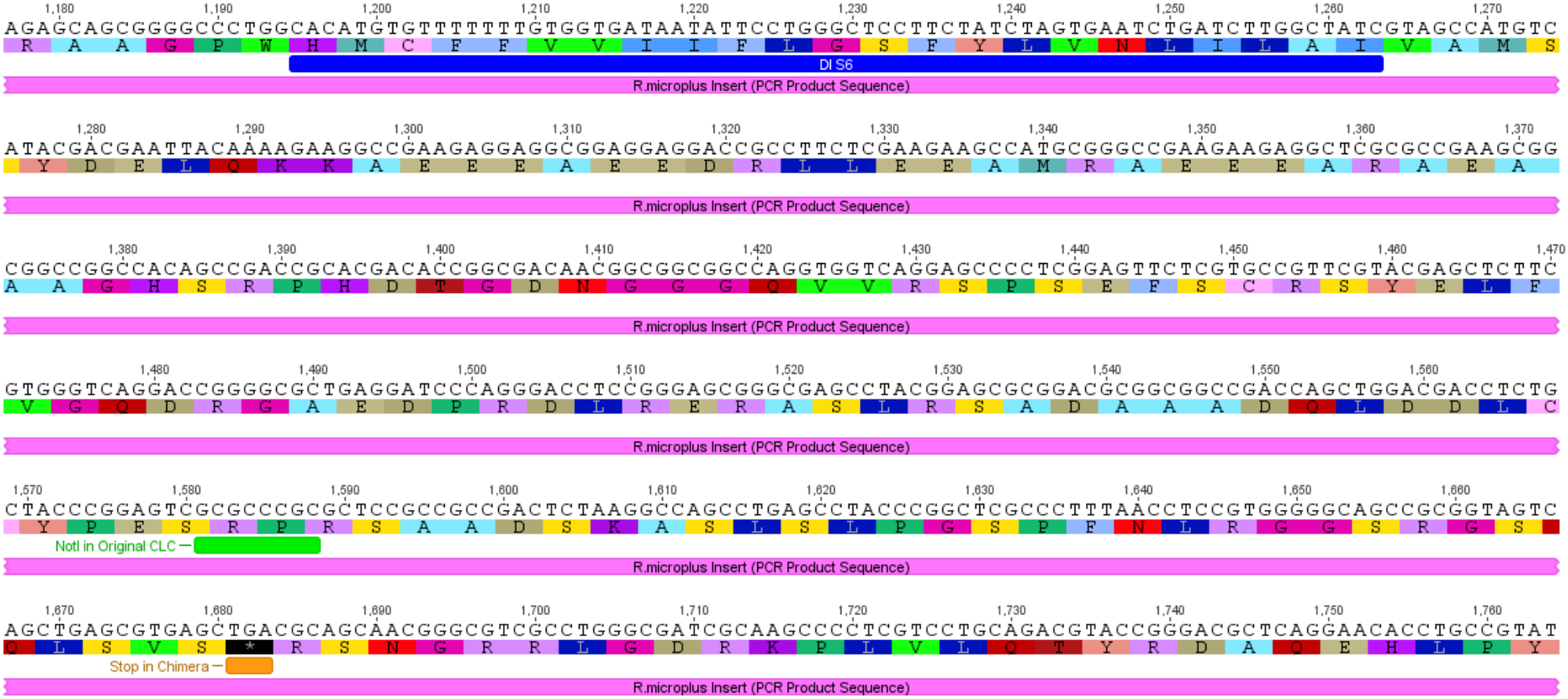
1,180 1,190 1,200 1,210 1,220 1,230 1,240 1,250 1,260 1,270
AGAGCAGCGGGGCCCTGGCACATGTGTTTTTTTGTGGTGATAATATTCCTGGGCTCCTTCTATCTAGTGAATCTGATCTTGGCTATCGTAGCCATGTC
R A A G P W H M C F F V V I I F L G S F Y L V N L I L A I V A M S
DI S6
R.microplus Insert (PCR Product Sequence)
1,280 1,290 1,300 1,310 1,320 1,330 1,340 1,350 1,360 1,370
ATACGACGAATTACAAAAGAAGGCCGAAGAGGAGGCGGAGGAGGACCGCCTTCTCGAAGAAGCCATGCGGGCCGAAGAAGAGGCTCGCGCCGAAGCGG
Y D E L Q K K A E E E A E E D R L L E E A M R A E E E A R A E A
R.microplus Insert (PCR Product Sequence)
1,380 1,390 1,400 1,410 1,420 1,430 1,440 1,450 1,460 1,470
CGGCCGGCCACAGCCGACCGCACGACACCGGCGACAACGGCGGCGGCCAGGTGGTCAGGAGCCCCTCGGAGTTCTCGTGCCGTTCGTACGAGCTCTTC
A A G H S R P H D T G D N G G G Q V V R S P S E F S C R S Y E L F
R.microplus Insert (PCR Product Sequence)
1,480 1,490 1,500 1,510 1,520 1,530 1,540 1,550 1,560
GTGGGTCAGGACCGGGGCGCTGAGGATCCCAGGGACCTCCGGGAGCGGGCGAGCCTACGGAGCGCGGACGCGGCGGCCGACCAGCTGGACGACCTCTG
V G Q D R G A E D P R D L R E R A S L R S A D A A A D Q L D D L C
R.microplus Insert (PCR Product Sequence)
1,570 1,580 1,590 1,600 1,610 1,620 1,630 1,640 1,650 1,660
CTACCCGGAGTCGCGCCCGCGCTCCGCCGCCGACTCTAAGGCCAGCCTGAGCCTACCCGGCTCGCCCTTTAACCTCCGTGGGGGCAGCCGCGGTAGTC
Y P E S R P R S A A D S K A S L S L P G S P F N L R G G S R G S
NotI in Original CLC
R.microplus Insert (PCR Product Sequence)
1,670 1,680 1,690 1,700 1,710 1,720 1,730 1,740 1,750 1,760
AGCTGAGCGTGAGCTGACGCAGCAACGGGCGTCGCCTGGGCGATCGCAAGCCCCTCGTCCTGCAGACGTACCGGGACGCTCAGGAACACCTGCCGTAT
Q L S V S * R S N G R R L G D R K P L V L Q T Y R D A Q E H L P Y
Stop in Chimera
R.microplus Insert (PCR Product Sequence)

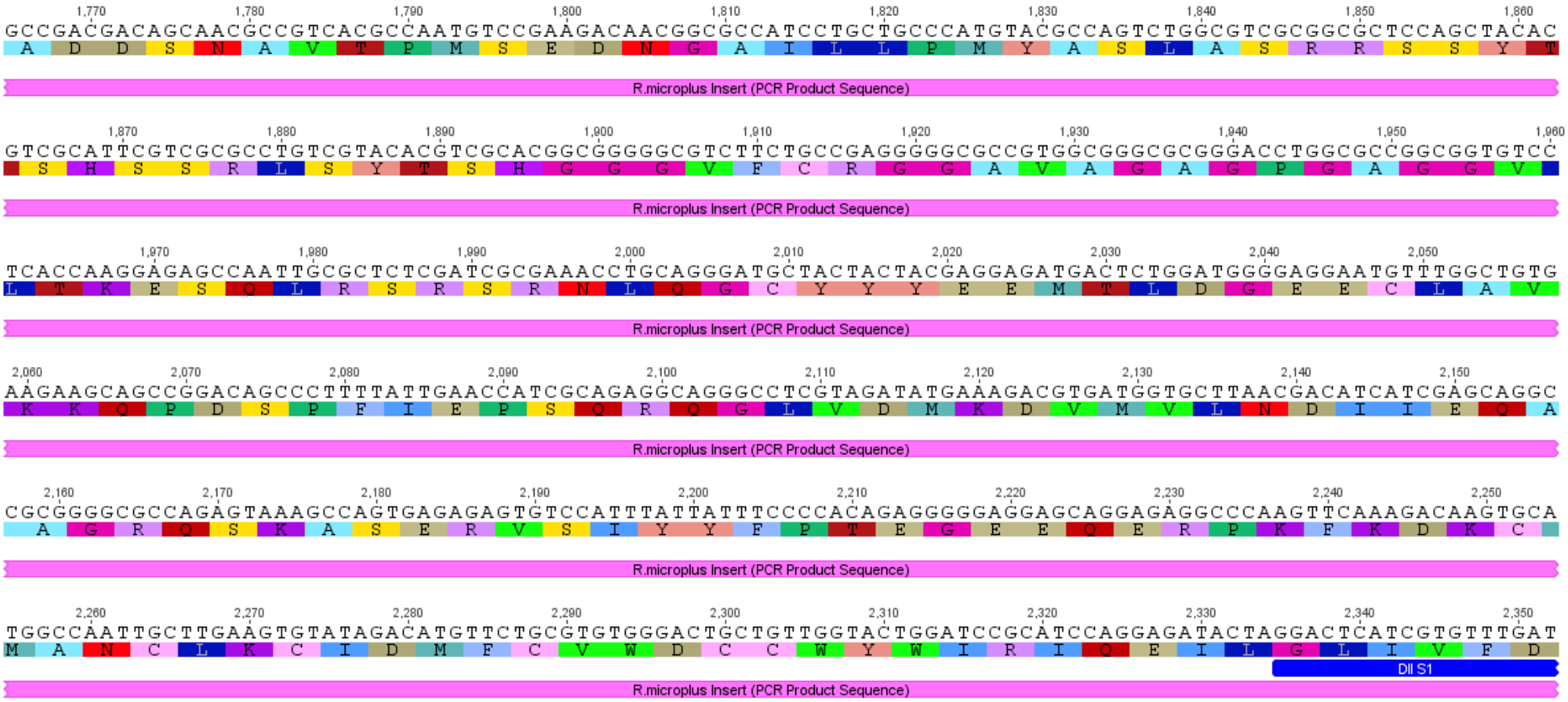
1,770 1,780 1,790 1,800 1,810 1,820 1,830 1,840 1,850 1,860
GCCGACGACAGCAACGCCGTCACGCCAATGTCCGAAGACAACGGCGCCATCCTGCTGCCCATGTACGCCAGTCTGGCGTCGCGGCGCTCCAGCTACAC
A D D S N A V T P M S E D N G A I L L P M Y A S L A S R R S S Y T
R.microplus Insert (PCR Product Sequence)
1,870 1,880 1,890 1,900 1,910 1,920 1,930 1,940 1,950 1,960
GTCGCATTCGTCGCGCCTGTCGTACACGTCGCACGGCGGGGGCGTCTTCTGCCGAGGGGGCGCCGTGGCGGGCGCGGGACCTGGCGCCGGCGGTGTCC
S H S S R L S Y T S H G G G V F C R G G A V A G A G P G A G G V
R.microplus Insert (PCR Product Sequence)
1,970 1,980 1,990 2,000 2,010 2,020 2,030 2,040 2,050
TCACCAAGGAGAGCCAATTGCGCTCTCGATCGCGAAACCTGCAGGGATGCTACTACTACGAGGAGATGACTCTGGATGGGGAGGAATGTTTGGCTGTG
L T K E S Q L R S R S R N L Q G C Y Y Y E E M T L D G E E C L A V
R.microplus Insert (PCR Product Sequence)
2,060 2,070 2,080 2,090 2,100 2,110 2,120 2,130 2,140 2,150
AAGAAGCAGCCGGACAGCCCTTTTATTGAACCATCGCAGAGGCAGGGCCTCGTAGATATGAAAGACGTGATGGTGCTTAACGACATCATCGAGCAGGC
K K Q P D S P F I E P S Q R Q G L V D M K D V M V L N D I I E Q A
R.microplus Insert (PCR Product Sequence)
2,160 2,170 2,180 2,190 2,200 2,210 2,220 2,230 2,240 2,250
CGCGGGGCGCCAGAGTAAAGCCAGTGAGAGAGTGTCCATTTATTATTTCCCCACAGAGGGGGAGGAGCAGGAGAGGCCCAAGTTCAAAGACAAGTGCA
A G R Q S K A S E R V S I Y Y F P T E G E E Q E R P K F K D K C
R.microplus Insert (PCR Product Sequence)
2,260 2,270 2,280 2,290 2,300 2,310 2,320 2,330 2,340 2,350
TGGCCAATTGCTTGAAGTGTATAGACATGTTCTGCGTGTGGGACTGCTGTTGGTACTGGATCCGCATCCAGGAGATACTAGGACTCATCGTGTTTGAT
M A N C L K C I D M F C V W D C C W Y W I R I Q E I L G L I V F D
DII S1
R.microplus Insert (PCR Product Sequence)

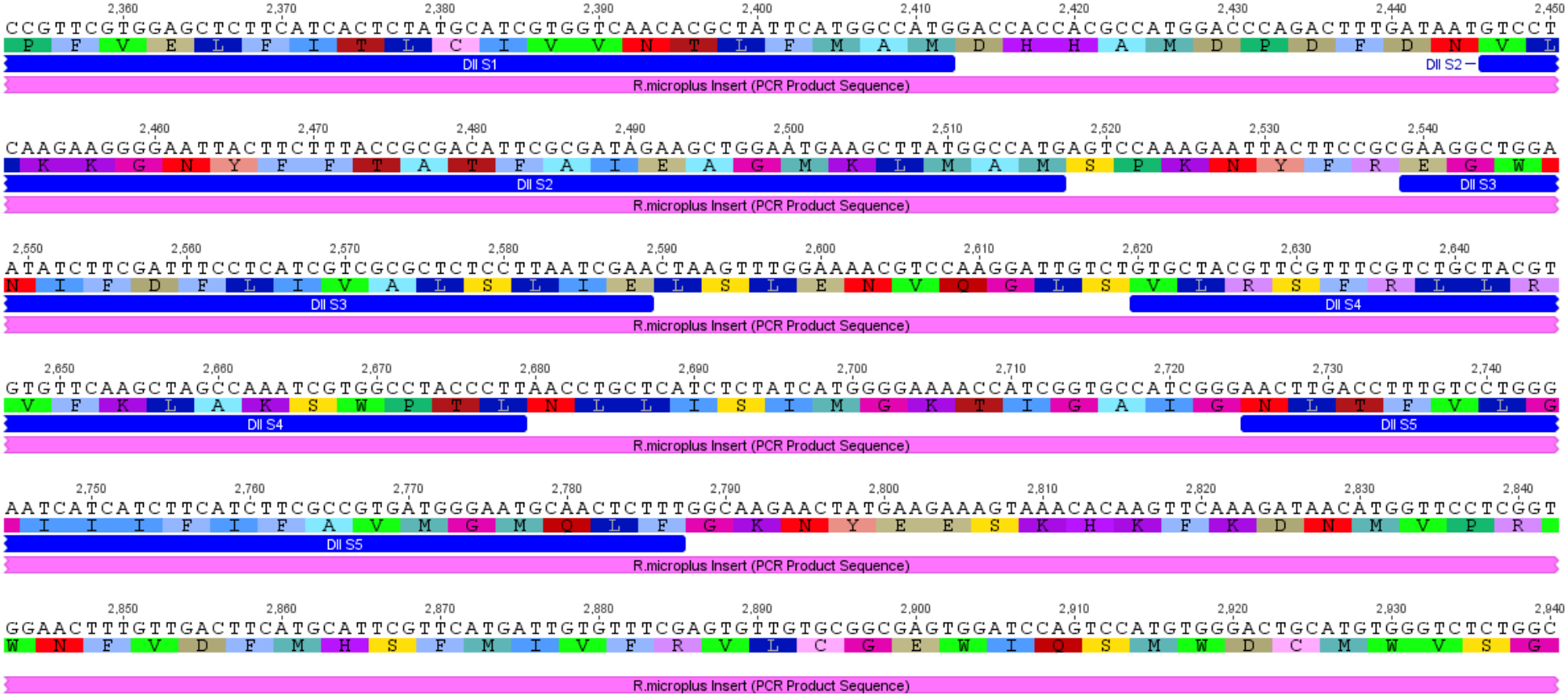
2,360 2,370 2,380 2,390 2,400 2,410 2,420 2,430 2,440 2,450
CCGTTCGTGGAGCTCTTCATCACTCTATGCATCGTGGTCAACACGCTATTCATGGCCATGGACCACCACGCCATGGACCCAGACTTTGATAATGTCCT
P F V E L F I T L C I V V N T L F M A M D H H A M D P D F D N V L
DII S1
DII S2
R.microplus Insert (PCR Product Sequence)
2,460 2,470 2,480 2,490 2,500 2,510 2,520 2,530 2,540
CAAGAAGGGGAATTACTTCTTTACCGCGACATTCGCGATAGAAGCTGGAATGAAGCTTATGGCCATGAGTCCAAAGAATTACTTCCGCGAAGGCTGGA
K K G N Y F F T A T F A I E A G M K L M A M S P K N Y F R E G W
DII S2
DII S3
R.microplus Insert (PCR Product Sequence)
2,550 2,560 2,570 2,580 2,590 2,600 2,610 2,620 2,630 2,640
ATATCTTCGATTTCCTCATCGTCGCGCTCTCCTTAATCGAACTAAGTTTGGAAAACGTCCAAGGATTGTCTGTGCTACGTTCGTTTCGTCTGCTACGT
N I F D F L I V A L S L I E L S L E N V Q G L S V L R S F R L L R
DII S3
DII S4
R.microplus Insert (PCR Product Sequence)
2,650 2,660 2,670 2,680 2,690 2,700 2,710 2,720 2,730 2,740
GTGTTCAAGCTAGCCAAATCGTGGCCTACCCTTAACCTGCTCATCTCTATCATGGGGAAAACCATCGGTGCCATCGGGAACTTGACCTTTGTCCTGGG
V F K L A K S W P T L N L L I S I M G K T I G A I G N L T F V L G
DII S4
DII S5
R.microplus Insert (PCR Product Sequence)
2,750 2,760 2,770 2,780 2,790 2,800 2,810 2,820 2,830 2,840
AATCATCATCTTCATCTTCGCCGTGATGGGAATGCAACTCTTTGGCAAGAACTATGAAGAAAGTAAACACAAGTTCAAAGATAACATGGTTCCTCGGT
I I I F I F A V M G M Q L F G K N Y E E S K H K F K D N M V P R
DII S5
R.microplus Insert (PCR Product Sequence)
2,850 2,860 2,870 2,880 2,890 2,900 2,910 2,920 2,930 2,940
GGAACTTTGTTGACTTCATGCATTCGTTCATGATTGTGTTTCGAGTGTTGTGCGGCGAGTGGATCCAGTCCATGTGGGACTGCATGTGGGTCTCTGGC
W N F V D F M H S F M I V F R V L C G E W I Q S M W D C M W V S G
R.microplus Insert (PCR Product Sequence)

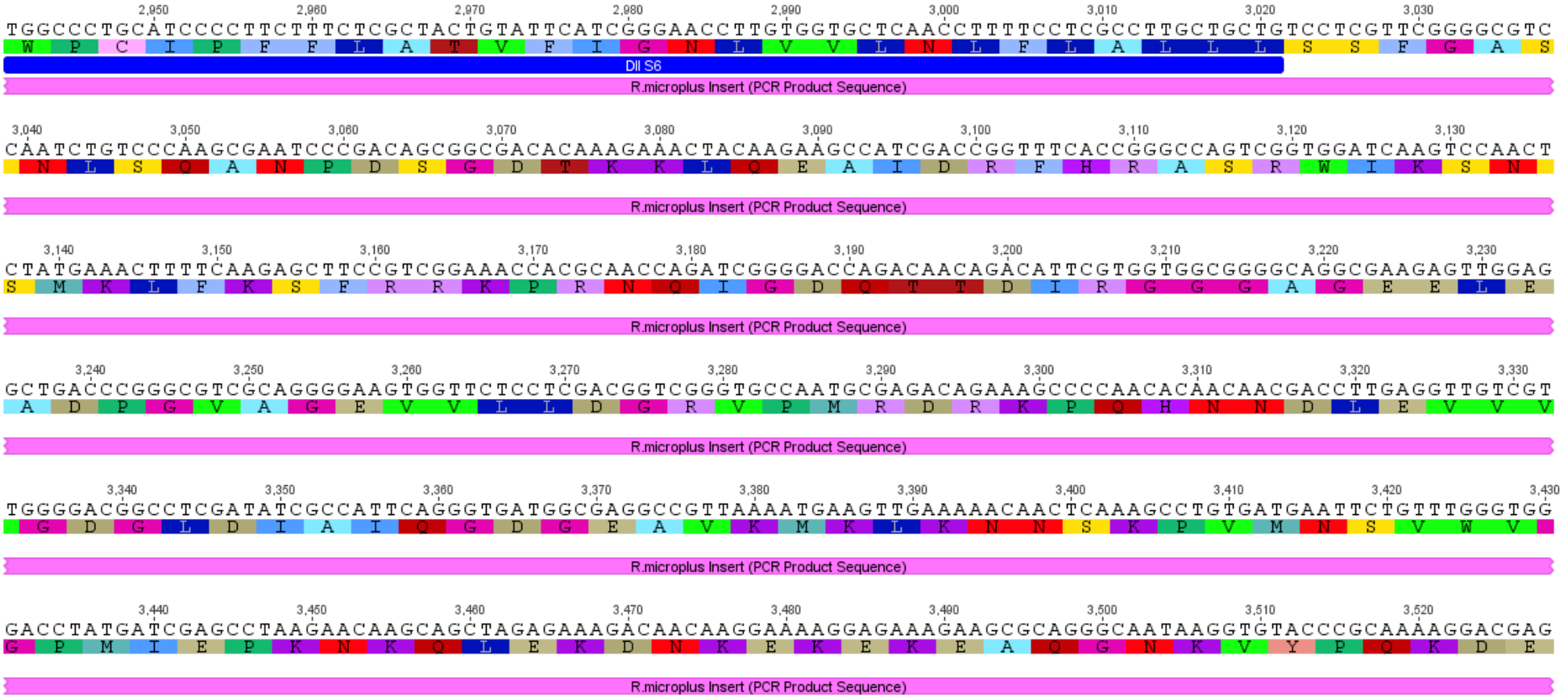
2,950 2,960 2,970 2,980 2,990 3,000 3,010 3,020 3,030
TGGCCCTGCATCCCCTTCTTTCTCGCTACTGTATTCATCGGGAACCTTGTGGTGCTCAACCTTTTCCTCGCCTTGCTGCTGTCCTCGTTCGGGGCGTC
W P C I P F F L A T V F I G N L V V L N L F L A L L L S S F G A S
DII S6
R.microplus Insert (PCR Product Sequence)
3,040 3,050 3,060 3,070 3,080 3,090 3,100 3,110 3,120 3,130
CAATCTGTCCCAAGCGAATCCCGACAGCGGCGACACAAAGAAACTACAAGAAGCCATCGACCGGTTTCACCGGGCCAGTCGGTGGATCAAGTCCAACT
N L S Q A N P D S G D T K K L Q E A I D R F H R A S R W I K S N
R.microplus Insert (PCR Product Sequence)
3,140 3,150 3,160 3,170 3,180 3,190 3,200 3,210 3,220 3,230
CTATGAAACTTTTCAAGAGCTTCCGTCGGAAACCACGCAACCAGATCGGGGACCAGACAACAGACATTCGTGGTGGCGGGGCAGGCGAAGAGTTGGAG
S M K L F K S F R R K P R N Q I G D Q T T D I R G G G A G E E L E
R.microplus Insert (PCR Product Sequence)
3,240 3,250 3,260 3,270 3,280 3,290 3,300 3,310 3,320 3,330
GCTGACCCGGGCGTCGCAGGGGAAGTGGTTCTCCTCGACGGTCGGGTGCCAATGCGAGACAGAAAGCCCCAACACAACAACGACCTTGAGGTTGTCGT
A D P G V A G E V V L L D G R V P M R D R K P Q H N N D L E V V V
R.microplus Insert (PCR Product Sequence)
3,340 3,350 3,360 3,370 3,380 3,390 3,400 3,410 3,420 3,430
TGGGGACGGCCTCGATATCGCCATTCAGGGTGATGGCGAGGCCGTTAAAATGAAGTTGAAAAACAACTCAAAGCCTGTGATGAATTCTGTTTGGGTGG
G D G L D I A I Q G D G E A V K M K L K N N S K P V M N S V W V
R.microplus Insert (PCR Product Sequence)
3,440 3,450 3,460 3,470 3,480 3,490 3,500 3,510 3,520
GACCTATGATCGAGCCTAAGAACAAGCAGCTAGAGAAAGACAACAAGGAAAAGGAGAAAGAAGCGCAGGGCAATAAGGTGTACCCGCAAAAGGACGAG
G P M I E P K N K Q L E K D N K E K E K E A Q G N K V Y P Q K D E
R.microplus Insert (PCR Product Sequence)

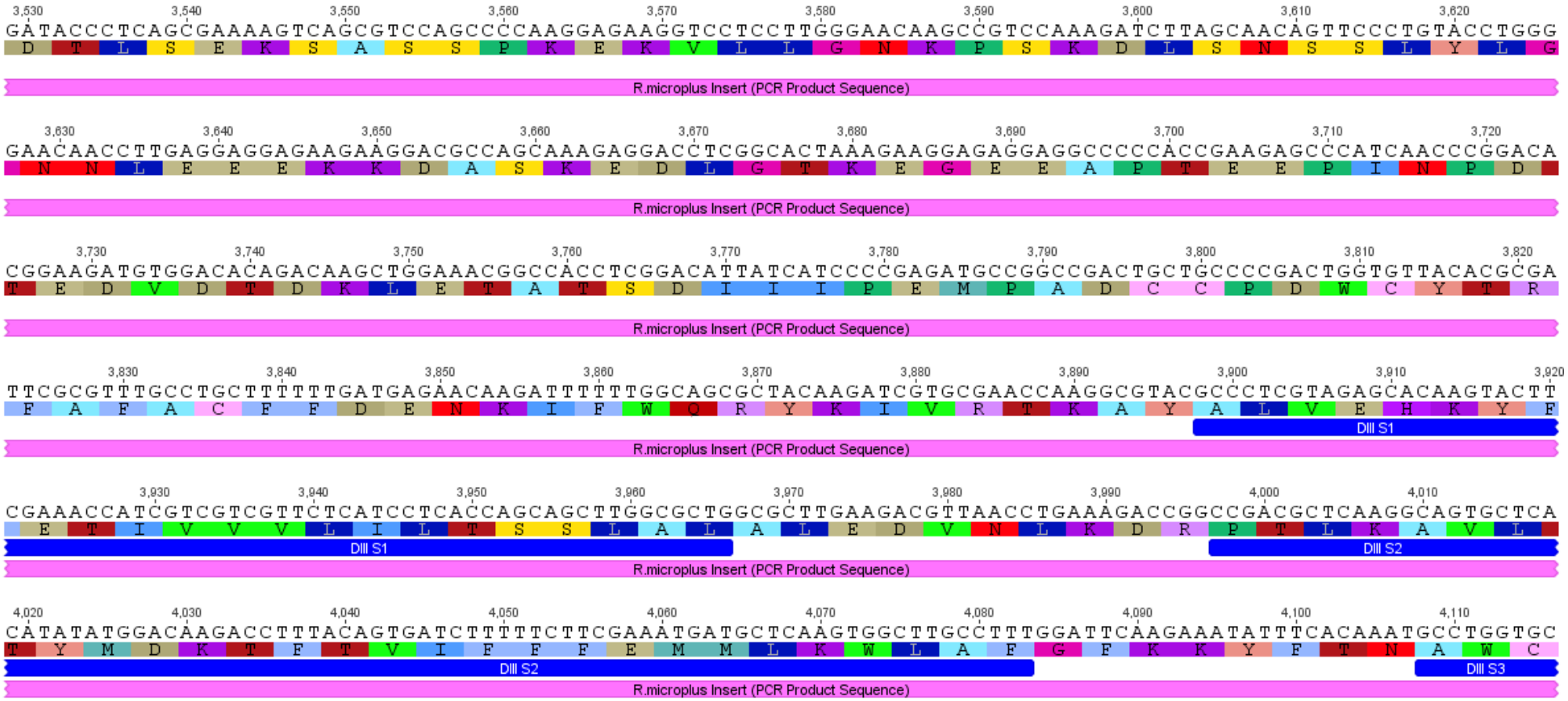
3,530 3,540 3,550 3,560 3,570 3,580 3,590 3,600 3,610 3,620
GATACCCTCAGCGAAAAGTCAGCGTCCAGCCCCAAGGAGAAGGTCCTCCTTGGGAACAAGCCGTCCAAAGATCTTAGCAACAGTTCCCTGTACCTGGG
D T L S E K S A S S P K E K V L L G N K P S K D L S N S S L Y L G
R.microplus Insert (PCR Product Sequence)
3,630 3,640 3,650 3,660 3,670 3,680 3,690 3,700 3,710 3,720
GAACAACCTTGAGGAGGAGAAGAAGGACGCCAGCAAAGAGGACCTCGGCACTAAAGAAGGAGAGGAGGCCCCCACCGAAGAGCCCATCAACCCGGACA
N N L E E E K K D A S K E D L G T K E G E E A P T E E P I N P D
R.microplus Insert (PCR Product Sequence)
3,730 3,740 3,750 3,760 3,770 3,780 3,790 3,800 3,810 3,820
CGGAAGATGTGGACACAGACAAGCTGGAAACGGCCACCTCGGACATTATCATCCCCGAGATGCCGGCCGACTGCTGCCCCGACTGGTGTTACACGCGA
T E D V D T D K L E T A T S D I I I P E M P A D C C P D W C Y T R
R.microplus Insert (PCR Product Sequence)
3,830 3,840 3,850 3,860 3,870 3,880 3,890 3,900 3,910 3,920
TTCGCGTTTGCCTGCTTTTTTGATGAGAACAAGATTTTTTGGCAGCGCTACAAGATCGTGCGAACCAAGGCGTACGCCCTCGTAGAGCACAAGTACTT
F A F A C F F D E N K I F W Q R Y K I V R T K A Y A L V E H K Y F
DIII S1
R.microplus Insert (PCR Product Sequence)
3,930 3,940 3,950 3,960 3,970 3,980 3,990 4,000 4,010
CGAAACCATCGTCGTCGTTCTCATCCTCACCAGCAGCTTGGCGCTGGCGCTTGAAGACGTTAACCTGAAAGACCGGCCGACGCTCAAGGCAGTGCTCA
E T I V V V L I L T S S L A L A L E D V N L K D R P T L K A V L
DIII S1
DIII S2
R.microplus Insert (PCR Product Sequence)
4,020 4,030 4,040 4,050 4,060 4,070 4,080 4,090 4,100 4,110
CATATATGGACAAGACCTTTACAGTGATCTTTTTCTTCGAAATGATGCTCAAGTGGCTTGCCTTTGGATTCAAGAAATATTTCACAAATGCCTGGTGC
T Y M D K T F T V I F F F E M M L K W L A F G F K K Y F T N A W C
DIII S2
DIII S3
R.microplus Insert (PCR Product Sequence)

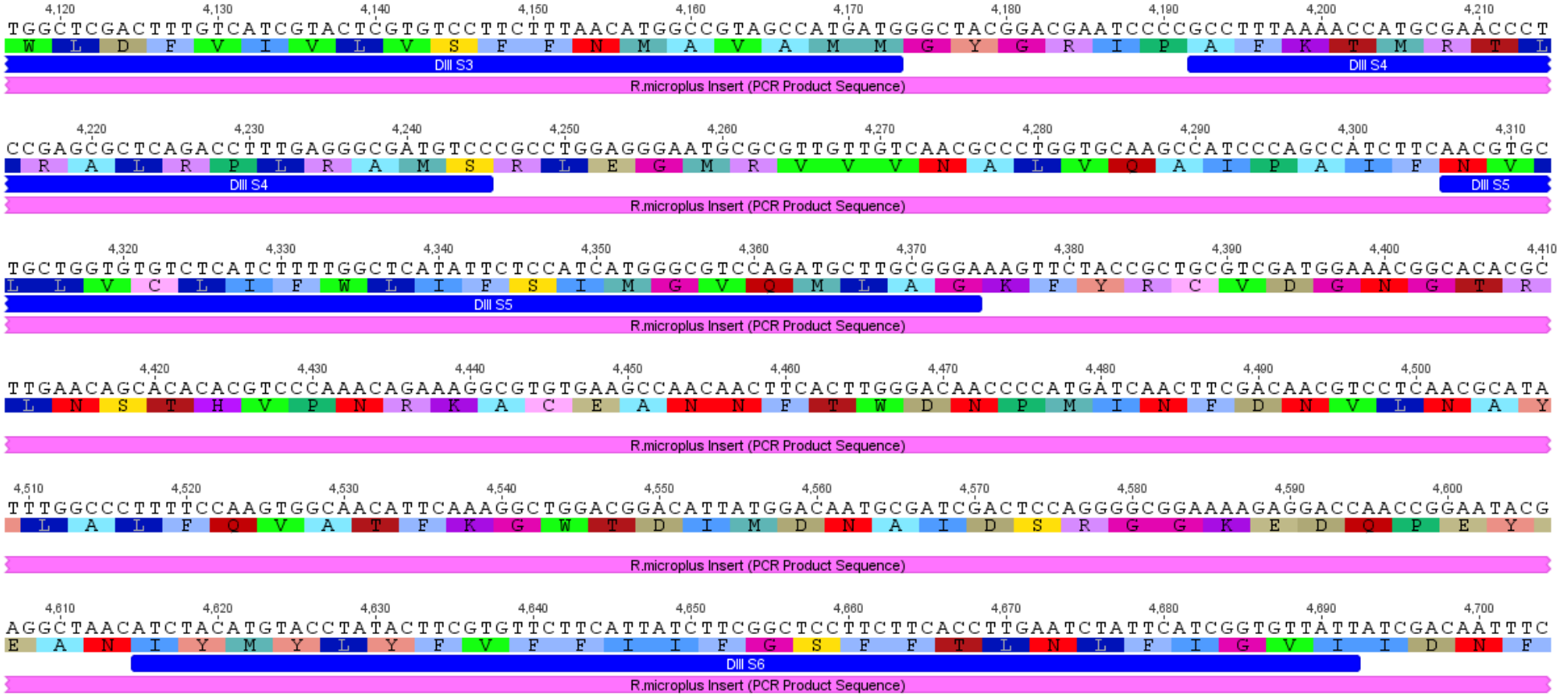
4,120 4,130 4,140 4,150 4,160 4,170 4,180 4,190 4,200 4,210
TGGCTCGACTTTGTCATCGTACTCGTGTCCTTCTTTAACATGGCCGTAGCCATGATGGGCTACGGACGAATCCCCGCCTTTAAAACCATGCGAACCCT
W L D F V I V L V S F F N M A V A M M G Y G R I P A F K T M R T L
DIII S3
DIII S4
R.microplus Insert (PCR Product Sequence)
4,220 4,230 4,240 4,250 4,260 4,270 4,280 4,290 4,300 4,310
CCGAGCGCTCAGACCTTTGAGGGCGATGTCCCGCCTGGAGGGAATGCGCGTTGTTGTCAACGCCCTGGTGCAAGCCATCCCAGCCATCTTCAACGTGC
R A L R P L R A M S R L E G M R V V V N A L V Q A I P A I F N V
DIII S4
DIII S5
R.microplus Insert (PCR Product Sequence)
4,320 4,330 4,340 4,350 4,360 4,370 4,380 4,390 4,400 4,410
TGCTGGTGTGTCTCATCTTTTGGCTCATATTCTCCATCATGGGCGTCCAGATGCTTGCGGGAAAGTTCTACCGCTGCGTCGATGGAAACGGCACACGC
L L V C L I F W L I F S I M G V Q M L A G K F Y R C V D G N G T R
DIII S5
R.microplus Insert (PCR Product Sequence)
4,420 4,430 4,440 4,450 4,460 4,470 4,480 4,490 4,500
TTGAACAGCACACACGTCCCAAACAGAAAGGCGTGTGAAGCCAACAACTTCACTTGGGACAACCCCATGATCAACTTCGACAACGTCCTCAACGCATA
L N S T H V P N R K A C E A N N F T W D N P M I N F D N V L N A Y
R.microplus Insert (PCR Product Sequence)
4,510 4,520 4,530 4,540 4,550 4,560 4,570 4,580 4,590 4,600
TTTGGCCCTTTTCCAAGTGGCAACATTCAAAGGCTGGACGGACATTATGGACAATGCGATCGACTCCAGGGGCGGAAAAGAGGACCAACCGGAATACG
L A L F Q V A T F K G W T D I M D N A I D S R G G K E D Q P E Y
R.microplus Insert (PCR Product Sequence)
4,610 4,620 4,630 4,640 4,650 4,660 4,670 4,680 4,690 4,700
AGGCTAACATCTACATGTACCTATACTTCGTGTTCTTCATTATCTTCGGCTCCTTCTTCACCTTGAATCTATTCATCGGTGTTATTATCGACAATTTC
E A N I Y M Y L Y F V F F I I F G S F F T L N L F I G V I I D N F
DIII S6
R.microplus Insert (PCR Product Sequence)

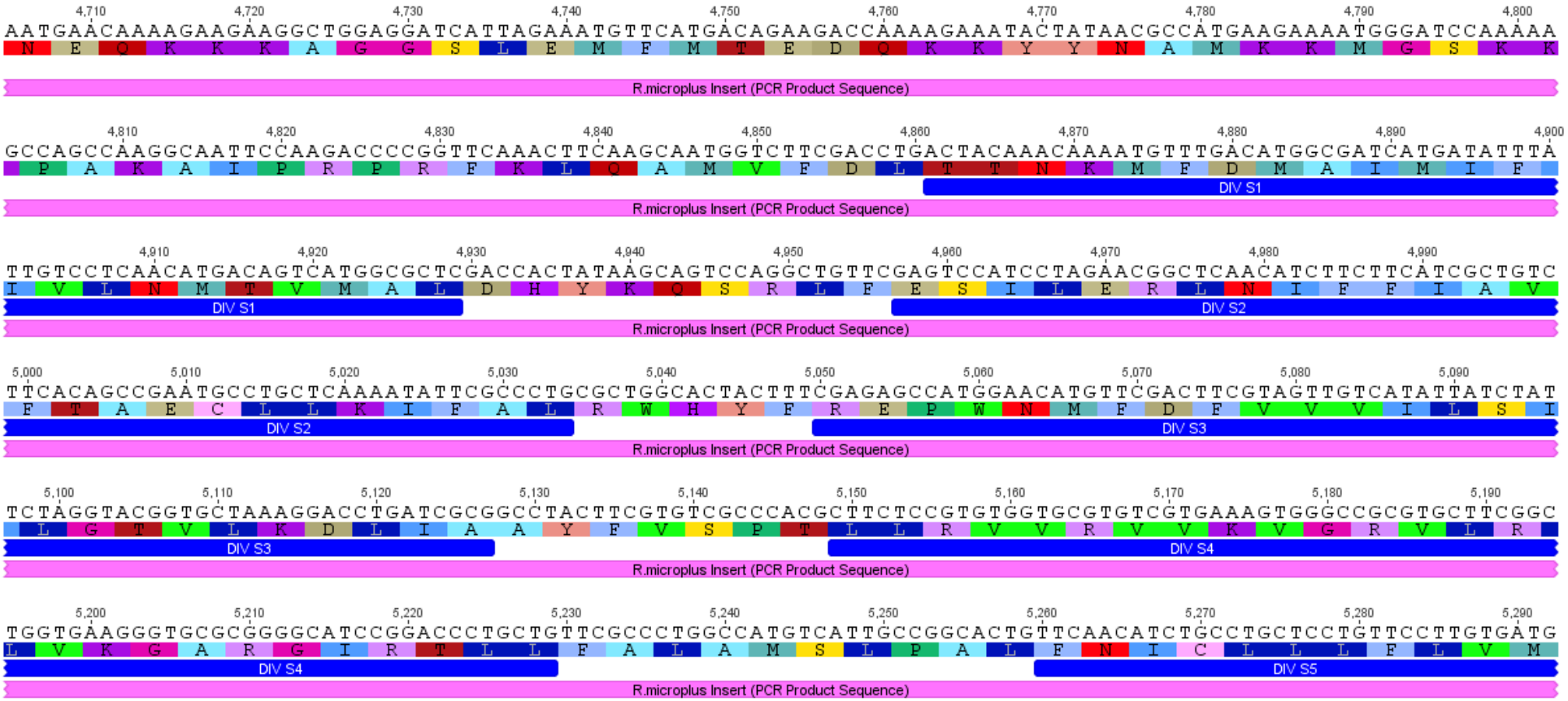
4,710 4,720 4,730 4,740 4,750 4,760 4,770 4,780 4,790 4,800
AATGAACAAAAGAAGAAGGCTGGAGGATCATTAGAAATGTTCATGACAGAAGACCAAAAGAAATACTATAACGCCATGAAGAAAATGGGATCCAAAAA
N E Q K K K A G G S L E M F M T E D Q K K Y Y N A M K K M G S K K
R.microplus Insert (PCR Product Sequence)
4,810 4,820 4,830 4,840 4,850 4,860 4,870 4,880 4,890 4,900
GCCAGCCAAGGCAATTCCAAGACCCCGGTTCAAACTTCAAGCAATGGTCTTCGACCTGACTACAAACAAAATGTTTGACATGGCGATCATGATATTTA
P A K A I P R P R F K L Q A M V F D L T T N K M F D M A I M I F
DIV S1
R.microplus Insert (PCR Product Sequence)
4,910 4,920 4,930 4,940 4,950 4,960 4,970 4,980 4,990
TTGTCCTCAACATGACAGTCATGGCGCTCGACCACTATAAGCAGTCCAGGCTGTTCGAGTCCATCCTAGAACGGCTCAACATCTTCTTCATCGCTGTC
I V L N M T V M A L D H Y K Q S R L F E S I L E R L N I F F I A V
DIV S1
DIV S2
R.microplus Insert (PCR Product Sequence)
5,000 5,010 5,020 5,030 5,040 5,050 5,060 5,070 5,080 5,090
TTCACAGCCGAATGCCTGCTCAAAATATTCGCCCTGCGCTGGCACTACTTTCGAGAGCCATGGAACATGTTCGACTTCGTAGTTGTCATATTATCTAT
F T A E C L L K I F A L R W H Y F R E P W N M F D F V V V I L S I
DIV S2
DIV S3
R.microplus Insert (PCR Product Sequence)
5,100 5,110 5,120 5,130 5,140 5,150 5,160 5,170 5,180 5,190
TCTAGGTACGGTGCTAAAGGACCTGATCGCGGCCTACTTCGTGTCGCCCACGCTTCTCCGTGTGGTGCGTGTCGTGAAAGTGGGCCGCGTGCTTCGGC
L G T V L K D L I A A Y F V S P T L L R V V R V V K V G R V L R
DIV S3
DIV S4
R.microplus Insert (PCR Product Sequence)
5,200 5,210 5,220 5,230 5,240 5,250 5,260 5,270 5,280 5,290
TGGTGAAGGGTGCGCGGGGCATCCGGACCCTGCTGTTCGCCCTGGCCATGTCATTGCCGGCACTGTTCAACATCTGCCTGCTCCTGTTCCTTGTGATG
L V K G A R G I R T L L F A L A M S L P A L F N I C L L L F L V M
DIV S4
DIV S5
R.microplus Insert (PCR Product Sequence)

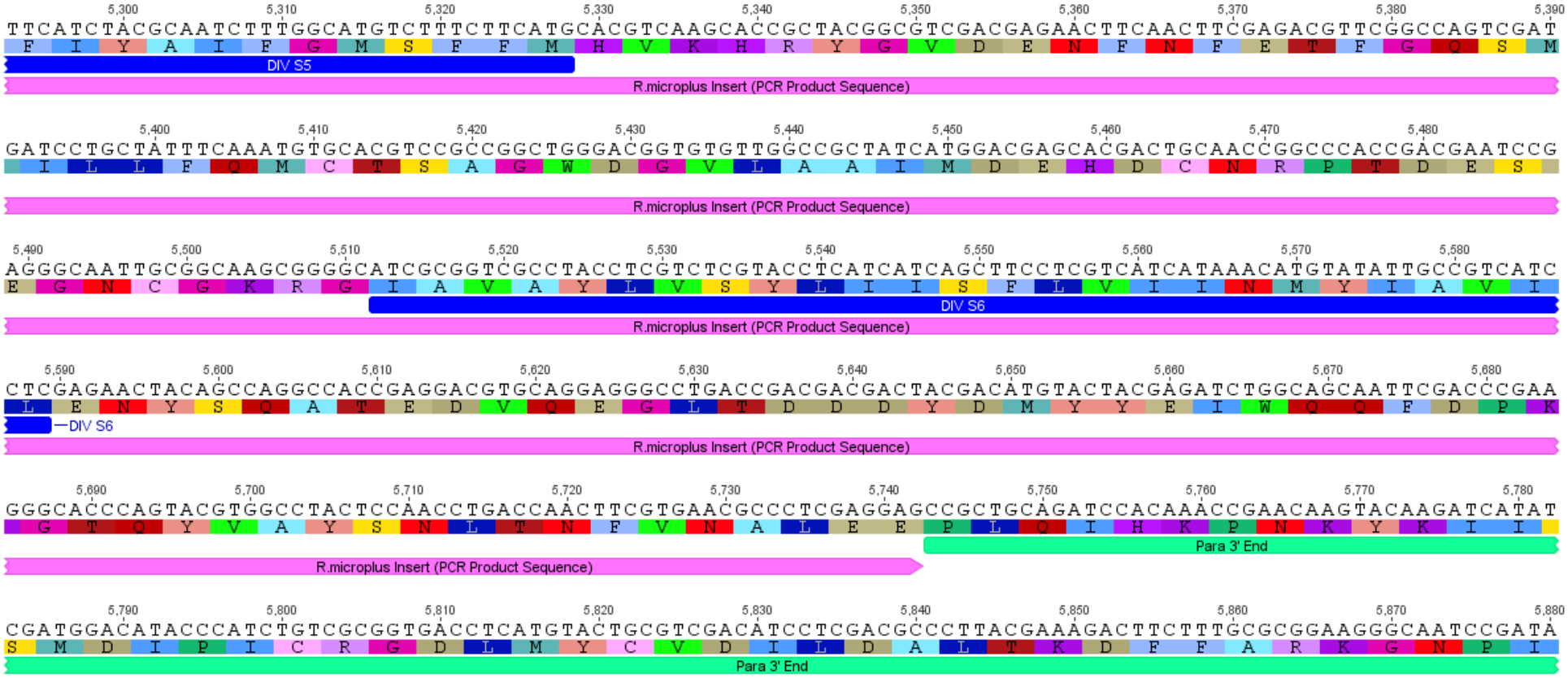
5,300 5,310 5,320 5,330 5,340 5,350 5,360 5,370 5,380 5,390
TTCATCTACGCAATCTTTGGCATGTCTTTCTTCATGCACGTCAAGCACCGCTACGGCGTCGACGAGAACTTCAACTTCGAGACGTTCGGCCAGTCGAT
F I Y A I F G M S F F M H V K H R Y G V D E N F N F E T F G Q S M
DIV S5
R.microplus Insert (PCR Product Sequence)
5,400 5,410 5,420 5,430 5,440 5,450 5,460 5,470 5,480
GATCCTGCTATTTCAAATGTGCACGTCCGCCGGCTGGGACGGTGTGTTGGCCGCTATCATGGACGAGCACGACTGCAACCGGCCCACCGACGAATCCG
I L L F Q M C T S A G W D G V L A A I M D E H D C N R P T D E S
R.microplus Insert (PCR Product Sequence)
5,490 5,500 5,510 5,520 5,530 5,540 5,550 5,560 5,570 5,580
AGGGCAATTGCGGCAAGCGGGGCATCGCGGTCGCCTACCTCGTCTCGTACCTCATCATCAGCTTCCTCGTCATCATAAACATGTATATTGCCGTCATC
E G N C G K R G I A V A Y L V S Y L I I S F L V I I N M Y I A V I
DIV S6
R.microplus Insert (PCR Product Sequence)
5,590 5,600 5,610 5,620 5,630 5,640 5,650 5,660 5,670 5,680
CTCGAGAACTACAGCCAGGCCACCGAGGACGTGCAGGAGGGCCTGACCGACGACGACTACGACATGTACTACGAGATCTGGCAGCAATTCGACCCGAA
L E N Y S Q A T E D V Q E G L T D D D Y D M Y Y E I W Q Q F D P K
DIV S6
R.microplus Insert (PCR Product Sequence)
5,690 5,700 5,710 5,720 5,730 5,740 5,750 5,760 5,770 5,780
GGGCACCCAGTACGTGGCCTACTCCAACCTGACCAACTTCGTGAACGCCCTCGAGGAGCCGCTGCAGATCCACAAACCGAACAAGTACAAGATCATAT
G T Q Y V A Y S N L T N F V N A L E E P L Q I H K P N K Y K I I
Para 3' End
R.microplus Insert (PCR Product Sequence)
5,790 5,800 5,810 5,820 5,830 5,840 5,850 5,860 5,870 5,880
CGATGGACATACCCATCTGTCGCGGTGACCTCATGTACTGCGTCGACATCCTCGACGCCCTTACGAAAGACTTCTTTGCGCGGAAGGGCAATCCGATA
S M D I P I C R G D L M Y C V D I L D A L T K D F F A R K G N P I
Para 3' End

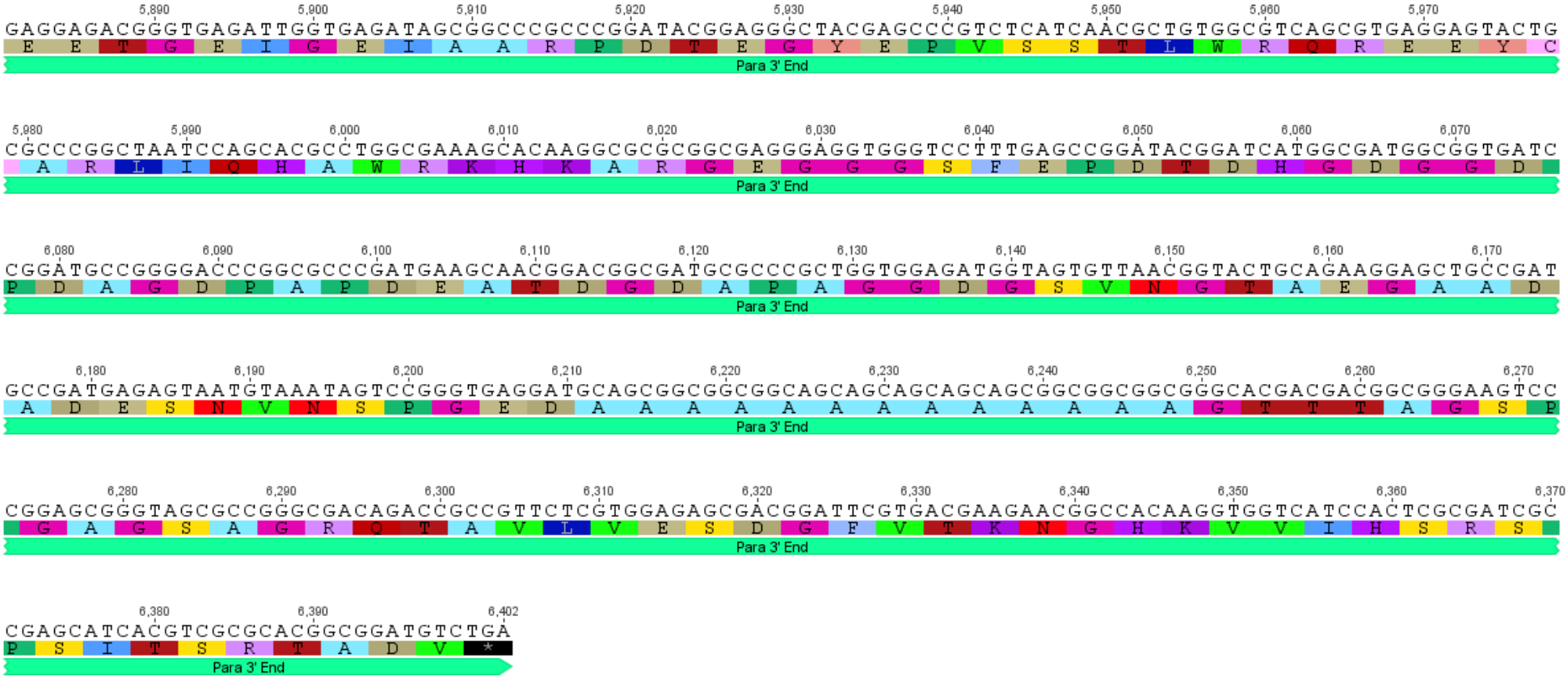
5,890 5,900 5,910 5,920 5,930 5,940 5,950 5,960 5,970
GAGGAGACGGGTGAGATTGGTGAGATAGCGGCCCGCCCGGATACGGAGGGCTACGAGCCCGTCTCATCAACGCTGTGGCGTCAGCGTGAGGAGTACTG
E E T G E I G E I A A R P D T E G Y E P V S S T L W R Q R E E Y C
Para 3' End
5,980 5,990 6,000 6,010 6,020 6,030 6,040 6,050 6,060 6,070
CGCCCGGCTAATCCAGCACGCCTGGCGAAAGCACAAGGCGCGCGGCGAGGGAGGTGGGTCCTTTGAGCCGGATACGGATCATGGCGATGGCGGTGATC
A R L I Q H A W R K H K A R G E G G G S F E P D T D H G D G G D
Para 3' End
6,080 6,090 6,100 6,110 6,120 6,130 6,140 6,150 6,160 6,170
CGGATGCCGGGGACCCGGCGCCCGATGAAGCAACGGACGGCGATGCGCCCGCTGGTGGAGATGGTAGTGTTAACGGTACTGCAGAAGGAGCTGCCGAT
P D A G D P A P D E A T D G D A P A G G D G S V N G T A E G A A D
Para 3' End
6,180 6,190 6,200 6,210 6,220 6,230 6,240 6,250 6,260 6,270
GCCGATGAGAGTAATGTAAATAGTCCGGGTGAGGATGCAGCGGCGGCGGCAGCAGCAGCAGCAGCGGCGGCGGCGGGCACGACGACGGCGGGAAGTCC
A D E S N V N S P G E D A A A A A A A A A A A A G T T T A G S P
Para 3' End
6,280 6,290 6,300 6,310 6,320 6,330 6,340 6,350 6,360 6,370
CGGAGCGGGTAGCGCCGGGCGACAGACCGCCGTTCTCGTGGAGAGCGACGGATTCGTGACGAAGAACGGCCACAAGGTGGTCATCCACTCGCGATCGC
G A G S A G R Q T A V L V E S D G F V T K N G H K V V I H S R S
Para 3' End
6,380 6,390 6,402
CGAGCATCACGTCGCGCACGGCGGATGTCTGA
P S I T S R T A D V *
Para 3' End

10.4 Appendix 4

Raw data from range-finding pyrethroid contact bioassays with tick species and *V. destructor* mites. Each tick species was tested with all four pyrethroids on the same day. Five adult acari were used per test vial, giving a total n = 5 per concentration. *V. destructor* mites were tested with one pyrethroid per day due to mite availability (as stated in Section 8.2.2). *A = Affected in these tables, the sum total of knockdown and dead individuals for the given pyrethroid dose or control.

Species and Species Details: *Amblyomma americanum*. Hatched 03/04/16. Delivered 06/05/16.

Compound	Concentration (mg/Ha)	Concentration (ppm)	Time								
			4 Hours			24 Hours			48 Hours		
			A*	Kdr	Dead	A	Kdr	Dead	A	Kdr	Dead
Deltamethrin	Blank Control	Blank Control	0	0	0	0	0	0	0	0	0
Deltamethrin	Acetone Only Control	Acetone Only Control	0	0	0	0	0	0	0	0	0
Deltamethrin	1000	1650	5	5	0	5	5	5	5	3	2
Deltamethrin	100	165	5	5	0	5	3	2	5	2	3
Deltamethrin	10	16.5	5	5	0	5	5	0	5	4	1
Deltamethrin	1	1.65	3	3	0	0	0	0	0	0	0
Deltamethrin	0.1	0.165	0	0	0	0	0	0	0	0	0
Deltamethrin	0.01	0.0165	0	0	0	0	0	0	0	0	0
Deltamethrin	0.001	0.00165	0	0	0	0	0	0	0	0	0
Deltamethrin	0.0001	0.000165	0	0	0	0	0	0	0	0	0
Flumethrin	Blank Control	Blank Control	0	0	0	0	0	0	0	0	0
Flumethrin	Acetone Only Control	Acetone Only Control	0	0	0	0	0	0	0	0	0
Flumethrin	1000	1650	5	1	4	5	1	4	5	0	0
Flumethrin	100	165	4	4	0	5	3	2	5	0	0
Flumethrin	10	16.5	3	3	0	5	4	1	5	0	0
Flumethrin	1	1.65	0	0	0	5	3	2	5	2	3
Flumethrin	0.1	0.165	0	0	0	0	0	0	3	3	0
Flumethrin	0.01	0.0165	0	0	0	0	0	0	0	0	0
Flumethrin	0.001	0.00165	0	0	0	0	0	0	0	0	0
Flumethrin	0.0001	0.000165	0	0	0	0	0	0	0	0	0

Compound	Concentration (mg/Ha)	Concentration (ppm)	Time								
			4 Hours			24 Hours			48 Hours		
			A	Kdr	Dead	A	Kdr	Dead	A	Kdr	Dead
Permethrin	Blank Control	Blank Control	0	0	0	0	0	0	0	0	0
Permethrin	Acetone Only Control	Acetone Only Control	0	0	0	0	0	0	0	0	0
Permethrin	1000	1650	5	5	0	5	5	0	5	1	4
Permethrin	100	165	5	5	0	5	4	1	4	0	4
Permethrin	10	16.5	5	5	0	1	1	0	0	0	0
Permethrin	1	1.65	0	0	0	0	0	0	0	0	0
Permethrin	0.1	0.165	0	0	0	0	0	0	0	0	0
Permethrin	0.01	0.0165	0	0	0	0	0	0	0	0	0
Permethrin	0.001	0.00165	0	0	0	0	0	0	0	0	0
Permethrin	0.0001	0.000165	0	0	0	0	0	0	0	0	0
Tau-Fluvalinate	Blank Control	Blank Control	0	0	0	0	0	0	0	0	0
Tau-Fluvalinate	Acetone Only Control	Acetone Only Control	0	0	0	0	0	0	0	0	0
Tau-Fluvalinate	1000	1650	0	0	0	5	5	0	5	5	0
Tau-Fluvalinate	100	165	0	0	0	1	1	0	3	3	0
Tau-Fluvalinate	10	16.5	0	0	0	0	0	0	0	0	0
Tau-Fluvalinate	1	1.65	0	0	0	0	0	0	0	0	0
Tau-Fluvalinate	0.1	0.165	0	0	0	0	0	0	0	0	0
Tau-Fluvalinate	0.01	0.0165	0	0	0	0	0	0	0	0	0
Tau-Fluvalinate	0.001	0.00165	0	0	0	0	0	0	0	0	0
Tau-Fluvalinate	0.0001	0.000165	0	0	0	0	0	0	0	0	0

Species and Species Details: *Dermacentor variabilis*. Hatched 01/12/15. Delivered 13/01/16.

Compound	Concentration (mg/Ha)	Concentration (ppm)	Time								
			4 Hours			24 Hours			48 Hours		
			A	Kdr	Dead	A	Kdr	Dead	A	Kdr	Dead
Deltamethrin	Blank Control	Blank Control	0	0	0	0	0	0	0	0	0
Deltamethrin	Acetone Only Control	Acetone Only Control	0	0	0	0	0	0	0	0	0
Deltamethrin	1000	1650	5	5	0	5	3	2	5	4	1
Deltamethrin	100	165	5	5	0	5	3	2	5	1	4
Deltamethrin	10	16.5	3	2	1	3	2	1	3	2	1
Deltamethrin	1	1.65	0	0	0	0	0	0	0	0	0
Deltamethrin	0.1	0.165	0	0	0	0	0	0	0	0	0
Deltamethrin	0.01	0.0165	0	0	0	0	0	0	0	0	0
Deltamethrin	0.001	0.00165	0	0	0	0	0	0	0	0	0
Deltamethrin	0.0001	0.000165	0	0	0	0	0	0	0	0	0
Flumethrin	Blank Control	Blank Control	0	0	0	0	0	0	0	0	0
Flumethrin	Acetone Only Control	Acetone Only Control	0	0	0	0	0	0	0	0	0
Flumethrin	1000	1650	5	5	0	5	0	5	5	0	5
Flumethrin	100	165	3	3	0	5	1	4	5	0	5
Flumethrin	10	16.5	1	1	0	5	4	1	5	0	5
Flumethrin	1	1.65	0	0	0	5	4	1	5	4	1
Flumethrin	0.1	0.165	0	0	0	3	3	0	4	4	0
Flumethrin	0.01	0.0165	0	0	0	0	0	0	0	0	0
Flumethrin	0.001	0.00165	0	0	0	0	0	0	0	0	0
Flumethrin	0.0001	0.000165	0	0	0	0	0	0	0	0	0

Compound	Concentration (mg/Ha)	Concentration (ppm)	Time								
			4 Hours			24 Hours			48 Hours		
			A	Kdr	Dead	A	Kdr	Dead	A	Kdr	Dead
Permethrin	Blank Control	Blank Control	0	0	0	0	0	0	0	0	0
Permethrin	Acetone Only Control	Acetone Only Control	0	0	0	0	0	0	0	0	0
Permethrin	1000	1650	5	5	0	5	2	3	5	0	5
Permethrin	100	165	2	2	0	5	5	0	2	1	1
Permethrin	10	16.5	0	0	0	0	0	0	0	0	0
Permethrin	1	1.65	0	0	0	0	0	0	0	0	0
Permethrin	0.1	0.165	0	0	0	0	0	0	0	0	0
Permethrin	0.01	0.0165	0	0	0	0	0	0	0	0	0
Permethrin	0.001	0.00165	0	0	0	0	0	0	0	0	0
Permethrin	0.0001	0.000165	0	0	0	0	0	0	0	0	0
Tau-Fluvalinate	Blank Control	Blank Control	0	0	0	0	0	0	0	0	0
Tau-Fluvalinate	Acetone Only Control	Acetone Only Control	0	0	0	0	0	0	0	0	0
Tau-Fluvalinate	1000	1650	5	5	0	5	5	0	5	3	2
Tau-Fluvalinate	100	165	5	5	0	5	5	0	5	4	1
Tau-Fluvalinate	10	16.5	0	0	0	0	0	0	0	0	0
Tau-Fluvalinate	1	1.65	0	0	0	0	0	0	0	0	0
Tau-Fluvalinate	0.1	0.165	0	0	0	0	0	0	0	0	0
Tau-Fluvalinate	0.01	0.0165	0	0	0	0	0	0	0	0	0
Tau-Fluvalinate	0.001	0.00165	0	0	0	0	0	0	0	0	0
Tau-Fluvalinate	0.0001	0.000165	0	0	0	0	0	0	0	0	0

Species and Species Details: *Ixodes ricinus*. From Stables 06/04/2016.

Compound	Concentration (mg/Ha)	Concentration (ppm)	Time								
			4 Hours			24 Hours			48 Hours		
			A	Kdr	Dead	A	Kdr	Dead	A	Kdr	Dead
N/A	Blank Control	Blank Control	0	0	0	0	0	0	0	0	0
N/A	Blank Control	Blank Control	0	0	0	0	0	0	0	0	0
N/A	Blank Control	Blank Control	0	0	0	0	0	0	0	0	0
N/A	Acetone Only Control	Acetone Only Control	0	0	0	0	0	0	0	0	0
N/A	Acetone Only Control	Acetone Only Control	0	0	0	0	0	0	0	0	0
N/A	Acetone Only Control	Acetone Only Control	0	0	0	0	0	0	0	0	0
Deltamethrin	1000	1650	5	0	5	5	0	5	5	0	5
Deltamethrin	100	165	5	1	4	5	0	5	5	0	5
Deltamethrin	10	16.5	5	0	5	5	0	5	5	0	5
Deltamethrin	1	1.65	5	0	5	5	0	5	5	0	5
Deltamethrin	0.1	0.165	5	0	5	5	0	5	5	0	5
Deltamethrin	0.01	0.0165	4	0	4	4	0	4	4	0	4
Deltamethrin	0.001	0.00165	0	0	0	1	0	1	1	0	1
Deltamethrin	0.0001	0.000165	0	0	0	0	0	0	0	0	0
Flumethrin	1000	1650	5	2	3	5	0	5	5	0	5
Flumethrin	100	165	5	1	4	5	0	5	5	0	5
Flumethrin	10	16.5	5	0	5	5	0	5	5	0	5
Flumethrin	1	1.65	5	2	3	5	0	5	5	0	5
Flumethrin	0.1	0.165	3	3	0	4	1	3	5	0	5
Flumethrin	0.01	0.0165	3	1	2	4	1	3	5	0	5
Flumethrin	0.001	0.00165	3	1	2	4	0	4	5	0	5
Flumethrin	0.0001	0.000165	0	0	0	0	0	0	0	0	0

Compound	Concentration (mg/Ha)	Concentration (ppm)	Time								
			4 Hours			24 Hours			48 Hours		
			A	Kdr	Dead	A	Kdr	Dead	A	Kdr	Dead
Permethrin	1000	1650	5	1	4	5	0	5	5	0	5
Permethrin	100	165	5	1	4	5	0	5	5	0	5
Permethrin	10	16.5	5	1	4	5	0	5	5	0	5
Permethrin	1	1.65	3	1	2	5	1	4	5	0	5
Permethrin	0.1	0.165	0	0	0	1	0	1	1	0	1
Permethrin	0.01	0.0165	0	0	0	0	0	0	0	0	0
Permethrin	0.001	0.00165	0	0	0	0	0	0	0	0	0
Permethrin	0.0001	0.000165	0	0	0	0	0	0	0	0	0
Tau-Fluvalinate	1000	1650	5	1	4	5	0	5	5	0	5
Tau-Fluvalinate	100	165	5	1	4	5	0	5	5	0	5
Tau-Fluvalinate	10	16.5	5	2	3	5	0	5	5	0	5
Tau-Fluvalinate	1	1.65	3	0	3	3	0	3	3	0	3
Tau-Fluvalinate	0.1	0.165	0	0	0	0	0	0	0	0	0
Tau-Fluvalinate	0.01	0.0165	0	0	0	0	0	0	0	0	0
Tau-Fluvalinate	0.001	0.00165	0	0	0	0	0	0	0	0	0
Tau-Fluvalinate	0.0001	0.000165	0	0	0	0	0	0	0	0	0

Species and Species Details: *Rhipicephalus sanguineus*. Hatched 04/03/16. Delivered 06/04/16.

Compound	Concentration (mg/Ha)	Concentration (ppm)	Time								
			4 Hours			24 Hours			48 Hours		
			A	Kdr	Dead	A	Kdr	Dead	A	Kdr	Dead
Deltamethrin	Blank Control	Blank Control	0	0	0	0	0	0	0	0	0
Deltamethrin	Acetone Only Control	Acetone Only Control	0	0	0	0	0	0	0	0	0
Deltamethrin	50	1650	5	4	1	5	2	3	5	1	4
Deltamethrin	5	165	5	5	0	5	5	0	5	5	0
Deltamethrin	0.5	16.5	5	5	0	3	1	2	4	2	2
Deltamethrin	0.05	1.65	3	3	0	2	1	1	1	0	1
Deltamethrin	0.005	0.165	0	0	0	1	1	0	1	1	0
Deltamethrin	0.0005	0.0165	0	0	0	0	0	0	0	0	0
Deltamethrin	0.00005	0.00165	0	0	0	0	0	0	0	0	0
Deltamethrin	0.000005	0.000165	0	0	0	0	0	0	0	0	0
Flumethrin	Blank Control	Blank Control	0	0	0	0	0	0	0	0	0
Flumethrin	Acetone Only Control	Acetone Only Control	0	0	0	0	0	0	0	0	0
Flumethrin	50	1650	5	0	5	5	2	3	5	0	5
Flumethrin	5	165	5	0	5	5	2	3	5	0	5
Flumethrin	0.5	16.5	5	2	3	5	3	2	5	0	5
Flumethrin	0.05	1.65	2	2	0	5	5	0	5	5	0
Flumethrin	0.005	0.165	0	0	0	3	2	1	4	2	2
Flumethrin	0.0005	0.0165	0	0	0	0	0	0	1	1	0
Flumethrin	0.00005	0.00165	0	0	0	0	0	0	0	0	0
Flumethrin	0.000005	0.000165	0	0	0	0	0	0	0	0	0

Compound	Concentration (mg/Ha)	Concentration (ppm)	Time								
			4 Hours			24 Hours			48 Hours		
			A	Kdr	Dead	A	Kdr	Dead	A	Kdr	Dead
Permethrin	Blank Control	Blank Control	0	0	0	0	0	0	0	0	0
Permethrin	Acetone Only Control	Acetone Only Control	0	0	0	0	0	0	0	0	0
Permethrin	50	1650	5	5	0	5	1	4	5	0	5
Permethrin	5	165	5	5	0	5	1	4	5	0	5
Permethrin	0.5	16.5	3	3	0	5	3	2	5	1	4
Permethrin	0.05	1.65	1	1	0	2	2	0	5	2	3
Permethrin	0.005	0.165	0	0	0	0	0	0	0	0	0
Permethrin	0.0005	0.0165	0	0	0	0	0	0	0	0	0
Permethrin	0.00005	0.00165	0	0	0	0	0	0	0	0	0
Permethrin	0.000005	0.000165	0	0	0	0	0	0	0	0	0
Tau-Fluvalinate	Blank Control	Blank Control	0	0	0	0	0	0	0	0	0
Tau-Fluvalinate	Acetone Only Control	Acetone Only Control	0	0	0	0	0	0	0	0	0
Tau-Fluvalinate	50	1650	5	5	0	5	4	1	5	3	2
Tau-Fluvalinate	5	165	5	5	0	5	5	0	5	5	0
Tau-Fluvalinate	0.5	16.5	0	0	0	5	5	0	1	1	0
Tau-Fluvalinate	0.05	1.65	0	0	0	0	0	0	1	1	0
Tau-Fluvalinate	0.005	0.165	0	0	0	0	0	0	0	0	0
Tau-Fluvalinate	0.0005	0.0165	0	0	0	0	0	0	0	0	0
Tau-Fluvalinate	0.00005	0.00165	0	0	0	0	0	0	0	0	0
Tau-Fluvalinate	0.000005	0.000165	0	0	0	0	0	0	0	0	0

Species and Species Details: *Varroa destructor*. From The Honey Farm, Imkerei Ullmann, Erlensee, Germany. Summer 2016.

Compound	Concentration (mg/Ha)	Concentration (ppm)	Time														
			2 Hours			4 Hours			6 Hours			8 Hours			10 Hours		
			A	Kdr	Dead	A	Kdr	Dead	A	Kdr	Dead	A	Kdr	Dead	A	Kdr	Dead
N/A	Blank Control	Blank Control	0	0	0	0	0	0	1	1	0	1	1	0	1	1	0
N/A	Acetone Only Control	Acetone Only Control	0	0	0	0	0	0	0	0	0	0	0	0	2	2	0
Deltamethrin	100	165	5	5	0	5	3	2	5	2	3	5	0	5	5	0	5
Deltamethrin	10	16.5	5	5	0	5	5	0	5	4	1	5	2	3	5	0	5
Deltamethrin	1	1.65	5	5	0	5	5	0	5	5	0	5	5	0	3	3	0
Deltamethrin	0.1	0.165	1	1	0	2	2	0	3	3	0	5	5	0	3	3	0
Deltamethrin	0.01	0.0165	0	0	0	0	0	0	1	1	0	2	0	2	4	2	2
Deltamethrin	0.001	0.00165	0	0	0	0	0	0	0	0	0	0	0	0	0	0	0
N/A	Blank Control	Blank Control	0	0	0	2	2	0	0	4	0	4	3	1	4	0	4
N/A	Acetone Only Control	Acetone Only Control	0	0	0	0	0	0	0	0	0	0	0	0	3	3	0
Flumethrin	100	165	5	4	1	5	1	4	5	0	5	5	0	5	5	0	5
Flumethrin	10	16.5	3	3	0	5	1	4	5	0	5	5	0	5	5	0	5
Flumethrin	1	1.65	3	3	0	5	4	1	5	3	2	5	0	5	5	0	5
Flumethrin	0.1	0.165	0	0	0	3	2	1	5	3	2	5	2	3	5	1	4
Flumethrin	0.01	0.0165	0	0	0	0	0	0	1	0	1	3	2	1	4	2	1
Flumethrin	0.001	0.00165	0	0	0	0	0	0	2	2	2	5	2	3	5	1	4
N/A	Blank Control	Blank Control	0	0	0	0	0	0	0	0	0	1	1	0	3	3	0
N/A	Acetone Only Control	Acetone Only Control	0	0	0	0	0	0	1	1	0	0	0	0	3	2	1
Permethrin	100	165	5	5	0	5	4	1	5	1	4	5	0	5	5	0	5
Permethrin	10	16.5	5	5	0	5	5	0	5	5	0	5	3	2	5	3	2
Permethrin	1	1.65	5	5	0	5	5	0	5	4	1	5	4	1	5	4	1
Permethrin	0.1	0.165	0	0	0	0	0	0	4	4	0	4	4	0	4	4	0
Permethrin	0.01	0.0165	0	0	0	0	0	0	0	0	0	0	0	0	1	0	1
Permethrin	0.001	0.00165	0	0	0	0	0	0	1	0	1	1	0	1	4	3	1

Compound	Concentration (mg/Ha)	Concentration (ppm)	Time														
			2 Hours			4 Hours			6 Hours			8 Hours			10 Hours		
			A	Kdr	Dead	A	Kdr	Dead	A	Kdr	Dead	A	Kdr	Dead	A	Kdr	Dead
N/A	Blank Control	Blank Control	0	0	0	0	0	0	2	2	0	4	4	0	4	1	3
N/A	Acetone Only Control	Acetone Only Control	0	0	0	3	3	0	2	0	2	2	0	2	4	1	3
Tau-Fluvalinate	100	165	5	5	0	5	5	0	5	5	0	4	1	3	5	0	5
Tau-Fluvalinate	10	16.5	5	5	0	5	5	0	5	5	0	5	2	3	4	0	4
Tau-Fluvalinate	1	1.65	0	0	0	0	0	0	1	1	0	1	1	0	2	0	2
Tau-Fluvalinate	0.1	0.165	0	0	0	0	0	0	1	1	0	3	3	0	3	0	3
Tau-Fluvalinate	0.01	0.0165	0	0	0	0	0	0	2	2	0	3	3	0	3	3	0
Tau-Fluvalinate	0.001	0.00165	0	0	0	0	0	0	0	0	0	2	2	0	0	0	0

10.5 Appendix 5

Dose-response curves for tick species and *M. domestica* from comparative pyrethroid contact bioassays. Five adult arthropods were used per test vial with three repeats, giving a total of n = 15 for each pyrethroid concentration. Probit analysis/logistic regression assumed a common slope parameter across species for each insecticide at each assessment time, allowing a comparison of the EC_{50} values via assessment of differences in the logit proportion intercept parameter for each tick species relative to that for *M. domestica*. Differences in intercept parameter values were assessing using a z-test, with a significant difference ($p < 0.05$) in intercept values indicating a significant difference ($p < 0.05$) in the associated EC_{50} estimates.

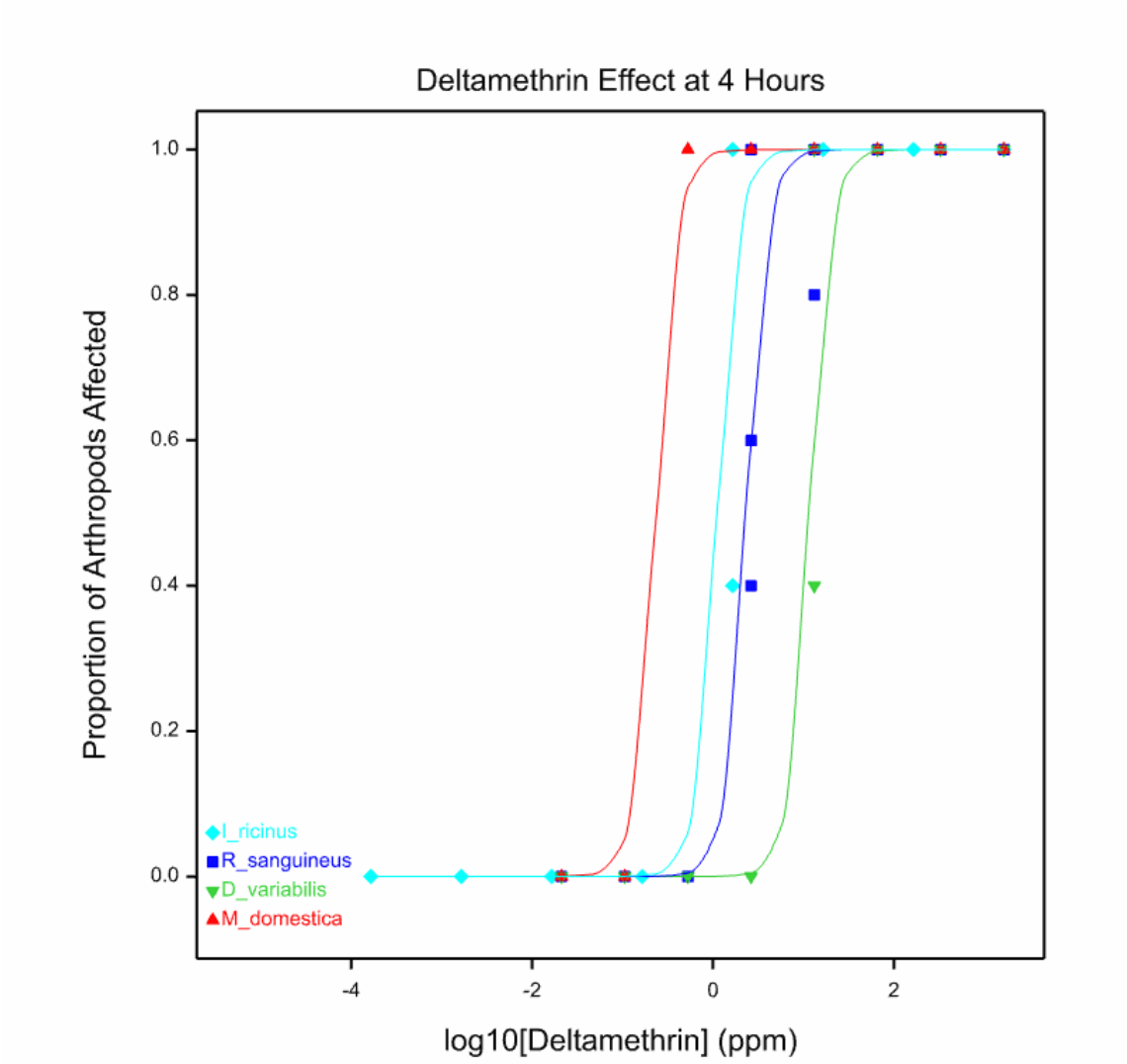

Species	Difference in intercept parameter relative to *M. domestica* (proportion)	Standard Error (s.e.)	z-statistic	p-value
D. variabilis	-14.14	3.34	-4.23	<.001
R. sanguineus	-8.33	2.15	-3.88	<.001
I. ricinus	-5.64	1.86	-3.03	0.002

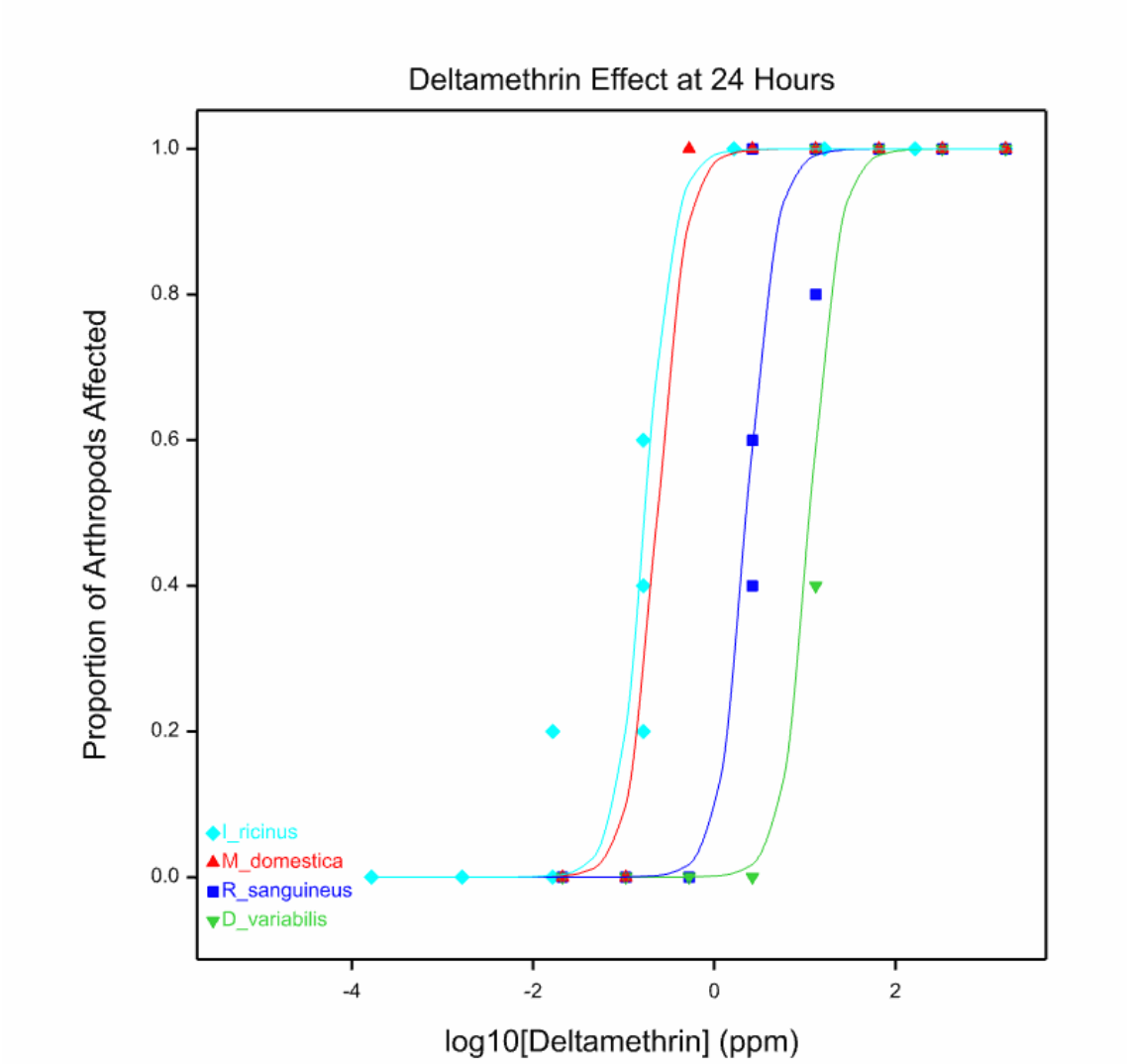

Species	Difference in intercept parameter relative to *M. domestica* (proportion)	Standard Error (s.e.)	z-statistic	p-value
D. variabilis	-10.64	2.06	-5.17	<.001
R. sanguineus	-6.23	1.37	-4.53	<.001
I. ricinus	0.849	0.811	1.05	0.295

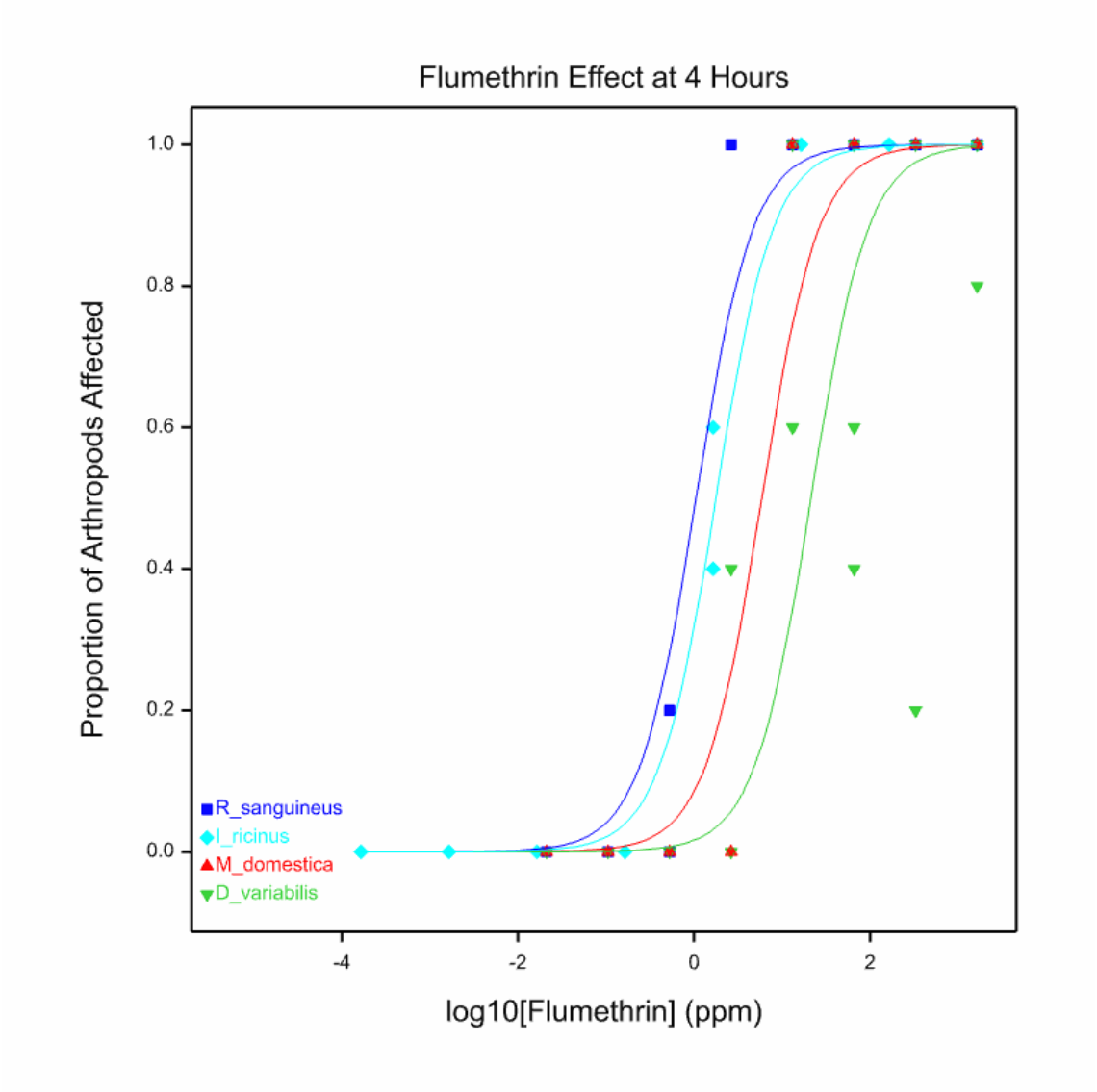

Species	Difference in intercept parameter relative to *M. domestica* (proportion)	Standard Error (s.e.)	z-statistic	p-value
D. variabilis	-1.729	0.570	-3.03	0.002
R. sanguineus	2.308	0.595	3.88	<.001
I. ricinus	1.614	0.612	2.64	0.008

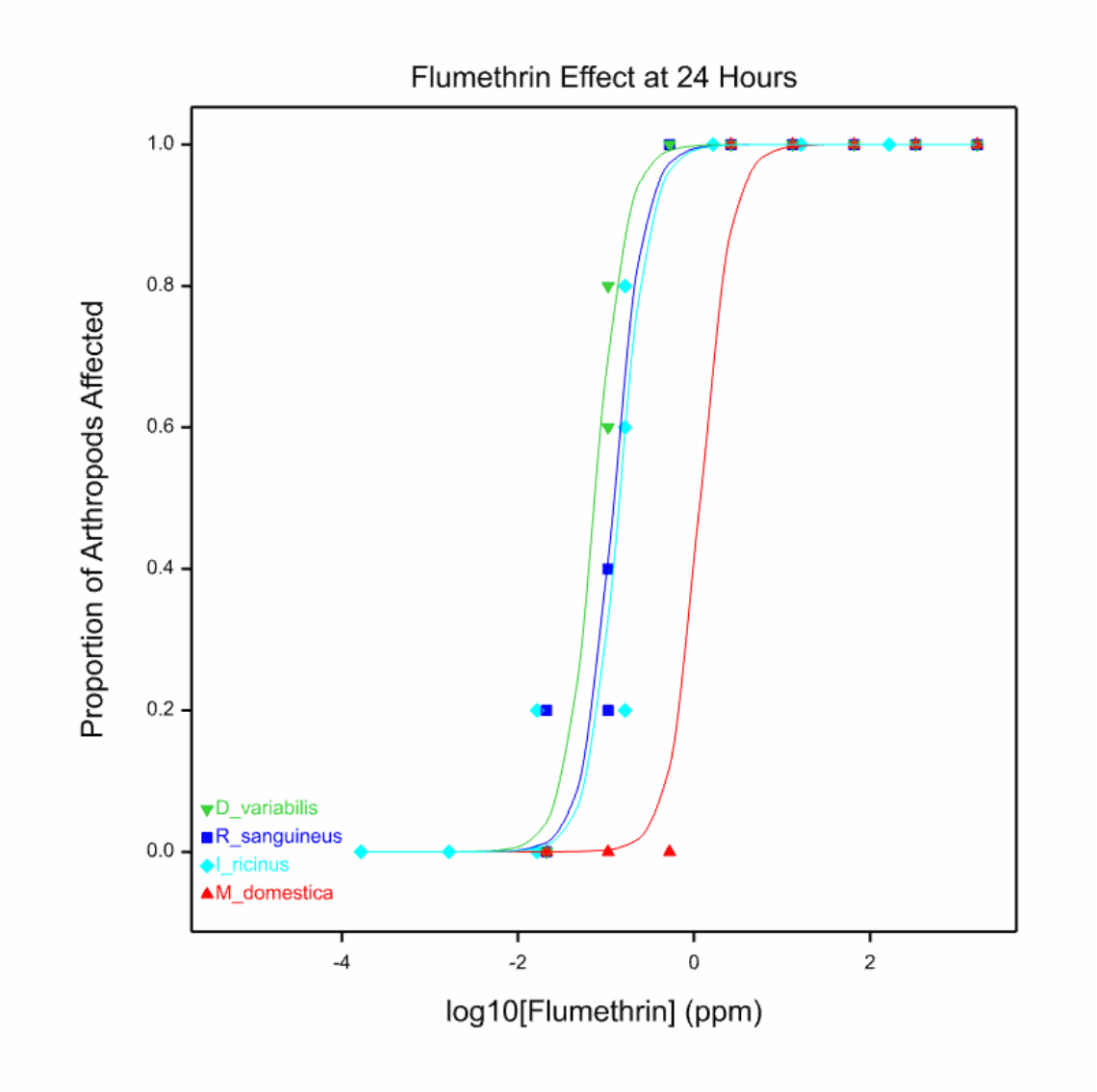

Species	Difference in intercept parameter relative to *M. domestica* (proportion)	Standard Error (s.e.)	z-statistic	p-value
D. variabilis	6.81	1.28	5.34	<.001
R. sanguineus	5.62	1.18	4.75	<.001
I. ricinus	5.26	1.09	4.81	<.001

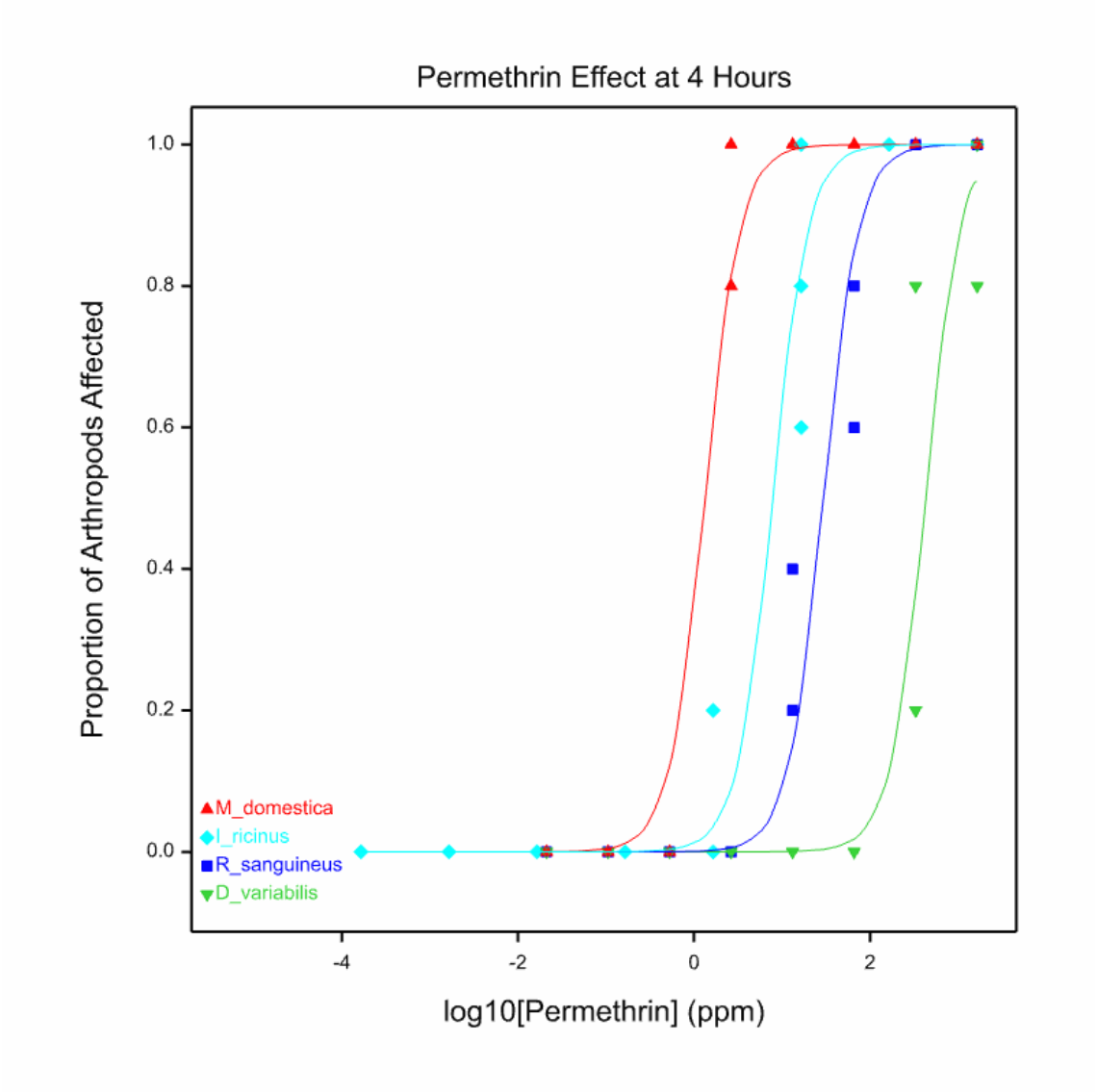

Species	Difference in intercept parameter relative to *M. domestica* (proportion)	Standard Error (s.e.)	z-statistic	p-value
D. variabilis	-12.41	1.77	-7.01	<.001
R. sanguineus	-6.67	1.13	-5.89	<.001
I. ricinus	-3.809	0.992	-3.84	<.001

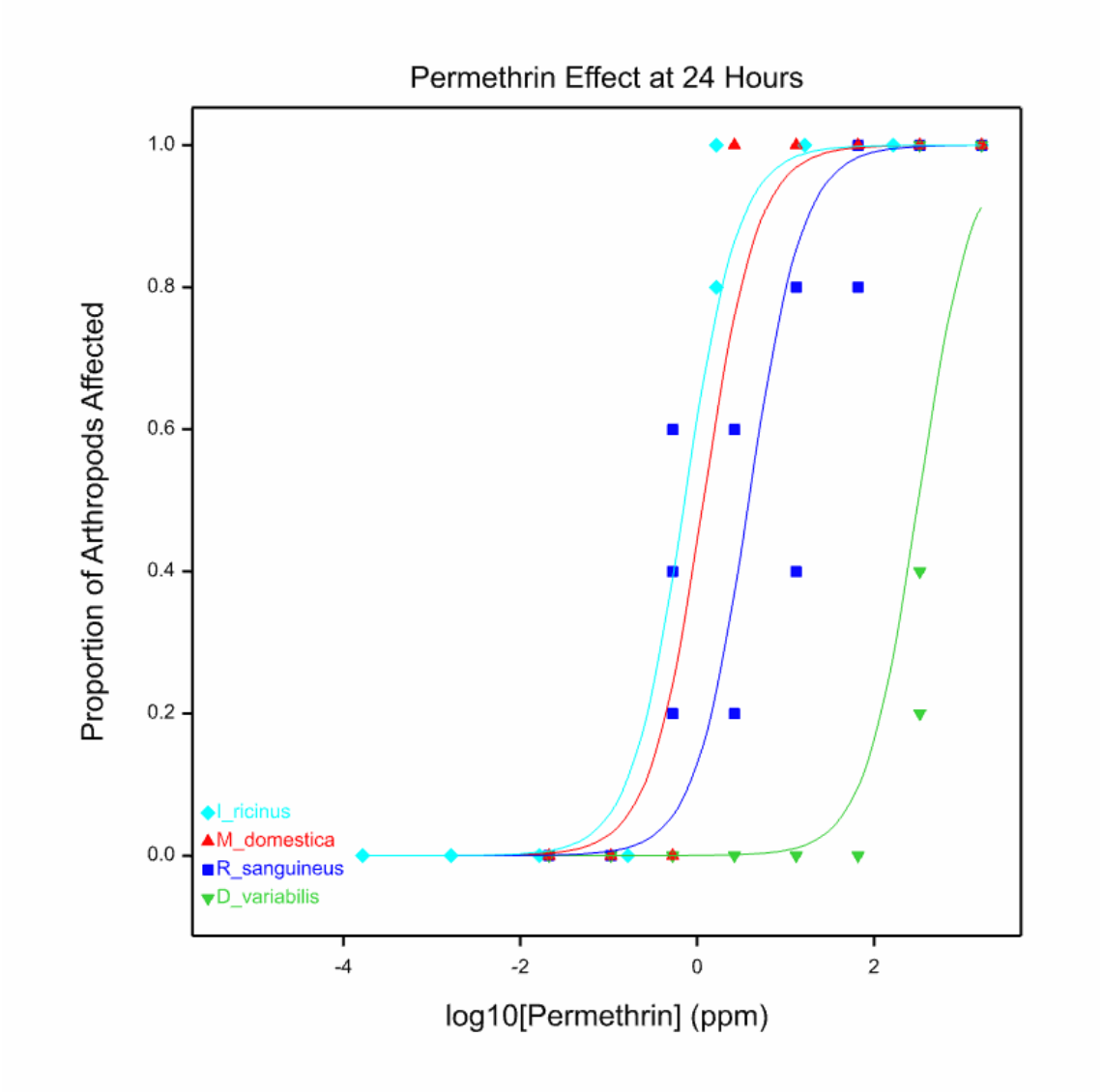

Species	Difference in intercept parameter relative to *M. domestica* (proportion)	Standard Error (s.e.)	z-statistic	p-value
D. variabilis	-7.99	1.06	-7.54	<.001
R. sanguineus	-1.683	0.586	-2.87	0.004
I. ricinus	0.703	0.621	1.13	0.258

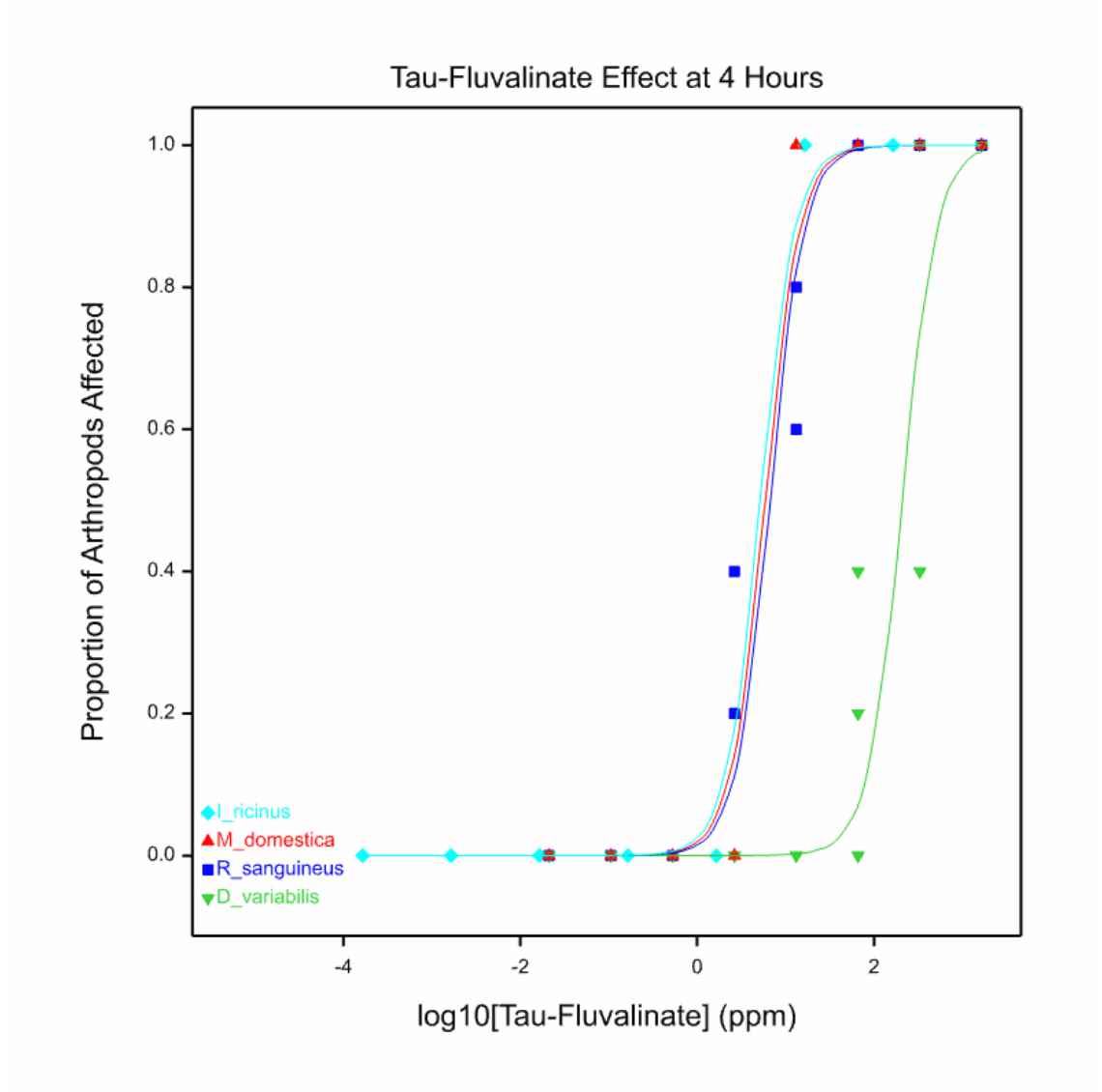

Species	Difference in intercept parameter relative to *M. domestica* (proportion)	Standard Error (s.e.)	z-statistic	p-value
D. variabilis	-8.00	1.28	-6.23	<.001
R. sanguineus	-0.264	0.728	-0.36	0.717
I. ricinus	0.277	0.879	0.31	0.753

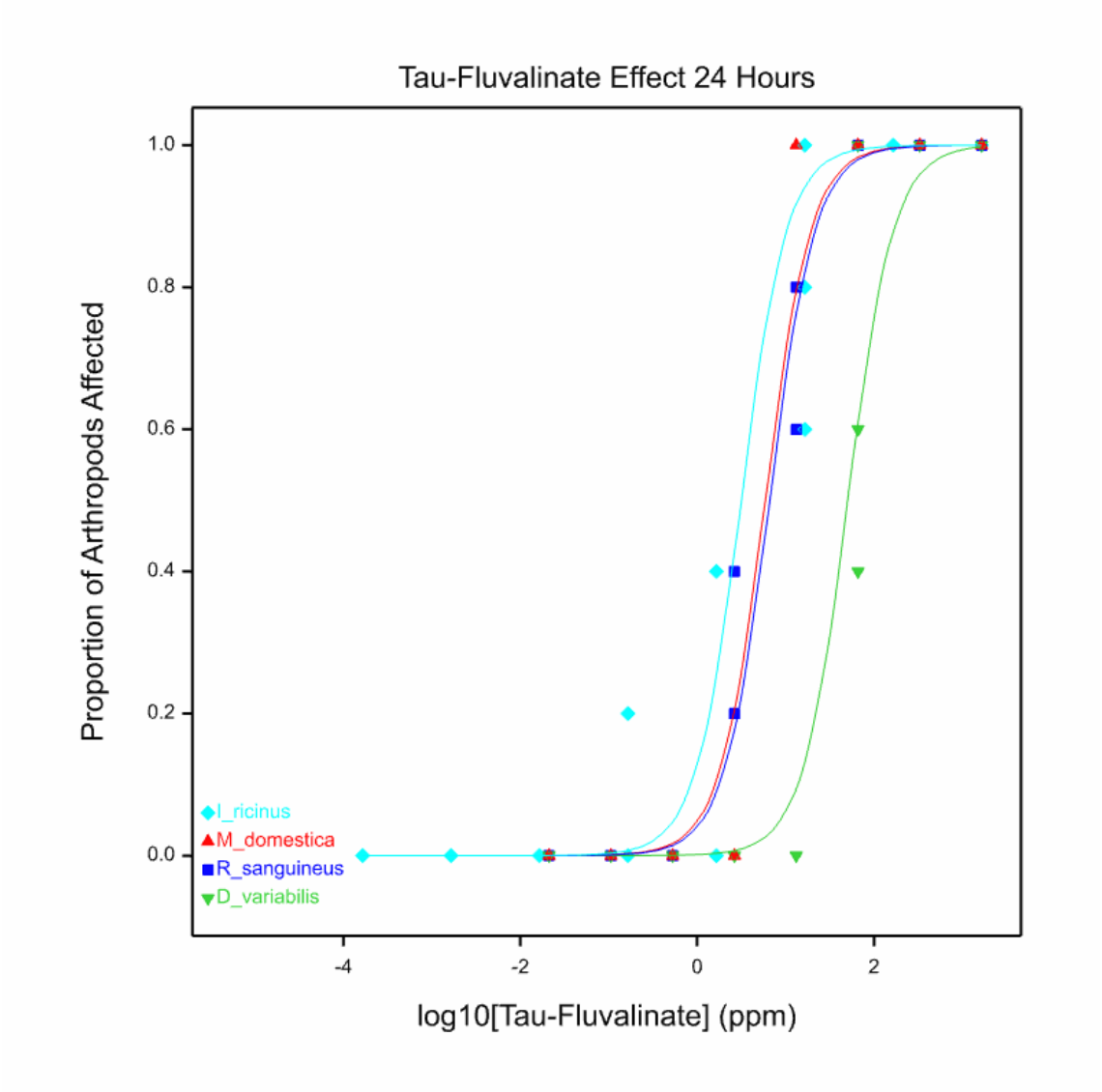

Species	Difference in intercept parameter relative to *M. domestica* (proportion)	Standard Error (s.e.)	z-statistic	p-value
D. variabilis	-3.626	0.747	-4.85	<.001
R. sanguineus	-0.185	0.607	-0.30	0.761
I. ricinus	1.06	0.691	1.54	0.125

11 Online References

Babraham Bioinformatics (2016) FastQC **http://www.bioinformatics.babraham.ac.uk/projects/fastqc/** Accessed September 2016

Centers for Disease control and Prevention (2016) Diagnosis and Management of Tick-borne Rickettsial Diseases: Rocky Mountain Spotted Fever and Other Spotted Fever Group Rickettsioses, Ehrlichioses, and Anaplasmosis - United States. A Practical Guide for Health Care and Public Health Professionals **http://www.cdc.gov/mmwr/volumes/65/rr/rr6502a1.htm?s_cid=rr6502a1_w** Accessed September 2016

Centers for Disease control and Prevention (2015) Lyme Disease **http://www.cdc.gov/lyme/** Accessed September 2016

Centers for Disease control and Prevention (2015b) Preventing Tick Bites **http://www.cdc.gov/ticks/avoid/on_people.html** Accessed September 2016

ChemSpider (2016) **http://www.chemspider.com/**
Cypermethrin: CSID
Deltamethrin: CSID 37079
Flumethrin: CSID 82804
Permethrin: CSID 36845
Pyrethrin I: CSID 4444510
Pyrethrin II: CSID 4444882
Tau-fluvalinate: CSID 82865
Accessed September 2016

Encyclopædia Britannica (2016) Acarid **http://www.britannica.com/animal/acarid** Accessed September 2016

European Centre for Disease Prevention and Control (2016) Communication Toolkit on Tick-Borne Diseases **http://ecdc.europa.eu/en/healthtopics/emerging_and_vector-borne_diseases/tick_borne_diseases/public_health_measures/pages/communication_toolkit.aspx** Accesses September 2016

Health Protection Agency (2012) Tick Surveillance Scheme **https://www.gov.uk/guidance/tick-surveillance-scheme** Accessed September 2016

Health Protection Agency (2013) Lyme Borreliosis Epidemiology and Surveillance (In England and Wales) **https://www.gov.uk/government/publications/lyme-borreliosis-epidemiology/lyme-borreliosis-epidemiology-and-surveillance** Accessed September 2016

Monsanto AgBio™ (2014) Met52®EC Liquid Bioinsecticide **http://www.monsanto.com/sitecollectiondocuments/bioag/united-states/dsm-hort-met52ec-lr.pdf** Accessed September 2016

Alain Migeon And Franck Dorkeld Spider Mites Web: A Comprehensive Database for the Tetranychidae (2006-2015) **http://www.montpellier.inra.fr/CBGP/spmweb** Accessed September 2016

World Health Organisation (1959) Joint WHO/FAO Expert Committee on Zoonoses: Second Report **https://extranet.who.int/iris/restricted/handle/10665/40435** Accessed September 2016

World Health Organisation (2011) Immunization, Vaccines and Biologicals: Tick-Borne Encephalitis **http://www.who.int/immunization/topics/tick_encephalitis/en/index.html** Accessed September 2016

World Health Organisation Regional Office for South East Asia (2016) Frequently Asked Questions Scrub Typhus **http://www.searo.who.int/entity/emerging_diseases/CDS_faq_Scrub_Typhus.pdf?ua=1** Accessed September 2016

World Organisation for Animal Health (2016) OIE-Listed Diseases, Infections and Infestations in Force in 2016 **http://www.oie.int/animal-health-in-the-world/oie-listed-diseases-2016/** Accessed September 2016

12 Bibliography

Abolins, S., Thind, B., Jackson, V., Luke, B., Moore, D., Wall, R., and Taylor, M. A. (2007). Control of the sheep scab mite *Psoroptes ovis in vivo* and *in vitro* using fungal pathogens. *Veterinary Parasitology* **148**, 310-317.

Agnew, W. S., Moore, A. C., Levinson, S. R., and Raftery, M. A. (1980). Identification of a large molecular-weight peptide associated with a tetrodotoxin binding-protein from the electroplax of *Electrophorus electricus*. *Biochemical and Biophysical Research Communications* **92**, 860-866.

Alao, O. R., and Decker, C. F. (2012). Lyme Disease. *Disease-a-Month* **58**, 335-345.

Alessandra, T., and Santo, C. (2012). Tick-borne diseases in sheep and goats: Clinical and diagnostic aspects. *Small Ruminant Research* **106**, 6-11.

Aljamali, M. N., Sauer, J. R., and Essenberg, R. C. (2002). RNA interference: Applicability in tick research. *Experimental and Applied Acarology* **28**, 89-96.

Alquisira-Ramirez, E., Paredes-Gonzalez, J. R., Hernandez-Velazquez, V. M., Ramirez-Trujillo, J. A., and Pena-Chora, G. (2014). In vitro susceptibility of *Varroa destructor* and *Apis mellifera* to native strains of *Bacillus thuringiensis*. *Apidologie* **45**, 707-718.

Attia, S., Grissa, K. L., Lognay, G., Bitume, E., Hance, T., and Mailleux, A. C. (2013). A review of the major biological approaches to control the worldwide pest *Tetranychus urticae* (Acari: Tetranychidae) with special reference to natural pesticides. *Journal of Pest Science* **86**, 361-386.

Barzman, M., Barberi, P., Birch, A. N. E., Boonekamp, P., Dachbrodt-Saaydeh, S., Graf, B., Hommel, B., Jensen, J. E., Kiss, J., Kudsk, P., Lamichhane, J. R., Messean, A., Moonen, A. C., Ratnadass, A., Ricci, P., Sarah, J. L., and Sattin, M. (2015). Eight principles of integrated pest management. *Agronomy for Sustainable Development* **35**, 1199-1215.

Bertani, G. (1951). Studies on Lysogenesis 1: The Mode of Phage Liberation by Lysogenic *Escherichia coli Journal of Bacteriology* **62**, 293-300.

Beugnet, F., and Franc, M. (2012). Insecticide and acaricide molecules and/or combinations to prevent pet infestation by ectoparasites. *Trends in Parasitology* **28**, 267-279.

Bloomquist, J. R. (1996). Ion channels as targets for insecticides. *Annual Review of Entomology* **41**, 163-190.

Brackenbury, W. J., and Isom, L. L. (2011). Na+ channel beta subunits: overachievers of the ion channel family. *Frontiers in Pharmacology* **2**, 11.

Bugeme, D. M., Knapp, M., Ekesi, S., Chabi-Olaye, A., Boga, H. I., and Maniania, N. K. (2015). Efficacy of *Metarhizium anisopliae* in controlling the two-spotted spider mite *Tetranychus urticae* on common bean in screenhouse and field experiments. *Insect Science* **22**, 121-128.

Burgess, S. T. G., Nunn, F., Nath, M., Frew, D., Wells, B., Marr, E. J., Huntley, J. F., McNeilly, T. N., and Nisbet, A. J. (2016). A recombinant subunit vaccine for the control of ovine psoroptic mange (sheep scab). *Veterinary Research* **47**, 1-8.

Burton, M. J. (2012). Molecular basis of pyrethroid sensitivity and resistance, The University of Nottingham, Nottingham; UK.

Burton, M. J., Mellor, I. R., Duce, I. R., Davies, T. G. E., Field, L. M., and Williamson, M. S. (2011). Differential resistance of insect sodium channels with kdr mutations to deltamethrin, permethrin and DDT. *Insect Biochemistry and Molecular Biology* **41**, 723-732.

Busvine, J. R. (1951). Mechanism of Resistance to Insecticide in Houseflies. *Nature* **168**, 193-195.

Campbell, E. M., Budge, G. E., and Bowman, A. S. (2010). Gene-knockdown in the honey bee mite *Varroa destructor* by a non-invasive approach: Studies on a glutathione S-transferase. *Parasites & Vectors* **3**, 1-10.

Campbell, N. A., Reece, J. B., Urry, L. A., Cain, M. L., Wasserman, S. A., Minorsky, P. V., and Jackson, R. B. (2015). "Biology: A Global Approach," Tenth Edition/Ed. Pearson Education Limited, Harlow; UK.

Carroll, J. F., Klun, J. A., and Debboun, M. (2005). Repellency of deet and SS220 applied to skin involves olfactory sensing by two species of ticks. *Medical and Veterinary Entomology* **19**, 101-106.

Casida, J. E. (1980). Pyrethrum flowers and pyrethroid insecticides. *Environmental Health Perspectives* **34**, 189-202.

Casida, J. E., Gammon, D. W., Glickman, A. H., and Lawrence, L. J. (1983). Mechanisms of Selective Action of Pyrethroid Insecticides. *Annual Review of Pharmacology and Toxicology* **23**, 413-438.

Catterall, W. A. (1980). Neurotoxins that act on voltage-sensitive sodium channels in excitable membranes. *Annual Review of Pharmacology and Toxicology* **20**, 15-43.

Catterall, W. A. (2000). From ionic currents to molecular mechanisms: The structure and function of voltage-gated sodium channels. *Neuron* **26**, 13-25.

Catterall, W. A. (2012). Voltage-gated sodium channels at 60: Structure, function and pathophysiology. *The Journal of Physiology* **590**, 2577-2589.

Clover, J. R., and Lane, R. S. (1995). Evidence Implicating Nymphal *Ixodes Pacificus* (Acari, Ixodidae) in the Epidemiology of Lyme-Disease in California. *American Journal of Tropical Medicine and Hygiene* **53**, 237-240.

Cock, M. J. W., van Lenteren, J. C., Brodeur, J., Barratt, B. I. P., Bigler, F., Bolckmans, K., Consoli, F. L., Haas, F., Mason, P. G., and Parra, J. R. P. (2010). Do new access and benefit sharing procedures under the convention on biological diversity threaten the future of biological control? *Biocontrol* **55**, 199-218.

Colwell, D. D., Dantas-Torres, F., and Otranto, D. (2011). Vector-borne parasitic zoonoses: Emerging scenarios and new perspectives. *Vet Parasitol* **182**, 14-21.

Cong, L., Ran, F. A., Cox, D., Lin, S. L., Barretto, R., Habib, N., Hsu, P. D., Wu, X. B., Jiang, W. Y., Marraffini, L. A., and Zhang, F. (2013). Multiplex Genome Engineering Using CRISPR/Cas Systems. *Science* **339**, 819-823.

Dantas-Torres, F., Chomel, B. B., and Otranto, D. (2012). Ticks and tick-borne diseases: A one health perspective. *Trends in Parasitology* **28**, 437-446.

Dascal, N. (2001). Voltage clamp recordings from *Xenopus* oocytes. *Current protocols in neuroscience* **10**, 1-6.

Davies, T. G. E., Field, L. M., Usherwood, P. N. R., and Williamson, M. S. (2007). DDT, pyrethrins, pyrethroids and insect sodium channels. *Iubmb Life* **59**, 151-162.

Davies, T. G. E., O'Reilly, A. O., Field, L. M., Wallace, B. A., and Williamson, M. S. (2008). Knockdown resistance to DDT and pyrethroids: From target-site mutations to molecular modelling. *Pest Management Science* **64**, 1126-1130.

Day, M. J. (2011). The immunopathology of canine vector-borne diseases. *Parasites & Vectors* **4**, 1-13.

de Faria, M. R., and Wraight, S. P. (2007). Mycoinsecticides and mycoacaricides: A comprehensive list with worldwide coverage and international classification of formulation types. *Biological Control* **43**, 237-256.

de la Fuente, J., Almazan, C., Naranjo, V., Blouin, E. F., Meyer, J. M., and Kocan, K. M. (2006). Autocidal control of ticks by silencing of a single gene by RNA interference. *Biochemical and Biophysical Research Communications* **344**, 332-338.

de Miranda, J. R., and Genersch, E. (2010). Deformed wing virus. *Journal of Invertebrate Pathology* **103**, 48-61.

Decourtye, A., Mader, E., and Desneux, N. (2010). Landscape enhancement of floral resources for honey bees in agro-ecosystems. *Apidologie* **41**, 264-277.

Deplazes, P., Eckert, J., Mathis, A., Samson-Himmelstjerna, G. V., and Zahner, H. (2016). "Parasitology in veterinary medicine," Wageningen Academic Publishers, Wageningen; NL.

Dietemann, V., Pflugfelder, J., Anderson, D., Charriere, J. D., Chejanovsky, N., Dainat, B., de Miranda, J., Delaplane, K., Dillier, F. X., Fuch, S., Gallmann, P., Gauthier, L., Imdorf, A., Koeniger, N., Kralj, J., Meikle, W., Pettis, J., Rosenkranz, P., Sammataro, D., Smith, D., Yanez, O., and Neumann, P. (2012). Varroa destructor: Research avenues towards sustainable control. *Journal of Apicultural Research* **51**, 125-132.

Dong, K., Du, Y. Z., Rinkevich, F. D., Nomura, Y., Xu, P., Wang, L. F., Silver, K., and Zhorov, B. S. (2014). Molecular biology of insect sodium channels and pyrethroid resistance. *Insect biochemistry and molecular biology* **50**, 1-17.

Drexler, N. A., Dahlgren, F. S., Heitman, K. N., Massung, R. F., Paddock, C. D., and Behravesh, C. B. (2016). National Surveillance of Spotted Fever Group Rickettsioses in the United States, 2008-2012. *American Journal of Tropical Medicine and Hygiene* **94**, 26-34.

Du, Y. Z., Khambay, B., and Dong, K. (2011). An important role of a pyrethroid-sensing residue F1519 in the action of the N-alkylamide insecticide BTG 502 on the cockroach sodium channel. *Insect Biochemistry and Molecular Biology* **41**, 446-450.

Du, Y. Z., Liu, Z. Q., Nomura, Y., Khambay, B., and Dong, K. (2006). An alanine in segment 3 of domain III (IIIS3) of the cockroach sodium channel contributes to the low pyrethrold sensitivity of an alternative splice variant. *Insect Biochemistry and Molecular Biology* **36**, 161-168.

Du, Y. Z., Nomura, Y., Liu, Z. Q., Huang, Z. Y., and Dong, K. (2009a). Functional expression of an arachnid sodium channel reveals residues responsible for tetrodotoxin resistance in invertebrate sodium channels. *Journal of Biological Chemistry* **284**, 33869-33875.

Du, Y. Z., Nomura, Y., Luo, N., Liu, Z., Lee, J. E., Khambay, B., and Dong, K. (2009b). Molecular determinants on the insect sodium channel for the specific action of type II pyrethroid insecticides. *Toxicology and Applied Pharmacology* **234**, 266-272.

Du, Y. Z., Nomura, Y., Satar, G., Hu, Z. N., Nauen, R., He, S. Y., Zhorov, B. S., and Dong, K. (2013). Molecular evidence for dual pyrethroid-receptor sites on a mosquito sodium channel. *Proceedings of the National Academy of Sciences of the United States of America* **110**, 11785-11790.

Dunstand-Guzman, E., Pena-Chora, G., Hallal-Calleros, C., Perez-Martinez, M., Hernandez-Velazquez, V. M., Morales-Montor, J., and Flores-Perez, F. I. (2015). Acaricidal effect and histological damage induced by *Bacillus thuringiensis* protein extracts on the mite *Psoroptes cuniculi*. *Parasites & Vectors* **8**, 1-9.

Eiden, A. L., Kaufman, P. E., Oi, F. M., Allan, S. A., and Miller, R. J. (2015). Detection of permethrin resistance and fipronil tolerance in *Rhipicephalus sanguineus* (Acari: Ixodidae) in the United States. *Journal of Medical Entomology* **52**, 429-436.

Eisen, R. J., Eisen, L., Castro, M. B., and Lane, R. S. (2003). Environmentally related variability in risk of exposure to Lyme disease spirochetes in northern California: Effect of climatic conditions and habitat type. *Environmental Entomology* **32**, 1010-1018.

Eisen, R. J., Mun, J. M., Eisen, L., and Lane, R. S. (2004). Life stage-related differences in density of questing ticks and infection with *Borrelia burgdorferi* sensu lato within a single cohort of *Ixodes pacificus* (Acari : Ixodidae). *Journal of Medical Entomology* **41**, 768-773.

Eldursi, N., Mellor, I. R., and Usherwood, P. N. R. (1997). Comparison of NMDA receptors expressed in *Xenopus laevis* oocytes following injection of rat brain RNA and mRNA encoding the NR1A subunit. *British Journal of Pharmacology* **122**, P64-P64.

Elliott, M. (1989). The pyrethroids - Early discovery, recent advances and the future. *Pesticide Science* **27**, 337-351.

Estrada-Pena, A., and Mans, B. J. (2014). Tick-induced paralysis and toxicoses. *In* "Biology of Ticks" (D. E. Sonenshine, Roe, R.M., ed.), Vol. 2, pp. 313-332. Oxford University Press, New York; USA.

Feng, G. P., Deak, P., Chopra, M., and Hall, L. M. (1995). Cloning and functional analysis of Tipe, a novel membrane protein that enhances *Drosophila para* sodium channel function. *Cell* **82**, 1001-1011.

Fiddes, M. D., Le Gresley, S., Parsons, D. G., Epe, C., Coles, G. C., and Stafford, K. A. (2005). Prevalence of the poultry red mite (*Dermanyssus gallinae*) in England. *Veterinary Record* **157**, 233-235.

Finney, D. J. (1947). "Probit analysis," Cambridge University Press, Cambridge; UK.

Flamini, G. (2006). Acaricides of natural origin. Part 2. Review of the literature (2002-2006). *Natural Product Communications* **1**, 1151-1158.

Foelix, R. F., and Axtell, R. C. (1972). Ultrastructure of Haller's organ in the tick *Amblyoma americanum* (L.). *Zeitschrift Fur Zellforschung Und Mikroskopische Anatomie* **124**, 275-292.

Garbian, Y., Maori, E., Kalev, H., Shafir, S., and Sela, I. (2012). Bidirectional transfer of RNAi between honey bee and *Varroa destructor: Varroa* gene silencing reduces *Varroa* population. *Plos Pathogens* **8**, 1-9.

Genersch, E., and Aubert, M. (2010). Emerging and re-emerging viruses of the honey bee (*Apis mellifera* L.). *Veterinary Research* **41**, 1-20.

George, D. R., Guy, J. H., Arkle, S., Harrington, D., De Luna, C., Okello, E. J., Shiel, R. S., Port, G., and Sparagano, O. A. E. (2008). Use of plant-derived products to control arthropods of veterinary importance: A review. *In* "Animal Biodiversity and Emerging Diseases: Prediction and Prevention" (O. A. E. Sparagano, J. C. Maillard and J. V. Figueroa, eds.), Vol. 1149, pp. 23-26. Blackwell Publishing, Oxford; UK.

Ghosh, S., Azhahianambi, P., and Yadav, M. P. (2007). Upcoming and future strategies of tick control: A review. *Journal of vector borne diseases* **44**, 79-89.

Goldin, A. L. (2001). Resurgence of sodium channel research. *Annual Review of Physiology* **63**, 871-894.

Goldin, A. L. (2006). Expression of ion channels in *Xenopus* oocytes. *In* "Expression and Analysis of Recombinant Ion Channels", pp. 1-25. Wiley-VCH Verlag GmbH & Co. KGaA.

Gonzalez-Cabrera, J., Davies, T. G. E., Field, L. M., Kennedy, P. J., and Williamson, M. S. (2013). An amino acid substitution (L925V) associated with resistance to pyrethroids in *Varroa destructor*. *Plos One* **8**.

Grabherr, M. G., Haas, B. J., Yassour, M., Levin, J. Z., Thompson, D. A., Amit, I., Adiconis, X., Fan, L., Raychowdhury, R., Zeng, Q. D., Chen, Z. H., Mauceli, E., Hacohen, N., Gnirke, A., Rhind, N., di Palma, F., Birren, B. W., Nusbaum, C., Lindblad-Toh, K., Friedman, N., and Regev, A. (2011). Full-length transcriptome assembly from RNA-Seq data without a reference genome. *Nature Biotechnology* **29**, 644–652.

Guerrero, F. D., Lovis, L., and Martins, J. R. (2012). Acaricide resistance mechanisms in *Rhipicephalus* (*Boophilus*) *microplus*. *Brazilian journal of veterinary parasitology* **21**, 1-6.

Guzman-Cornejo, C., Robbins, R. G., Guglielmone, A. A., Montiel-Parra, G., and Perez, T. M. (2011). The *Amblyomma* (Acari: Ixodida: Ixodidae) of Mexico: Identification keys, distribution and hosts. *Zootaxa* **2998**, 16-38.

Halos, L., Baneth, G., Beugnet, F., Bowman, A. S., Chomel, B., Farkas, R., Franc, M., Guillot, J., Inokuma, H., Kaufman, R., Jongejan, F., Joachim, A., Otranto, D., Pfister, K., Pollmeier, M., Sainz, A., and Wall, R. (2012). Defining the concept of 'tick repellency' in veterinary medicine. *Parasitology* **139**, 419-423.

Hamiduzzaman, M. M., Sinia, A., Guzman-Novoa, E., and Goodwin, P. H. (2012). Entomopathogenic fungi as potential biocontrol agents of the ecto-parasitic mite, *Varroa destructor*, and their effect on the immune response of honey bees (*Apis mellifera* L.). *Journal of Invertebrate Pathology* **111**, 237-243.

Hanrahan, C. J., Palladino, M. J., Ganetzky, B., and Reenan, R. A. (2000). RNA editing of the drosophila para Na+ channel transcsipt: Evolutionary conservation and developmental regulation. *Genetics* **155**, 1149-1160.

Hanson, M. S., and Edelman, R. (2003). Progress and controversy surrounding vaccines against Lyme disease. *Expert Review of Vaccines* **2**, 683-703.

He, H., Chen, A. C., Davey, R. B., Ivie, G. W., and George, J. E. (1999). Identification of a point mutation in the *para*-type sodium channel gene from a pyrethroid-resistant cattle tick. *Biochem Biophys Res Commun* **261**, 558-61.

Hebert, D., and Eschner, A. (2010). Seroprevalence of *Borrelia burgdorferi*-specific C-6 antibody in dogs before and after implementation of a nonadjuvanted recombinant outer surface Protein A vaccine in a Rhode Island small animal clinic. *Veterinary Therapeutics* **11**, 1-9.

Hille, B. (2001). "Ion Channels of excitable membranes," Third Edition/Ed. Sinauer, Massachusetts; USA.

Isman, M. B. (2000). Plant essential oils for pest and disease management. *Crop Protection* **19**, 603-608.

Isman, M. B. (2006). Botanical insecticides, deterrents, and repellents in modern agriculture and an increasingly regulated world. *Annual Review of Entomology* **51**, 45-66.

James, R. R., Hayes, G., and Leland, J. E. (2006). Field trials on the microbial control of *Varroa* with the fungus *Metarhizium anisopliae*. *American Bee Journal* **146**, 968-972.

Jameson, L. J., and Medlock, J. M. (2011). Tick surveillance in Great Britain. *Vector-Borne and Zoonotic Diseases* **11**, 403-412.

Jeppson, L. R., Keifer, H. H., and Baker, E. W. (1975). "Mites injurious to economic plants," University of California Press., California; USA.

Jongejan, F., and Uilenberg, G. (2004). The global importance of ticks. *Parasitology* **129**, 3-14.

Jonsson, N. N., Cutulle, C., Corley, S. W., and Seddon, J. M. (2010). Identification of a mutation in the para-sodium channel gene of the cattle tick Rhipicephalus microplus associated with resistance to flumethrin but not to cypermethrin. *International Journal for Parasitology* **40**, 1659-1664.

Kahl, O., Gern, L., Eisen, L., and Lane, R. S. (2002). "Ecological research on *Borrelia burgdorferi* sensu lato: Terminology and some methodological pitfalls.," CABI Publishing, Wallingford; UK.

Kamler, M., Nesvorna, M., Stara, J., Erban, T., and Hubert, J. (2016). Comparison of tau-fluvalinate, acrinathrin, and amitraz effects on susceptible and resistant populations of *Varroa destructor* in a vial test. *Experimental and Applied Acarology* **69**, 1-9.

Kanga, L. H. B., Adamczyk, J., Marshall, K., and Cox, R. (2010). Monitoring for resistance to organophosphorus and pyrethroid insecticides in *Varroa* mite populations. *Journal of Economic Entomology* **103**, 1797-1802.

Kanga, L. H. B., Jones, W. A., and James, R. R. (2003). Field trials using the fungal pathogen, *Metarhizium anisopliae* (Deuteromycetes: Hyphomycetes) to control the ectoparasitic mite, *Varroa destructor* (Acari: Varroidae) in honey bee, *Apis mellifera* (Hymenoptera: Apidae) colonies. *Journal of Economic Entomology* **96**, 1091-1099.

Katz, T. M., Miller, J. H., and Hebert, A. A. (2008). Insect repellents: Historical perspectives and new developments. *Journal of the American Academy of Dermatology* **58**, 865-871.

Khambay, B. P. S., and Jewess, P. J. (2005). Pyrethroids. *In* "Comprehensive Molecular Insect Science", Vol. 6, pp. 1-29. Elsevier, Oxford; UK.

Khila, A., and Grbic, M. (2007). Gene silencing in the spider mite *Tetranychus urticae*: dsRNA and siRNA parental silencing of the *Distal-less* gene. *Development Genes and Evolution* **217**, 241-251.

Kirkwood, A. C. (1967). Anaemia in poultry infested with red mite *Dermanyssus gallinae*. *Veterinary Record* **80**, 514-516.

Kirkwood, A. C. (1986). History, biology and control of sheep scab. *Parasitology Today* **2**, 302-307.

Kiss, T., Cadar, D., and Spinu, M. (2012). Tick prevention at a crossroad: New and renewed solutions. *Veterinary Parasitology* **187**, 357-366.

Kumar, S., Prakash, S., Kaushik, M. P., and Rao, K. M. (1992). Comparative Activity of 3 Repellents against the ticks *Rhipicephalus sanguineus* and *Argas persicus*. *Medical and Veterinary Entomology* **6**, 47-50.

Lane, R. S. (1989). Treatment of clothing with a permethrin spray for personal protection against the western black-legged tick, *Ixodes pacificus* (Acari: Ixodidae). *Experimental & Applied Acarology* **6**, 343-352.

Lee, S. H., Ingles, P. J., Knipple, D. C., and Soderlund, D. M. (2002). Developmental regulation of alternative exon usage in the house fly *Vssc1* sodium channel gene. *Invertebrate Neuroscience* **4**, 125-133.

Lee, S. H., Tsao, R., Peterson, C., and Coats, J. R. (1997). Insecticidal activity of monoterpenoids to western corn rootworm (Coleoptera: Chrysomelidae), two-spotted spider mite (Acari: Tetranychidae), and house fly (Diptera: Muscidae). *Journal of Economic Entomology* **90**, 883-892.

Lekimme, M., Focant, C., Farnir, F., Mignon, B., and Losson, B. (2008). Pathogenicity and thermotolerance of entomopathogenic fungi for the control of the scab mite, *Psoroptes ovis*. *Experimental and Applied Acarology* **46**, 95-104.

Li, J., Waterhouse, R. M., and Zdobnov, E. M. (2011). A remarkably stable TipE gene cluster: evolution of insect Para sodium channel auxiliary subunits. *Bmc Evolutionary Biology* **11**.

Lim, C., and Dudev, T. (2016). Potassium versus sodium selectivity in monovalent ion channel selectivity filters. *Metal ions in life sciences* **16**, 325-47.

Lin, W. H., Gunay, C., Marley, R., Prinz, A. A., and Baines, R. A. (2012). Activity-dependent alternative splicing increases persistent sodium current and promotes seizure. *Journal of Neuroscience* **32**, 7267-7277.

Lin, W. H., Wright, D. E., Muraro, N. I., and Baines, R. A. (2009). Alternative splicing in the voltage-gated sodium channel DmNa(v) regulates activation, inactivation, and persistent current. *Journal of Neurophysiology* **102**, 1994-2006.

Liu, D. T., Tibbs, G. R., and Siegelbaum, S. A. (1996). Subunit stoichiometry of cyclic nucleotide-gated channels and effects of subunit order on channel function. *Neuron* **16**, 983-990.

Liu, Z. Q., Song, W. Z., and Dong, K. (2004). Persistent tetrodotoxin-sensitive sodium current resulting from U-to-C RNA editing of an insect sodium channel. *Proceedings of the National Academy of Sciences of the United States of America* **101**, 11862-11867.

Liu, Z. Q., Tan, J. G., Huang, Z. Y., and Dong, K. (2006). Effect of a fluvalinate-resistance-associated sodium channel mutation from varroa mites on cockroach sodium channel sensitivity to fluvalinate, a pyrethroid insecticide. *Insect Biochemistry and Molecular Biology* **36**, 885-889.

Loughney, K., Kreber, R., and Ganetzky, B. (1989). Molecular analysis of the *para* locus, a sodium channel gene in *Drosophila*. *Cell* **58**, 1143-1154.

Luz, C., D'Alessandro, W. B., Rodrigues, J., and Fernandes, E. K. K. (2016). Efficacy of water- and oil-in-water-formulated *Metarhizium anisopliae* in *Rhipicephalus sanguineus* eggs and eclosing larvae. *Parasitology Research* **115**, 143-149.

Mans, B. J., Gothe, R., and Neitz, A. W. H. (2004). Biochemical perspectives on paralysis and other forms of toxicoses caused by ticks. *Parasitology* **129**, 95-111.

Marangi, M., Morelli, V., Pati, S., Camarda, A., Cafiero, M. A., and Giangaspero, A. (2012). Acaricide residues in laying hens naturally infested by red mite *Dermanyssus gallinae*. *Plos One* **7**, 1-6.

Marcelino, I., de Almeida, A. M., Ventosa, M., Pruneau, L., Meyer, D. F., Martinez, D., Lefrancois, T., Vachiery, N., and Coelho, A. V. (2012). Tick-borne diseases in cattle: Applications of proteomics to develop new generation vaccines. *Journal of Proteomics* **75**, 4232-4250.

Marcic, D. (2012). Acaricides in modern management of plant-feeding mites. *Journal of Pest Science* **85**, 395-408.

McCusker, E. C., Bagneris, C., Naylor, C. E., Cole, A. R., D'Avanzo, N., Nichols, C. G., and Wallace, B. A. (2012). Structure of a bacterial voltage-gated sodium channel pore reveals mechanisms of opening and closing. *Nature Communications* **3**, 1102-1109.

McNair, C. M. (2015). Ectoparasites of medical and veterinary importance: Drug resistance and the need for alternative control methods. *Journal of Pharmacy and Pharmacology* **67**, 351-363.

Mehlhorn, H. (2001). "Encyclopedic reference of parasitology: Biology, structure, function," Springer-Verlag, Berlin; DE.

Meikle, W. G., Mercadier, G., Holst, N., Nansen, C., and Girod, V. (2007). Duration and spread of an entomopathogenic fungus, *Beauveria bassiana* (Deuteromycota: Hyphomycetes), used to treat *Varroa* mites (Acari: Varroidae) in honey bee (Hymenoptera: Apidae) hives. *Journal of Economic Entomology* **100**, 1-10.

Meinkoth, J. H., and Kocan, A. A. (2005). Feline cytauxzoonosis. *Veterinary Clinics of North America-Small Animal Practice* **35**, 89-101.

Merino, O., Almazan, C., Canales, M., Villar, M., Moreno-Cid, J. A., Estrada-Pena, A., Kocan, K. M., and de la Fuente, J. (2011). Control of *Rhipicephalus* (*Boophilus*) *microplus* infestations by the combination of subolesin vaccination and tick autocidal control after subolesin gene knockdown in ticks fed on cattle. *Vaccine* **29**, 2248-2254.

Miledi, R., Parker, I., and Sumikawa, K. (1982). Synthesis of chick brain gaba receptors by frog oocytes. *Proceedings of the Royal Society Series B-Biological Sciences* **216**, 509-515.

Miller, R. J., George, J. E., Guerrero, F., Carpenter, L., and Welch, J. B. (2001). Characterization of acaricide resistance in *Rhipicephalus sanguineus* (Latreille) (Acari: Ixodidae) collected from the Corozal Army Veterinary Quarantine Center, Panama. *Journal of Medical Entomology* **38**, 298-302.

Miresmailli, S., and Isman, M. B. (2006). Efficacy and persistence of rosemary oil as an acaricide against two-spotted spider mite (Acari: Tetranychidae) on greenhouse tomato. *Journal of Economic Entomology* **99**, 2015-2023.

Morgan, J. A. T., Corley, S. W., Jackson, L. A., Lew-Tabor, A. E., Moolhuijzen, P. M., and Jonsson, N. N. (2009). Identification of a mutation in the *para*-sodium channel gene of the cattle tick *Rhipicephalus* (*Boophilus*) *microplus* associated with resistance to synthetic pyrethroid acaricides. *International Journal for Parasitology* **39**, 775-779.

Morin, S., Williamson, M. S., Goodson, S. J., Brown, J. K., Tabashnik, B. E., and Dennehy, T. J. (2002). Mutations in the *Bemisia tabaci para*-sodium channel gene associated with resistance to a pyrethroid plus organophosphate mixture. *Insect Biochemistry and Molecular Biology* **32**, 1781-1791.

Mowbray, F., Amlot, R., and Rubin, G. J. (2012). Ticking all the boxes? A systematic review of education and communication interventions to prevent tick-borne disease. *Vector-Borne and Zoonotic Diseases* **12**, 817-825.

Naik, P. R. H., and Shekharappa. (2009). Field evaluation of different entomopathogenic fungal formulations against sucking pests of okra. *Karnataka Journal of Agricultural Sciences* **22**, 575-578.

Nicholson, W. L., Allen, K. E., McQuiston, J. H., Breitschwerdt, E. B., and Little, S. E. (2010). The increasing recognition of rickettsial pathogens in dogs and people. *Trends in Parasitology* **26**, 205-212.

Noda, M., Shimizu, S., Tanabe, T., Takai, T., Kayano, T., Ikeda, T., Takahashi, H., Nakayama, H., Kanaoka, Y., Minamino, N., Kangawa, K., Matsuo, H., Raftery, M. A., Hirose, T., Inayama, S., Hayashida, H., Miyata, T., and Numa, S. (1984). Primary structure of *Electrophorus electricus* sodium channel deduced from cDNA sequence. *Nature* **312**, 121-127.

Nolan, J., Wilson, J. T., Green, P. E., and Bird, P. E. (1989). Syntheitc pyrethroid resistance in field samples in the cattle tick (*Boophilus microplus*). *Australian Veterinary Journal* **66**, 179-182.

O' Brien, D. J., Gray, J. S., and Oreilly, P. F. (1994). Survival and retention of infectivity of the mite *Psoroptes ovis* off the host. *Veterinary Research Communications* **18**, 27-36.

O'Dowd, D. K., and Aldrich, R. W. (1988). Voltage-clamp analysis of sodium-channels in wild-type and mutant *Drosophila* neurons. *Journal of Neuroscience* **8**, 3633-3643.

O'Reilly, A. O., Khambay, B. P. S., Williamson, M. S., Field, L. M., Wallace, B. A., and Davies, T. G. E. (2006). Modelling insecticide-binding sites in the voltage-gated sodium channel. *Biochemical Journal* **396**, 255-263.

O'Reilly, A. O., Williamson, M. S., Gonzalez-Cabrera, J., Turberg, A., Field, L. M., Wallace, B. A., and Davies, T. G. E. (2014). Predictive 3D modelling of the interactions of pyrethroids with the voltage-gated sodium channels of ticks and mites. *Pest Management Science* **70**, 369-377.

Olson, R. O., Liu, Z. Q., Nomura, Y., Song, W. Z., and Dong, K. (2008). Molecular and functional characterization of voltage-gated sodium channel variants from Drosophila melanogaster. *Insect Biochemistry and Molecular Biology* **38**, 604-610.

Papke, R. L., and Smith-Maxwell, C. (2009). High throughput electrophysiology with *Xenopus* oocytes. *Combinatorial Chemistry & High Throughput Screening* **12**, 38-50.

Parizi, L. F., Reck, J., Oldiges, D. P., Guizzo, M. G., Seixas, A., Logullo, C., de Oliveira, P. L., Termignoni, C., Martins, J. R., and Vaz, I. D. (2012). Multi-antigenic vaccine against the cattle tick *Rhipicephalus* (*Boophilus*) *microplus*: A field evaluation. *Vaccine* **30**, 6912-6917.

Park, Y., Taylor, M. F. J., and Feyereisen, R. (1999). Voltage-gated sodium channel genes *hscp* and *hDSC1* of *Heliothis virescens* F-genomic organization. *Insect Molecular Biology* **8**, 161-170.

Payandeh, J., Scheuer, T., Zheng, N., and Catterall, W. A. (2011). The crystal structure of a voltage-gated sodium channel. *Nature* **475**, 353-104.

Perez de Leon, A. A., Vannier, E., Almazan, C., and Krause, P. (2014). Tick-Borne protozoa. *In* "Biology of Ticks" (D. E. Sonenshine, Roe, R.M., ed.), Vol. 2, pp. 147-179. Oxford university Press, New York; USA.

Philippou, D., Field, L. M., Wegorek, P., Zamojska, J., Andrews, M. C., Slater, R., and Moores, G. D. (2011). Characterising metabolic resistance in pyrethroid-insensitive pollen beetle (*Meligethes aeneus* F.) from Poland and Switzerland. *Pest Management Science* **67**, 239-243.

Piesman, J., and Eisen, L. (2008). Prevention of tick-borne diseases. *Annual Review of Entomology* **53**, 323-343.

Plapp, F. G. J., McWhorter, G. M., and Vane, W. M. (1987). Monitoring for pyrethroid resistance in the tobacco budworm in Texas - 1986. *In* "Proceedings of the Beltwide Cotton Production Research Conferences", Dallas; USA.

Plummer, N. W., McBurney, M. W., and Meisler, M. H. (1997). Alternative splicing of the sodium channel SCN8A predicts a truncated two-domain protein in fetal brain and non-neuronal cells. *Journal of Biological Chemistry* **272**, 24008-24015.

Pretorius, A. M., Jensenius, M., Clarke, F., and Ringertz, S. H. (2003). Repellent efficacy of DEET and KBR 3023 against *Amblyomma hebraeum* (Acari: Ixodidae). *Journal of Medical Entomology* **40**, 245-248.

Puinean, A. M., Lansdell, S. J., Collins, T., Bielza, P., and Millar, N. S. (2013). A nicotinic acetylcholine receptor transmembrane point mutation (G275E) associated with resistance to spinosad in *Frankliniella occidentalis*. *Journal of Neurochemistry* **124**, 590-601.

Randolph, S. E. (2010). To what extent has climate change contributed to the recent epidemiology of tick-borne diseases? *Veterinary Parasitology* **167**, 92-94.

Regnault-Roger, C., Vincent, C., and Arnason, J. T. (2012). Essential oils in insect control: Low-risk products in a high-stakes world. *In* "Annual Review of Entomology", Vol. 57, pp. 405-424.

Reichard, M. V., Edwards, A. C., Meinkoth, J. H., Snider, T. A., Meinkoth, K. R., Heinz, R. E., and Little, S. E. (2010). Confirmation of Amblyomma americanum (Acari: Ixodidae) as a Vector for Cytauxzoon felis (Piroplasmorida: Theileriidae) to Domestic Cats. *Journal of Medical Entomology* **47**, 890-896.

Richter, P. J. J., Kimsey, R. B., Madigan, J. E., Barlough, J. E., Dumler, J. S., and Brooks, D. L. (1996). Ixodes pacificus (Acari: Ixodidae) as a vector of Ehrlichia equi (Rickettsiales: Ehrlichieae). *Journal of Medical Entomology* **33**, 1-5.

Rinkevich, F. D., Du, Y. Z., and Dong, K. (2013). Diversity and convergence of sodium channel mutations involved in resistance to pyrethroids. *Pesticide Biochemistry and Physiology* **106**, 93-100.

Rosen, S., Yeruham, I., and Braverman, Y. (2002). Dermatitis in humans associated with the mites *Pyemotes tritici*, *Dermanyssus gallinae*, *Ornithonyssus bacoti* and *Androlaelaps casalis* in Israel. *Medical and Veterinary Entomology* **16**, 442-444.

Sambrook, J., and Green, M. R. (2012). "Molecular cloning: A laboratory manual," Fourth Edition/Ed. Cold Spring Harbor Laboratory Press, New York; USA.

Sammataro, D., Gerson, U., and Needham, G. (2000). Parasitic mites of honey bees: Life history, implications, and impact. *Annual Review of Entomology* **45**, 519-548.

Sargison, N., Roger, P., Stubbings, L., Baber, P., and Morris, P. (2007). Controlling sheep scab by eradication. *Veterinary Record* **160**, 491-492.

Sawicki, R. M. (1978). Unusual response of DDT-resistant houseflies to carbinol analogs of DDT. *Nature* **275**, 443-444.

Schetters, T. (2005). Vaccination against canine babesiosis. *Trends in Parasitology* **21**, 179-184.

Schreck, C. E., Snoddy, E. L., and Spielman, A. (1986). Pressurized sprays of permethrin or deet on military clothing for personal protection against *Ixodes dammini* (Acari: Ixodidae). *Journal of Medical Entomology* **23**, 396-399.

Service, M. (2012). "Medical Entomology for Students," Cambridge University Press, New York; USA.

Shaalan, E. A. S., Canyon, D., Younes, M. W. F., Abdel-Wahab, H., and Mansour, A. H. (2005). A review of botanical phytochemicals with mosquitocidal potential. *Environment International* **31**, 1149-1166.

Shao, Y. M., Dong, K., Tang, Z. H., and Zhang, C. X. (2009). Molecular characterization of a sodium channel gene from the Silkworm *Bombyx mori*. *Insect Biochemistry and Molecular Biology* **39**, 145-151.

Shi, W. B., and Feng, M. G. (2006). Field efficacy of application of *Beauveria bassiana* formulation and low rate pyridaben for sustainable control of citrus red mite *Panonychus citri* (Acari: Tetranychidae) in orchards. *Biological Control* **39**, 210-217.

Shi, W. B., Zhang, L. L., and Feng, M. G. (2008). Field trials of four formulations of *Beauveria bassiana* and *Metarhizium anisoplae* for control of cotton spider mites (Acari: Tetranychidae) in the Tarim basin of China. *Biological Control* **45**, 48-55.

Shkap, V., de Vos, A. J., Zweygarth, E., and Jongeian, F. (2007). Attenuated vaccines for tropical theileriosis, babesiosis and heartwater: The continuing necessity. *Trends in Parasitology* **23**, 420-426.

Singh, O. P., Dykes, C. L., Das, M. K., Sabyasachi, P., Bhatt, R. M., Agrawal, O. P., and Tridibes, A. (2010). Presence of two alternative kdr-like mutations, L1014F and L1014S, and a novel mutation, V1010L, in the voltage-gated Na+ channel of *Anopheles culicifacies* from Orissa, India. *Malaria Journal* **9**, 1-6.

Smit, R. (2012). Cost-effectiveness of tick-borne encephalitis vaccination in Slovenian adults. *Vaccine* **30**, 6301-6306.

Soderlund, D. M. (2012). Molecular mechanisms of pyrethroid insecticide neurotoxicity: Recent advances. *Archives of Toxicology* **86**, 165-181.

Soderlund, D. M., and Bloomquist, J. R. (1989). Neurotoxic actions of pyrethroid insecticides. *Annual Review of Entomology* **34**, 77-96.

Solberg, V. B., Klein, T. A., Mcpherson, K. R., Bradford, B. A., Burge, J. R., and Wirtz, R. A. (1995). Field-evaluation of deet and a piperidine repellent (Ai3-37220) against *Amblyomma americanum* (Acari: Ixodidae). *Journal of Medical Entomology* **32**, 870-875.

Solomon, S., Qin, D., Manning, M., Chen, Z., Marquis, M., Averyt, K. B., Tignor, M., and Miller, H. L. (2007). "Climate change 2007: The physical science basis.." Cambridge University Press, Cambridge;UK And New York; USA.

Song, W. Z., Liu, Z. Q., Tan, J. G., Nomura, Y., and Dong, K. (2004). RNA editing generates tissue-specific sodium channels with distinct gating properties. *Journal of Biological Chemistry* **279**, 32554-32561.

Sonoda, S., Igaki, C., Ashfaq, M., and Tsumuki, H. (2006). Pyrethroid-resistant diamondback moth expresses alternatively spliced sodium channel transcripts with and without T929I mutation. *Insect Biochemistry and Molecular Biology* **36**, 904-910.

Sparagano, O. A. E., and De Luna, C. J. (2008). From population structure to genetically engineered vectors: New ways to control vector-borne diseases? *Infection Genetics and Evolution* **8**, 520-525.

Stanneck, D., Ebbinghaus-Kintscher, U., Schoenhense, E., Kruedewagen, E. M., Turberg, A., Leisewitz, A., Jiritschka, W., and Krieger, K. J. (2012). The synergistic action of imidacloprid and flumethrin and their release kinetics from collars applied for ectoparasite control in dogs and cats. *Parasites & Vectors* **5**.

Steenberg, T., and Kilpinen, O. (2014). Synergistic interaction between the fungus *Beauveria bassiana* and desiccant dusts applied against poultry red mites (*Dermanyssus gallinae*). *Experimental and Applied Acarology* **62**, 511-524.

Steere, A. C., Malawista, S. E., Snydman, D. R., Shope, R. E., Andiman, W. A., Ross, M. R., and Steele, F. M. (1977). Lyme arthritis - Epidemic of oligoarticular arthritis in children and adults in 3 connecticut communities. *Arthritis and Rheumatism* **20**, 7-17.

Steere, A. C., Sikand, V. K., Meurice, F., Parenti, D. L., Fikrig, E., Schoen, R. T., Nowakowski, J., Schmid, C. H., Laukamp, S., Buscarino, C., and Krause, D. S. (1998). Vaccination against Lyme disease with recombinant *Borrelia burgdorferi* outer-surface lipoprotein A with adjuvant. *New England Journal of Medicine* **339**, 209-215.

Suarez, C. E., and Noh, S. (2011). Emerging perspectives in the research of bovine babesiosis and anaplasmosis. *Veterinary Parasitology* **180**, 109-125.

Sutherst, R. W. (2004). Global change and human vulnerability to vector-borne diseases. *Clinical Microbiology Reviews* **17**, 136-173.

Talleklint-Eisen, L., and Lane, R. S. (2000). Spatial and temporal variation in the density of *Ixodes pacificus* (Acari : Ixodidae) nymphs. *Environmental Entomology* **29**, 272-280.

Tan, J. G., Liu, Z. Q., Nomura, Y., Goldin, A. L., and Dong, K. (2002). Alternative splicing of an insect sodium channel gene generates pharmacologically distinct sodium channels. *Journal of Neuroscience* **22**, 5300-5309.

Taylor, M. A. (2001). Recent developments in ectoparasiticides. *Veterinary Journal* **161**, 253-268.

Telford, S. R., and Goethert, H. K. (2004). Emerging tick-borne infections: rediscovered and better characterized, or truly 'new'? *Parasitology* **129**, 301-327.

Thackeray, J. R., and Ganetzky, B. (1994). Developmentally-Regulated Alternative Splicing Generates a Complex Array of *Drosophila-Para* Sodium-Channel Isoforms. *Journal of Neuroscience* **14**, 2569-2578.

Thackeray, J. R., and Ganetzky, B. (1995). Conserved Alternative Splicing Patterns and Splicing Signals in the *Drosophila* Sodium-Channel Gene *para*. *Genetics* **141**, 203-214.

Tunc, I., and Sahinkaya, S. (1998). Sensitivity of two greenhouse pests to vapours of essential oils. *Entomologia Experimentalis Et Applicata* **86**, 183-187.

Ullah, M. S., and Lim, U. T. (2015). Laboratory bioassay of *Beauveria bassiana* against *Tetranychus urticae* (Acari: Tetranychidae) on leaf discs and potted bean plants. *Experimental and Applied Acarology* **65**, 307-318.

Usherwood, P. N. R., Davies, T. G. E., Mellor, I. R., O'Reilly, A. O., Peng, F., Vais, H., Khambay, B. P. S., Field, L. M., and Williamson, M. S. (2007). Mutations in DIIS5 and the DIIS4-S5 linker of *Drosophila melanogaster* sodium channel define binding domains for pyrethroids and DDT. *Febs Letters* **581**, 5485-5492.

Usherwood, P. N. R., Vais, H., Khambay, B. P. S., Davies, T. G. E., and Williamson, M. S. (2005). Sensitivity of the *Drosophila para* sodium channel to DDT is not lowered by the super-kdr mutation M918T on the IIS4-S5 linker that profoundly reduces sensitivity to permethrin and deltamethrin. *Febs Letters* **579**, 6317-6325.

Uzzell, D., Vasileiou, K., Marcu, A., and Barnett, J. (2012). Whose Lyme is it anyway? Subject positions and the construction of responsibility for managing the health risks from Lyme disease. *Health & Place* **18**, 1101-1109.

Vais, H., Goodson, S., Eldursi, N., Williamson, M., Devonshire, A. L., Cohen, C. J., and Usherwood, P. N. R. (2000a). Cooperativity between pyrethroid-resistance mutations (kdr and super-kdr) upon insertion into the *Drosophila para* sodium channel. *In* "Society for Neuroscience Abstracts", Vol. 26, pp. Abstract No.-418.12.

Vais, H., Williamson, M. S., Devonshire, A. L., and Usherwood, P. N. R. (2001). The molecular interactions of pyrethroid insecticides with insect and mammalian sodium channels. *Pest Management Science* **57**, 877-888.

Vais, H., Williamson, M. S., Goodson, S. J., Devonshire, A. L., Warmke, J. W., Usherwood, P. N. R., and Cohen, C. J. (2000b). Activation of Drosophila sodium channels promotes modification by deltamethrin - Reductions in affinity caused by knock-down resistance mutations. *Journal of General Physiology* **115**, 305-318.

Vais, H., Williamson, M. S., Hick, C. A., Eldursi, N., Devonshire, A. L., and Usherwood, P. N. R. (1997). Functional analysis of a rat sodium channel carrying a mutation for insect knock-down resistance (kdr) to pyrethroids. *Febs Letters* **413**, 327-332.

Valiente Moro, C., Chauve, C., and Zenner, L. (2005). Vectorial role of some dermanyssoid mites (Acari: Mesostigmata, Dermanyssoidea). *Parasite* **12**, 99-109.

van den Broek, A. H. M., Huntley, J. F., Machell, J., Taylor, M., Bates, P., Groves, B., and Miller, H. R. P. (2000). Cutaneous and systemic responses during primary and challenge infestations of sheep with the sheep scab mite, *Psoroptes ovis*. *Parasite Immunology* **22**, 407-414.

Van Leeuwen, T., Tirry, L., Yamamoto, A., Nauen, R., and Dermauw, W. (2015). The economic importance of acaricides in the control of phytophagous mites and an update on recent acaricide mode of action research. *Pesticide Biochemistry and Physiology* **121**, 12-21.

Van Leeuwen, T., Vontas, J., Tsagkarakou, A., Dermauw, W., and Tirry, L. (2010a). Acaricide resistance mechanisms in the two-spotted spider mite *Tetranychus urticae* and other important Acari: A review. *Insect Biochemistry and Molecular Biology* **40**, 563-572.

Van Leeuwen, T., Witters, J., Nauen, R., Duso, C., and Tirry, L. (2010b). The control of eriophyoid mites: State of the art and future challenges. *Experimental and Applied Acarology* **51**, 205-224.

van Lenteren, J. C. (2012). The state of commercial augmentative biological control: Plenty of natural enemies, but a frustrating lack of uptake. *Biocontrol* **57**, 1-20.

Wakeling, E. N., Neal, A. P., and Atchison, W. D. (2012). Pyrethroids and their effects on ion channels *In* "Pesticides - Advances in Chemical and Botanical Pesticides" (D. R. P. Soundararajan, ed.). InTech

Walter, D. E., and Proctor, H. (1999). "Mites: Ecoloy, evolution and behaviour," CABI Publishing, Wallingford; UK.

Wang, R. W., Huang, Z. Y., and Dong, K. (2003). Molecular characterization of an arachnid sodium channel gene from the varroa mite (*Varroa destructor*). *Insect Biochemistry and Molecular Biology* **33**, 733-739.

Warmke, J. W., Reenan, R. A. G., Wang, P. Y., Qian, S., Arena, J. P., Wang, J. X., Wunderler, D., Liu, K., Kaczorowski, G. J., VanderPloeg, L. H. T., Ganetzky, B., and Cohen, C. J. (1997). Functional expression of *Drosophila para* sodium channels - Modulation by the membrane protein TipE and toxin pharmacology. *Journal of General Physiology* **110**, 119-133.

Willadsen, P. (2001). The molecular revolution in the development of vaccines against ectoparasites. *Veterinary Parasitology* **101**, 353-367.

Williamson, M. S., Bell, C. A., Denholm, I., and Devonshire, A. L. (1993a). Cloning of a housefly sodium channel gene linked to pyrethroid resistance. *Opportunities for Molecular Biology in Crop Production* **55**, 329-330.

Williamson, M. S., Denholm, I., Bell, C. A., and Devonshire, A. L. (1993b). Knockdown resistance (Kdr) to DDT and pyrethroid insecticides maps to a sodium channel gene locus in the housefly (*Musca domestica*). *Molecular & General Genetics* **240**, 17-22.

Williamson, M. S., MartinezTorres, D., Hick, C. A., and Devonshire, A. L. (1996). Identification of mutations in the housefly *para*-type sodium channel gene associated with knockdown resistance (kdr) to pyrethroid insecticides. *Molecular and General Genetics* **252**, 51-60.

Wrzesinska, B., Czerwoniec, A., Wieczorek, P., Wegorek, P., Zamojska, J., and Obrepalska-Steplowska, A. (2014). A survey of pyrethroid-resistant populations of *Meligethes aeneus* F. in Poland indicates the incidence of numerous substitutions in the pyrethroid target site of voltage-sensitive sodium channels in individual beetles. *Insect Molecular Biology* **23**, 682-693.

Yang, X. L., and Cox-Foster, D. L. (2005). Impact of an ectoparasite on the immunity and pathology of an invertebrate: Evidence for host immunosuppression and viral amplification. *Proceedings of the National Academy of Sciences of the United States of America* **102**, 7470-7475.

Zhang, Z. Q., Hooper, J. N. A., Van Soest, R. W. M., Pisera, A., Crowther, A. L., Tyler, S., Schilling, S., Eschmeyer, W. N., Fong, J. D., Blackburn, D. C., Wake, D. B., Wilson, D. E., Reeder, D. M., Fritz, U., Hodda, M., Guidetti, R., Bertolani, R., Mayer, G., Oliveira, I. D., Zhang, Z. Q., Adrain, J. M., Bamber, R. N., Kury, A. B., Prendini, L., Harvey, M. S., Beaulieu, F., Dowling, A. P. G., Klompen, H., de Moraes, G. J., Walter, D. E., Zhang, Z. Q., Fan, Q. H., Pesic, V., Smit, H., Bochkov, A. V., Khaustov, A. A., Baker, A., Wohltmann, A., Wen, T. H., Amrine, J. W., Beron, P., Lin, J. Z., Gabrys, G., Husband, R., Bolton, S., Uusitalo, M., Zhang, Z. Q., Schatz, H., Behan-Pelletier, V. M., Oconnor, B. M., Norton, R. A., Dunlop, J. A., Penney, D., Minelli, A., Shear, W., Ahyong, S. T., Lowry, J. K., Alonso, M., Bamber, R. N., Boxshall, G. A., Castro, P., Gerken, S., Karaman, G. S., Goy, J. W., Jones, D. S., Meland, K., Rogers, D. C., Svavarsson, J., Janssens, F., Christiansen, K. A., Ingrisch, S., Brock, P. D., Marshall, J., Beccaloni, G. W., Eggleton, P., Mound, L. A., Slipinski, S. A., Leschen, R. A. B., Lawrence, J. F., Holzenthal, R. W., Morse, J. C., Kjer, K. M., van Nieukerken, E. J., Kaila, L., Kitching, I. J., Kristensen, N. P., Lees, D. C., Minet, J., Mitter, C., Mutanen, M., Regier, J. C., Simonsen, T. J., Wahlberg, N., Yen, S. H., Zahiri, R., Adamski, D., Baixeras, J., Bartsch, D., Bengtsson, B. A., Brown, J. W., et al. (2011). Animal biodiversity: An outline of higher-level classification and taxonomic richness. *Zootaxa* **3148**, 7-237.

Zlotkin, E. (1999). The insect voltage-gated sodium channel as target of insecticides. *Annual Review of Entomology* **44**, 429-455.